SEP -4

REPORT DOCUMENTATION PAGE

AFRL-SR-AR-TR-02-

0323

1. REPORT DATE (DD-MM-YYYY)	2. REPORT TYPE	3. DATES COVERED (From - To)
September 3, 2002	Final	9/01/1995 to 12/31/2001

4. TITLE AND SUBTITLE
RESEARCH AND EDUCATIONAL ACTIVITIES AT THE FAST CENTER FOR STRUCTURAL INTEGRITY OF AEROSPACE SYSTEMS

5a. CONTRACT NUMBER

5b. GRANT NUMBER
F49620-95-1-0518

5c. PROGRAM ELEMENT NUMBER

6. AUTHOR(S)
Roberto A. Osegueda and Carlos M. Ferregut

5d. PROJECT NUMBER

5e. TASK NUMBER

5f. WORK UNIT NUMBER

7. PERFORMING ORGANIZATION NAME(S) AND ADDRESS(ES)
FAST Center for Structural Integrity of Aerospace Systems
The University of Texas at El Paso
Burges Hall, Room 206
El Paso, Texas 79968

8. PERFORMING ORGANIZATION REPORT NUMBER

9. SPONSORING / MONITORING AGENCY NAME(S) AND ADDRESS(ES)
US Air Force of Scientific Research/NM
801 North Randolph St.
Arlington, VA 22203-1977

10. SPONSOR/MONITOR'S ACRONYM(S)
AFOSR

12. DISTRIBUTION / AVAILABILITY STATEMENT
Approved for public release;
distribution unlimited.

20021008 012

13. SUPPLEMENTARY NOTES

14. ABSTRACT

This report describes the technical research activities that were carried out at the Future Aerospace Science and Technology (FAST) Center for Structural Integrity of Aerospace Systems, the University of Texas at El Paso, under funding from the US Air Force Office of Scientific Research. Also included is a brief description of the efforts to educate minority scientists and engineers. The technical mission was to conduct basic research to contribute to improvements of the reliability and maintainability of aerospace structures. The Center involved an interdisciplinary core group of Engineering and Science faculty and collaborators with scientists and engineers from various USAF, DOE and NASA centers and laboratories and other universities.

Technical accomplishments are included in this report on four different research projects addressing issues on ultrasonic nondestructive evaluation of aircraft, the characterization of structural damage and materials degradation, vibrational NDE methods using laser Doppler velocimetry and neural networks and pattern recognition techniques to process NDE data. The research performed resulted in more than 70 publications in conference proceedings and referred journals, 6 doctorate dissertations, 31 masters' theses, and contributed to the education of 73 students.

15. SUBJECT TERMS
Aircraft Structures, Global Vibrational NDE, Damage Detection, Large Area NDE, Corrosion, Ultrasonic Inspection, Lamb Waves

16. SECURITY CLASSIFICATION OF:			17. LIMITATION OF ABSTRACT	18. NUMBER OF PAGES	19a. NAME OF RESPONSIBLE PERSON
a. REPORT	b. ABSTRACT	c. THIS PAGE			Roberto Osegueda
Unclassified	Unclassified	Unclassified	Unclassified	220	19b. TELEPHONE NUMBER (include area code) (915) 747-7891

RESEARCH AND EDUCATIONAL ACTIVITIES AT THE FAST CENTER FOR STRUCTURAL INTEGRITY OF AEROSPACE SYSTEMS

A Final Report

Grant No. F49620-95-1-0518

Prepared by

Roberto A. Osegueda
Carlos M. Ferregut
FAST Center for Structural Integrity of Aerospace Systems
The University of Texas at El Paso
Burges Hall, Room 206
El Paso, Texas 79968

Submitted to

US Air Force of Scientific Research/NM
801 North Randolph St.
Arlington, VA 22203-1977
Program Manager: Dr. Spencer Wu

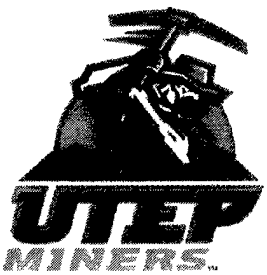

September 3, 2002

RESEARCH AND EDUCATIONAL ACTIVITIES AT THE FAST CENTER FOR STRUCTURAL INTEGRITY OF AEROSPACE SYSTEMS

EXECUTIVE SUMMARY

This report describes the technical research activities that were carried out at the Future Aerospace Science and Technology (FAST) Center for Structural Integrity of Aerospace Systems, the University of Texas at El Paso, under funding from the US Air Force Office of Scientific Research. Also included is a brief description of the efforts to educate minority scientists and engineers. The technical mission was to conduct basic research to contribute to improvements of the reliability and maintainability of aerospace structures. The Center involved an interdisciplinary core group of Engineering and Science faculty and collaborators with scientists and engineers from various USAF, DOE and NASA centers and laboratories and other universities.

Technical accomplishments are included in this report on four different research projects addressing issues on ultrasonic nondestructive evaluation of aircraft, the characterization of structural damage and materials degradation, vibrational NDE methods using laser Doppler velocimetry and neural networks and pattern recognition techniques to process NDE data. The research performed resulted in more than 70 publications in conference proceedings and referred journals, 6 doctorate dissertations, 31 masters' theses, and contributed to the education of 73 students.

ACKNOWLEDGMENTS

The efforts documented here were sponsored by the Air Force Office of Scientific Research, Air Force Materiel Command, USAF, under grant number F49620-95-1-0518. The US Government is authorized to reproduce and distribute reprints for Governmental purposes notwithstanding any copyright notation thereon. The continuing mentoring of Dr. Spencer Wu, program manager, is greatly appreciated. The fruitful involvement of all the students listed in Appendix A is greatly acknowledged. Without their desire to obtain an education, this work would not have been possible. Furthermore, the involvement of the following individuals is greatly recognized. From UTEP: Soheil Nazarian, Larry Murr, Roy Arrowood, Joseph Pierluissi, Jorge Lopez, Vladik Kreinovich, John McClure, Cesar Carrasco; from US Air Force: Tom Moran, Tobey Cordell, Claudia Kropas-Hughes, Don Nieser and Don Groner; from Sandia National Labs: Tom Paez, Bruce Hansche, Pat Barney, George James and Tom Baca; From NASA JSC: Rodney Rocha, Mike Grygier; From Los Alamos: Charles Farrar & Norman Hunter; and from other universities: Norris Stubbs (TAMU), Gabriel Garcia (UCLA), Ajit Mal (UCLA) & Dale Chimenti (Iowa State Univeristy).

TABLE OF CONTENTS

Page

LIST OF FIGURES

Figure **Page**

Figure **Page**

Figure **Page**

Figure **Page**

LIST OF TABLES

CHAPTER 1

INTRODUCTION

1.1 Introduction

The University of Texas at El Paso received funding from the US Air Force Office of Scientific Research to establish a Center for Structural Integrity of Aerospace Systems under the Future Aerospace Science and Technology Program (FAST). The technical mission of the center was to conduct basic research to contribute to improvements of the reliability and maintainability of aerospace structures. The educational mission of the Center was to produce qualified graduate minority scientists, and engineers in fields relevant to Air Force needs. The Center was formed with an interdisciplinary core group of faculty members from the Colleges of Engineering and Science and a significant number of students. In addition, the Center established collaborations, at the project level, with scientists and engineers from Jet Propulsion Laboratories, Sandia National Laboratories, Los Alamos National Laboratories and Texas A&M University. These organizations were initially approached because of their involvement on research on aging aircraft and structural health monitoring. Through the years, however, additional collaborations were established with scientists and engineers from Air Force Research Labs in Dayton Ohio, USAF Oklahoma City Air Logistic Center, University of California at Los Angeles, Iowa State University, NASA Johnson Space Center and Boeing.

In addition to conducting basic research, UTEP's FAST Center facilitated summer fellowships to students and faculty, established a series of technical seminars, and networked with the majority of organizations dealing with aging aircraft issues

The core faculty consisted of members of the departments of Civil Engineering, Metallurgical and Materials Engineering, Electrical Engineering, Computer Science and Physics who have traditionally worked together conducting research and have extensively contributed to the education of a vast number of students in Science and Engineering. During the six years of AF funding the Center sponsored from 15 to 25 students per year to participate in the program.

Four different research projects were initiated at UTEP's FAST Center under AFOSR funding. These projects addressed issues on ultrasonic nondestructive evaluation of aircraft, the characterization of structural damage and materials degradation, NDE methods using laser Doppler velocimetry, global NDE vibrational methods, neural networks and pattern recognition techniques to process NDE data.

1.2 General Problem Statement

The trend to extend the use of old military aircraft, rather than replacing them with new models, has increased their probability of structural failure as a result of aging. This trend added a great degree of urgency to the ongoing needs for reliable and efficient NDE methods and better understanding of the flaws formation and growth under service conditions. Aging of aircraft is

associated with fatigue cracking and corrosion of the metallic structures; whereas in composite components the material degrades, and there is an increased probability of impact damage and initiation of delaminations. Effective NDE methods for detecting and characterizing flaws are needed to provide advanced warning, before defects reach critical size that could lead to catastrophic failure, or to allow safe repair or part replacement.

Military aircraft are exposed to service conditions that lead to the degradation of the quality and performance of their structural materials. This degradation is costly, can cause loss in humans and property if left undetected and requires a periodic maintenance to assure both the residual life and the protection of the structure. Figure 1.1 depicts some of the factors that can cause degradation. These are static and cyclic mechanical and thermal loads, humidity, exposure to extreme range of temperatures, impulse loading including impact damage, thermal spikes, service fluids, radiation damage and erosion. These conditions are causing damage and material deterioration in a form that alters their properties from the design allowable and eventually to an uncontrolled critical failure of the structure. Figure 1.2 illustrates typical forms of damage.

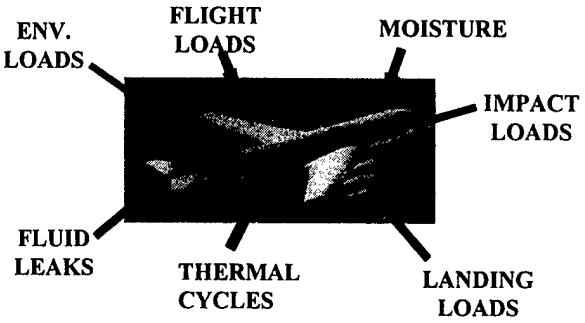

Figure 1.1 Causes of Damage.

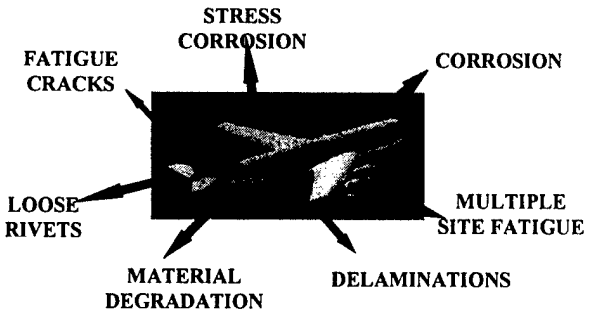

Figure 1.2 Typical Forms of Damage.

Inspection of aging aircraft using current technology is time consuming, demands great attention to details by the inspectors and, in many cases, requires a costly disassembly of the structure. The reliability of the test results depends heavily on the type of instrument used, the condition of the instrument, the methods and environment under which it is used and above all, the interpretation of the inspectors. The inspector's interpretation depends critically on his/her experience and attentiveness. The work performed at the FAST Center addressed issues on corrosion in metallic structures and defects in metallic and composite airframes using local and global NDE methods

1.2.1 Metallic Materials (Corrosion)

Corrosion of primary aircraft components and structures can have serious consequences in terms of safety and cost to the Air Force. Corrosion is a term used for the oxidation degradation of metals and can appear in many forms, depending on the metals and the damage mechanism. The detection of each type of corrosion may require different NDE methodology depending on the distinct characteristics of the corrosion process. Corrosion is a form of

deterioration of metallic structure that results from exposure to humid or corrosive environments. Its process converts the metal into its oxide or hydroxide resulting in a deterioration of the metal's mechanical characteristics.

Despite the existing preventive measures, corrosion does occur and is mostly due to insufficient inhibitors or leakage of solutions into traps within elements of the structures. The severity of corrosion attack varies with aircraft types, design techniques, operating environments, and operator's maintenance program. In general, there are common areas of aircraft structures that are subject to corrosion; for example, floor and structures in the vicinity of fluid flow systems, structures surrounding doors, wing-to-body joint fittings, etc.

Currently, no reliable cost-effective technology is available for the detection and evaluation of corrosion damage in structural components. Corrosion on aluminum alloys and plated steel surfaces can often be recognized by dulling or pitting of the area, and sometimes by white or red powdery deposits. Such an indication may be the origin for, or revealed by, lamination, cracking, metal thinning, fretting, etc. For hidden corrosion, as in engine blades or fuel tanks, several NDE methods are presently used which are very expensive and time consuming. These techniques include X-ray and thermal-neutron radiography, ultrasonics, eddy current and acoustic emission. All existing NDE methods for detection of corrosion are limited in capability and sensitivity; therefore, it is not uncommon that corrosion is detected only after several subsequent inspection schedules have elapsed, in which case the damage is fairly extensive.

1.2.2 Composite Materials

Primary structural components of several new military aircraft are constructed of fiber-reinforced composites. These structures are designed with high demand on their performance using the unique properties of composites. Besides their radar reflectance characteristics, these materials are selected for their relatively low weight that is accompanied by high stiffness, strength, fatigue resistance and damage tolerance. Further, these materials offer a unique mix of formability and toughness allowing sensors and actuators to be imbedded in the material and to form active/adaptive (i.e., smart) structures. However, composites are very sensitive to manufacturing processes and service conditions, which can induce defects and seriously degrade the material performance.

In contrast to metals, the failure mechanisms of structural composites are much more complex. Further, the ability of composite structures to sustain loads can be critically affected by conditions to which metals are more tolerant. For example, internal damage, caused by low velocity foreign object impact or by rapidly applied localized thermal loads, can critically deteriorate the structure durability. Another major difficulty that hampers a wide use of composites is the lack of sufficient theoretical and experimental understanding of the material behavior at the micromechanical or fundamental level. This deficiency needs to be accounted for in the design allowable and it has led to the use of conservative safety margins. These safety margins are involved with weight penalties, reduce the low-weight advantage of composites and increase the manufacturing cost in material and processing.

Composite materials tend to degrade due to exposure to service conditions. Fire and heat

are examples of sources of material properties degradation, which depends on the level of oxygen that is involved in the process. Heat causes polymer chain scission leading to polymer degradation, namely, formation of shorter polymer chains. The chain scission produces highly reactive radical species that can react with oxygen, participate in radical/radical recombination reactions, and cause abstraction of hydrogen and/or form terminations. These reactions can occur on the fiber epoxy interface damaging the interfacial bond as well as in the matrix causing strength reduction. Generally, thermal degradation of epoxy resins starts around 250°C (about 480° F), but some weight loss measurements can be detected to initiate even around 200°C (about 390° F).

1.2.3 NDE of Aging Aircraft

Most NDE methods that are used for inspection in field conditions provide detailed information about a limited region of the structure. These methods include, but are not limited to, penetrating radiation, optics, electromagnetics, ultrasonics, acoustic emission and magnetic flux analysis. By far, the most developed and utilized methods are those based on visual inspection, electromagnetics (i.e. eddy current) and ultrasonics. The method to be used in a given situation depends on the expected nature of the defect to be detected, the required sensitivity, reliability of the measurement, the cost and practicality of inspection.

In recent years, efforts were exerted to develop NDE methods that can cover large areas at high speed. These methods include: laser induced ultrasonic C-scan, shearography, thermography and the analysis of vibrational response of the structure (or component). The FAST Center developed a vibration analysis technique which takes advantage of the fact that structures have a unique set of resonant frequencies, modal damping ratios, and characteristic mode shapes. These fundamental quantities are unique functions of the mass, stiffness and the damping characteristics of the structure. A change in any one of the latter produces a change in the modal response. In principle, aircraft structures can be monitored periodically to detect changes in their response and the information can be used to detect, locate and quantify defects and material degradation. Traditionally, the vibrational response methods have depended on the determination of the modal parameters via experimental modal analysis, typically using transducer sensors such as accelerometers that are mounted on several points of the structure. Damage detection algorithms based on modal information, however, have exhibited limitations on the resolution of the damage that can be detected. This has been partially attributed to the fact that the damage predictions have been proven sensitive to the limited number of measured points and the uncertainties in the measurements, structural modes, boundary conditions, as well as material and geometric properties.

To overcome the limitations listed above, new methods were developed using neural networks, pattern recognition techniques, damage detection theories, and laser optical sensing instruments. These methods are allowing higher density of measurements, more reliable information, and better techniques to process information from limited number of sensors. This progress is making the vibrational approach more attractive as a potential tool, not only for inspecting large areas but also for on-line evaluation of structural integrity and in-flight damage monitoring. Further, global NDE methods based on the vibrational approach can be used for high speed screening to assess the integrity of large structures. For decision making regarding the reparability or acceptability of the structure integrity, the results can be verified and

determined in details by local type NDE methods. The global NDE techniques investigated in the center were based on the laser Doppler velocimetry, as well as those based on accelerometers accompanied with Artificial Neural Networks and Pattern Recognition techniques to develop damage assessment models with limited information.

1.3 Summary of Technical Projects

Four projects initiated the research activities of the FAST Center. These projects addressed issues on ultrasonic nondestructive evaluation of aircraft, the characterization of structural damage and materials degradation, NDE methods using laser Doppler velocimetry and shearography, global NDE vibrational methods, neural networks and pattern recognition techniques to process NDE data.

1.3.1 Ultrasonic Wave Propagation Methods for Evaluation of Damage to Metallic Structures and Degradation in Composite Materials

The project was directed by Drs. Soheil Nazarian and Joseph H. Pierluissi of UTEP in collaboration with Dr. Yoseph Bar-Cohen of the Jet Propulsion Laboratory (JPL) and Dr. Dale Chimenti of Iowa State University (ISU). Dr. Jorge Lopez from UTEP's Physics department also contributed to the project. A summary of the work accomplished under this project is included in Chapter 3 of this report.

The cracking and corrosion of the metallic components as well as delamination, impact damage and material degradation of composite materials are becoming of great concern as aircraft are aging. UTEP, in collaboration with JPL and ISU, investigated ultrasonic NDE methods to detect and characterize defects and material degradation. The focus was on methods that are reliable, simple to operate and can be practical for use in the field to perform high speed inspection.

The emphasis of this project was on ultrasonic NDE methods since they offer a base of quantitative NDE techniques for detection and characterization of flaws and for the determination of the material stiffness properties. Most practical efforts in ultrasonic NDE had been focused on metallic components. Composites as multi-layered anisotropic media have posed a challenge to the NDE research community for many years and successful results have been reported in several areas.

UTEP, in collaboration with JPL, conducted studies of ultrasonic wave propagation and scattering in metallic and multi-layer structures. The emphasis was towards adapting the spectral analysis of surface waves techniques to the metallic and composite materials. The propagation of symmetrical and anti-symmetrical modes of vibration of elastic waves in plates with or without defects was modeled and studied. Flaws in a generic form representing corrosion and cracks were introduced into the models and studied to predict the responses. Experiments were conducted to verify the theoretical predictions. Efforts were also made to determine the characteristics of detected flaws. Also, the practical travel distance and the number of travel orientations along the plate required to obtain reliable data was studied. Finally, this project in close collaboration with a parallel project in the Center developed algorithms based on Artificial

Neural Networks for identifying potential damages in a given member.

1.3.2 Characterization of Structural Damage and Materials Degradation using analysis on the micro- and macro-scales

This project was directed by Drs. Lawrence E. Murr and Roy Arrowood from UTEP. The majority of their efforts focused on corrosion issues associated with Aluminum aircraft. Very close collaborations existed in this project with the USAF Oklahoma Air Logistic Center and with USAF Wright Patterson Lab. Some of the technical achievements in this project are documented in Chapter 4 of this report.

Background

Incipient damage as a result of chemical/environmental reaction/interaction (e.g., corrosion) or cyclic/static stresses (e.g., fatigue) are critical elements of aircraft structures loss of integrity. To be able to assess the effect of such damage it is important to be able to link the damage at the characteristics at both the micro and macro- scales. In order to examine incipient defects, UTEP used scanning electron microscopy and other state of the art equipment. Tests results were compared with data obtained by destructive tests using scanning electron microscopy, transmission electron microscopy and energy-dispersive X-ray spectrometry. The mechanism of composite materials degradation on the microscopic level will be studied.

In addition, corrosion on metal structures and primary aircraft components was also examined using combinations of approaches outlined above in an effort to identify microstructural features of corrosion and an elucidation of fundamental mechanisms involved. Corrosion is a difficult issue to address using NDE approaches since none to date have been effective in early diagnostic detection. By conducting fundamental studies of corrosion using transmission electron microscopy and scanning electron microscopy it was possible to identify features unique to corrosion at very early stages. Considerable time was spent, of necessity, attempting to document and characterize the most important corrosion issues, especially those more amenable to observation and characterization because the corrosion issues are numerous.

Objectives

The specific objectives of this research component involved the application of observational and analytical tools - transmission and scanning electron microscopy to characterize structural damage and degradation in aircraft materials: corrosion of metal components, erosion and failure of composite materials, and the development of diagnostic, to early detection of damage and degradation. In dealing with these issues, of necessity, the mechanisms involved in the various aspects of degradation and damage were explored. An important initial objective involved the development of a matrix of the most important degradation/damage problems in the most important aircraft materials systems and components.

1.3.3 Modal-based Laser Doppler Velocimetry for large area NDE of aircraft structures

This project was directed by Drs. Osegueda and Ferregut from UTEP, in collaboration with Drs. Norris Stubbs from Texas A&M University, George James, III and Tom Paez from Sandia National Labs, and from Michael Grygier from NASA JSC. The technical accomplishments under this particular project were documented separately by Osegueda and

Ferregut in an accompanying report.

Most commonly used NDE methods for the inspection of aircraft structures are capable of providing detailed information only about a limited region of the structure. The most developed and utilized methods are those based on visual inspection, electromagnetics (i.e. eddy current) and ultrasonics. One major problem faced, however, is the detection of defects in hidden members or members deep inside the aircraft. Although, the above mentioned techniques are effective in detecting cracks and other forms of damage, these require access so that sensors and/or instrumentation be placed at/or near the vicinity of the flaw. For these methods to be effective to detect flaws in hidden or deep structural members, disassembly is almost always mandatory. Disassembly requires grounding of the aircraft for weeks. Thus alternative methods for aircraft inspection, that could reduce the time airplanes are out of service, are desirable. This project dealt with large area inspection of aircraft structures using vibrational nondestructive evaluation techniques

The vibrational NDE methods take advantage of the fact that structures have a unique set of resonant frequencies, modal damping ratios, and characteristic mode shapes. These fundamental quantities are unique functions of the mass, stiffness and the damping characteristics of the structure. A change in any one of the latter produces a change in the modal response. In principle, aircraft structures can be monitored periodically to detect changes in their response and the information can be used to detect, locate and quantify defects and material degradation. Traditionally, vibrational NDE methods have depended on the determination of the modal parameters via experimental modal analysis using transducer sensors such as accelerometers that are mounted on several points of the structure. This poses a limitation on the amount of effort associated with mounting a large number of sensors not withstanding that the mass of the structure is artificially increased. The added mass could be significant when the number of sensors is large. To overcome these limitations laser optical sensing instruments currently exist that allows for a rapid set-up of the required instrumentation required. Furthermore, the laser sensing also allows higher density of measurements without adding extra mass or even contacting the specimen. This technology is making the vibrational approach more attractive as a potential tool for inspecting large areas in aircraft structures.

The vibrational NDE techniques that were investigated primarily relied on measurements obtained with a Laser Doppler Velocimeter (LDV) accompanied with data fusion methodologies to develop damage assessment tools with limited information. The LDV is a device based on the Michelson's interferometer that provides non-contact measurements of dynamic velocity. The LDV used in the investigations has scanning mirrors that allow for the targeting of the laser beam on any point within an area limited by 25° by 25° of mirror rotation. In addition, the LDV is capable of obtaining velocity measurements from objects at a distance of 200-meters, which allows for scanning large structural areas.

The vibrational NDE methods considered are based on modal strain energy differences between the elements of the structure at a damaged and a healthy state. The method uses the strain energy in the structural elements due to modal deformation, and compares them to similar energy quantities for a healthy reference state to obtain indicators of damage as a function of the structure location. The damage severity can be determined from the relative changes in the

modal strain energy. The method, however, requires a mode-pairing process to match the mode shapes of the damaged state to those of the healthy state. The mode-pairing seems to have an effect on the detectability of damage. The differences in the element strain energy due to the deformations of the paired modes then provide features for the detection of damage. Furthermore, the mode pairs may lack sensitivity to detect damage at given locations, especially if the locations have relatively low modal strain energy content. For this reason, damage is usually detected using several pairs of modes. Then the issue is how to best combine the information extracted from individual mode-pairs to make a final determination of the potential damage.

1.3.4 Neural Networks to Evaluate and Identify Types of Damage in Airframe Systems

This project was directed by Dr. Carlos Ferregut and Dr. Roberto A. Osegueda from UTEP, in cooperation with Dr. Tom Paez, Sandia National Labs and Charles Farrar, Los Alamos National Labs. Through the development of this project collaboration with Professor Ajit Mal from UCLA also emerged. The technical accomplishments under this particular project are described in Chapter 6 of this report. Perhaps one of the critical challenges of the research community is to investigate some of the fundamental issues associated with the development of hybrid NDE systems. For some time now, it has been recognized that all single NDE techniques have limitations on sensitivities to the size, type and location of the defects they can detect. No single method currently used is capable to detect all forms of defects. For that reason the development of hybrid systems that combine two or more NDE methods are attractive. Fundamental research issues that are critical here include the processing of the data coming from the systems at real time. Artificial neural networks (ANN) have the potential to provide the needed processing speed and robustness that multiple sensor NDE require. In this project several applications of ANN to process NDE information were attempted.

One of the major elements that is usually ignored in NDE is the post-inspection decision making process. Among the issues that can be identified are the characterization of defects and the determination of their significance on the reliability of the structure. In most cases NDE techniques do not provide quantitative assessments about the integrity and reliability of the damaged structure. Two projects that explored the feasibility of probabilistic methods and fractal theory to assess the effect of pitting corrosion damage are also summarized in Chapter 6.

The objectives of this project were to develop and test alternative methodologies for NDE data processing that: would be (1) computationally faster than traditional methods; (2) more reliable in the detection of the damage, by better processing data which are contaminated with noise or incomplete; (3) more sensitive to detect smaller defects; (4) able to discriminate among types of damage once they are detected; and (5) be able to detect the existence of multiple damages.

1.4 Collaborations

Establishing technical and educational collaborations with other institutions was and is a continuous goal of the FAST Center. Collaborative work enhances our research capacity and

provides educational and developmental activities to our faculty and students. It also provides the venue to network with other researchers who are conducting similar work and the opportunity to obtain constructive criticism from them regarding our research activities.

Over the period covered in this report, researchers at the FAST center have conducted collaborative work with: (a) four universities - Texas A&M University, Iowa State University, New Mexico State University and The University of California at Los Angeles; (b) five federal research laboratories - NASA Jet Propulsion Laboratory, Sandia National Laboratories, Los Alamos National Laboratory, NASA (JSC), US Air Force Research Labs at Wright Patterson AFB and; (c) one company, Boeing. A brief description of the activities conducted with each of our collaborators follows.

Jet Propulsion Laboratory

The main collaborator from the Jet Propulsion Laboratory was Dr. Yoseph Bar-Cohen. Dr Bar-Cohen was very instrumental in providing training and technical expertise associated with Project 1. Dr. Bar-Cohen and co-workers assisted UTEP in developing NDE technology for aging aircraft. Their efforts involved the transfer of technology to establish on-site capability, at UTEP. More specifically, JPL supported UTEP in studying ultrasonic wave propagation in multi-layer structures. The emphasis was on the transfer of JPL technology to study aging aircraft structures made of metallic and composite materials. Also, JPL provided training and assistance to the UTEP team in making the technology transition from civil structures to aerospace structures. In addition, JPL assisted in the development of an algorithm for the evaluation of the global elastic constant of multi-layered composite panels. Furthermore, JPL also assisted in establishing the capabilities of laser-induced ultrasonics.

Texas A&M University

Dr. Norris Stubbs, Professor of Civil Engineering, was our main collaborator at this institution. He worked closely with Dr. Roberto Osegueda in the development of techniques that use pattern recognition methods for processing structural vibrational information for damage detection. One of Dr. Stubbs' students who got involved in this collaborative work while pursuing his Ph.D. degree continues to collaborate with Dr. Osegueda after graduating and becoming a faculty member in the Department of Mechanical Engineering at New Mexico State University. Dr. Stubbs also sponsored Texas A&M University students under FAST sponsorship in topics associated with project three. Summary of his technical contributions are evident from the publications abstracts and theses summaries in the Appendices of this report.

Iowa State University

The collaborative efforts with this university involved Dr. Dale Chimenti, Professor of Aerospace Engineering and Engineering Mechanics. Dr. Chimenti worked with Dr. Nazarian and assisted in the development of the analytical models to characterize ultrasonic wave propagations in thin metallic and composite plates. His collaboration was crucial for the technical work conducted by Eulalio Rodriguez under project 1.

Sandia National Laboratories

Collaborative work with Sandia National Laboratories was conducted with several members of the experimental dynamics group, mainly Dr. Thomas Paez,, Mr. Pat Barney, Dr.

Bruce Hansche and Dr. George James, III. Dr. Paez and Mr. Barney worked with Drs. Roberto Osegueda and Carlos Ferregut in the development of model validation techniques for deterministic and stochastic models using limited experimental data. Drs. Hansche and James collaborated in the development of experimental procedure to use the laser vibrometer as a tool for global nondestructive damage evaluation. Since the beginning of the collaboration in 1995, Sandia's and UTEP's researchers have met regularly. In addition, several students have participated on summer internships at Sandia where they have been supervised by the Sandia Collaborators. Students have worked on various topics ranging from damage detection in a DC-9 fuselage to applications of Artificial Neural Networks techniques to predict the response of nonlinear dynamic systems. Students who participate in internships at Sandia include Jaime Ortiz, Raul Meza, Doug Demming, Jose Gutierrez, Angel Urbina and James Brown. Mr. Urbina's Master's thesis was co-directed by Dr. Paez and Dr. Ferregut. They also co-directed the Master's thesis of Mr. Luis Perez.

Los Alamos National Laboratory

Collaboration with this Lab has been through Mr. Norman Hunter and Dr. Charles Farrar. Mr. Hunter collaborated with Dr. Osegueda, Ferregut and Paez in the development of techniques for model validation. Mr. Hunter also provided a summer internship to Mr. Angel Urbina when he was working on his master's thesis. Dr. Farrar has provided opportunities for our students to participate in the annual summer workshop that he and his team have been putting together for the past four years. Students that have participated in summer internships at Los Alamos include: Debra George, Sergio Castillo, Enrique Roldan and Luis Espino.

New Mexico State University

Dr. Gabriel Garcia, Associate Professor of Mechanical Engineering, conducted collaborative research with Dr. Roberto Osegueda. Dr. Garcia was funded from the FAST program while he was completing his Ph.D. dissertation at Texas A&M University. After graduation he secured a tenure-track line at NMSU. Dr. Garcia's work focused on the application of Auto Regressive Moving Average models to process vibrational information of damaged and undamaged structures for damage detection.

University of California at Los Angeles

Dr. Ajit Mal, Professor of Mechanical and Aerospace Engineering, collaborated with Dr. Carlos Ferregut in the development of probabilistic models to assess pitting corrosion damage in aluminum plates. One of Dr. Ferregut's Master students, Mr. Hugo Pardo spent a summer working with Dr. Mal on corrosion/fracture modeling issues.

AFRL, Wright-Patterson

In the summer of 1998 a team from the FAST Center spent two months in Dayton, Ohio working with researchers from the NDE section of Wright Patterson Lab. UTEP's team was integrated by Dr. Carlos Ferregut, Mr. Arturo Revilla (Ph.D. student) and Ms. Alina Nunez (undergraduate student). The team had close interactions with Mr. Tobey Cordell, Dr. Tom Moran and Mr. Charles Buynak. The team's work focused on NDE data fusion issues and on collecting a data base that could be used to develop and test data fusion models. As a result from the visit a proposal for conducting follow up work was written and subsequently funded. Since Mr. Cordell's retirement, we have been interacting with Ms Claudia Kropas-Hughes.

Captain Don Groner from AF Wright Patterson was instrumental in securing aircraft aluminum parts from KC-135 for the corrosion studies reported in Chapter 4.

Boeing

In the Fall 1998, Dr. Roberto Osegueda teamed with Dr. Michael Mohaghegh from Boeing and Dr. Edward Conley from NMSU to offer a distance learning course on the design of aircraft structures. The course was patterned after a course Boeing offers to their engineers and was simultaneously viewed at UTEP, NMSU and Boeing Seattle. More that 3 dozens of students took the course at the three institutions.

NASA Johson Space Center

Drs. Ferregut, Osegueda and Carrasco have had strong collaborative links with the technical staff of JSC for more than ten years, in particular with Mr. Rodney Rocha, Mr. Mike Grygier and Dr. George James while on leave from Sandia. Several of the research activities of the FAST center used data gathered from NASA's test articles such as a prototype of a vertical stabilizer of the space orbiter. This resulted in the reinforcement of professional links between UTEP's and NASA's staff.

USAF Oklahoma City Air Logistic Center (OC-ALC)

During the early years of the FAST Center, close ties were developed between the Metallurgy faculty, Drs. Roy Arrowood and Larry Murr, and managers of the aging aircraft program at OC-ALC, Mr. Don Nieser, in particular. Several collaborations were realized and resulted in the summer internship of Ms. Leticia Campuzano-Contreras at Tinker Air Force Base. Ms. Campuzano-Contreras worked at the PDM operations of the KC-135 during the summer 1997. Her internship was arranged though Boeing, who is the contractor for the KC-135 PDM program. Her graduate studies were based on the retrogression and reaging of post-service aluminum structural parts. This work described in Chapter 4 of this report.

1.5 Contents of Report

Chapter 2 provides an overview of the educational components associated with the FAST Center. It provides summaries of the students involved, student internships outside UTEP, and an overview of where the students have ended up.

Chapter 3 provides a summary of the technical accomplishments associated with Project 1, dealing with ultrasonic wave propagation methods for evaluation of damage.

Chapter 4 provides a description of the technical work accomplished by the Metallurgical and Materials Engineering faculty and students. Their efforts primarily focused on corrosion issues of aircraft Aluminum and retrofitting post-service aluminum parts.

Chapter 5 is a brief summary of all the work conducted on large area inspection of aircraft structures using vibrational NDE techniques under Project 3. Chapter 5 is a summary of another report already submitted.

Chapter 6 summarizes the work performed under Project 4. Their focus was on performing fundamental research on hybrid systems that combine two or more NDE methods, the use of ANN to provide the needed processing speed and robustness that multiple sensor NDE require. Chapter 6 illustrates several application examples of ANN to process NDE information. Also in this chapter, two projects that explored the feasibility of probabilistic methods and fractal theory to assess the effect of pitting corrosion damage are included. Furthermore, Chapter 6 also summarizes the work conducted to develop a statistical approach to model validation when the data on a system's response is limited.

Appendix A of this report lists all the students that participated in the FAST Center at UTEP together with the abstracts of their dissertations or theses for graduate students, or the way they contributed for the undergraduate students. This appendix also cites the publications which the students authored or co-authored and the latest whereabouts of the former students.

Appendix B lists all the technical publications and abstract that resulted from this grant.

CHAPTER 2

FAST CENTER EDUCATIONAL COMPONENT

2.1 Introduction

In fulfillment of its educational mission the FAST Center has prepared qualified graduate and post-graduate scientists and engineers that are ready to face the technical challenges associated with the aging of the USA Air Force fleet, as well as the challenges associated with the development of the next generation of fighter planes. The center has supported interested graduate and undergraduate students to conduct research at UTEP and at collaborating institutions. The goal has been to have a diversity of students from all the fields of interest to the center and all academic levels. The center has also tried to have a diversified pool of students mimicking UTEP students' demography. In particular the center has encouraged the involvement of female, Hispanic and other minority students. Our success is reflected by the more than 70 students that have been part of this program.

2.2 Summary of Students Involved

A total of 73 different students were supported by the FAST Center. Seven students were supported at the doctoral level, 42 at the Masters level, and 24 at the Bachelor's level. The number of undergraduate students only refers to those who were supported by the FAST program and did not continue for graduate school. The degrees earned by all students supported by the center include: 6 Ph.D., 31 Masters of Science and 15 Bachelors of Science degrees. Fifty percent of students who obtained a BS degree under FAST sponsorship have continued for Masters Studies. Also, 75% of the Masters students obtained their BS degrees from UTEP.

Seventy five percent of students supported are from the El Paso region. 61% are Hispanic or members of other minorities and 18% are international students.

A summary of the students involved follows. More information about their technical work while at the FAST Center can be found in Appendix A of this report. This appendix lists abstracts of the students' dissertations and theses for the graduate students, and describes the participation efforts of the undergraduate students.

Ph.D. students

Out of the seven doctoral students supported by the FAST Center four of them pursued their Ph.D. work at UTEP, two of them at Texas A & M University and one received her doctoral degree at the University of Mexico. One student is currently pursuing a Ph.D. degree at UTEP. The following is the list of Ph.D. students supported since 1995.

Dr. Eulalio Rodríguez
Doctor of Philosophy
Electrical and Computer Engineering, UTEP

Date: December 1998
Dissertation Title: Non-Destructive Determination of Elasticity Constants of Composite Plates by the Acousto-Ultrasonic Method
Supervisors: Drs. Joseph Pierluissi and Soheil Nazarian

Dr. Gabriel Garcia
Doctor of Philosophy
Mechanical Engineering, Texas A&M University
Date: August 1996
Dissertation Title: Evaluation of relative performance of classification algorithms for nondestructive damage detection
Supervisor: Dr. Norris Stubbs

Dr. Cesar Carrasco
Doctor of Philosophy
Materials Science and Engineering, UTEP
Date: July 2000
Dissertation Title: Development of a Constitutive Microdamage Model for Simulation of Damage and Fracture of Metallic Plates Caused by Hypervelocity Impact
Supervisors: Drs. John Eftis and Roberto Osegueda

Dr. Arturo Revilla
Doctor of Philosophy
Electrical and Computer Engineering, UTEP
Date: December 2000
Dissertation Title: Predicting Probe Impedance Change in Eddy Current Nondestructive Testing Using Finite Elements
Supervisor: Dr. Joseph Pierluissi

Dr. Maria Estela Calixto
Chemistry
Universidad Nacional Autonoma de México, UNAM
(National Autonomous University of Mexico)
June 2001
Dissertation Title: Characterization of Formation and Growth Mechanisms of Electro-Deposited $CuInSe_2$ Thin Films and their Applications to Solar Cells
Supervisors: Dr. Sebastian P. Joseph (UNAM) and Dr. John McClure (UTEP)

Dr. Sanghyun Choi
Doctor of Philosophy
Civil Engineering, Texas A&M University
Date: December 1999
Dissertation Title: Improved Performance of Damage Localization and Severity Estimation via Combining Multiple Damage Algorithms
Supervisor: Dr. Norris Stubbs

Fariba Ansari
MS in Physics
Ph.D. Candidate
Materials Science and Engineering
Expected Graduation Date: December 2002
Tentative Dissertation Title: Determination of Composite Materials Properties using Lamb-Waves

Masters Students

The Master's students supported have earned degrees in Civil Engineering (16), Mechanical Engineering (2), Metallurgical and Materials Engineering (6), Computer Science (2), Electrical and Computer Engineering (2) and Physics (2). Currently the center is supporting six Master's students. Five students were supported but left the program. Students that were also supported by the center while pursuing their Bachelor of Science degrees are identified with an asterisk. The following is the list of Master's students supported since 1995. Description of their work at the FAST center can be found in Appendix A.

Graduated
Raul Meza
*Luis Pérez, MSCE
David Doran, MSCE
Miguel Castro, MS Physics
Batu Batu, MS Physics
*Maria Posada, MSMME
*Cesar Tirado, MSCE
Gabriela Andre, MSCE
Angel Urbina, MSCE
Charles Miller, MS ME (TAMU)
Leopoldo Pereyra, MS CE
Ana Leticia Campuzano, MSMME
Walter Alvarez, MSCE
*Haydy Obispo, MSMME
Ravi Venugopalan, MS ECE
Murali Krishna, MS CS
Helder López, MSCE
Sudhir Prabhu, MS ME
Robert Cervantes, MS MME
*Mario Perez, MSCE
Miguel Orozco, MSCE
Moisés Macias, MSCE
*Hugo Pardo, MSCE
*Sergio Castillo, MSCE
*Francisco De Villa, MSCE
Daryl Little, MS MME (Univ. of Virginia)
*David Roberson, MS MME
*Benjamin Lopez, MSCE
Ulas Toros, MSCE
Manuel Celaya, MSCE
Victor Noriega, MS EE

Current MS Students
Rama Garigipati
Gabriel Carrera
Mohamed Khathib
*Enrique Roldan
*Jose Rodrigo Mares
Rama Karnati

Graduate Students who transferred out of UTEP
Ana Cristina Holguin
Siria Espino, MS CE
David Meza, MSCE
Xiafang Mu, MS ECE
Tony Prado

Undergraduate Students

Involvement of undergraduate students in research activities has become a tradition at UTEP. The FAST center has strived to attract undergraduate students interested on the center's activities. Since 1995, the FAST center has supported 24 students to work with faculty in the various research activities. The following is the list of students that have been supported by the center (The list does not include those students in the previous list that were supported while pursuing their bachelor degree nor the six students that were supported but left the program.)

Graduated
James Brown, Senior BSME
AdrianEnriquez, BSCE
Daniela Martinez, BS MME
Bryan Harms, BSCE
Adolfo Aguilera, BSME
Jose Gutierrez, BS ECE
Doug Deming, BS ECE
Scott Minke, BS Aero Eng. (TAMU)
Oscar Moguel, ME
Alina Nunez, ME
John Feighery, ME
Miguel Kanakoqui, ME
Patrick Dickerson, MME
Claudia Hunter CE
William Torres CE

Current students
Jessica Corral, MME
Jose Gabriela Mares, CE
Vanol Francois, ME

2.3 Summary of Internships

Internships give students the opportunity to complement their education and enhance their experience while working away from UTEP's campus. During an internship a student has the chance to work on technical problems of their interest and which are also closely related to the FAST center mission. Internships also provide a means for students to be exposed to other points of view about the research they conduct at the center and allow them to start a technical support network by interacting with researchers and students from other institutions. To date 19 students have obtained internships at several federal government laboratories and universities. A list with the names of students and laboratories that provided the internship follows.

Cesar Carrasco, NASA JSC (Summers of 95 & 97), conducted control damage modal tests on a model of a space station truss and on a prototype of the vertical stabilizer assembly of the space shuttle. His work at NASA was supervised by Mr. Rodney Rocha and Mr. Mike Grygier.

Raul Meza, SNL (Summer 96), conducted Modal Tests on composite panels and on the fuselage of a DC-9 aircraft airplane. His work at Sandia was supervised by Dr. George James, III.

Angel Urbina, Los Alamos (Fall 97), conducted work on nonlinear dynamic supervised by Mr. Norman Hunter. Sandia National Labs (Sum. 98 and Fall 98), performed work on the prediction of nonlinear vibrations using artificial neural networks. His work was supervised by Dr. Thomas Paez

Ana Leticia Campuzano, Oklahoma City Air Logistic Center & Boeing (Summer 97), worked at Tinker Air Force Base in the PDM program of the KC-135. She was supervised by Don Nieser. She familiarized herself with the KC-135 corrosion issues. Her thesis topic was a spin-off of her work at Tinker.

Gabriela Andre, NASA JSC (Summer 97), was a member of the team that performed modal tests of the vertical stabilizer assembly of the Space Shuttle.

David Meza, NASA JSC (Summer 95), was a member of the team that performed modal tests of a model of the space station.

James Brown, SNL (Summer 96), worked on Laser Velocimetry supervised by Dr. Bruce Hansche. While at Sandia, he developed algorithms to register the laser Velocimeter.

Bryan Harms, NASA JSC (Summer 95), member of team that performed control damage tests of a prototype truss for the space station.

Jose Gutierrez, SNL (Summmers 96 & 97), worked on the development of Artificial Neural Networks for predicting the behavior of nonlinear stochastic systems. His work at Sandia was supervised by Dr. Tom Paez.

Daryl Little, NIST (Summer 97), worked under the supervision of Dr. Richard Rickard performing corrosion tests.

Debra Lee Goerge, NASA Langley (Summer 97), worked in the Langley's NDE group supervised by Dr. William Winfree. Los Alamos Labs (Summer 98), worked on nonlinear dynamics problems supervised by Mr. Norman Hunter.

John Feighery, NASA JSC (Spring and Summer 97).

Alina Nunez, WPAFB (Summer 98), work in the computer tomography laboratory and the NDE section. Her work was supervised by Dr. Tom Moran.

Arturo Revilla, WPAFB (Summer 98), conducted ultrasonic and eddy current tests of composite structures. He was supervised by Mr. Tobey Cordell and Dr. Tom Moran.

Hugo Pardo, UCLA (Summer 98), developed FE models of crack initiation on corroded aluminum panels. His worked was supervised by Dr. Ajit Mal.

Ana Cristina Holguin, Univ. of Wisconsin, Madison (Summer 2000), performed research in the Mechanical Engineering Department analyzing dynamic images to study flow problems.

Sergio Castillo, Los Alamos (Summer 2000), participated in the summer dynamics workshop organized by Dr. Charles Farrar.

Enrique Roldan, Los Alamos (Summer 2000), participated in the summer dynamics workshop organized by Dr. Charles Farrar.

Miguel Orozco, NASA JSC (Summer 2000), collected archived data dealing with hypervelocity impact test targets

2.4 FAST Alumni Update

The FAST Center makes an effort to maintain contact with the majority of the students that have gone trough the program. This allows us to assess if our mission and goals are being achieved, and provide us with the valuable feed back from our former students once they move to industry or academia.

Three of the six doctoral graduates now hold tenure track positions in academia. Dr. Gabe Garcia is currently an Associate Professor of Mechanical Engineering at New Mexico State University. Dr. Cesar Carrasco has been an Assistant Professor of Civil Engineering at UTEP since September of 2000. Dr. Sanghyun Choi is an Assistant Professor in the College of Architecture at Texas A&M. Two of the doctoral graduates hold DoD-related positions. Dr. Arturo Revilla is a Computer Engineer with the Survivability/Lethality Analysis Directorate of the U.S. Army Research Laboratory at White Sands Missile Range. Dr. Eulalio Rodriguez is an Army contractor at Fort Bliss, El Paso, Radar and Electronic Countermeasures analysis. Dr.. Maria Estela Calixto has joined her husband at U.C. Berkeley where he is pursuing a Ph.D. degree.

The center has supported 32 master's graduates who are currently conducting the following activities: six are pursuing Ph.D. degrees at other universities; four are employed at government Labs; 14 work at private engineering firms, three are at electronics/software companies, one works for an oil company, and one is a high school teacher. Six of these students live in El Paso/Ciudad Juarez region.

Of the 15 BS graduates, who did not continue their studies at UTEP, six are employed in government or government contractor companies (e.g. Boeing, Raytheon, NASA, Sandia and Lockheed), four work for oil companies, three work at private engineering firms and two work at a State Department of Transportation. All graduates live outside El Paso.

Appendix A gives more detail about the current affiliation of all graduates.

CHAPTER 3

RESEARCH IN ULTRASONIC WAVE PROPAGATION METHODS FOR EVALUATION OF DAMAGE TO METALLIC STRUCTURES AND DEGRADATION IN COMPOSITE MATERIALS

3.1 Introduction

This chapter presents a technical summary of the research performed at the FAST Center under Project 1. The work described here was supervised by Dr. Nazarian of Civil Engineering, Dr. Pierluissi of Electrical Engineering and Dr. Lopez from Physics. Dr Yoseph Bar-Cohen from JPL and Dr. Dale Chimenti of ISU collaborated in this project and provided technical assistance in the experimental and analytical aspects of the research.

3.2 Non-Destructive Determination of Elasticity Constants of Composite Plates by the Acousto-Ultrasonic Method

The objective of the research performed by Rodriguez (1998) was to characterize thin homogeneous plates by using ultrasonic plate waves generated by piezoelectric transducers in direct contact with the plate. In this study, the characterization of a material consists of the estimation of its elasticity constants from ultrasonic wave velocity measurements. Aluminum and unidirectional graphite-epoxy composite plates were considered. Rodriguez performed an extensive literature review on the application of ultrasonic wave propagation to the nondestructive testing of plate like materials and on the inverse problem to determine the elasticity constants from experimental wave phase velocity and frequency measurements. This review can be found in Chapter 1 of his thesis (Rodriguez, 1998). He found that most of the methods described in this literature survey, required a laboratory-type set up to obtain the measurements, as well as specialized personnel to operate it. The methods that do not required immersion coupling, however, required special test specimens. He also concluded that the available techniques can not be applied for in situ characterization of plate-like structures. He presented a method suitable for field-testing to estimate experimentally the elasticity constants of homogeneous isotropic and anisotropic plates.

3.2.1 Measurements of Phase Velocity

A simple, fast and nondestructive system for measuring the elasticity constants of thin isotropic and anisotropic plates using ultrasonic plate waves was developed. This technique may be applied for in situ characterization of plate-like structures; that is, it is suitable for field testing. The measuring system is also easy to operate using a computer to control the equipment set up and data acquisition. The proposed method has an advantage over other methods that does not require an immersion coupling and that measures the phase velocity of the plate waves directly in real-time. The elasticity constants are estimated from experimental phase velocity data using a computerized inversion procedure. The procedure is performed automatically by a

computer interfaced to additional equipment to acquire data at desired frequencies. The experiments may be typically performed in the range of frequencies from 100 KHz to 1 MHz, where only the fundamental modes contain appreciable energy. In this section, a frequency domain method based on spectral analysis is presented to estimate the phase velocity and dispersion curves of a guided wave propagating in the lowest symmetric mode.

The method requires the determination of travel times in the frequency domain. First it is assumed that a wave moving in the positive x-direction in a non-attenuating medium is represented as

$$u(x,t) = \exp[j(\omega t - kx)] \tag{3.1}$$

where k is the wavenumber and ω is the circular frequency. In a dispersive medium k is a function of the frequency of excitation $k(\omega)$. When a wave propagates through a material and two transducers, separated a distance D, are used to receive the signals, the Fourier transforms of the waves at the second transducer is given by:

$$U(\omega) = U_o(\omega)\exp[jk(\omega)D] \tag{3.2}$$

where $U_o(\omega)$ is the Fourier transform of the first transducer signal. In polar form, $U_o(\omega)$ and $U(\omega)$ are expressed as:

$$U_o(\omega) = |U_o(\omega)|\exp(j\phi_o) \tag{3.3}$$

$$U(\omega) = |U_o(\omega)|\exp\{j[\phi_o + kD]\} \tag{3.4}$$

Where $\phi(\omega) = \phi_o + kD$ is the phase spectrum of the wave at the second transducer. The phase spectrum $\phi(\omega)$ can be measured experimentally, and the phase velocity can be obtained from the expression:

$$V_{ph}(\omega) = \frac{\omega}{k} = \frac{\omega D}{\phi(\omega) - \phi_o} \tag{3.5}$$

The cross spectrum between two time signals x(t) and y(t) may be defined as

$$S(\omega) = X^*(\omega)\cdot Y(\omega) \tag{3.6}$$

where X(ω) and Y(ω) are the Fourier transforms of x(t) and y(t), respectively. The cross-spectrum can be represented in polar notation as follows:

$$S(\omega) = |S(\omega)|e^{-j\theta(\omega)} \tag{3.7}$$

where $\theta(\omega)$ is the continuous (not cyclical) phase cross spectrum and $|S(\omega)|$ is the amplitude cross-spectrum. The time the wave takes to travel a distance D and the propagation velocity as a function of frequency are calculated from the continuous phase cross spectrum as

$$\tau(\omega) = \theta(\omega)/\omega \tag{3.8}$$

$$V_{ph} = D/\tau \tag{3.9}$$

or

$$V_{ph}(\omega) = \omega D/\theta(\omega) \tag{3.10}$$

Since Equation 3.10 is similar to Equation 3.5, the phase cross spectrum may be used to obtain the dispersion relation. The time t for a wave traveling at a given frequency to travel between two transducers separated a distance D is given by

$$t(\omega) = \frac{D}{V_{ph}(\omega)} \tag{3.11}$$

where $V_{ph}(\omega)$ is the phase velocity given by the theoretical dispersion curve. A theoretical phase spectrum is calculated by multiplying the time t of Equation 3.11 by the radial frequency ω to obtain

$$\phi(\omega) = \omega t = \frac{\omega D}{V_{ph}(\omega)} \tag{3.12}$$

The purpose of this process is to display the measured phase spectra $\theta(\omega)$ and the theoretical phase spectra $\phi(\omega)$ simultaneously, and to perform a visual fitting of the theoretical spectra to the measured spectra. The measured phase spectrum $\theta(\omega)$ is function of the phase velocity of the wave in the plate and of the distance between receivers; therefore it remains fixed. However, the theoretical phase spectrum $\phi(\omega)$ is function of the phase velocity given by the theoretical dispersion curve and of the distance between receivers. Hence, the theoretical phase spectrum may be adjusted to fit the measured phase spectrum by changing the theoretical dispersion curve. Once the phase spectra overlap, the modified theoretical dispersion curve corresponds to the "true" dispersion curve of the plate under test. Since the theoretical curve is a function of the elastic constants, then the constants of the material can be indirectly measured.

3.2.2 Phase Velocity Measurement Process

A block diagram of the complete process is shown in Figure 3.1. In the first step of the process, a fast Fourier algorithm is employed to calculate the cross power spectrum between the time signals representing the Lamb wave at two points. Based on the peak amplitude of the spectrum , the frequency range that contains strong Lamb wave energy is determined based on a threshold amplitude. The threshold is usually set to about 10 decibels below the peak. The range of frequencies, where the wave power level is at least 30 dB above the noise level is the usable frequency range. The usable range of the phase spectrum remains stable and free of noise as shown in Figure 3.2. This range of phase spectrum is defined as $\theta(\omega)$.

Numerical models are used to calculate the theoretical dispersion curve using typical parameters for the plate under test. The density and thickness must be measured accurately. This theoretical dispersion curve is converted to a theoretical phase spectrum using Equation 3.12. This is necessary since the phase cross spectrum as calculated by a fast Fourier transform algorithm also varies cyclically from $-\pi$ to $+\pi$. The basis of the measurement method to obtain a theoretical phase spectrum that is very similar to the measured phase spectrum within the usable range of frequencies. It is assumed that the phase spectrum in the frequency range below the usable range varies linearly with frequency at the same rate as the spectrum within the usable range. This assumption is supported by the fact that the phase velocity of the So mode remains constant in the low frequency range. Once the two phase spectra are very close within the usable range, the dispersion curve is calculated using Equation 5.16, with $\theta(\omega)$ being equal to the theoretical phase spectrum.

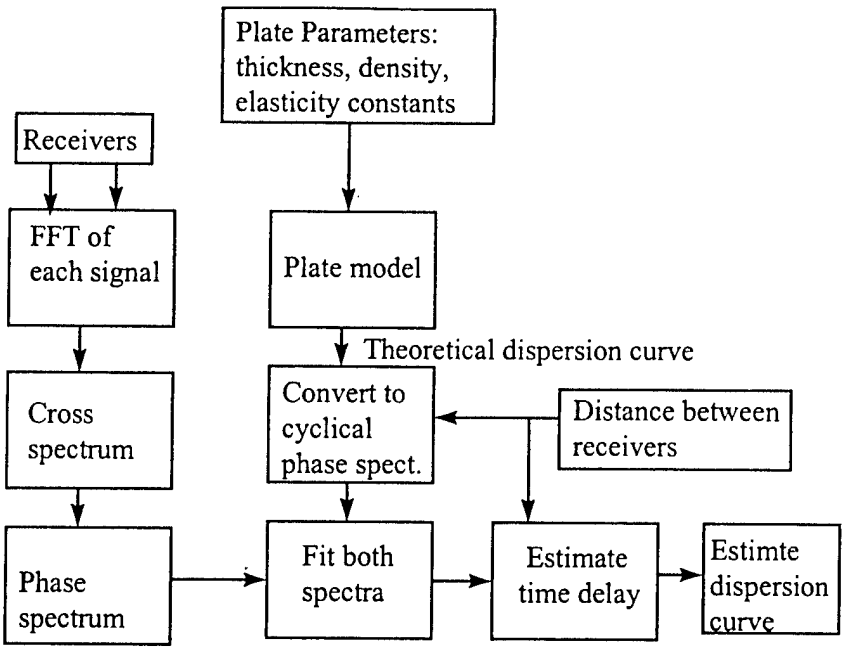

Figure 3.1 Block diagram of the procedure to obtain a dispersion curve

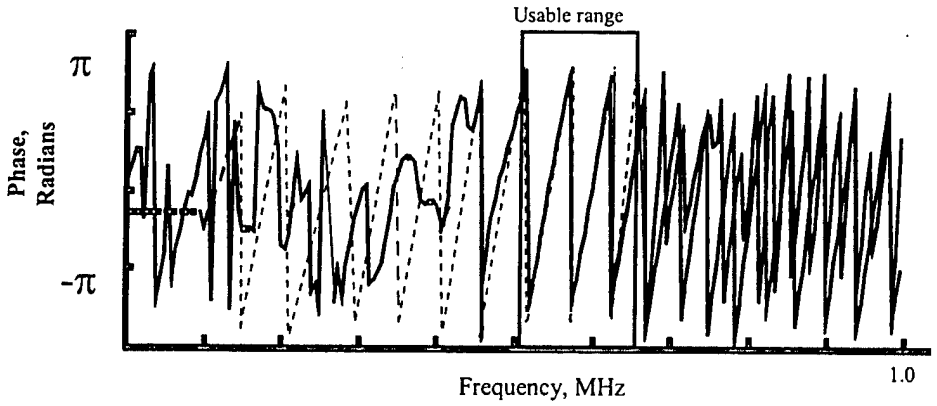

Figure 3.2 Measured and theoretical phase (--) cross spectra.

3.2.3 Experimental Aspects of Testing

A schematic diagram of the experimental setup for making phase velocity measurements is shown in Figure 3.3. The essential equipment required to measure the phase velocity of Lamb waves includes a two-channel digitizing oscilloscope or an A/D card; an arbitrary function generator; two wideband receivers and a transmitter adaptable to a Plexiglas variable-angle wedge. Figure 3.4 shows the experimental test setup. The arbitrary function generator is programmed to generate several cycles of a sine burst modulated with a Blackman window. The burst is generated every 10 ms (100 Hz repetition rate). This special excitation function has a narrow band spectrum at a selected center frequency, and together with a proper angle of incidence, a Lamb wave propagating in the fundamental symmetrical mode, S_0, is excited in the plate.

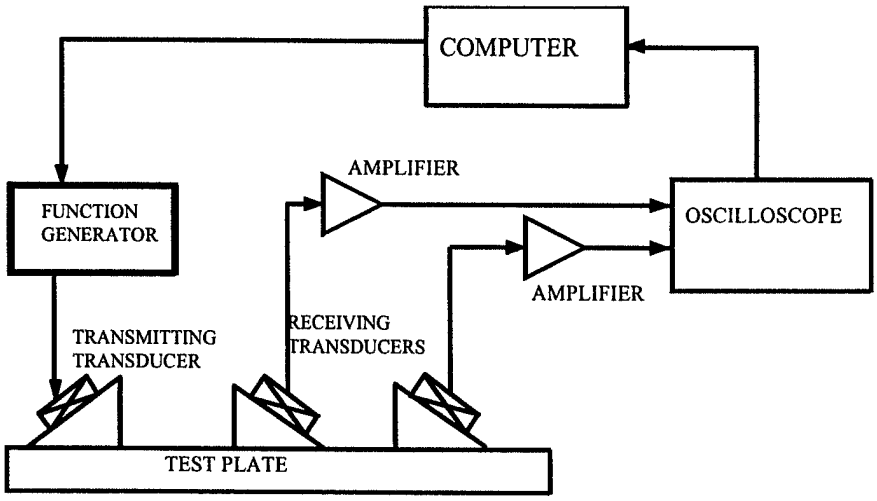

Figure 3.3 Block diagram of the experimental setup for making phase velocity measurements

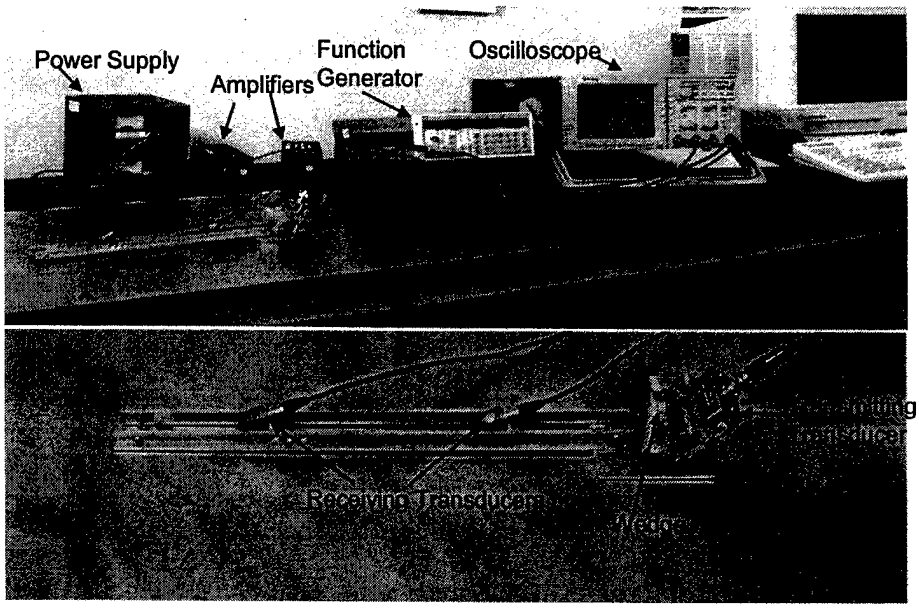

Figure 3.4 Experimental setup for making phase velocity measurements

The operation of the experimental apparatus is controlled by a Virtual Instrument using the LabView software. The LabView program consists of a main module which calls several submodules in sequence. The first module acquires the wave data from the oscilloscope and selects the section of the waves with a time window. The next module calculates the FFT transforms and selects the usable range of the spectrum. The next module reads the theoretical dispersion curve and transforms it to a cyclical phase spectrum. The main module displays the phase spectra, and calculates and displays the dispersion curves. When the frequency of the function generator needs to be changed, a virtual instrument is used to program the function generator with the desired frequency, amplitude, and number of cycles. Figure 3.5 shows the

control settings of the virtual instrument front panel to obtain the initial segment of the dispersion curve of an aluminum plate. The Virtual Instrument automatically performs all the steps required to measure the phase velocity as a function of the frequency, from which the dispersion curve of the plate was obtained. Using the dispersion curve as input to an inversion algorithm, the elasticity constants of plate materials are calculated.

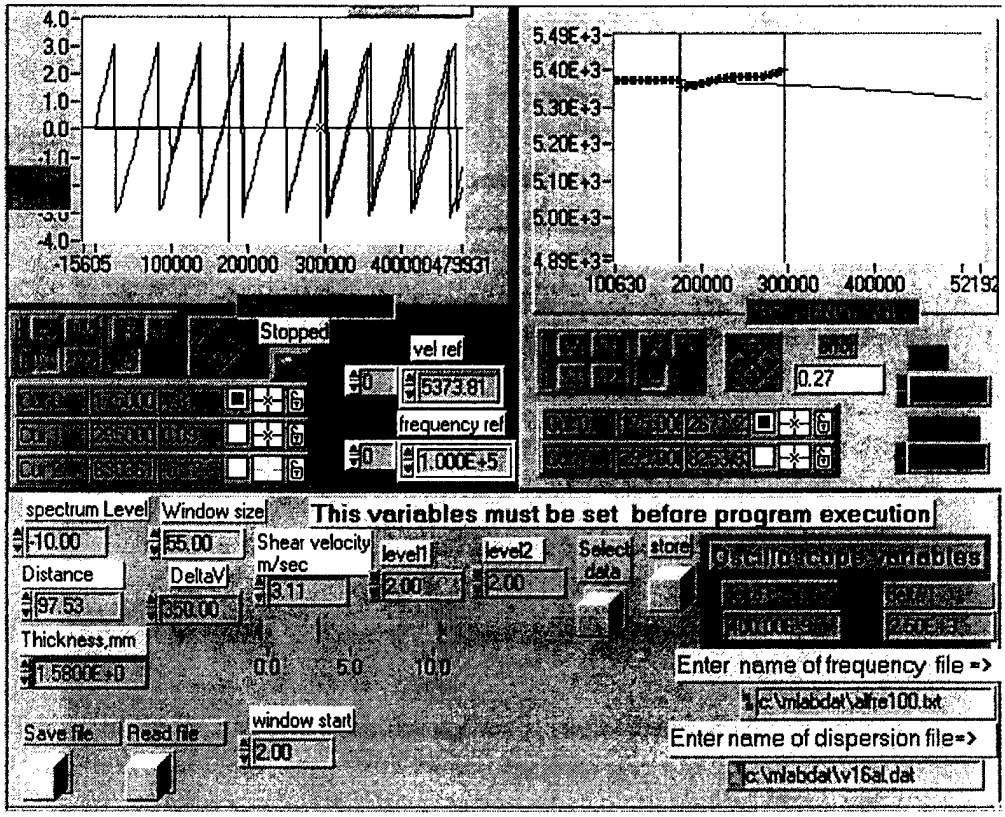

Figure 3.5 Computer screen of the virtual instrument

3.2.4 Determination of Elastic Constants of Composite Plates

The problem of determining the stiffness constants from phase velocity data was divided into three major areas: the forward modeling, the experimental system, and the inverse process. Numerical solutions were developed for the forward model and the inverse process based on an orthotropic model of the unidirectional graphite-epoxy composite plate. It was shown that a model for propagation along the fibers included the constants C_{11}, C_{33}, C_{13}, and C_{55}. The model for propagation in a direction perpendicular to the fibers included the constants C_{22}, C_{33}, C_{23}, and C_{44}. It was possible to estimate from phase velocity data of a wave propagating in the plane x-z (parallel to the fibers) the constants C_{11} and C_{33}, but the constants C_{13} and C_{55} had to be assumed. However, the values of these constants may be adjusted by observing how well a theoretical dispersion curve calculated with those constants fits the measured dispersion curve. If the fit was not acceptable, the inversion algorithm is executed with different values of C_{13} and C_{55} until a satisfactory fit was obtained. An RMS error of less than 1% was typically achieved. For propagation perpendicular to the fibers it was possible to estimate the constants C_{22} and C_{33}. The constants C_{44} and C_{23} were assumed as the typical values for the kind of composite under test.

The algorithm fits a theoretical dispersion curve to the measured data up the highest frequency data point by varying the parameters C_{22} and C_{33}, while keeping all other parameters constant. In this section the application of the spectral analysis method, discussed in the previous section, to measure phase velocity of a Lamb wave in a unidirectional composite plate and to estimate the elasticity constants are described.

The tests involved a specimen of a unidirectional graphite-epoxy plate, supplied by Jet Propulsion Laboratories (JPL). The 30-cm square plate was 1.2 mm thick. Phase velocity measurements on this specimen were made at JPL by the immersion method (Bar-Cohen et al, 1993) using an effective frequency range from 4.13 MHz to 8.13 MHz. They applied an inversion algorithm based on the simplex method to estimate the elasticity constants (Karim et al, 1990). Based on a sensitivity study, for the frequency range used in those experiments, the constants C_{22} and C_{23} greatly impact the shape of the dispersion curve. The constants reported for the plate are shown in Table 3.1.

Table 3.1 Constants of a Unidirectional Graphite-Epoxy Composite Plate Reported by JPL.

Stiffness Constant	C_{11}	C_{12}	**C_{22}**	**C_{23}**	C_{55}	C_{13}	C_{33}
Measured Value (GPa)	166.4	7.1	**16.8**	**7.5**	7.8	$7.1^{(1)}$	$16.8^{(1)}$

(1) Assuming $C_{33}=C_{22}$, $C_{13}=C_{12}$.

Several researchers have measured the elasticity constants of unidirectional graphite-epoxy composites (see Table 3.2) by methods involving leaky Lamb waves, bulk wave velocities measurements, and reflection coefficients.

The phase velocity of Lamb waves as a function of frequency in the composite specimen was measured. Lamb waves were established between 200 kHz and 1.2 MHz for propagation in fiber direction and between 200 kHz and 600 kHz for propagation perpendicular to the fibers. The composite plate tested highly attenuated the elastic wave energy. By means of the "Virtual Instrument" the dispersion curves in Figure 3.6 and 3.7 were obtained for the symmetric So mode propagating in the fibers direction and perpendicular to the fibers, respectively. The figures also show the theoretical dispersion curves calculated with the constants estimated at JPL. The phase velocity given by the JPL constants is 13% higher in the fiber direction, and 8.5% in the direction perpendicular to the fibers.

Table 3.2 Reference Measurements of Elasticity Constants of Unidirectional Graphite-Epoxy Composites. (Units are in GPa)

Reference	C11	C22	C33	C12	C13	C23	C44	C55	C66
Karim and Mal. (1990)	160.7	13.9		6.4		6.9		7.1	
Hosten and Castings (1993)	121	13.5		6.6		7.1	3.2	5.7	5.7
Rokhlin and Wang (1991)	162	17			11.8	8.2	4.4		8
Mal, et al (1993)	161	14		4.5		7.4		4.5	
Wu and Ho (1990)	142.4	14.6	15.5	7.5	7.5	7.3	4	6.4	6.4
Bar-Cohen, et al (1993)	166	16.1		7.1		7.5		7.8	
Rokhlin and Chimenti (90)	133	12.9	15.9	3.7	1.8	5.5	4.2	8.6	7.5
Mal, et al (1993)	161.8	13.9		6.5		6.9			7.1
Hsu, and Margetan (1992)	128.2	14.9		6.9	6.9	7.3	3.8	6.7	6.7
JPL Measurements	166.4	16.8		7.1		7.5		7.8	
This study	131.6	20.7	17.3	16.1	12.2	12.2	5.6	7.8	

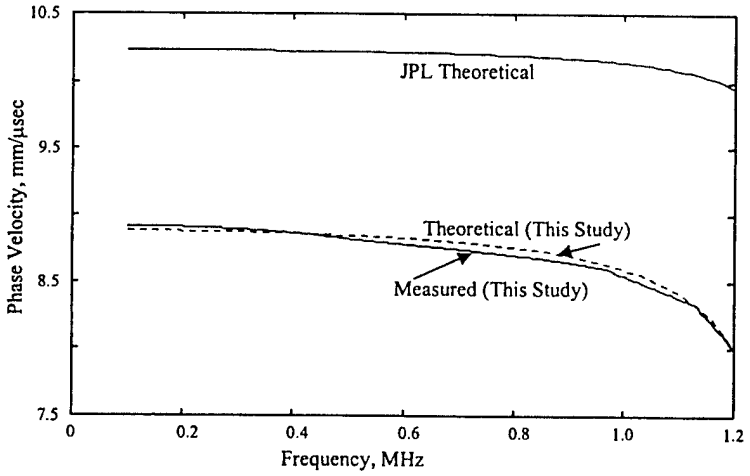

Figure 3.6 Measured and fitted dispersion curves for a unidirectional carbon- epoxy composite for propagation along the fiber direction. The measured constants are C_{11}=131.6 GPa, C_{33}=17.3 GPa, C_{55}=11.8 GPa, C_{13}=12.2 GPa.

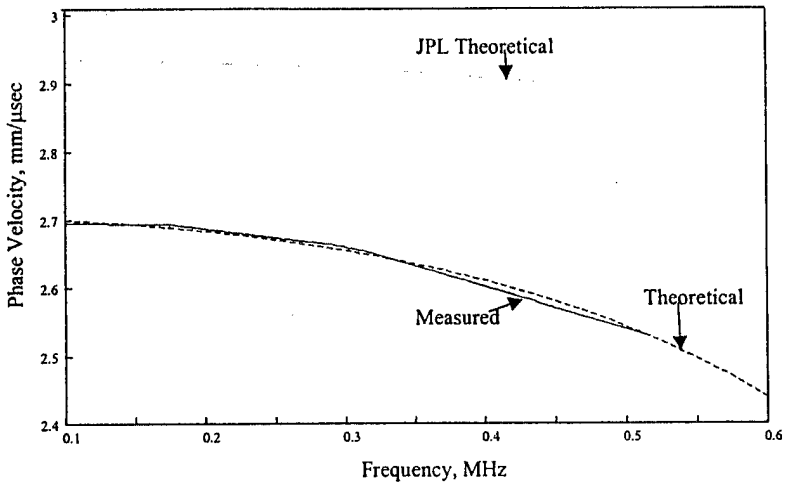

Figure 3.7 Measured (solid) and fitted (--) dispersion curves for propagation perpendicular to the fibers in a carbon-epoxy unidirectional composite. C_{22}= 20.7 GPa, C_{33}=16.1 GPa, C_{23} =12.2 GPa, C_{44}=5.6 GPa.

The inversion algorithm was executed to find iteratively a vector of constants, which minimizes the difference between the theoretical and measured data. Initial vectors of velocities and elasticity constants were input to the inversion algorithm before execution. The results of the inversion process are summarized in Table 3.3. Parameter C_{22} is approximately the same as C_{33}, which is consistent with the fact that the unidirectional plate may be considered as transversely isotropic.

Table 3.3 Elasticity Constants of a Unidirectional Composite Plate Estimated in this Study by the Spectral Analysis Method

C_{11}	C_{22}	C_{33}	C_{13}	C_{23}	C_{44}	C_{55}
131.6	20.7	17.3(1) 16.1(2)	12.2(3)	11.0(3)	5.6(3)	7.8(3)

(1) Value estimated from propagation in the fiber direction.
(2) Value estimated from propagations perpendicular to the fibers.
(3) Fixed values assigned to this parameter since low frequency dispersion curves are not sensitive to this constant

A two-dimensional simulation of wave propagation using the Dyna2D finite element program was performed simulating the experiments on the composite plate. The time histories of simulated waves in a composite plate are shown in Figure 3.8 for the different frequencies of excitation. The composite plate elastic parameters identified in the inversion procedure of Table 3.3 were used in the simulation. Figure 3.9 shows the experimental dispersion curves of a wave propagating along the fibers together with those obtained using the theoretical solution and determined by the finite element simulation with parameters obtained from the measurements. The three curves fit within 1% up to a frequency of about 1.2 MHz. Figure 3.10 shows the simulated, experimental and theoretical dispersion curve of a wave propagating perpendicularly

to the fibers in the same sample composite plate. The three curves agree to within 1% up to 600 KHz.

In this section the elasticity constants of a graphite-epoxy composite plate were measured using spectral analysis and an experimental system that obtains the dispersion curve of the lowest symmetric Lamb waves propagating along the principal directions of the composite plate. The maximum frequency at which a wave can still be detected in the composite is 600 KHz for propagation perpendicular to the fibers and 1.2 MHz for propagation along the fibers. Above these frequencies, signal to noise ratio is very small and no consistent spectra can be obtained. However, the inversion process worked satisfactorily with the portion of the dispersion curves measured by the experimental system. The results of the finite elements simulation of Lamb wave propagation in thin plates agreed to within 1% of the theoretical phase velocities and the elasticity constants.

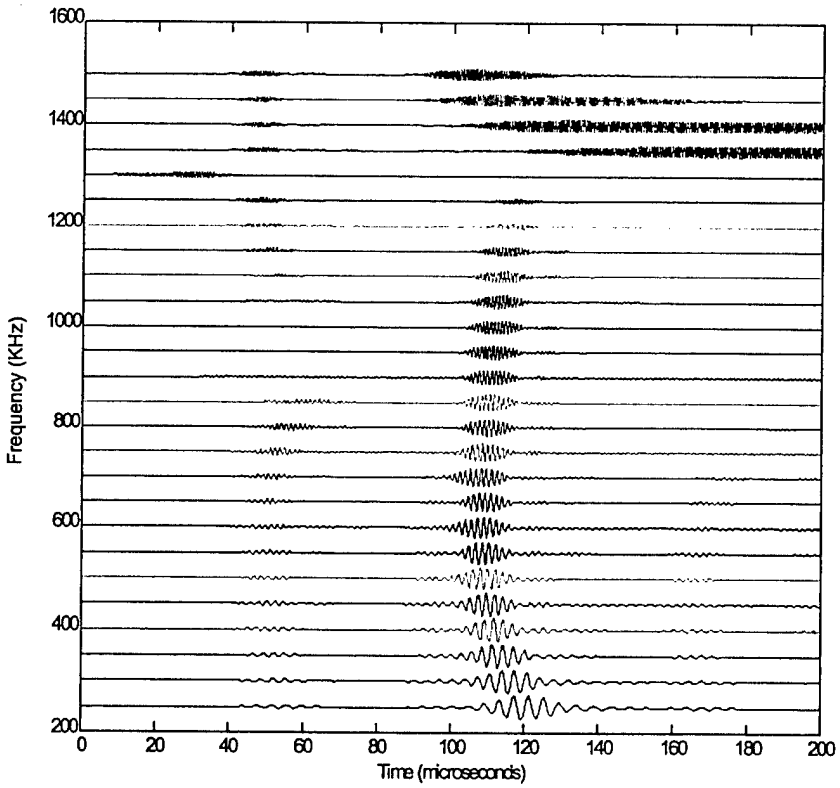

Figure 3.8 Time histories of simulated plate waves in a unidirectional composite with parameters obtained from phase velocity measurements. The simulation direction is along the fibers.

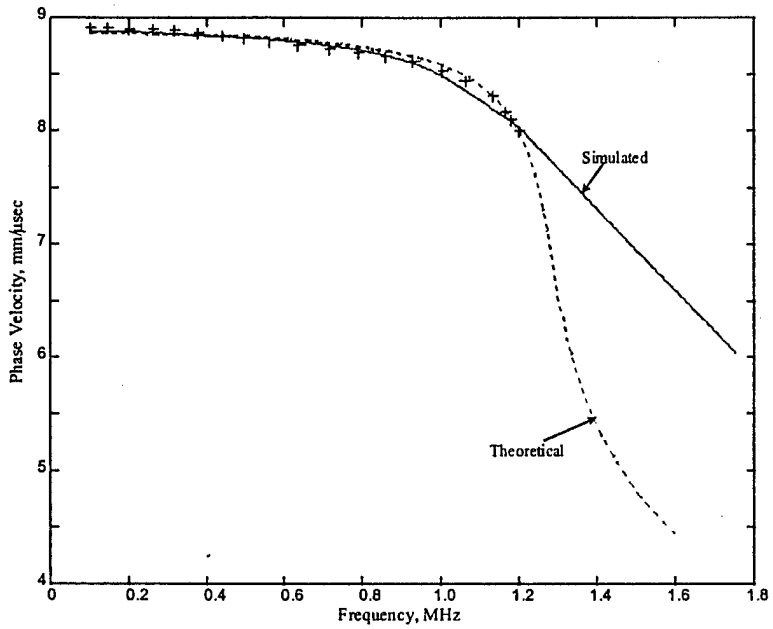

Figure 3.9 Experimental (+), theoretical (---) and simulated (solid) dispersion curves for an epoxy-graphite composite, 1.2 mm thick, for propagation in the fiber direction.

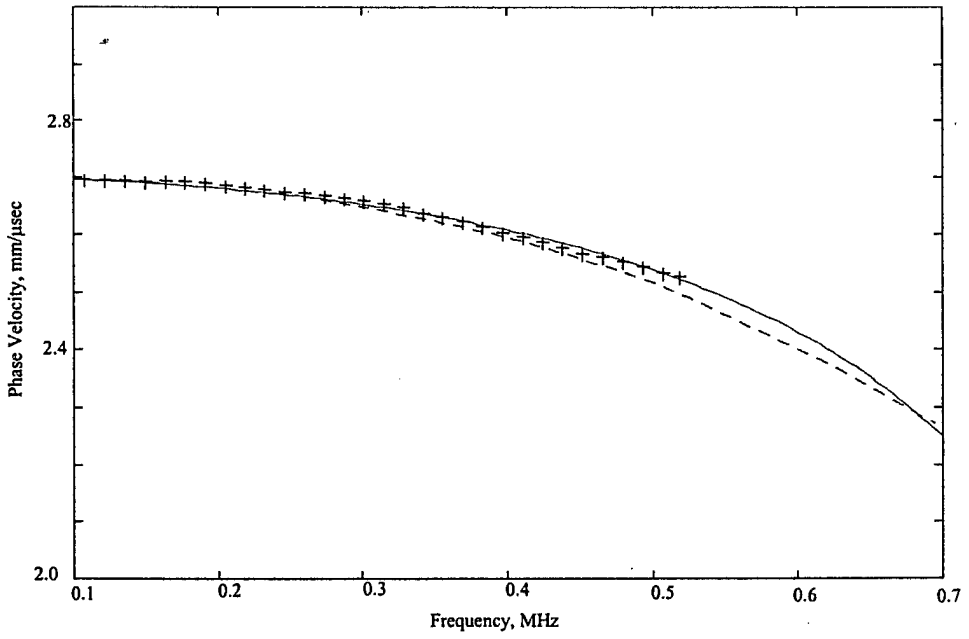

Figure 3.10 Experimental (+), theoretical (---) and simulated (solid) dispersion curves for an epoxy-graphite composite, 1.2 mm thick., for propagation perpendicular to the fibers.

3.3 Identification of Laser-Induced Lamb Waves in Aluminum Plates

The work performed by Castro (1998) aimed at generating Lamb waves in aluminum plates with a Nd:YAG laser light. The generation of Lamb waves with a laser is inherently a broadband process as compared to more traditional methods. The laser was focused to a line with a Gaussian profile with full-width half-maximum of 1 mm. In principle it was expected that the broadband excitation of wavenumbers extending from 0 to about 6 mm^{-1}. Similarly, the pulse from the Nd:YAG, with a 20 ns duration would contain a spectrum that extends to approximately 50 MHz. The source was able to excite frequencies within the mentioned regimes.

When a laser pulse of high power density is focused on the surface of the material, some of the material may ablate and/or plasma may be formed (Ready, 1971). These occurrences contribute to the generation of elastic waves in the material. When the laser power density is below the power density necessary for ablation, the interaction between the laser pulse and the material near the surface is purely thermoelastic (Rose, 1984). The thermoelastic generation of ultrasound occurs primarily because the incident laser light is intense enough to create a sharp localized thermal gradient in the surface illuminated by the laser pulse. The thermal gradient induces transient stresses on the surface of the material initiating ultrasonic waves (Rose, 1984). During experiments conducted the laser power density was kept below the ablation power density, avoiding any visible damage; the interaction between the laser and the material near the surface was then purely thermoelastic.

The instrumentation used in the experimental investigation is shown schematically in Figure 3.11. The laser had a synchronization signal that was used to trigger the digitizing oscilloscope. The fixed synchronization output is used thus to establish a time reference for all events. Broadband piezoelectric transducers with a bandwidth from 20 kHz to 1.5 MHz were used. The theoretical bandwidth of the laser generated ultrasound was broader than the bandwidth of the transducers. The piezoelectric transducer senses the surface deflections from waves induced by the laser as shown in Figure 3.12. The signal captured from the transducer is amplified and sent to the oscilloscope.

The arrangement of the optics consisted of an optical density filter, a plane-concave lens, a plane-convex lens, a cylindrical lens, and a high energy laser mirror. The density filter drops the laser energy down to a percentage transmittance of 0.01 with respect to the output value. The transmitted energy level is maintained below the damage threshold of the aluminum surface. Plane-concave and plane convex lenses, with effective focal lengths of -30 mm and 50 mm respectively, condense the laser beam from 6 mm down to 1 mm diameter. The cylindrical lens, 44 mm focal length, stretches the circular beam into a line, maintaining a 1 mm width dimension while allowing for varying the line length through altering the angle appropriately.

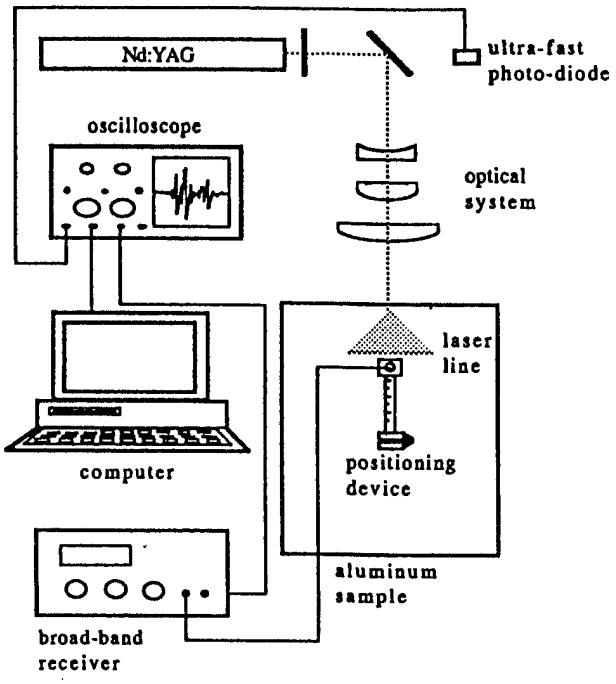

Figure 3.11 Experimental setup for laser-based ultrasonic system

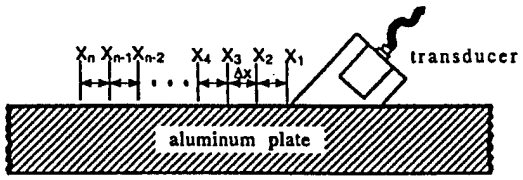

Figure 3.12 Displacement of transducer along aluminum plate

To capture the data, a LabView program was used. The program permits interfacing the oscilloscope to the computer through a GPIB board. A synchronization signal outputs the laser for triggering purposes. The data is collected while the transducer is displaced to 32 or 64 equally spaced points with the help of a micrometer as depicted in Figure 3.12. At each position 2500 time history points are stored. The measurements combined to 32 x 2048 or 64 x 2048 matrices. The acquired time data was treated with a two-dimensional Fourier transform (2D-FFT), to provide the amplitude of the generated waves as a function of frequency and wavenumber. Experiments were performed for 12, 24, 36, 47 and 56 mm laser line length modifying in each case the pulse-width, 16.8, 14.0, 13.6 and 13.4 ns. A total of 20 tests were conducted, of which the most significant are shown here.

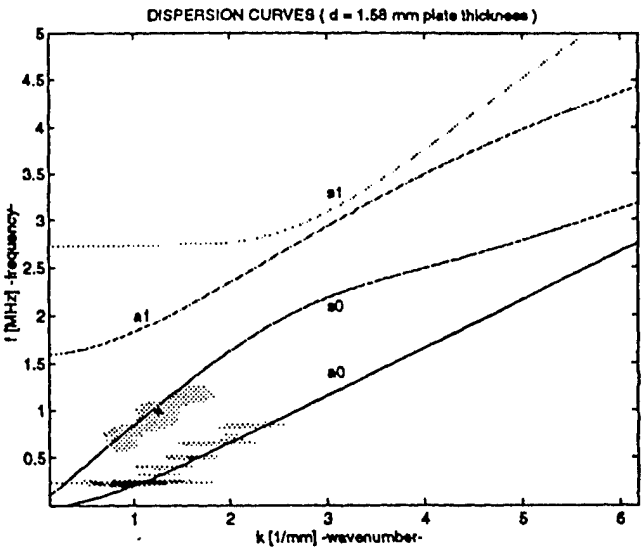

Figure 3.13 Two-dimensional FFT experimental data superimposed on numerically calculated dispersion curves, 13.6 ns pulse-width and 24 mm laser line-length (contour plot).

Figure 3.13 shows the main modes present in the aluminum plate for 13.6 ns and 24 mm laser line-length. In this case the relative amplitudes of modes along the s_0 dispersion curve reach one-half the amplitude of the a_0 mode. Likewise Figure 3.14 illustrates the case where the a_0 mode has more predominant presence. A dispersion curve induced by the same laser line-length of 24 mm but with a reduced pulse-width is shown in Figure 3.15.

This series of experiments demonstrated that Lamb waves can be generated in thin metallic structure using a Nd:YAG laser light. Furthermore, with the proper optical arrangement, the length of the laser light illumination projected on the specimen plate and the pulse duration can be used to control the content of the Lamb wave modes.

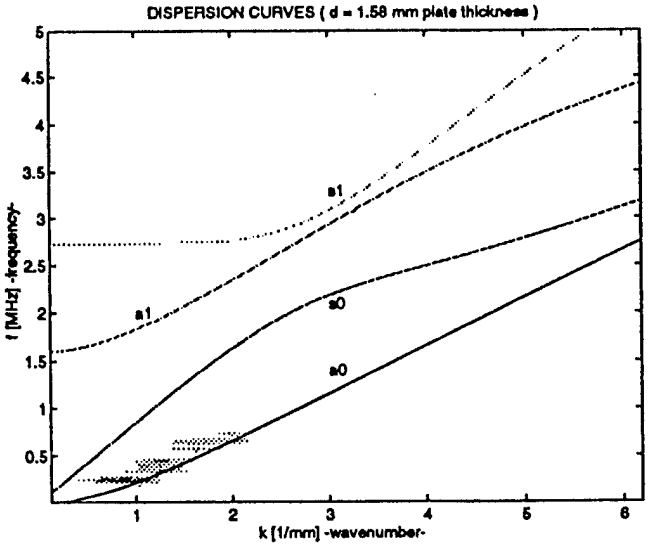

Figure 3.14 2D-FFT experimental data superimposed on numerically calculated Lamb wave dispersion curves, 14.0 ns pulse-width and 24 mm laser line-length.

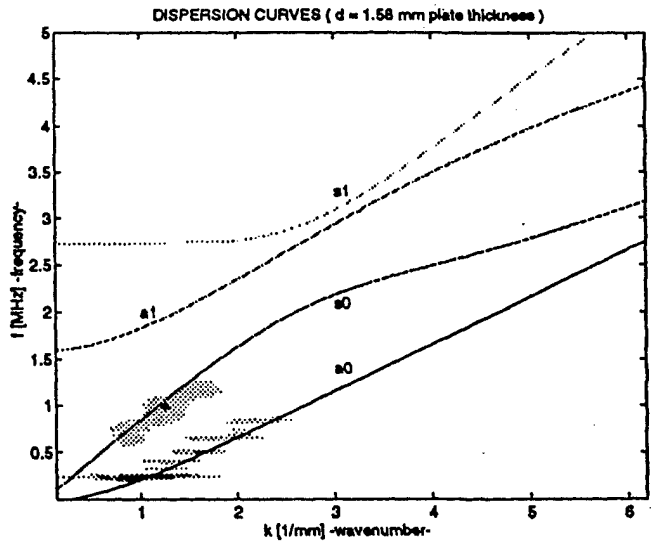

Figure 3.15 2D-FFT experimental data superimposed on numerically calculated Lamb wave dispersion curves, 13.4 ns pulse-width and 24 mm laser line-length.

3.4 Interaction of Lamb Waves A_0 and So Modes with Notched Aluminum Plates

The efforts reported in the previous section were then expanded by Batu (1998), who conducted preliminary experiments to generate Lamb waves with the laser and with a transmitter on aluminum plates with and without notches. The plate specimens had a thickness of 1/16 in. with dimensions of 2 ft by 3 ft. Six plates were tested, one with no notch and others with notches as shown in Table 3.4. In all case, the position of the notches was 220 mm away from one end of the plate.

Table 3.4 Characteristics of sample plates

plate	notch	width [in]	depth [in]	length [in]
1	no	-	-	-
2	yes	1/32	2/64	8
3	yes	3/32	2/64	8
4	yes	5/32	2/64	8
5	yes	5/32	1/64	8
6	yes	5/32	3/64	8

Batu used the set-up developed by Rodriguez (1998) to conduct the experiments involving the transmitter, and the set-up developed by Castro (1998) for the laser generation case. The transmitter setup produced Lamb waves mostly of the So-mode while the laser beam produced mostly the Ao-mode. In the transmitter-induced Lamb waves, Batu studied the So-mode reflection from notches, through-notch transmission and mode conversion due to the notches. In laser induced Lamb waves he studied the Ao-mode through-notch transmission and mode conversion due to the notches.

The So-mode reflection was more suitable for detecting the notches on plates. Notches modified the time record signal by adding reflections or echoes to them. The deeper the notch was, the stronger the reflection signal would become. Batu did not find an obvious relation between the reflected signal and the width of the notch. The presence of a reflection in the time record signals indicated the presence of a notch. If there was a notch, a reflection from the notch would occur that arrived ahead of that one from the end of the plate. The location of the notch caould be estimated from the arrival time.

In the through notch transmission case, a reduction in the amplitude of the signals was observed. However, a mode conversion from So to A_0 was observed for the transmitter case, and from A_0 to So for the laser induced case. The deeper the notch was, the larger the amplitude of the mode converted signal would become. In the laser-induced case, even though the modes excited were mostly A_0, there were still many other modes. Thus the time record signals were complicated and difficult to analyze directly.

3.5 Numerical Investigation on Propagation of Lamb Waves in Damage Plates

The objective of Tirado (1999) was to simulate the ultrasonic testing of thin plates using finite element (FEM) analysis. He simulated three plates made of aluminum, steel and graphite-epoxy. The composite plate was analyzed in the direction and perpendicular to the direction of the fibers. The FEM models considered the propagation of different modes of elastic waves in plates with and without defects. More specifically, the reflectivity and transmissivity of the waves due to the presence of a crack were studied. The two-dimensional FFT was used to analyze the propagation of multimode signals and to quantify Lamb wave interactions with defects. The changes in phase and group velocities due to the presence of damage were also studied.

The code DYNA2D was selected for the simulations. This code is an explicit, Lagrangian, finite element code designed for analyzing the transient dynamic response of two-dimensional solids (Whirley and Engelmann, 1992). The analysis process began with a physical description of the problem assisted by a mesh generator pre-processor. The plate was modeled as a plane-strain geometry, with dimensions of 1.0-m long by 1.6-mm thick, as shown in Figure 3.16.

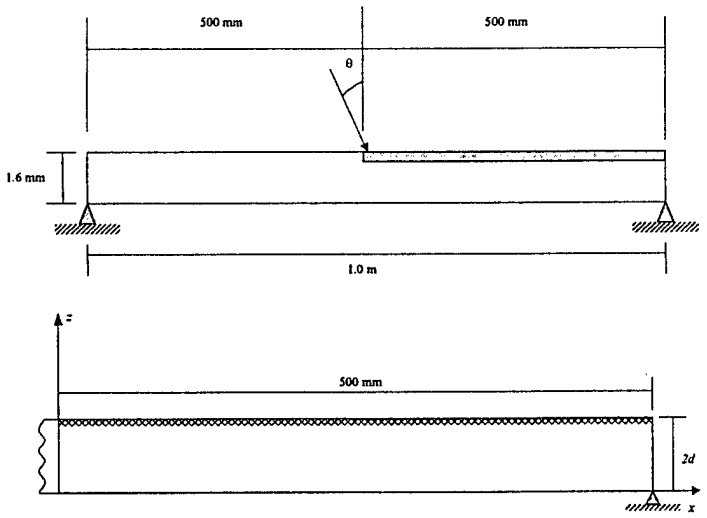

Figure 3.16 Setup of an undamaged plate

A 5-cycle sinusoidal load modulated by a Hanning window, was applied at the mid-length of the plate, at an angle appropriate to excite the symmetric mode as the dominant energy mode ($\theta = 31°$). The boundary conditions defined a pin supported plate, as shown in Figure 3.16. The grids were defined to conform to the criterion developed by Rousseau et al. (1996) to ensure proper modeling of wave propagation. In summary, the model of the plate consisted of 32,000 elements and 36,009 nodes. A similar mesh was developed for a similar plate but with a thickness of 3.2 mm. In all executions 2,048 time steps, lasting 0.1 μs, was selected to carry out the analysis. The time records obtained for nodes on top surface spaced at 1.0-mm the point where the signal was applied to the edge of the plate were selected for processing.

The simulated damaged plates had a notch located at 275 mm away from the source as shown in Figure 3.17a. The time histories for the nodes before the notch served as the basis for wave reflection analysis; those past the notch were used for transmission analysis as shown in Figure 3.17b.

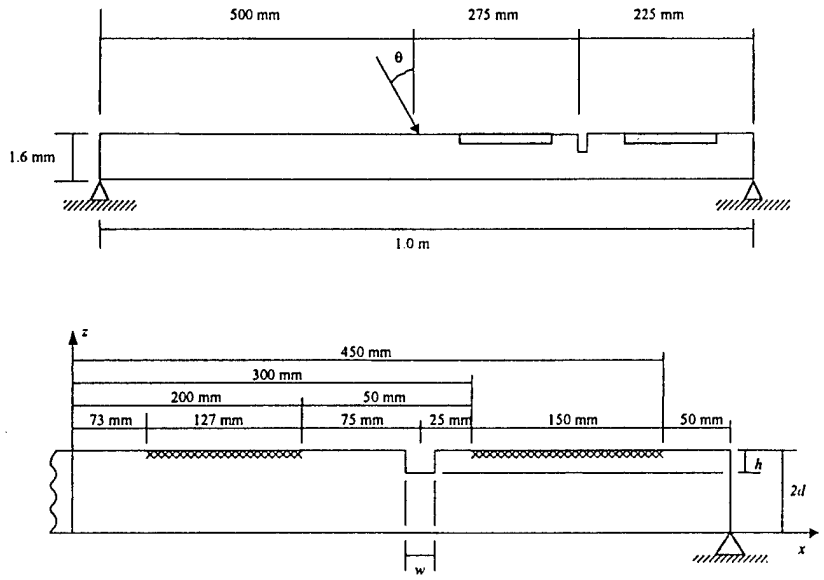

Figure 3.17 Setup of damaged plate

The identification of the amplitudes of the individual Lamb wave modes present in a multimode dispersive signal is important. To determine which modes and frequency-thickness regions are suitable with in the setup, time records for different burst frequencies at a point 300 mm away from the source was considered. Time records from frequencies ranging from 200 kHz to 1,500 kHz, at intervals of 50 kHz, obtained for the 1.6-mm thick aluminum plate are shown in Figure 3.18. At frequencies less than 1,100 kHz (frequency-thickness of 1.75 MHz-mm), the fundamental symmetrical and antisymmetrical modes are distinguishable. Past this frequency, it becomes more difficult to distinguish them individually from the time histories. Above that frequency, the a_1 mode appears with a significant energy level. At a frequency of 1,220 kHz (1.94 MHz-mm), the group velocity of the three modes (s_0, a_0 and a_1) are similar. Therefore, visually distinguishing the energy associated with these three modes became difficult. Practically speaking, performing tests at normalized frequencies above 2 MHz-mm with this method is not feasible.

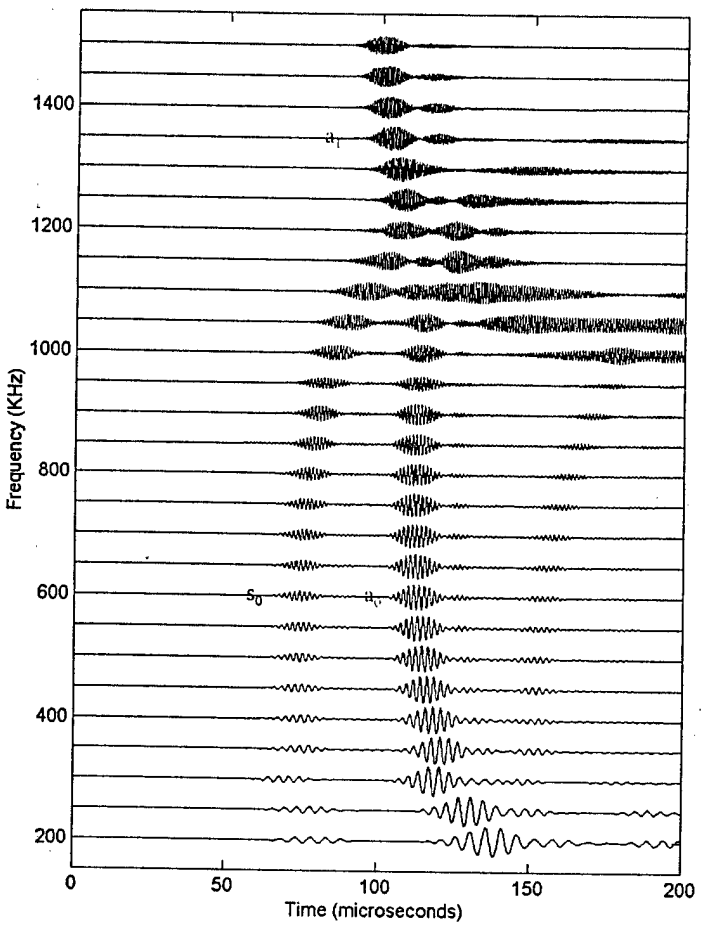

Figure 3.18 Variation in time records with frequency at 300 mm away from a source in a 1.6 mm aluminum plate.

After reviewing the most appropriate modes, four frequencies were selected as representatives of the ranges allowed to discern the modes. These frequencies were 200 kHz, 500 kHz, 800 kHz and 1,100 kHz. Since 8 elements are present across the thickness of the plate, the notch depth was created by removing each of these elements. Finally, three different widths were selected to carry out the analysis. All information related to the damage size is summarized on Table 3.5. This table presents the testing frequencies, and the notch dimensions in terms of the ratio of the notch depth, h, to plate thickness, $2d$, as well as the notch width, w.

Table 3.5 Notch dimensions

Testing Frequencies		200 kHz, 500 kHz, 800 kHz, 1,100 kHz
Notch Dimensions	$h/2d$	12.5%, 25.0%, 32.5%, 50.0%, 62.5%, 75.0%, 87.5%
	w	1.00 mm, 2.00 mm, 3.00 mm

As illustrated in Figure 3.18 the wave packets associated with different modes overlap in the time histories depending on the location and frequency; it was difficult to delineate them from the time records. This problem was also aggravated during the simulation of the damaged plates because of mode conversion due to reflections from and transmissions through the notches. The problem of mode recognition of the Lamb waves using the time histories was minimized by applying the two-dimensional FFT transformation. Figure 3.19 illustrates a typical set of time histories from the FE model from the nodes at the top located between the source and the edge of the plate. This particular data corresponds to a frequency input of 500 kHz. It can be seen that the input source generates to Lamb-waves traveling at two different velocities. The reflections for the edge are also observed. The time records of Figure 3.20 correspond to the same plate but with the presence of a 1.0-mm long notch extending a depth of 37.5% its thickness. At the defect, the energy associated with each mode is divided into two reflected Lamb waves of the same mode order (i.e. R_{s_0/s_0} and R_{a_0/s_0} for the s_0 mode, and R_{s_0/a_0} and R_{a_0/a_0} for the a_0 mode). Similarly, the transmitted Lamb waves are divided into two Lamb wave modes (i.e. T_{s_0/s_0} and T_{a_0/s_0} for the s_0 mode, and T_{s_0/a_0} and T_{a_0/a_0} for the a_0 mode). Energy in a mode is partially converted to the waves of the other mode. Figure 3.21 shows a similar set of time records but corresponding to a notch depth of 87.5% of the plate's thickness. The behavior of the waves is similar with the exception that the amplitudes of the reflections from and transmissions through the notch are different. The deeper the notch is, the greater the amplitude of the reflected waves will become. Conversely, the deeper the notch is, the smaller the amplitude of the transmitted waves through the notch will be. This phenomenon was studied quantitatively by examining the time records at selective points and by a double FFT procedure gating the data to only examine the wave packets of interest. The selective points for the time record analysis corresponded to nodes where the time records showed clearly defined wave packets with no overlaps.

The numerical simulations served as the basis to investigate the sensitivity of the symmetric and antisymmetric modes (s_0 and a_0) of Lamb wave energy to notches of varying depth. The results included here correspond to an excitation frequency of 500 kHz. Similar results but for other frequencies are available in Tirado's thesis. These results are in the form of reflection and transmission ratios graphed versus the notch depth normalized with respect to the wavelength of the mode. The reflection ratio is the amplitude of the reflected divide by the incident wave amplitude. The transmission ratio is the amplitude of the wave transmitted through the notch divided by the incident wave amplitude. The amplitude for the particular mode types can be obtained from the time histories at selected points or from double FFT analysis using the gating procedure. Both type of analysis yield almost identical results.

Figure 3.22 shows the reflection ratios as a function of the notch depth to wavelength ratio, for the symmetric and antisymmetric modes. The reflection ratios for the s_0 and a_0 modes increase almost linearly with the notch depth. Figure 3.23 shows the transmission ratios. The transmission ratios decrease proportionally to the notch depth. Similar analyses were conducted for steel and the unidirectional graphite epoxy materials. For the composite material the analysis was performed in the fiber direction and perpendicular to the fibers. Figures 3.24 and 3.25 compare the reflection and transmission ratios, respectively, for aluminum and steel. The elastic constants of the isotropic material do not appear to influence the results. However, the behavior was different for the composite material.

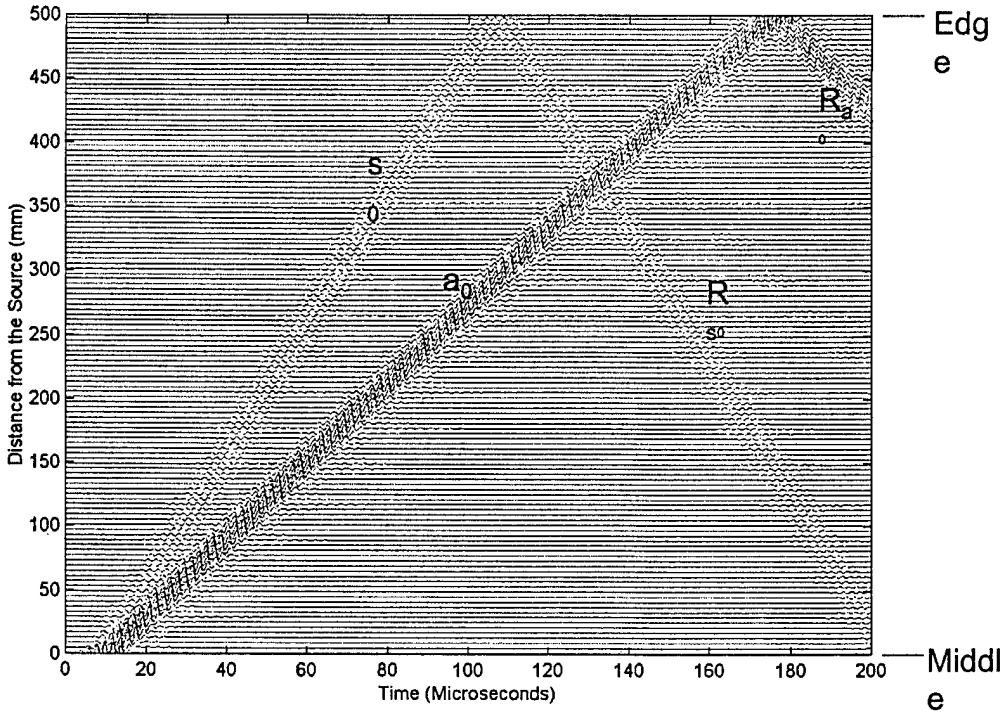

Figure 3.19 Typical set of time records for 1.6 mm aluminum plate at 500 kHz input sources.

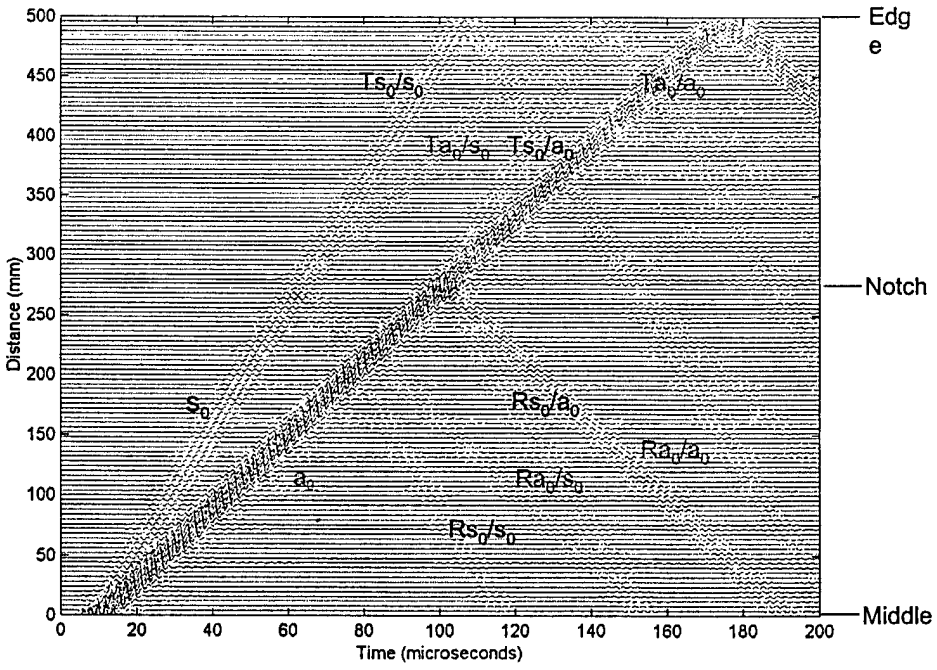

Figure 3.20 Set of Time history records for 1.6-mm aluminum plate, with a 500 kHz tone burst, and a notch depth of 37.5 % of plate thickness.

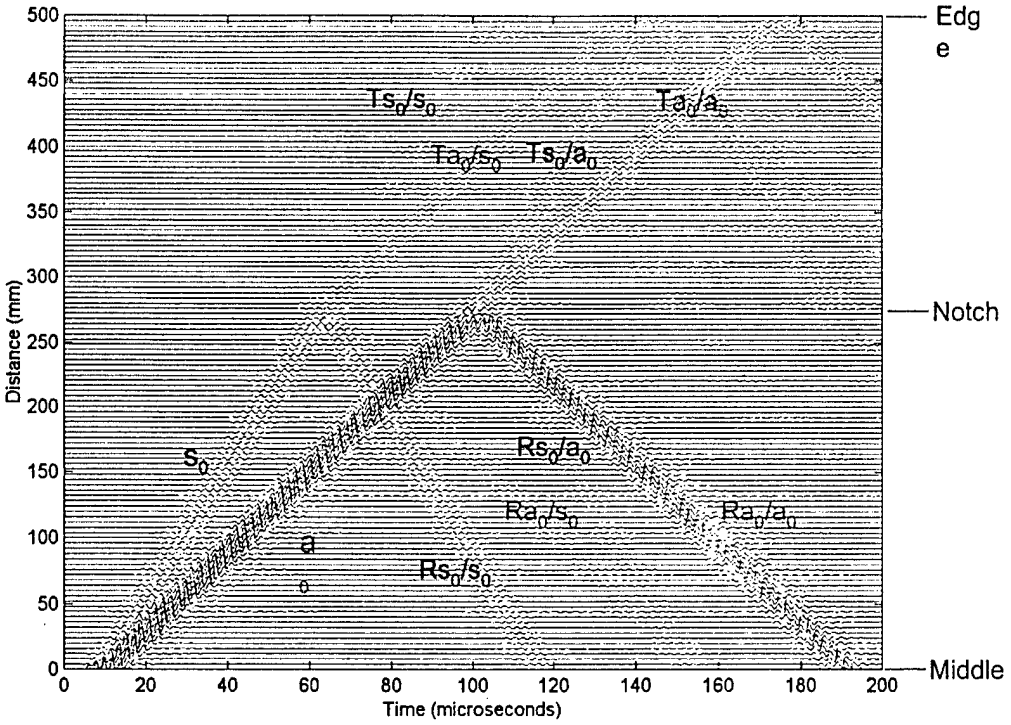

Figure 3.21 Time history plot of 1.6 mm thick, aluminum plate, with a 500 kHz incident tone burst, and a notch depth of 87.5 % of plate thickness.

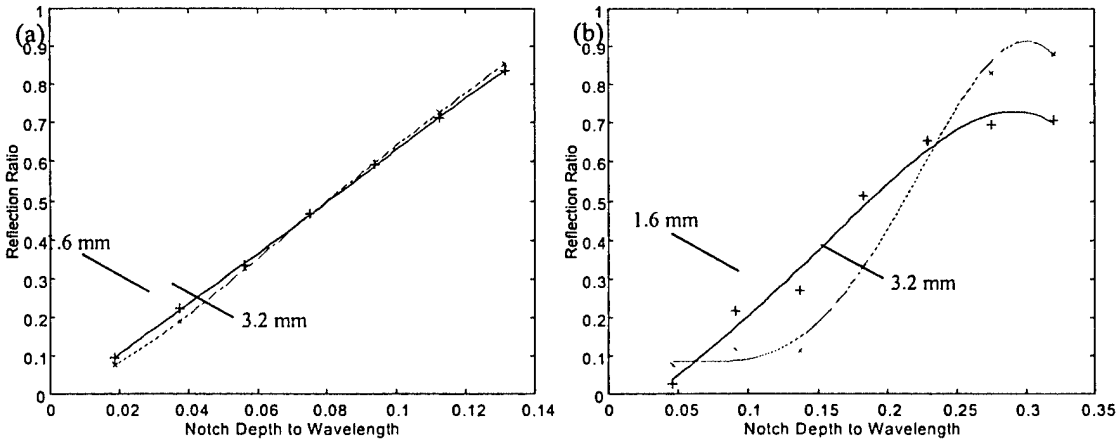

Figure 3.22 Reflection ratios as a function of notch depth to wavelength ratio (h/λ), for 1.6 mm thick and 3.2 mm thick aluminum plates, (a) for the s_0 mode, and (b) for the a_0 mode.

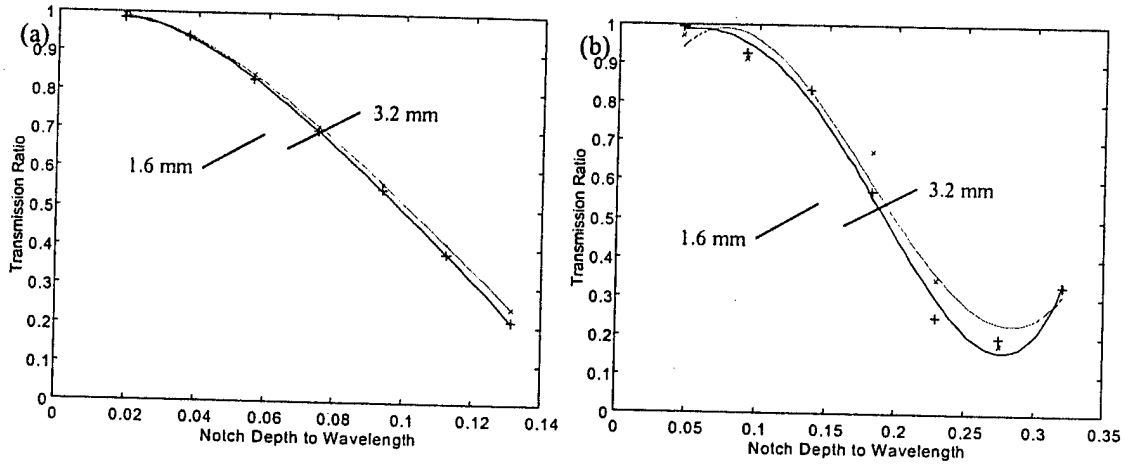

Figure 3.23 Transmission ratios as a function of notch depth to wavelength ratio (h/λ), for 1.6 mm thick and 3.2 mm thick aluminum plates, (a) for the s_0 mode, and (b) for the a_0 mode.

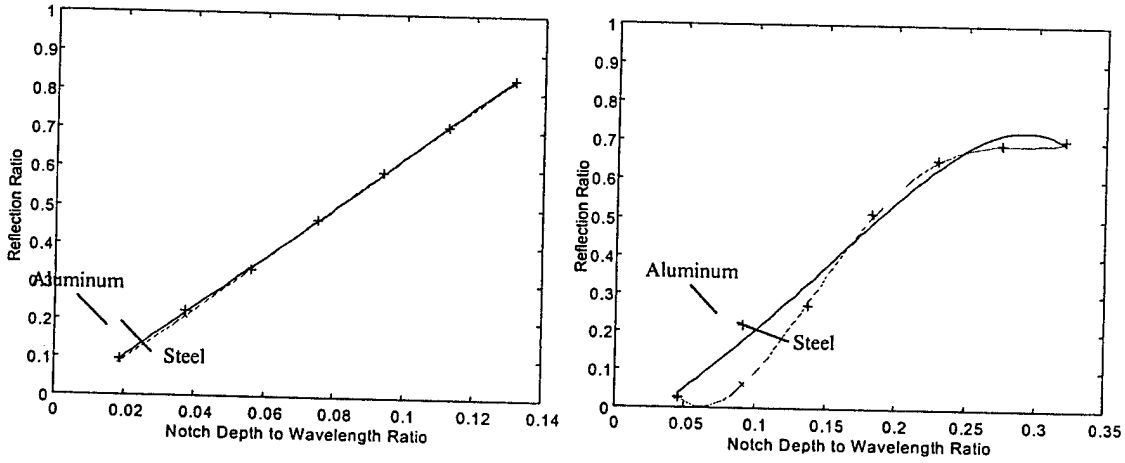

Figure 3.24 Reflection ratios as a function of notch depth to wavelength ratio (h/λ), for a 1.6 mm thick aluminum and steel plate, (a) for the s_0 mode, and (b) for the a_0 mode.

The propagation patterns along a plane parallel to the fibers and perpendicular to the fibers were considered. Figure 3.26 shows the reflection ratios as a function of the notch depth to wavelength ratio, for both the symmetric and antisymmetric modes. Similarly, Figure 3.27 shows the transmission ratios. A similar pattern is observed for the reflection and transmission ratios obtained for both directions except for the reflection values for the a_0 mode. In that case, the patterns are very similar but the values are shifted. This was attributed to the relative values of the elastic constants. The direction of the fibers, hence the material properties, do not seem to significantly affect the variation in reflection and transmission ratios with notch depth.

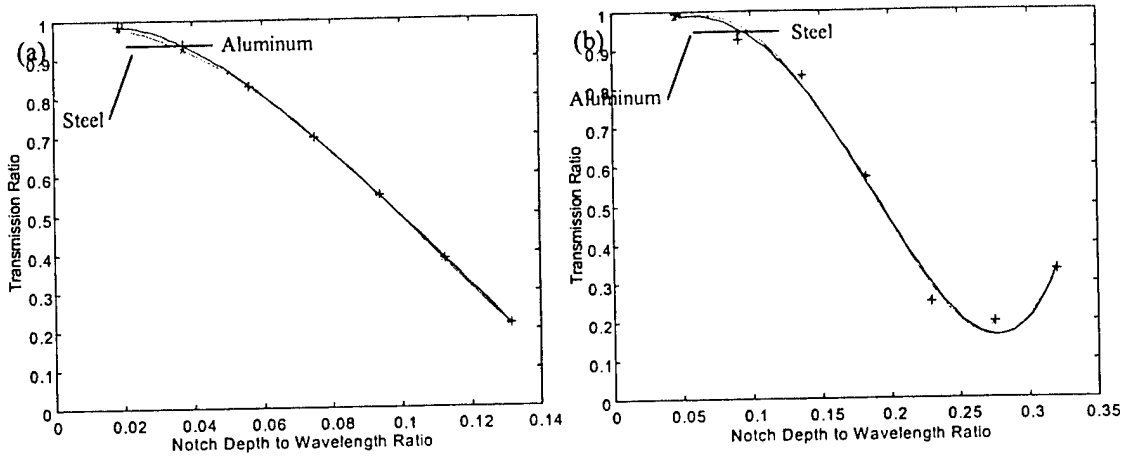

Figure 3.25 Reflection ratios as a function of notch depth to wavelength ratio (h/λ), for a 1.6 mm thick aluminum and steel plate, (a) for the s_0 mode, and (b) for the a_0 mode.

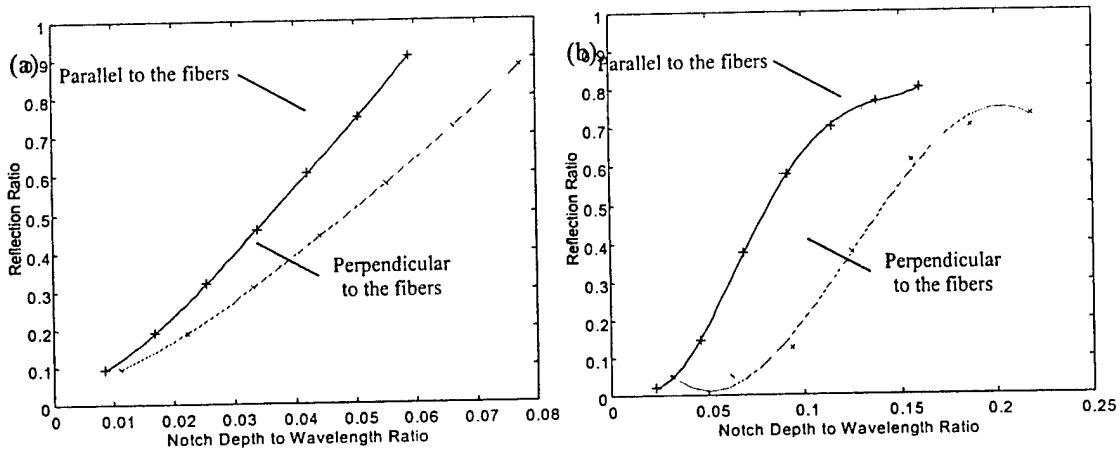

Figure 3.26 Reflection ratios as a function of notch depth to wavelength ratio (h/λ), for an epoxy plate (a) for the s_0 mode and (b) for the a_0 mode.

Another parameter that was studied from the FE simulations was the change in group velocity. The group velocity was calculated by determining the travel time of a given mode between two different points. The measurements were made by considering the peak of the first cycle as the starting point of the wave packet. The velocity of the wave after passing through the damage was normalized to the group velocity of an undamaged plate. The variation in group velocity ratio as a function of notch depth for a 1.6 mm thick aluminum plate is shown in Figure 3.28. As the notch becomes deeper, the s_0 mode group velocity ratio decreases. For the a_0 mode, the velocity ratio decreases only slightly as the notch becomes deeper. The reduction in velocity is rather small because the notch depth is very small relative to the wavelength associated with the induced frequency of 500 kHz. Furthermore, the change in phase velocity due to the notch was also studied. The phase velocity is the rate at which a point of constant phase travels along the

boundary. Measurements were made by considering a unique cycle within a wave packet and a known traveled distance. The phase velocity of a Lamb wave after passing through the damage was compared to the phase velocity of an undamaged plate. The variations in phase velocity ratios with notch depths for a 1.6 mm thick aluminum plate is shown in Figure 3.29. The phase velocity ratios of the s_0 mode and a_0 mode are minimally affected by the notch depth. The wavelength for the symmetric mode is on the order of $\lambda_{s_0} = 10.6$ mm, while the antisymmetric is $\lambda_{a_0} = 4.3$ mm for the induced frequency of 500 kHz. As such, the minimum wavelength to notch depth (λ/h) is 7.6 and 3.1 for the s_0 and a_0 modes, respectively. The velocities of the waves with such a large wavelength to notch depth ratios will not be affected by the damage.

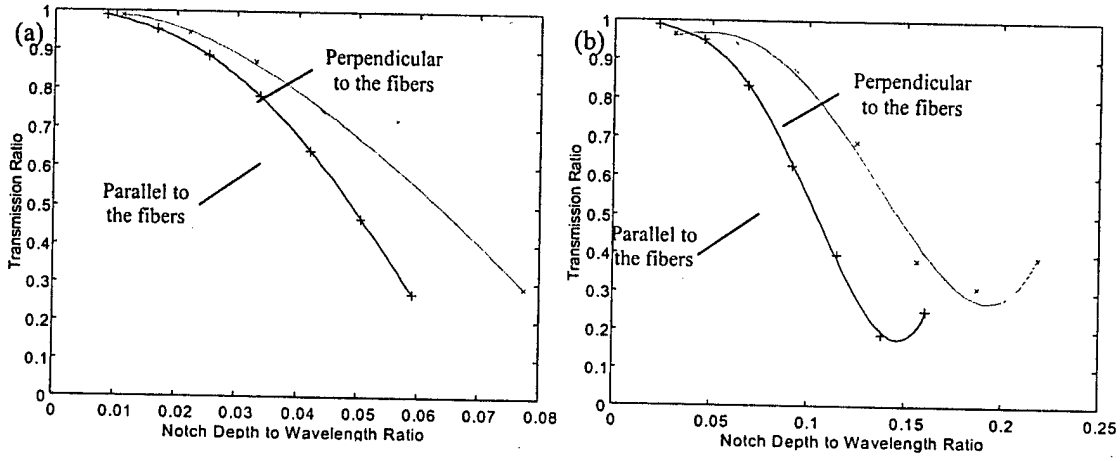

Figure 3.27 Transmission ratios as a function of notch depth to wavelength ratio (h/λ), for an epoxy plate (a) for the s_0 mode and (b) for the a_0 mode.

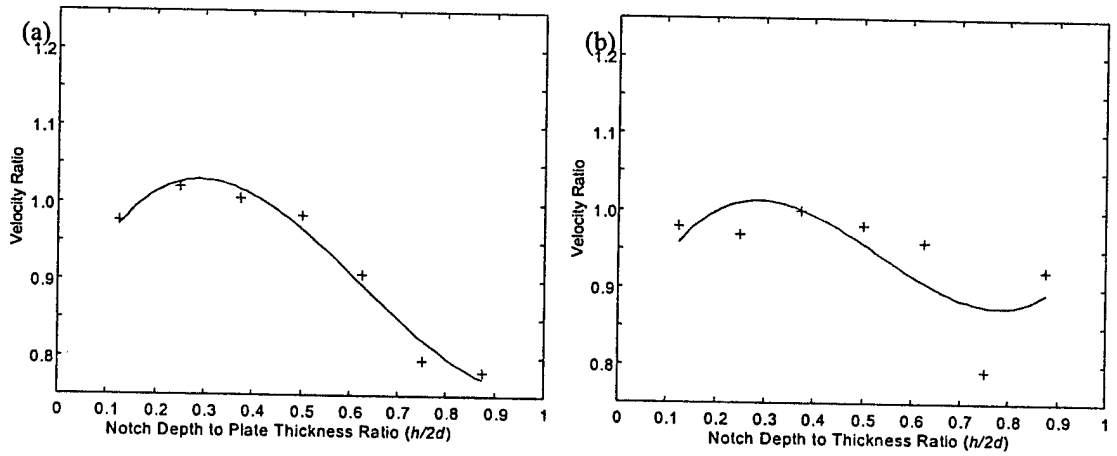

Figure 3.28 Variation in group velocity ratio as a function of notch depth to plate thickness ratio ($h/2d$) for an aluminum plate, (a) for the s_0 mode, and (b) for the a_0 mode.

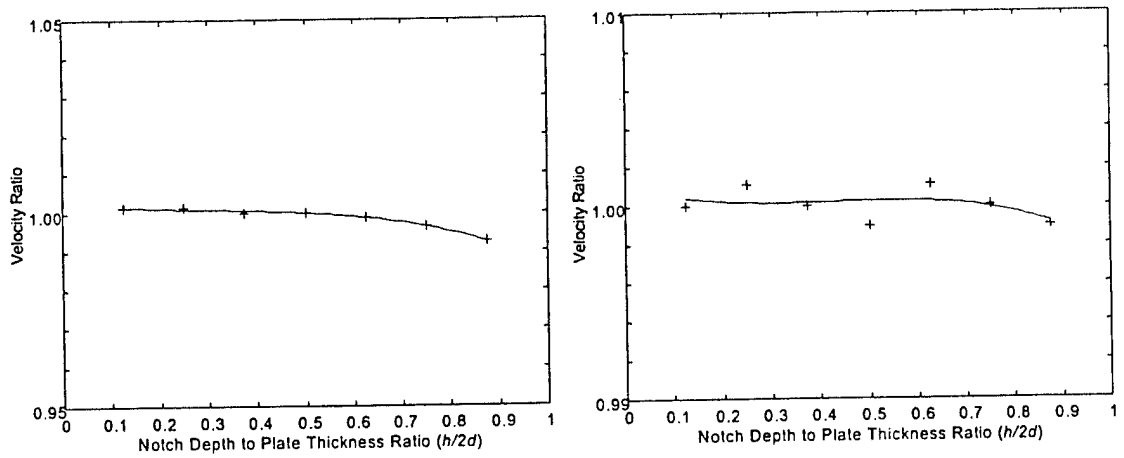

Figure 3.29 Variation of phase velocity as a function of notch depth to plate thickness ratio (*h/2d*) presented as a ratio between damaged to undamaged case for an aluminum plate, (a) for the s_0 mode, and (b) for the a_0 mode.

The following conclusions were derived from the Finite Element simulation studies done by Tirado (1999):

1. The use of explicit finite element analysis software to model wave propagation problems is practical.
2. The sensitivity of the individual Lamb waves to particular notches depends on the frequency-thickness product and the mode type and order.
3. The ratio of the notch depth to plate thickness was proven to be a controlling parameter for the measurement of the reflection and transmission ratios. For notch depth to plate thickness ratios greater than 70%, the transmission and reflection ratios become constant. Acceptable sensitivity associated with detecting the depth of a notch is attained for notch depth to wavelength ratios smaller than 0.25.
4. Reflection and transmission ratios are largely dependent on the notch depth.
5. Reflection and transmission ratios are insensitive to changes in the notch width.
6. The 2D-FFT methods can be used to quantify Lamb wave interactions with defects. The reflection and transmission 2D-FFT results can be used to determine the size of the notch. The reflection and transmission ratios obtained from time domain records are not robust in some instances.
7. The propagation velocities of Lamb waves only slightly decrease as the notch becomes deeper. The phase velocity of the antisymmetric mode a_0 was decreased by 5% for deep notches (notch depth to plate thickness of 0.75 and greater). Phase velocity for the symmetric mode s_0 varied by less than 0.5%.

3.6 Artificial Neural Network Models for Damage Detection Using Lamb Waves

The objectives of the research performed by Alvarez (2000) were to utilize the finite element models developed by Tirado (1999) to train an artificial neural network to detect notched-type defects, their location and their depths. The methodology proposed in his work is

illustrated in Figure 3.30. At one location of the plate a piezoelectric transducer excites a Lamb wave, which propagates through the plate and is reflected from the notch. At another point, a receiving transducer measures the resulting time history. The measurements collected contain information about the notch characteristics, i.e. its location and depth according to the work by Tirado (1999). The aim is to obtain quantitative information about the notch characteristics on the basis of these measurements. This requires an inverse problem to be solved using neural networks to process the measured waves with the goal of determining the size and location of the notch. For the training of the ANN, synthetically produced wave patterns were used. In this way the ANN builds up the wanted mapping between the time histories and corresponding notch characteristics. Eventually his ANN was successfully tested with experimental data.

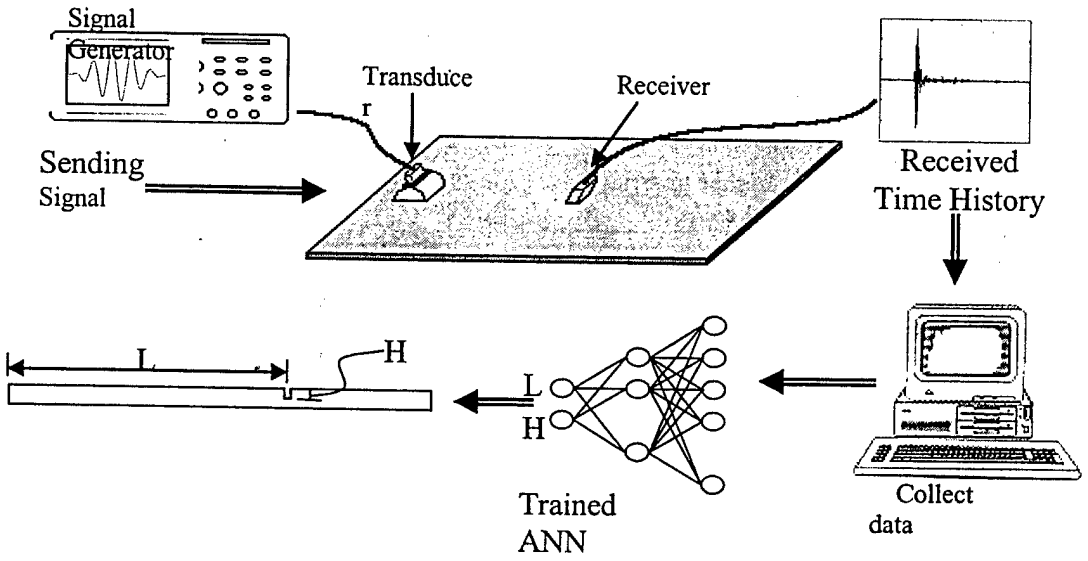

Figure 3.30 Proposed Methodology.

3.6.1 Database Generation Procedure

Artificial neural networks are built based on historical data where there is an unknown relationship between a set of input factors and an outcome. To develop a neural network it is necessary to have a representative set of examples of this unknown mapping. These examples are then used to train and test the neural network model. In this study each example consisted of an input vector whose elements are defined by the time response of the plate due to the Lamb-wave excitation, and an output vector, which is defined by the quantity that the model will predict. In this case, the quantities are the location and depth of the damage. The finite element method was used to model the propagation of ultrasonic waves to generate a comprehensive synthetic database covering a wide range of possible damage scenarios. The data was generated for the same 1.6-mm-thick aluminum, plates considered by Tirado.

The overall process employed to generate a synthetic database is graphically depicted in Figure 3.31. First, the parameters for the model were set (i.e. location of the transmitting and receiving transducers, and the notch). The first approach was to have a fixed source and 16 receivers at 20-mm intervals. This permitted the investigation of the effects of the distance between the transmitting and receiving transducers on the ANN performance. The location of the notch was set randomly through out the plate with some restrictions. Three notch depths where considered in this study, 25%, 50%, and 75% of the thickness of the plate. In step 2, the models of the aluminum plate to be analyzed by the finite element software were created. Next, in step 3, the model was analyzed by the finite element program using DYNA2D. After analyzing the model, an ASCII file was written. Such file contained the 16 time responses, one for each receiving transducer, of the plate. Each time response had 2,048 time steps. This process was repeated for every notch location on the plate until a comprehensive database was built (Step 5). The database was then composed of files, for each notch location, containing 16 time responses for each receiving transducer. Finally, in Step 6, from this comprehensive database, training and testing time responses from each file were selected to develop the ANN models. The inputs of the ANN models were based on the number of time steps of the time response.

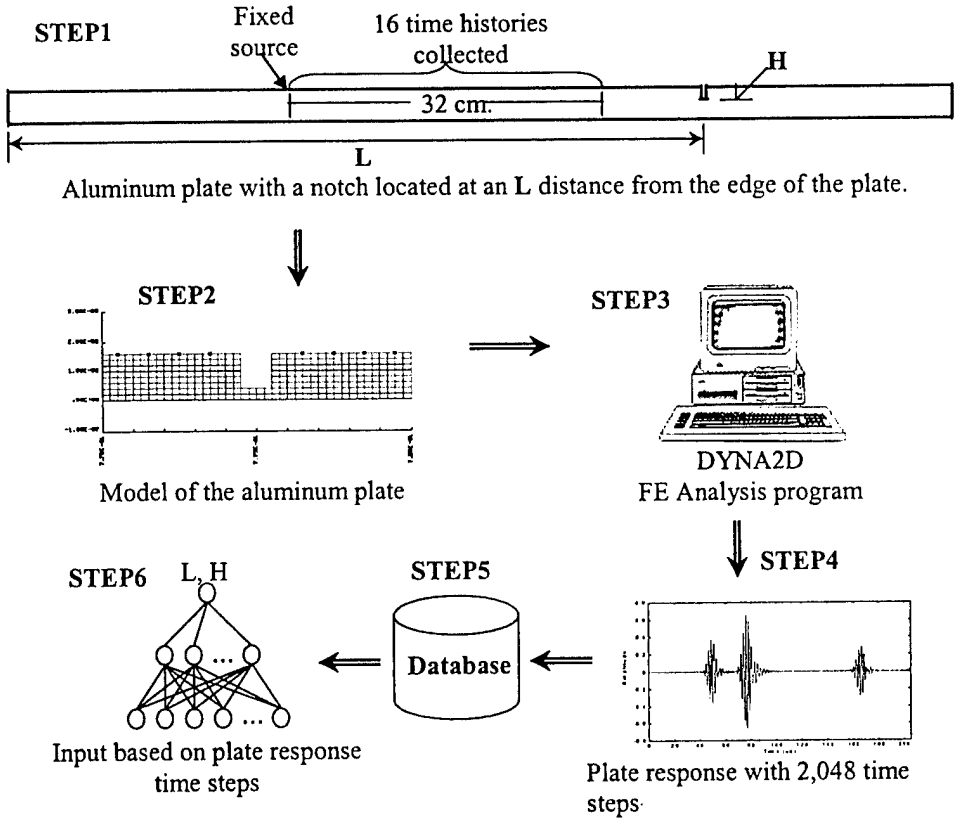

Figure 3.31 Synthetic Database Generation Process

3.6.2 Artificial Neural Network Models

All the neural networks models developed during this project were based on a multi-layer feed forward backpropagation algorithm. An adaptive gradient rate method was selected as the learning rule, to estimate the weights for the links that join the processing elements between two adjacent layers. The sigmoid function is used in the output layer to transfer the weighted sum to fit within certain specified bounds. The architectures for the final models consisted of three layers. The model with the best architecture was then tested and validated with a testing data file. A commercial software package, NeuralWorks Professional II by Neural Ware Inc., was used in this study. The ANN models developed were tested with experimental data presented and discussed in the next chapter.

There were three questions asked in this case. Is the plate damaged? If there is, where is the damage? And, how much damage is there? These questions influenced the development of the different types of ANN models in this study. The first network trained decided the presence of a defect, while a second network predicted the location. Once the decision that a defect is present and it is successfully located a third network was trained to predict the magnitude of the damage.

Three ANN models were created for evaluation of defects using simulated signals. One model was created to detect the presence of a defect, one to decide the location, and finally, another to determine the depth of the damage. Success was achieved in training an ANN model in detecting the existence of a defect. The final architecture for this model consisted of 256, 12, and 1 processing elements (PEs) in the input, hidden and output layers respectively. The model had a 95% correct classification. Good results were also obtained from the ANN model that localized the damage. The model had an 86% of the predictions within a ±10% error from the actual values when tested with time histories with the same notch depth as the training set. The model also showed good performance when tested with time histories from different notch depths. This model had a final architecture of 256, 15, 1 PEs in the input, hidden and output layer respectively. The final ANN model had 30-67% recognition of the different notch depths used in this study.

3.6.3 Validation with Experimental Data

After developing an ANN using synthetic data, the network was tested with experimental data to evaluate the performance of the ANN. There are several aspects on the differences between using simulated data and measured data. Some of these differences are due to generic problems presented when doing measurements, others are specific for the way measurements were done in this study, but they are all immediately related to the measurements.

The instrumentation used in the experimental investigation is similar to the one used by Rodriguez (1998) and is shown in Figure 3.32. The transmitting and the receiving transducers were placed perpendicular to the edge of the plate. This methodology was applied due to the presence of multiple modes (i.e. s_o, a_o) in the analytical time histories, even though the model was set up to excite only one fundamental mode (i.e. s_o). Placing the transducers in a vertical position will generate time histories similar to the analytical where both fundamental modes are present. This time histories are then input to the ANN for evaluation.

The aluminum plates used in the experimental investigation were 1.6 mm. thick, 0.3 m wide and 0.6 m long. Different plates were tested, one having no notch, and others having a notch as shown in Table 3.6. All notches were 0.8-mm-wide and 20 mm long.

Three different scenarios were used to investigate the capability of the ANN to detect and locate the damage independently of where the transmitter transducer was placed on the plate. The transmitter transducer was placed at 300 mm, 230 mm, and at 145 mm from the edge of the plate as shown in Figure 3.33.

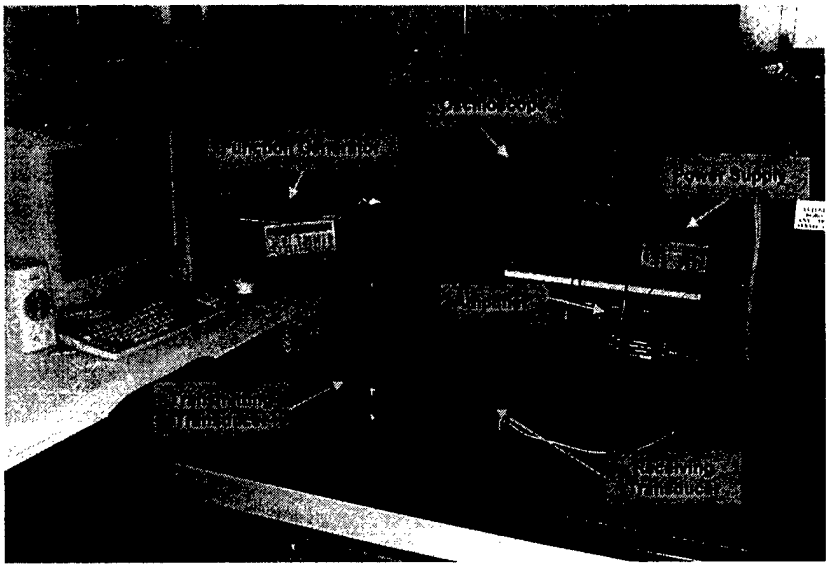

Figure 3.32 Actual Experimental Setup.

Table 3.6 Characteristics of sample plates.

Plate	Notch	Width (mm)	Length (mm)	Depth (mm)	Location (mm)
1	No	-	-	-	-
2	Yes	0.8	20	1.2	750
3	Yes	0.8	20	0.4	530
4	Yes	0.8	20	0.8	640
5	Yes	0.8	20	0.8	820

The first step was to record the time history from the oscilloscope and transfer it to a PC where the file was read and processed in order to be input to the ANN models. The file consisted of a time history with a time period of 0.1 μs and a total of 2500 time steps. The time history was then cut to 2048 time steps and then decimated to 256 time steps before input to the ANN models. The time histories for all scenarios were recorded for each of the 5 specimens and input to the three ANN models. Table 3.7 lists the results for Scenario I. The percent errors are shown in Table 3.8 and Figure 3.34 graphically illustrates the results of Scenario I. Figure 3.35 and 3.36 graphically illustrate the results for Scenarios II and III, respectively.

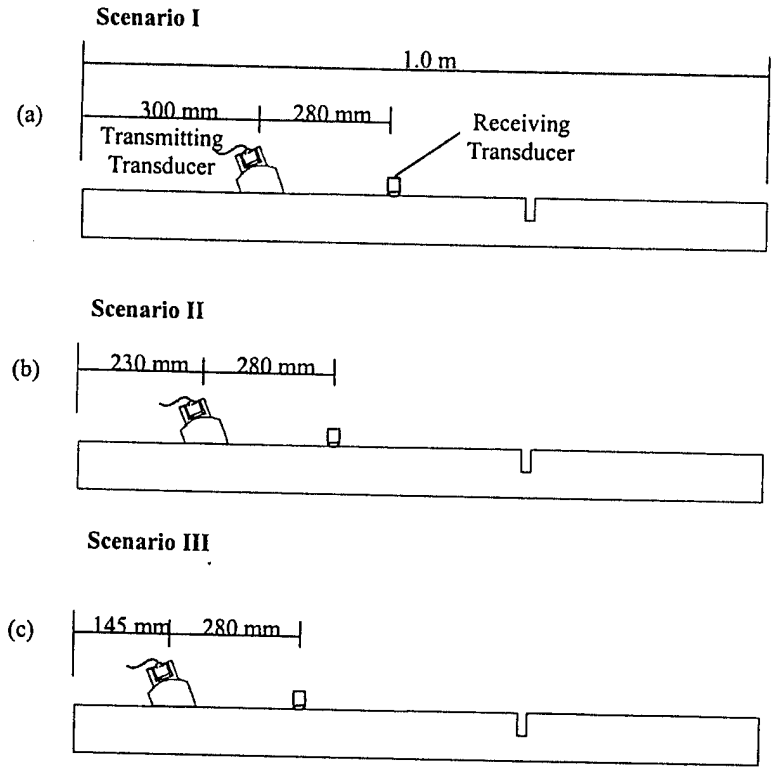

Figure 3.33 Transmitter position at (a) 300 mm, (b) 230 mm, and (c) 145 mm.

Table 3.7 Results for ANN Models for Scenario I.

	ANN Models					
	Damage Detection		Damage Location (mm)		Depth Prediction (mm)	
Plate	Actual	Predicted	Actual	Predicted	Actual	Predicted
1	0	0	-	-	-	-
2	1	1	750	781	1.2	0.4
3	1	1	530	552	0.4	1.2
4	1	1	640	668	0.8	0.8
5	1	1	820	760	0.8	0.5

Table 3.8 Percent Error in ANN Results for Scenario I.

Plate	Damage Location	Depth Prediction
2	3.1 %	50.0 %
3	2.2 %	50.0 %
4	2.8 %	0.0 %
5	6.0 %	18.7 %

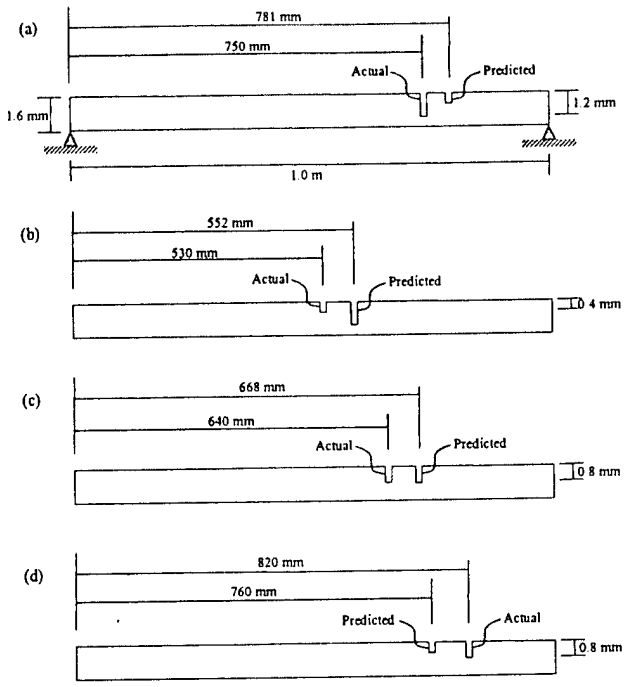

Figure 3.34 Predicted and actual locations of defects for Scenario I.

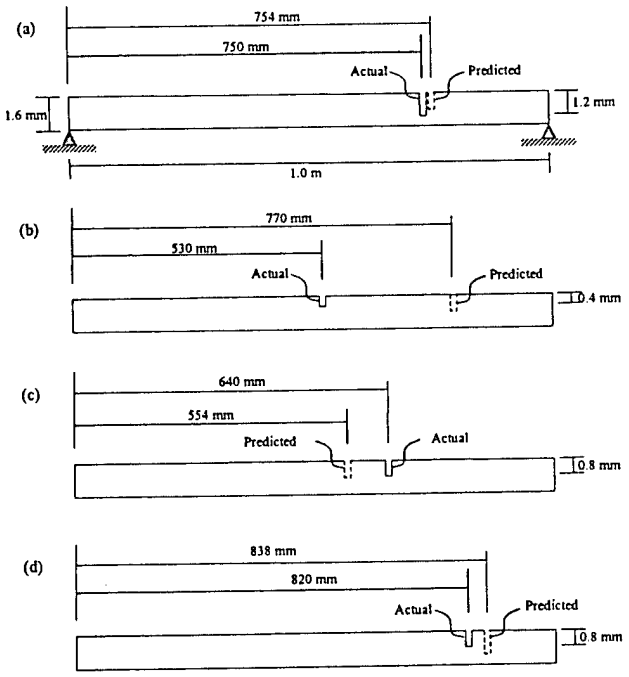

Figure 3.35 Predicted and actual locations of defects for Scenario II.

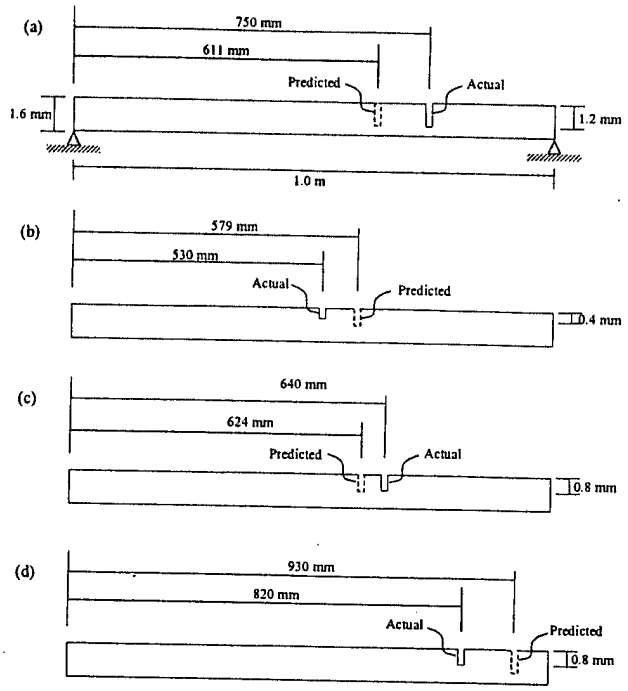

Figure 3.36 Predicted and actual locations of defects for Scenario III.

For the ANN model that detected the presence of damage, the network returned a value of 1.0 for all damaged plates and a value of 0.0 for the undamaged plate successfully for the three scenarios investigated in this thesis. The ANN models that predicted the location and depth had a performance of 2.2 – 6.0% and a 0.0 – 50% error respectively.

For Scenario II, the performance for the ANN models for damage localization was of a 0.4 – 24% error. The depth was predicted within a 6.2 – 25% error for all of the test plates. Scenario III had similar results as the other two scenarios, where the percent error fell between 1.6 – 13.9% and 0.0 – 25% for the localization and depth prediction respectively.

The ANN models for damage detection and localization showed good performance for the analytical and experimental data. However, the ANN model for depth prediction showed inconsistent results and larger errors. The amplitudes of the reflection and transmission modes from the notch are the characteristics that distinguish the time histories for each of the three depths used in this study.

3.6.4 Conclusions on ANN to predict damage using Lamb Waves

The following conclusions were derived form the research done by Alvarez (2000):

1. The use of explicit finite element analysis software to model wave propagation problems was practical for developing databases to train and test ANN models.
2. The ANN model for damage detection exhibited satisfactory results in identifying the existence of a defect.
3. Damage location results for most of the experimental cases were acceptable.

4. The ANN model for depth identification showed inconsistent results. This is because there is a significant increase in the reflection modes amplitudes when comparing the analytical and experimental time histories.
5. The ANN models for damage detection and location proved to be effective in their predictions independently of where the transmitter transducer was placed on the plate.
6. Damage locations where successfully predicted when tested with time histories form different notch depth, even though the ANN model was trained with only one notch depth.

3.7 References

Alvarez, W. (2000), "Artificial Neural Network Models for Damage Detection Using Lamb Waves", Master of Science in Civil Engineering, The University of Texas at El Paso, EL Paso, Texas, May 2000.

Bar-Cohen,Y., A.K. Mal, S.S. Lih, " NDE of Composite Materials Using Ultrasonic

Oblique Insonification", *Materials Evaluation*, November 1993, pp 1285-1296.

Batu, B., "Interaction of Lamb Waves A_0 and So Modes with Notched Aluminum Plates", Master of Science in Physics, The University of Texas at El Paso, El Paso, Texas, July 1998.

Burger, C. P., and Duffer, C. E. (1993). "Thermal-acousto-photonics remote monitoring of damage and dynamic response inside complex structures," A*MD-Experiments in Smart, J. Acoust. Soc. Am.*,100, (5), pp. 3070.

Castro, Miguel, "Identification of Laser-Induced Lamb Waves in Aluminum Plates", Master of Science in Physics, The University of Texas at El Paso, El Paso, Texas, July 1998.

Hosten, B. and M. Castings, "An Acoustic Method to Predict the Effective Elastic Constants of Orthotropic and Symmetric Laminates", *Review of Progress in Quantitative Nondestructive Evaluation*, Vol. 12, 1993, pp 1201-1207.

Hsu, D.K. and F.J. Margetan, "Analysis of Acousto-Ultrasonic Signals in Unidirectional Thick Composites Using the Slowness Surfaces", *Journal of Composite Materials* , Vol. 26, No. 7, 1992.

Karim M.R, A.K. Mal, and Y. Bar-Cohen, "Inversion of Leaky Lamb Wave Data by Simplex Algorithm", *Journal Acoustic Society of America*, Vol. 88, 1990, pp 482-491.

Mal, A.K., S.S.Lih, Y. Bar-Cohen, "Ultrasonic Determination of the Elastic Properties of Unidirectional Composites", *Review of Progress in Quantitative Nondestructive Evaluation*, Vol. 12, 1993, pp. 1233-1240.

Nazarian, S., and M.R. Desai, "Automated Surface Wave Method: Field Testing", *Journal of Geotechnical Engineering*, American Society of Civil Engineering,Vol. 119, No. 7, July 1993.

Ready, J. F. (1971). *Effects of high power laser radiation.* Academic Press.

Rodriguez, E. , "Non-Destructive Determination of Elasticity Constants of Composite Plates by the Acousto-Ultrasonic Method", Ph.D. Dissertation, Electrical and Computer Engineering, The University of Texas at El Paso, El Paso, Texas, December 1998.

Rokhlin, S.I., and D.E. Chimenti, "Reconstruction of Elastic Constants from Ultrasonic Reflectivity Data in a Fluid Coupled Composite Plate", *Review of Progress in Quantitative Nondestructive Evaluation*, Vol. 9, 1990, Plenum Press, New York, NY.

Rokhlin S.I. and W. Wang, "Ultrasonic Evaluation of In-plane and Out-of -Plane Elastic Properties of Composite Materials", *Review of Progress in Quantitative Nondestructive Evaluation*, Vol. 8B, 1989.

Rose, L. R. F. (1984). *Point source representation for laser-generated ultrasound,* J. Acoust. Soc. Am., 75, (3), pp. 723-733.

Tirado, Cesar (1999), "Numerical Investigation on Propagation of Lamb Waves in Damage Plates," Master of Science in Civil Engineering, The University of Texas at El Paso, El Paso, Texas, May 1999.

Whirley, R.G., and Engelmann B.E., "DYNA2D, A Nonlinear, Explicit, Two-Dimensional Finite Element Code for Solid Mechanics User Manual," Lawrence Livermore National Laboratory, April 1992.

Wu, T.T. and Z. H. Ho, " Anisotropic Wave Propagation and Its Applications to NDE of Composite Materials", *Experimental Mechanics*, December 1990,

CHAPTER 4

CHARACTERIZATION OF STRUCTURAL DAMAGE AND MATERIALS DEGRADATION USING ANALYSIS ON THE MICRO- AND MACRO-SCALES

4.1 Introduction

The specific objectives of this research component involved the application of observational and analytical tools - transmission and scanning electron microscopy to characterize structural damage and degradation in aircraft materials, primarily corrosion of aluminum components and the development of diagnostic, to early detection of damage and degradation. In dealing with these issues, of necessity, the mechanisms involved in the various aspects of degradation and damage were explored. The work described in this chapter is based on the theses of Posada (1998), Campuzano-Contreras (2000), Obispo (1999) and Cervantes (2000).

4.2 Problem Statement

Presently, one of the major concerns in the aircraft and aerospace industry is corrosion. This is especially true of aging aircraft when structural strength is compromised by corrosion. Corrosion is the natural or induced degradation of metal, which is irreversible but controllable in intensity by means of engineering design (Taylor, 1997). The potential of malfunctioning of aircraft components and systems have proven tragic in many cases and corrosion prevention has been a primary concern to the military and aerospace industry. The economic losses to contractor and customer are overwhelming due to natural or induced corrosion. In the United States, corrosion maintenance and repair for military aircraft weapons systems is costing over 3 billion dollars annually (Agarwala, 1998).

Current down sizing and new acquisition policies for the U.S. Department of Defense (DoD) have ordered that older aircraft (greater than 30 years) continue in service for another 40 years to meet mission requirements (Agarwala, 1998). Several aircraft that have reached maturity of 30 years of age or beyond include: P-3s, C-135s, C-141s, C-5s, B-52s, H-46s, F-4s, and F-14s. The minimum age at which an aircraft has been retired due to corrosion issues and/or airworthiness is 40 years of age.

In an effort to acquire corrosion control and prevention, several processes are routinely performed. Inspection periods to check electrical and avionics housing and hydraulic systems are based upon an aircraft safety performance assessment (ASPA). This scheduled depot level maintenance (SDLM) varies from aircraft to aircraft. On the average, most fixed wing aircraft go through ASPAs every 5 to 7 years. If the aircraft fails these types of safety inspections, it is due primarily (eight percent of the time) to corrosion and stress cracking (Agarwala, 1998). Paint stripping is done approximately every seven years. However, coating is done frequently and over-painting is very common. By the time an aircraft comes to SDLM it probably has 25 mil (0.063 cm)

thick coating versus the specification requirement of 3 mil (~0.008 cm) thick coating. The extra paint adds to the weight of the aircraft which results in increased fuel costs and less cargo capacity.

Corrosion control and prevention processes can fall into three categories: organizational (O), intermediate (I), and depot (D) type. At the organizational level, simple tasks are performed such as washing, cleaning, sealant and touch-up paint. This organizational work is performed on carriers, ships and operational sites during deployment. This is where aircraft dwell for most of the time. Unfortunately, the longer their stay is, the greater the corrosion damage. Since there are no in-situ corrosion detection technologies or equipment on board for hidden corrosion, corrosion prevention is simply limited to corrosion preventive compounds (CPCs) and sealants.

4.3 Exfoliation Corrosion Occurring in 2024 Al Alloy Aging Aircraft

There has been a recent interest, a renewal of sorts, in understanding corrosion phenomena in aircraft sheet metals, particularly 2XXX and 7XXX aluminum alloys. This interest stems from the fact that many aircraft, especially KC-135 military aircraft or the 707 equivalent may be expected to be operational for another 40 plus years as mentioned earlier. Although, in the case of the KC-135, actual flight hours are minimal many aircraft are exhibiting a variety of corrosion problems, including exfoliation corrosion in body skins is particularly notable.

Maria Posada (1998) re-examined severe exfoliation in aluminum alloy skins (1.8 mm-thick sheet samples) from military KC-135 aircraft utilizing a wide range of materials characterization protocols in an effort to develop a broad, yet detailed analysis and comparison of precipitation within the grains and in the grain boundaries as well as the examination of elemental depletion profiles at grain boundaries by using analytical transmission electron microscopy and EDS. In addition, detailed crystallographic comparisons involving specific grain boundary rotations corresponding to in-plane and through-thickness interfaces were also made utilizing combinations of electron backscatter diffraction patterns and transmission electron microscopy techniques; including selected-area electron diffraction from adjacent grains characterizing these specific boundaries (interfaces). The overall objective of her research was to gain a fundamental understanding of the exfoliation corrosion mechanism in an effort to eliminate or retard exfoliation corrosion. To achieve this, the fundamental microstructure and microchemistry in-plane and through-thickness grain boundaries were explored utilizing transmission electron microscopy as a primary tool.

4.3.1 Exfoliation Corrosion Mechanisms

Exfoliation corrosion is characterized by intergranular corrosion and occurs along elongated grain boundaries in which the sheets of pan-cake like grains tend to lift and separate in a lamellar direction parallel to the surface. This creates a pastry dough effect, with a corresponding weakening of the sheet. Typical features of exfoliation corrosion can be seen in Figure 4.1 and the sequence of nucleation and propagation of exfoliation is shown schematically in Figure 4.2. According to Habashi et al (1983), the corrosion process is active in the grain boundaries containing precipitates and in the free precipitated zone (FPZ) around the grain boundaries. The electrochemical reactions between the precipitates and the FPZ promote micro-galvanic cell which initiates the active corrosion path and consequently the formation of the corrosion products. If the volume of the

corrosion products exceeds the volume of the metal from which it formed then wedging stresses arise which lift the surface grains. The role of the wedging stresses is thought also to be responsible for the propagation of exfoliation through the grain boundaries by a stress corrosion mechanism (Robinson 1988).

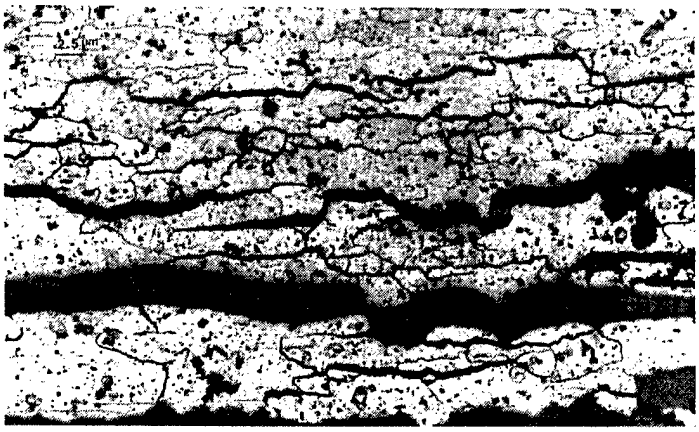

Figure 4.1 Typical features of exfoliation corrosion where leafing and layering is evident as the grains tend to lift and separate.

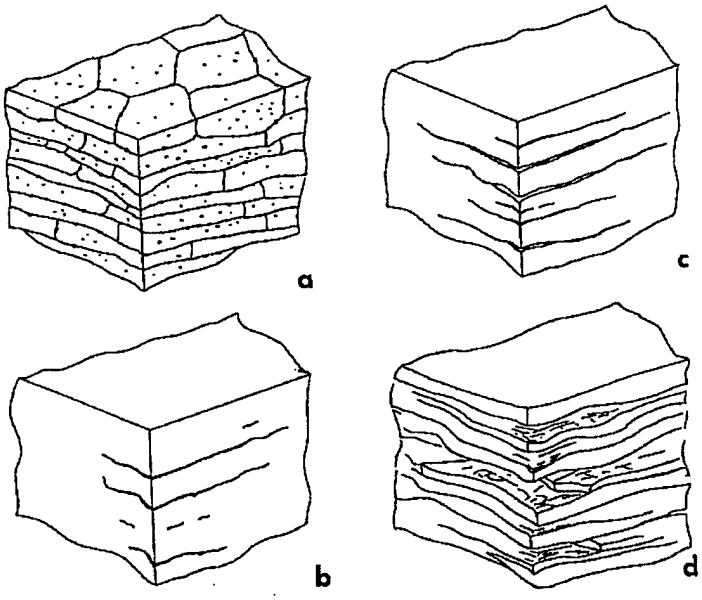

Figure 4.2 Schematic sequence illustrating the evolution of exfoliation structures in 2024 aluminum sheet or plate: (a) plate corner showing elongated grain structure and precipitation (b) corrosion onset within grain boundaries (c) linking of corrosion sites and delamination (cracking between grain layers and multi-layers by corrosion product wedge action (d) leafing and compete loss of sheet thickness integrity (Posada, et al, 1997).

Robinson (1983) has attributed exfoliation to a stress corrosion cracking (SCC) mechanism driven by the wedging of corrosion products in the elongated grain boundary. These wedging forces are attributed to the aspect ratio of the elongated grains, and increase with increasing aspect ratio. This is a relatively new approach to exfoliation in aluminum alloy sheet, and based in part on earlier work by oxide wedging to form SCC cracks in stainless steel. In fact, Habashi et al (1983) as well as Robinson (1983) in earlier work, have demonstrated that exfoliation is primarily an SCC mechanism. Habashi et al, have demonstrated this by using a special device which measures the forces developed by the corrosion products during the exfoliation process on several aluminum alloys. They found that the variation of the exfoliation force as a function of exposure time in Exco solution could be divided into two stages: an incubation period t_i was followed by an increase in the forces to a level corresponding a time of exfoliation equal to 240 h (F_{240h}). The time of incubation t_i increases when F_{240h} decreases. t_i increases also when the SCC Sc% decreases. Sc%decreases when the copper content decreases. They concluded that t_i may be taken as an exfoliation criterion and that the mechanism of exfoliation and that of SCC is thought to be the same (5). However, a fundamental mechanism is lacking and it is unclear why aspect ratio, as a simple geometrical condition, would nucleate and propagate exfoliation corrosion.

Aluminum and magnesium alloys and high strength alloy steels used for the construction of aircraft are active metals which react with, and interact with the environment to cause corrosion. In addition, when these materials are joined with other materials, especially less active or nobler materials such as titanium, stainless steels, and graphite composites, their coupling creates anodic/cathodic contacts and causes serious galvanic corrosion. Composites have also become a large player in the manufacture of aircraft and their use as patch repairs has further elevated the corrosion concerns because these materials (carbon, boron, and metal oxide matrices) are more cathodic (noble) in an electrochemical nature. Therefore, when coupled to aluminum a greater potential difference is created.

In a much more microscopic approach, Robinson (1983) and Jones (1993) attributed the exfoliation corrosion mechanism to electrochemical effects between grain boundary precipitates and adjacent, solute depleted zones. The markedly directional microstructure and temper of these aluminum alloys apparently create intergranular precipitates and related phenomena which contribute to localized compositional variations. These variations have been attributed to copper depletion as a consequence of grain boundary precipitation in the 2XXX series alloys, for example, and are said to create preferential anodic sites that sensitize the material to corrosion when coupled with a severe corrosive environment. This corrosive environment may include high humidity, high temperatures, salt containing sea waters (with varying concentrations and temperatures), and contaminants in air; including sulfur dioxide fumes. These are all conditions which the KC-135 aircraft experience. However, Posada et al (1997) failed to provide any evidence for copper depletion in or near elongated grain boundaries along the in-plane or the transverse surface areas for 2024 aluminum body skins from KC-135 aircraft. There was, however, a slight variation in the overall precipitate composition in the matrix and within the grain boundaries (1997).

The nature of exfoliation corrosion in aluminum alloy sheet such as 2024 seems to be complicated by several interconnected phenomena. First, the corrosion product must nucleate and

fracture along (and within) the grain boundary plane. Third, there appears to be some simultaneity in these events because the exfoliation failures can occur along each grain layer or multiple grain layers to create the characteristic leafing or french dough appearance (Figures 4.1 and 4.2). There is usually no apparent (external) (resolved) stress acting to promote the exfoliation process, and a wedging action therefore seems quite plausible. However the question remains: how (or why) does it nucleate and propagate within elongated grain boundaries?

Campuzano-Contreras et al (1997) demonstrated that 2024 aluminum alloy corrosion products contain high concentrations of bayerite ($AlO(OH)_3$) and boemite (AlO(OH)), and it is difficult to understand the overall nature of rapid grain boundary decohesion which must contribute as a significant aspect of exfoliation even if wedging by corrosion products is important.

4.3.2 Summary of Experimental Work

Samples of the KC-135 aircraft fuselage skin sections, which are similar to the 707 commercial aircraft body skin, were obtained with a nominal thickness of 1.81 mm. Figure 4.3 shows the as-received sample, and Figure 4.4 shows a magnification of exfoliated area. A 25.4 mm by 35.4 mm sample was cut from the base material and sent out for laboratory analysis (Charles C. Kawin Company, Broadview, Illinois) to determine elemental composition of the thin plate. The thin-plate skin had the following composition (wt%): Cu: 3.81, Mg: 1.41, Mn: 0.63, Fe: 0.21, Si: 0.09, Zn: 0.05, Ti: 0.02, Cr: 0.01, and balance Al.

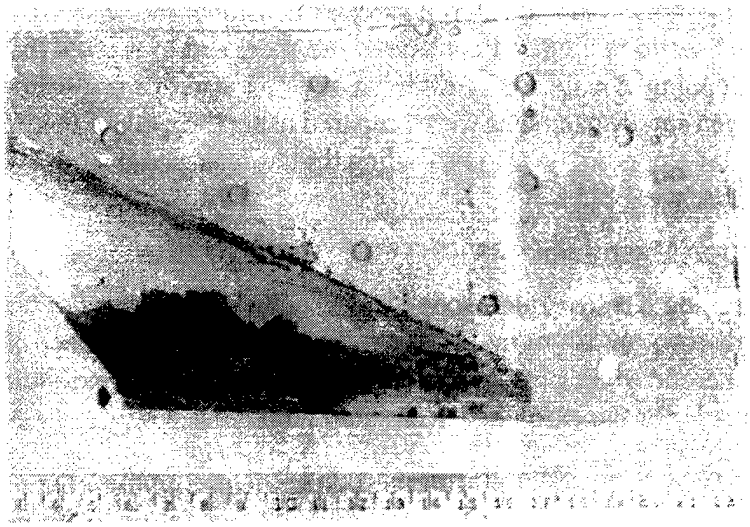

Figure 4.3 As-received sample of KC-135 aircraft fuselage skin demonstrating a severe case of exfoliation corrosion.

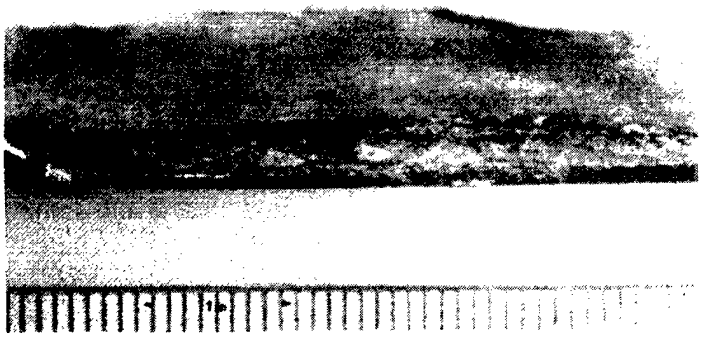

Figure 4.4 Magnified view of exfoliated region.

Optical Metallography

To serve as a control or reference specimen a 12.7 mm by 12.7 mm sample was sectioned from the skin on an area in which corrosion was not present. This sample was mounted in plastic for easy handling. The top and two sides perpendicular to each other were ground to a 1200 grit finish, polished with 1μm alumina in suspension, 0.3 μm alumina in suspension, and colloidal silica in suspension, respectively. All three surfaces were chemically etched with Keller's reagent (2.5 mL HNO3, 1.5 mL HCl, 1.0 mL HF, 95.0 mL H2O) to reveal the microstructure. Optical microscopy methods were used to examine and develop a three-dimensional model of the microstructure by creating metallographic section views in the plane of the sheet and in each of the through-thickness sheet directions. Extending collages of exfoliated regions also were developed by using light metallography. A second set of specimens were prepared using the methodology described above and sent to TSL labs for EBSD analysis. A corresponding three-dimensional model was made from these samples to use as a reference.

Scanning Electron Microscopy

An ISI-DS scanning electron microscope was used to analyze the as-received sample of the corroded section to observe the topography. Energy dispersive x-ray spectroscopy was used to observe and analyze the corrosion products on a section cut from the exfoliated area of the skin section. A map was made for the exfoliated area shown in Figure 4.4.

Transmission Electron Microscopy

Transmission electron microscope samples were prepared from small area of noncorroded control specimens. Specimens were cut from both the in-plane and transverse sides of the plate (see Figure 4.5). The thin strips were sectioned and ground on both sides to a 600 grit finish until a final thickness of 0.2 mm was obtained. The samples from the in-plane view were punched into normal 3 mm discs as shown in Figure 4.5. A modification was necessary for samples prepared from the in-thickness sides since the plates thickness was only 1.8 mm. TEM samples were modified to a rectangular shape with dimensions of 1.8 mm by 3.5 mm. The discs and the rectangular shaped samples were jet polished, with the use of a Tenupol 3 dual-jet polisher, to allow transmission through the thinned area in the vicinity of the hole produced by the electrolyte. The electrolyte used was composed of 20% HNO3 in methanol at a temperature of -24EC. Transmission electron sample were

were examined in a Hitachi H-8000 scanning transmission electron microscope operated at 200 kV accelerating potential and employing a goniometer-tilt stage.

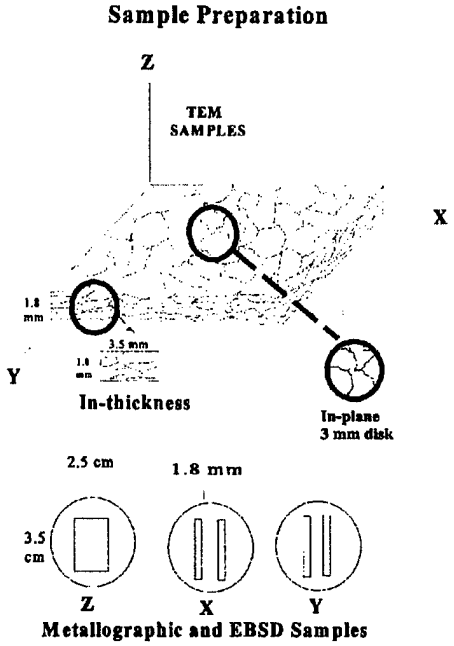

Figure 4.5 Schematic illustration of samples prepared from the in-plane and through thickness sections for TEM, metallographic, and EBSD analysis.

Electron Backscatter Diffraction

Electron backscatter diffraction was performed at TSL Laboratories, Inc., Provo, UT. The details on the scans are as follows: A) Z: 600 μm x 350 μm x 2 μm steps (in-plane surface), B) Z: 1000 μm x 1000 μm x 5 μm steps (in-plane surface), C) X: 600 μm x 900 μm x 2 μm steps (transverse side) and D) Y: 40 μm x 540 μm x 2 μm steps (transverse side). Several plots showing texture and boundary structures were generated.

4.3.3 Results and Discussion

Figure 4.6 illustrates a typical 3-D section view from a representative 2024 aluminum sheet specimen from a well-preserved and non-corroded portion of a KC-135 aircraft body skin. This view illustrates the occurrence of second-phase precipitates and an elongated grain structure similar to the schematic view in Figure 4.2 a. The average aspect ratio (grain length/grain thickness) for the elongated grain structure was found to be about 8. The average grain size of the in-plane view of the sheet (Z axis), and correspondingly the average grain length of the in-thickness transverse sections (X and Y axis) was 175 μm. The grain structure in the plane of the sheet was generally equiaxed as a consequence of cross-rolling schedules during the plate manufacture and elongated grain boundaries were created along each of the transverse sides of the plate.

The microstructure shown in Figure 4.6 illustrates large, second phase precipitates. However,

these precipitates are the largest of a range of different types of precipitates and inclusions. The larger particles are actually impurities created during early alloy solidification and development. Typical features of these large inclusions are illustrated in Fig. 4.7. The more common precipitates which resulted primarily by thermal treatment, and which are more or less uniformly distributed throughout the grain volumes in the aircraft body skin samples, are illustrated in the comparative, tilt-contrast bright-field TEM images shown in Fig. 4.7. There were, as is apparent from Figure 4.6, few examples of the large inclusions associated with the elongated grain boundaries; thereby providing for anodic sites to initiate corrosion assisted exfoliation.

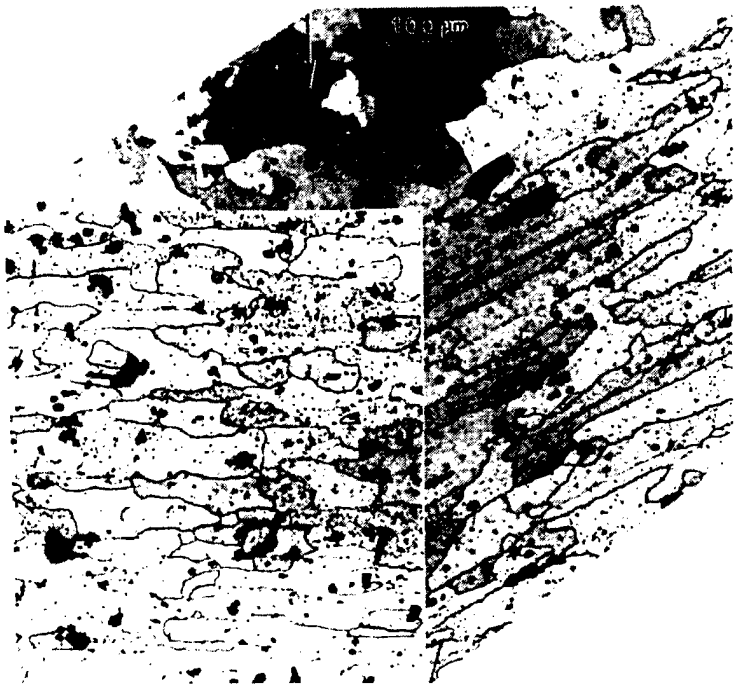

Figure 4.6 Three dimensional structure for a representative 2024 aluminum body skin specimen from KC-135 aircraft.l The arrow indicates the normal to the plane of the sheet.

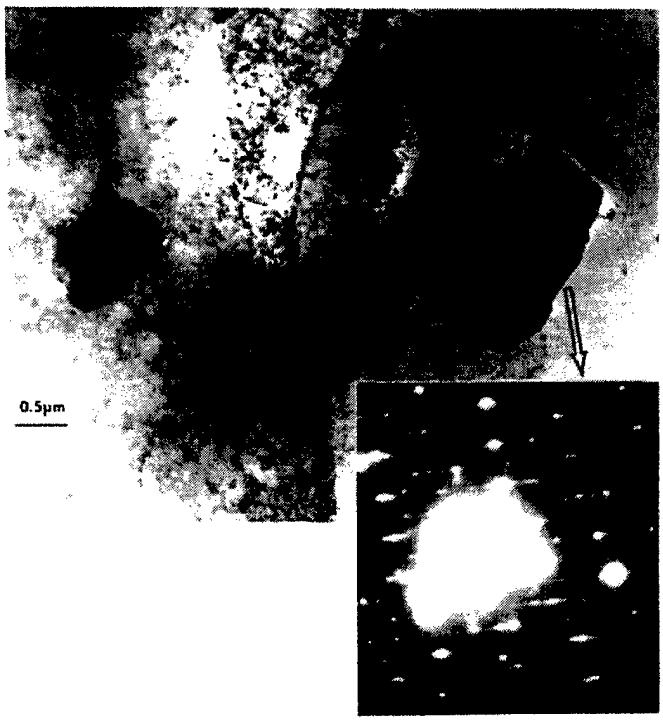

Figure 4.7 Transmission electron micrographic bright-field image showing large inclusion layer structure possibly due to particle shear of faulting during continued sheet rolling. The SAD pattern inset shows the presence of regular domains perpendicular to the diffraction streaks.

A systematic analysis of individual (and generally larger) precipitates in the grain interiors and in the grain boundaries revealed some subtle differences. These differences are illustrated on comparing representative EDX spectra for grain boundary precipitates with precipitates in the grain interior (grain matrix) in Figure 4.8. Figure 4.9 shows a more quantitative and statistically qualitative comparison of the incidence of elemental compositions for grain-boundary precipitates and matrix precipitates. It is observed in the elemental histogram that some grain boundary precipitates contain Si while some matrix precipitates contain less Si, and the difference is replaced by Mn. The majority of the precipitates were of the type CuAl2 and FeCuAlx; with Si and Mn, (CuAl)Si, CuAl(Mn), FeCuAlx(Si) or (FeCuAlx)Mn. These were also numerous AlFex and (AlFex)Si precipitates in the matrix and occasionally in the boundaries. Since Si is more anodic than Mn, this difference may create a tendency for corrosion or oxidation initiation in the grain boundaries in contrast to the matrix. On the other hand, Si combined in an intermetallic would not necessarily be anodic. In this context, it is of interest to note that very recent studies by Wei, et al (1997) in 2024-T3 aluminum have not only identified typical phases to be CuAl2, CuMgAl2, Fe4CuAl23 and a (Fe, Cu, Mn, Si)Al phase, which are somewhat different from those we have identified in these 2024 aluminum aircraft skin samples, but they have also noted matrix dissolution around Fe and Mn-containing particles such as Fe4CuAl23 and (Fe, CuMn, Si)Al; as well as CuAl2 particles. CuMgAl2 particles tended to exhibit matrix dissolution also aerated 0.5 M NaCl solution; consistent with SEM pitting corrosion observations. We did not observe Mg-containing precipitates, and the Mg was observed to be somewhat uniformly distributed throughout the aircraft skin alloy.

Since there are a number of heat treatments (T2, T3, T4, etc.) schedules for 2024 aluminum also sheet, there are a wide range of compositions and morphologies of second phase particles which can occur. This may in fact be a complicating feature in examining aging aircraft skins as well as efforts to elucidate specific corrosion mechanisms.

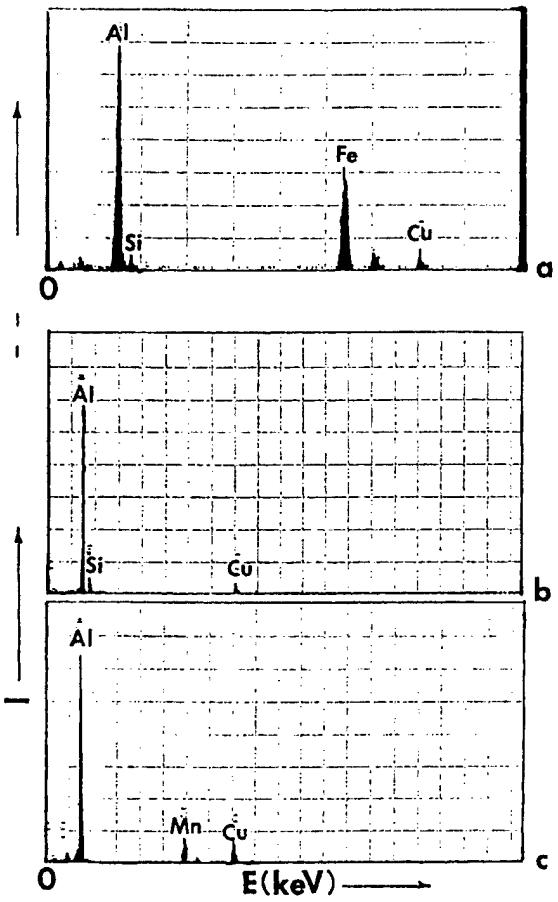

Figure 4.8 Energy-dispersive x-ray spectra: (a) grain boundary precipitate (10.24 KeV full scale); (b) grain boundary precipitate (20.48 Kev full scale); (c) grain interior (matrix) precipitates (20.48 KeV full scale). Note that energy scale is (a) is half that in (b) and (c). Relative intensity is denoted by I.

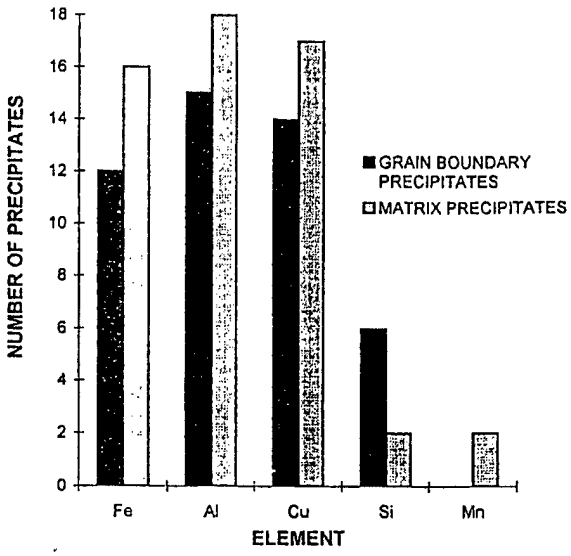

Figure 4.9 Elemental composition histograms for grain boundary and grain matrix precipitate along in-plane view as determined from energy-dispersive x-ray spectra illustrated in Fig. 4.4.

Since the exfoliation illustrated in Fig. 4.1 is unique to the elongated grain boundaries in 2024 aluminum plate thickness, its origin has historically been associated with either grain boundary precipitation, or an anodic feature specific to grain boundary depletion or other elemental concentration (or segregation). Copper depletion, as noted earlier, has been touted as the principal cause for anodic-behaving grain boundaries. However, in dozens of convergent electron beam scans across a variety of grain boundaries along in-plane direction, and between precipitates spaced sufficiently within the grain boundary there have been no indications of either elemental segregation or depletion of copper. While the grain boundary is problematic because it has a rather steep inclination, several analytical profiles across grain boundaries perpendicular to the thin film surfaces also did not illustrate systematic variations in scanned elements, Al, Cu, Si, Mn, Mg, and Fe. In the same context, similar analysis was performed across elongated grain boundaries along the in-thickness direction to determine whether there may exist any variations of scanned elements that would differ from the previous investigation of elemental analysis across grain boundaries along the in-plane direction where grains are not elongated. Table 4.1 illustrates the data obtained at the grain boundary and moving away from the grain boundary at increments of 3 x 10-2 nm. The results are shown in Cu to Al ratios and Mn to Al ratios for the areas under the curves obtained from the EDX spectra. It is interesting to note that Al, Cu and Mn where the only elements that were identifiable across these grain boundaries and as seen in the chemical analysis of the precipitates, there was no evidence of Mg.

Table 4.1. Data obtained from EDX scans across elongated grain boundaries

Ratio of areas	At GB	$3x10^{-2}$ nm	$6x10^{-2}$ nm	$9x10^{-2}$ nm	$12x10^{-2}$ nm
Cu/Al	0.23	0.25	0.24	0.24	0.25
Mn/Al	0	0	0	0	.008
Cu/Al	0.23	0.23	0.25	0.26	-------
Mn/Al	0	0	0.008	0.017	-------
Cu/Al	0.11	0.11	0.11	0.12	0.12
Mn/Al	0	0	0	0	0
Cu/Al	0.11	0.11	0.13	0.12	0.11
Mn/Al	0	0.007	0.022	0	0
Cu/Al	0.12	0.11	0.11	0.11	0.12
Mn/Al	0	0	0	0	0
Cu/Al	0.31	0.38	0.38	0.36	
Mn/Al	0	0.016	0	0	
Cu/Al	0.28	0.28	0.36	0.30	0.31
Mn/Al	0.008	0	0	0	0.017
Cu/Al	0.28	0.27	0.25	0.28	0.28
Mn/Al	0.008	0	0	0.018	0.011
Cu/Al	0.08	0.09	0.09	0.09	0.09
Mn/Al	0.004	0.007	0.007	0.008	0.005
Cu/Al	0.08	0.10	0.09	0.09	0.09
Mn/Al	0.004	0.009	0	0.006	0.009

From the data seen in the Table 4.1, there is no evidence to suggest that there is any elemental segregation or depletion of Cu across the grain boundaries since the Al/Cu ratios are consistent across the grain boundary, however, there does seem to be variations in the amount of the copper/aluminum ratio concentrations from grain to grain which may be attributed to the precipitation phenomena occurring during the heat treatment process. Another peculiarity observed is the variance in the disbursement of Mn from grain to grain which again may be a result of precipitation. However, the data does not display any consistent patterns or trends in the elemental variations that could be attributed to the exfoliation phenomenon in the aluminum alloy sheet metal. Nonetheless, this data may strongly suggest that the traditional theory of exfoliation may be erroneous or incomplete. Many of the previous work performed to examine the exfoliation mechanism has either been performed on a pure Al-Cu system in which they have demonstrated that the potentials become greater at the grain boundaries indicative of anodic behaving grain boundaries as a result of precipitation.

Specimen sections representing each of the three orthogonal views (Figure 4.1 (a)) for exfoliated sheet samples in 2024 aluminum alloy from KC-135 aircraft body skin sections were examined in an SEM in the EBSD mode by TSL Laboratories, Provo, Utah. A 3-D model of the microstructure was developed from the image quality and grain boundary map using the EBSD technique (Figure 4.10). The microstructure seen is very similar the metallographic micrographs obtained. Single-grain kikuchi patterns illustrated in Figure 4.10 were utilized in developing ODFs and frequency distributions for each of these sections Figure 4.11 illustrates the information for one of the sections. This data, which includes essentially similar pole figures and distributions for all orientations X, Y, and Z, illustrates essentially random grain orientation distributions or textures for each of the three orthogonal sections through the sheet specimens, and this seems rather surprising considering the aspect ratio variations in the grains (Figure 4.10) but it points up the fact that grain boundaries in the elongated directions in the sheet thickness do not exhibit any obvious mesotexture either, and direct examination of the mesotexture and microtexture associated with actual exfoliated grains did not exhibit any distinctive features. This is illustrated in Fig. 4.12. However, there is a shift in the misorientation histogram in Fig. 4.12 (b) in contrast to the in-plane analysis shown in Fig. 4.12 (c). The misorientation curves for both the in-plane and in-thickness specimens have a tendency for high misorientation angles.

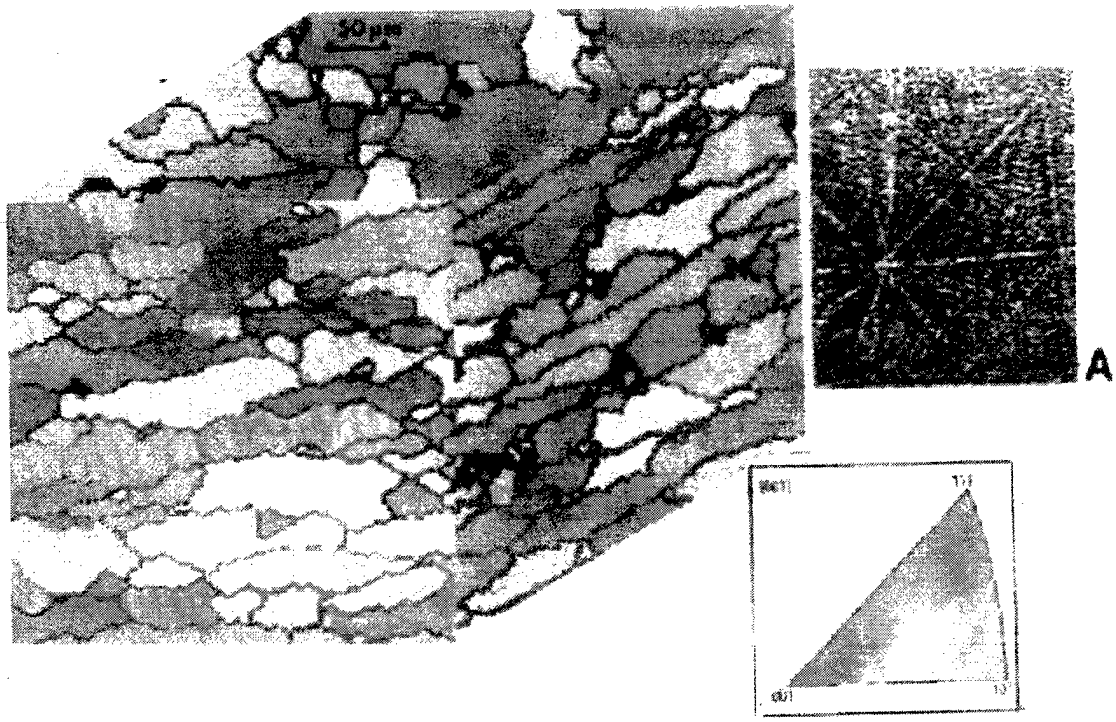

Figure 4.10 SEM generated EBSD data for 2024 aluminum alloy aircraft sheet samples. (A) Reconstructed 3-D view for comparison grain Kikuchi patterns (13). The inverse pole figure insert shows a color scale for the grain orientations shown.

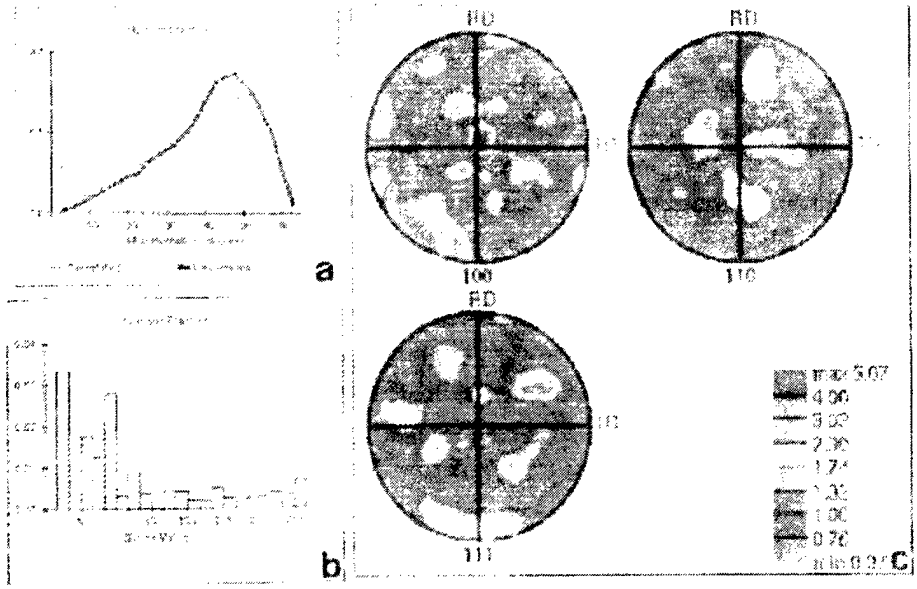

Figure 4.11 (a) Grain misorientation distribution plot for in-plane (Z-axis) data, with pole figure insert (top). (b) Experimental Σ-boundary (mesotexture) frequency plot corresponding to (a). The correlated curves in the distribution shown are the measured distribution while the uncorrelated curves show the distribution determined from texture measurement assuming that no spatial crystallite correlation exists.

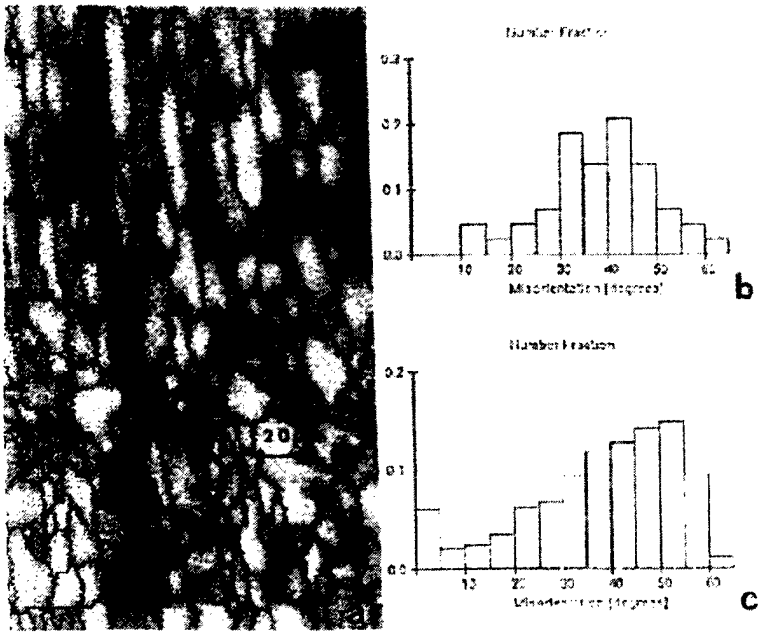

Figure 4.12 SEM-generated EBSD data specific to exfoliation cracks. (a) In-thickness (longitudinal) elongated grains composing exfoliated segment. (b) Random grain misorientation distribution plot composed from EBSD data. (c) In-plane misorientation histogram for comparison with (b).

In the TEM studies to be reported herein, misorientations were measured for (110) and (112) and grain surface orientations, i.e. the misorientation angle (Θ) was measured as the minimum angle between [11-0] directions extended as traces in grains A and B. Preliminary distributions of these (110) boundary misorientations are shown in Fig. 4.13 (a) and (b) which correspond to the transverse and in-plane directions, respectively. Figure 4.13 (c) and (d) shows for comparison a corresponding misorientation distribution histogram for (112) in the transverse direction and (100) and (112) for the in-plane direction. Fig. 4.13 (e) shows the combined measurements of the distribution of the grain boundary asymmetry angles, ϕ, for the elongated grain boundaries in the transverse direction. The data in Fig. 4.13 (a) and (c) show a curious bimodal distribution of low-angle and high-angle boundaries. Since two different orientations ((110) and (112)) show the same trends, there is a compulsion to believe that this trend is a valid one in spite of the dearth of measurements which is in stark contrast to the data generated in the EBSD analysis. Fig. 4.13 (b) and (d) do not follow a strict bimodal distribution rather they have a more even distribution of misorientation angles along the equiaxed (in-plane) grains. This is expected since exfoliation occurs along the elongated (transverse) planes and not along the equiaxed (in-plane) grains. The bimodal distribution that is evident along the in-thickness (elongated) section is an interesting observation since this is the section in which exfoliation is occurring. There seems to be some texturing along the (112) and (110) directions, whereas in this same analysis along the in-plane (equiaxed) grains where corrosion is not occurring texturing is not as obvious (with the addition of one more direction (100)) and the misorientation distribution is much more evenly distributed. However, this may not be statistically correct since there were only a minimal amount of grain boundaries were observed and perhaps the analysis was preferential to these directions. It should be noted, of course, that the low-angle boundaries noted in Figs. 4.13 (a) and (c) are correspondingly low energy boundaries and not special boundaries. Moreover, since there are only two measurements which exceed ϕ– 26E, these trends would tend to reflect interfacial energy regimes implicit in the histograms of Figs. 4.13 (a) and (c).

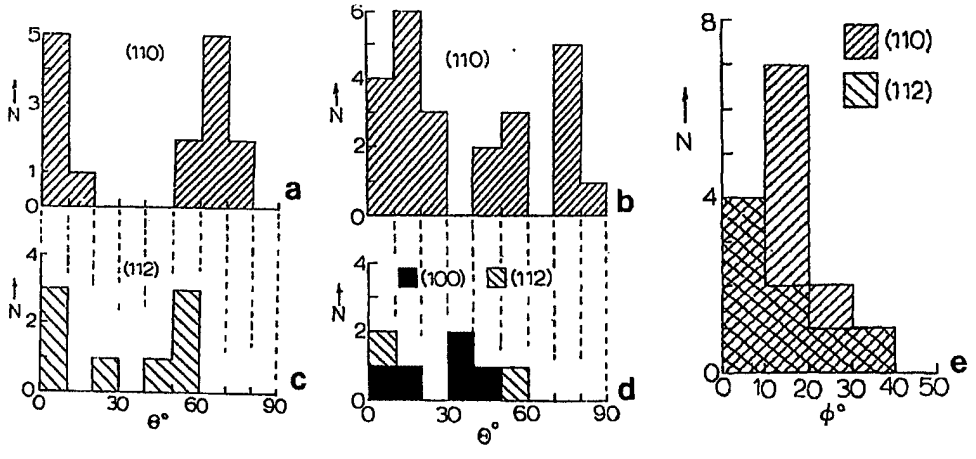

Figure 4.13 TEM measurements of misorientation (Θ) and asymmetry (ϕ) distributions for both in-thickness and longitudinal sheet thickness. (a) and (b) misorientation distribution histogram for (110) for transverse and in-plane sections, respectively. (c) Misorientation distribution histogram for (112) in the transverse view, and (d) misorientation distribution histogram for (112) and (100) along the in-plane view. (e) Asymmetry angle distribution for both (110) and (112) orientations.

4.3.4 A model for exfoliation corrosion

In the absence of any compelling evidence for electrochemical variations (anodic sites, etc.) at the in-plane grain boundaries (10), and the absence of textures or other orientation effects (including mesostructures), as well as preliminary TEM data which suggests the prospects for a peculiar, bimodal, grain boundary energy distribution (Fig. 4.13), a curious dilemma exists. There seems to be no obvious mechanism for nucleating and growing exfoliation crack except for the wedging action of the corrosion products! It is not well understood how boundary precipitates, such as they are, contribute in a significant way to exfoliation, and there is little morphological distinction between matrix precipitates and those observed to be associated with the elongated grain boundaries. However, there must be some simple thermodynamic and kinetic features connected with the migration of oxygen or water vapor (or both) to the crack tip to form AlO(OH) and AlOH wedge products (Figure 4.14). It is possible that as the crack tip advances, new surface (on the grain boundary) could be further embrittled by oxygen or H2O molecular dissociation on the interface, simultaneously creating a corrosion product wedge, and advancing the crack. This might be characterized by a type of dynamic embrittlement which has been described for other systems which crack uncharacteristically (38). Figure 4.15 illustrates the exfoliated cross-section of the fraying aluminum sheet and figure 4.14 shows an SEM view of a similar exfoliated area along with magnified views of the hard and brittle corrosion products seen on the layers. Figure 4.16 is an attempt to depict such a mechanism schematically, utilizing the concepts developed in Chapter 2 of Posadas's thesis (1998). It will be important to attempt to look more critically into the advancing exfoliation cracks in the future in an effort to observe some of these features, and it will be necessary to verify more quantitatively the implications of Fig. 4.2 (a)- (d). If may be, as recently demonstrated by Wei, et al (1997), that anodic precipitates can themselves nucleate corrosion, and this further complicates the process because there is obviously a role played by precipitates in nucleating corrosion.

Figure 4.14 Scanning electron micrograph of the exfoliated 2024 aluminum body skin section shown in Fig. 4.11. The right-hand part of (a) is near the edge of a rivet hole. Insets (b) and (c) show magnified views of specific areas exhibiting heavy corrosion products.

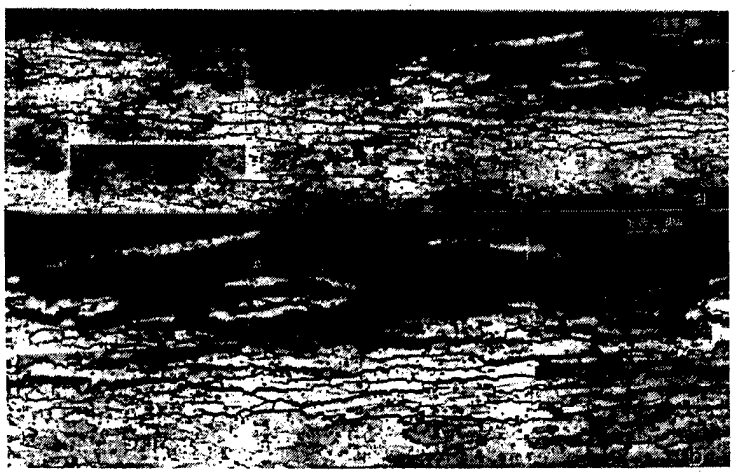

Figure 4.15 Light microscope composition showing extensive exfoliation behavior in 2024 aluminum body skin section: (a) sectional view showing extensive exfoliation; (b) magnified view showing extension of (a) to the right. AA@ is the point of reference.

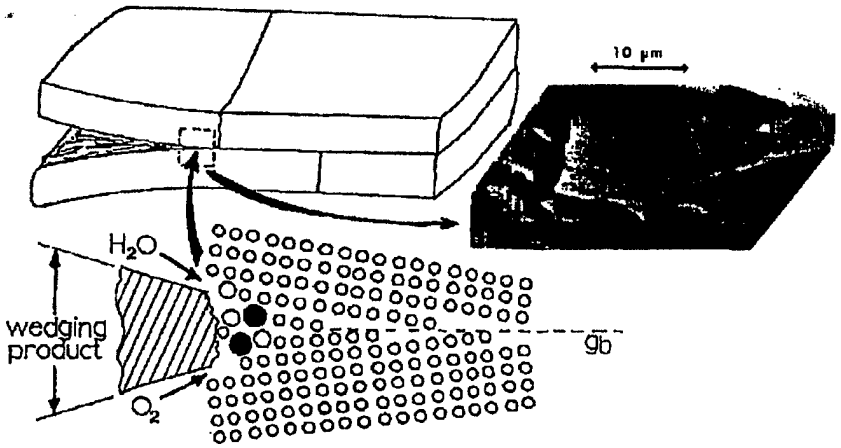

Figure 4.16 Dynamic embrittlement and corrosion product wedging model for exfoliation in 2024 aluminum alloy sheet which incorporates analytical and experimental issues presented in this paper. The SEM insert illustrates the typical appearance of corrosion product on exfoliated surfaces.

4.3.5 Summary and Conclusions of Posada's Thesis

The aircraft skin samples revealed the familiar, definitive features of exfoliation corrosion: numerous intergranular separations parallel to the plane of the sheet, penetrating long distances into

the material along in-plane directions, with voluminous corrosion products apparently wedging between sheets of pancake-shaped grains. However, several of the observations are at odds with conventional concepts of exfoliation mechanisms in 2XXX series alloys. In particular, no copper-depleted zones were found in the boundaries of the in-plane and the transverse sections of the plate, which were examined carefully by using state-of-the art electron microscopic and microanalytical techniques.

The boundaries parallel to the plane of the rolled sheet lie at high angles to the plane of the sheet, whereas the other boundaries which are the elongated grain boundaries along the transverse section of the plate lie at low angles. The included boundaries lack the copper-depleted zones that have been viewed as being characteristic of Al-Cu and 2XXX alloys exhibiting intergranular attack.

The results of this study indicate the conventional picture of exfoliation susceptible microstructures is erroneous or, at least incomplete. The parallel boundaries (elongated boundaries which clearly are participating in classical exfoliation in these samples) also lack copper-depleted zones, but concentrations although constant across the individual boundary, the concentrations varied from grain to grain.

Electron backscatter diffraction and scanning electron microscope were used to examine the microtexture and mesotexture in each of the three orthogonal planes characterizing (3D) sections of 2024 aluminum alloy sheet specimens in exfoliated regions of KC-135 body skin samples. Surprisingly, these comparative measurements and plots of misorientation and distributions for special grain boundaries failed to illustrate any significant anomalies in the elongated grain boundary direction in the sheet thickness, and in fact, pole figure diagrams (and inverse pole figure diagrams) illustrated no significant texture variations; with a random distribution of grain orientations. However, direct measurements of simple misorientations of identical (110) and (112) contiguous grains composing elongated (in-thickness) grain boundaries utilizing transmission electron microscopy and selected-area diffraction techniques revealed a consistent bimodal distribution. The misorientation angles grouped in both the low-angle and high-angle regimes corresponding to low and high energy boundaries respectively as illustrated analytically through model development from first principles utilizing a Read-Shockley dislocation approach. The other grain boundaries along the in-plane view (equiaxed grains) demonstrated a more even distribution throughout the range of misorientations.

In the absence of any compelling evidence of elemental deficiencies or excesses at the grain boundaries for this 2024 Al alloy, there must be some other contributions to an effective grain boundary embrittlement promoting or facilitating exfoliation. Corrosion product formation may also affect embrittlement and create crack-tip stresses to propagate cracks. A simple model has been developed which attempts to illustrate these possible features.

Finally, we have attempted to illustrate the utility of EBSD analysis in evaluating prospects for microstructure and mesostructure variations which may contribute to corrosion problems in sheet specimens. Even though the results are not particularly helpful in delineating the mechanisms of exfoliation in 2024 aluminum alloy sheet from a KC-135 aircraft, the approach may have potential in other related aluminum alloy sheet problems, and may provide or provoke new analytical directions or other innovative approaches. This effect would only occur dynamically, that is, at the time oxygen

presented by the elongated grains in the thickness section; consistent with the aspect (geometrical) features which have already been documented. Tenacious coatings to prevent O_2 and H_2O access, especially along the sheet edges, around rivet holes, etc. This concept might be proposed in future studies.

4.4 Retrogression and Reaging Heat Treatment on Post Service KC-135 Sections

Programmed Depot Maintenance (PDM) are performed every four years on the KC-135. A KC-135 at its PDM at Tinker Air Force Base is shown in Figure 4.17. This maintenance requires the aircraft body be carefully inspected for any problems such as corrosion or cracks, hydraulics, electrical and avionics systems. Paint stripping is required at PDM assess corrosion damage. The environment KC-135 aircraft fly in and the number of years in service have caused corrosion degradation problems.

Stress corrosion cracking (SCC) has been observed in bulkheads, stringer ties, wing spar chord, wing production breaks, floor beams, wing terminal fittings, and upper wing skins of the KC-135. The majority of these parts are made of 7075-T6 aluminum alloy. Some KC-135 aircraft structural parts made of Al 7075-T6 alloy have been replaced with Al 7075-T73. Corrosion resistance of the T6 alloy can be improved by overaging to the T73 condition. The T73 offers better resistance to stress corrosion cracking and exfoliation corrosion. However, a tradeoff of the T73 heat treatment is the loss of material strength. The yield strength of 7075-T73 is about 10-15% lower than that of 7075-T6 (Rajan, et al., 1982). Many aircraft components requiring high strength and wear properties cannot transition from a 7075-T6 to a T73 aluminum alloy due to this decrease in strength. A new heat treatment that may be used instead of T73 is retrogression and reaging (RRA) heat treatment. Researchers believe that the Retrogression Reaging (RRA) heat treatment improves the corrosion resistance of Al 7075-T6 alloy without affecting the strength as much as the T73-treatment (Cina, et al, 1973 & 1974).

The purpose of the research performed by Campuzano-Contreras (2000) was to investigate if parts that have been in service on the KC-135 could be removed from the aircraft and heat-treated to the RRA temper in order to improve the properties of the part. A combination of T6 strength and T73 stress corrosion resistance was sought. Several researchers have investigated the effects of the retrogression and reaging heat treatment on new samples of aluminum alloy 7075, but only a few have studied the effect it has on parts that have been in service. A potential payoff of the retrogression and reaging heat treatment was that the resistance to SCC can be improved at minimal cost for parts that have been or are in service. Technicians would not have to wait for new parts; they could perform the RRA heat treatment instead. Reducing the amount of days in the PDM process reduces cost. RRA treatment also could achieve lower total labor costs and conservation of materials and energy because the part will not be replaced by a new one. For parts that are no longer in production, the setup costs to produce small numbers of new replacements can be very high.

Figure 4.17 KC-135 fuel tanker at its Programmed Depot Maintenance (PDM) at Tinker Air Force Base. The paint has been removed.

One of the parts that was of major interest was the bulkhead. The large size and weight of the bulkhead make it inconvenient to work with in laboratories; therefore, smaller stringer ties, with similar properties, were used for her investigation. Stringer ties are forged and made of 7075-T6 aluminum alloy. A typical stringer tie is shown in Figure 4.18. Figure 4.19 demonstrates where some stringer ties are located in the aircraft. They are tying the stringers together. The stringer ties were obtained from thirty to thirty-five year old KC-135s from Tinker Air Force Base. The years of service and the actual environment the stringer ties were in service were unknown.

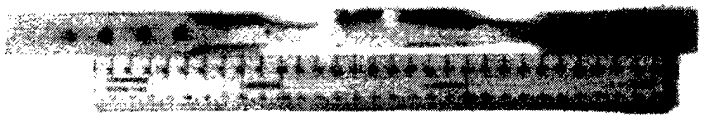

Figure 4.18 Stringer tie taken from a KC-135.

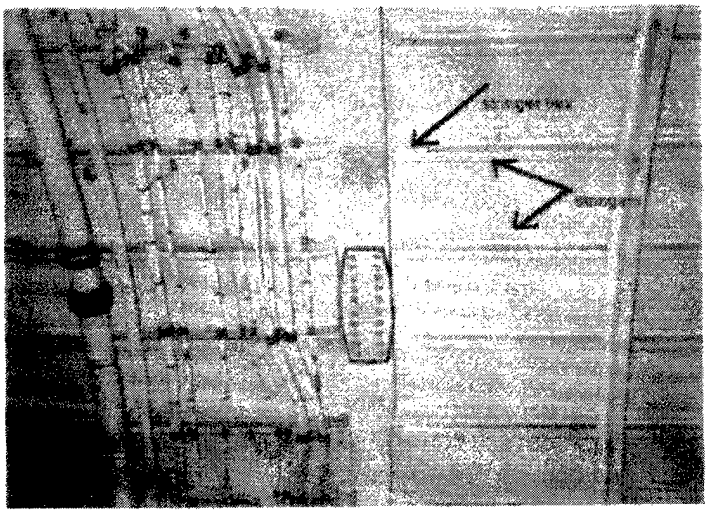

Figure 4.19 Inside a KC-135 showing a location where stringers and stringer ties are located.

Cina et al. (1973, 1974) developed a retrogression and reaging (RRA) heat treatment in search of a method of substantially reducing the susceptibility to stress corrosion cracking of the 7000 series aluminum alloys while still retaining their original mechanical strength. Retrogression and reaging heat treatment consists of a short time retrogression anneal in a temperature range within the two-phase ($\alpha + \eta$) region of the phase diagram (Park & Ardell, 1984). In other words, the retrogression step is in a temperature range above that of aging, but below that of the solution treatment. After the retrogression anneal the material is water quenched followed by a reaging treatment.

4.4.1 Summary of Experimental Work

The stringer tie sections were used to study the effects the overaging treatment (T7X) and the retrogression and reaging heat treatment would have on the post service parts. Hardness, conductivity, polarization resistance and tensile strength values were examined. Transmission electron microscopy (TEM) was also conducted to follow the microstructural evolution with heat treatment, look at the size and amount of precipitates, and to establish any existing relationship between the properties of the material and the precipitates.

Specimens used for transmission electron microscopy, optical metallography, and polarization tests were cut from the stringer ties and measured 2-cm in length, 1 cm in thickness, and 2 cm in width. For tensile strength determinations samples as seen in Figure 4.20 were used. Conductivity values were obtained to verify if the heat treatments performed/obtained were in the range of their perspective conductivity values. Tensile strength experiments were performed to correlate the hardness to their perspective heat treatment.

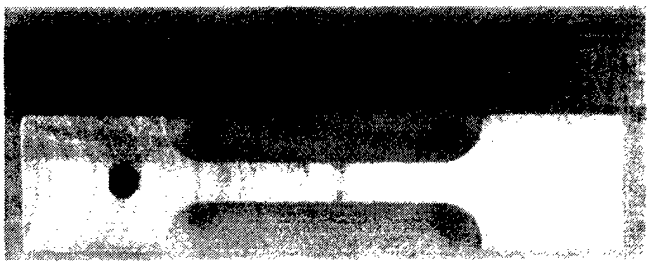

Figure 4.20 Sample of a test specimen used for tensile testing, the thickness is approximately 0.25 inches.

In order to obtain the overaging treatment (T7X) and the retrogression and reaging heat treatment the following was performed. Heat treatments were carried out on the specimens and silicone oil baths were used for the RRA and T73 heat treatments. The following times were used for the retrogression anneal: 5 seconds, 10 seconds, 30 seconds, 60 seconds, 5 minutes, 10 minutes, 15 minutes, 20 minutes, 30 minutes, and 60 minutes. The retrogression temperature used was 220^{0}C. The retrogressed samples were analyzed with optical metallography, microhardness measurements, conductivity measurements, and the TEM. The samples were then aged at 120^{0}C for 24 hours to complete the retrogression and reaging heat treatment. The T73-like samples were heat treated to their overage condition. To obtain an overage temper, similar to the T73 temper, the as-received samples underwent a dual heat treatment. The samples were not solutionized before performing the dual heat treatment. They were first aged at 105^{0}C for 8 hours, water quenched and aged at 175^{0}C for 8 hours.

4.4.2 Summary of RRA Results

The post-service material retrogression and reaging results obtained by Campuzano-Contreras (2000) were generally consistent with published information. Hardness values obtained by retrogression and reaging were similar to published results in almost every case. However, one of the stringer ties showed anomalous post-RRA hardness (and conductivity). This specimen had an atypical, large-grained microstructure that almost certainly resulted from some anomaly in the original T6 heat treatment.

For retrogression times of one minute or less at 220 C, the electrical conductivity values were similar to those of the as-received (T6) material. After longer retrogression times (30-60 minute), the RRA-treated material approaches the conductivity of the T73-like condition. These trends agree with the published literature. However, the samples in the T73-like condition have conductivity of only 38% IACS, which barely meets the minimum that is sometimes specified for 7075-T73. Published values are higher, about 40 to 42% IACS, for T73 and longer-time RRA tempers.

In 3.5% NaCl solution, these samples all displayed free corrosion potentials of -672 to -695 mV relative to the saturated calomel electrode (SCE). Anodic polarization scans showed the T6 and one-minute RRA specimens were at or near a localized film-breakdown condition at the free corrosion potential. The T73-like condition exhibited passive behavior during this test. The specimens regressed for longer times (5 and 60 minutes) showed a fragile passivity, with the localized film breakdown potential only 5-8 mV higher than the free corrosion potential. These observations

observations suggest that the susceptibility of the RRA tempers to localized, grain-boundary corrosion is slightly better than that of the T6 condition, but not as good as that of the T73 condition.

Average yield strength values for post-service stringer tie samples that underwent the RRA heat treatment were greater than the published T6 yield strength values for alloy 7075.

4.5 Pitting Corrosion of Aluminum Alloys

Initially, the research performed by Obispo (1999) was directed towards the observation of second-phase particles, in order to determine their role in pitting corrosion. It seems that the second-phase particles, especially the larger particles (> 2 mm), were preferential sites for pitting. Optical microscopy and scanning electron microscopy were employed on polished samples both before and after corrosion testing, where the same areas on the samples were analyzed in order to determine the location of pits and/or corrosion products.

In addition, samples were observed at high magnification in the scanning electron microscope; and using energy dispersive x-ray spectrometer, copper-rich particles were identified. These copper-rich particles were observed to be plating preferentially on iron-containing or iron-rich precipitates. The importance of the presence of copper-rich particles can be attributed to the role these may have in the pitting corrosion of aluminum.

Following these initial observations of apparent copper plating, a replica-based lift-off technique to extract especially intact copper particles from aluminum alloy 2024 surfaces after exposure to NaCl solutions, ranging in pH from 3 to 11, was used. These replicas were then observed using transmission and scanning electron microscopy.

In addition, transmission electron microscopy and energy dispersive x-ray spectroscopy were used to identify the different types of second-phase particles present, and to develop an inventory of these particles in the 2024 aluminum alloy.

In general, the objective of Obispo's research was to attain a better understanding of the pitting corrosion of the aluminum alloys, and the different factors, especially the presence of copper-rich particles, that play a a role in the corrosion process.

4.5.1 Overview of Pitting Corrosion

Pitting corrosion is a localized attack where the rate of attack is much greater at certain small areas on the surface, while other areas of the materials are unaffected. Pitting corrosion is the least predictable type of corrosion. Pitting may cause perforation of the material, and subsequently cause failure of the component in use (Jones 1992; Schweitzer 1996).

Pitting corrosion involves two principal stages, pit initiation and propagation. The propagation of pits is well understood, however, there has been mayor complication in order to

develop a good understanding of the initiation of the pits. There are many factors, such as the presence of an oxide layer, pitting potential, alloying elements, and second phase particles, to be considered in order to have a better understanding of the corrosion of aluminum and especially aluminum alloys.

Aluminum owes its corrosion resistance to a thin oxide layer that forms naturally on the surface of the metal. This film has a thickness of approximately 5 nm (50 A) when formed in air, but the thickness can be increased by formation at elevated temperatures or in the presence of water or water vapor (Schweitzer 1996, Hatch 1984). The oxide layer is very stable in air and neutral solution or in solution with a pH range of 4 to 8.5 (Jones 1992). The oxide film, however, is not very homogenous, and therefore weak. The film is non-homogenous due to the presence of impurities, which form new structures and destroy the continuity of the film. As a consequence, localized corrosion initiates at the weak points, causing the breakdown of the oxide film (Jones 1992). Three possible mechanisms for the initiation of pitting corrosion, due to the presence of chloride ions are shown in Figure 4.21. Pitting may initiate due to incorporation of anions (e.g. Cl^-) into the passive oxide layer, or due to adsorption of the anions, or through tearing of the oxide layer. However, there are other factors, such as impurities, that have an influence on how the oxide layer behaves (Kaesche 1985). Furthermore, the film becomes less homogenous due to the heat treatments performed on the aluminum and its alloys, and thereby decreasing the corrosion resistance of the metal. The electrochemical stability of the protective passive film and the ability of the film to repair itself in an environment determine its resistance to pitting corrosion (Chen et al. 1996).

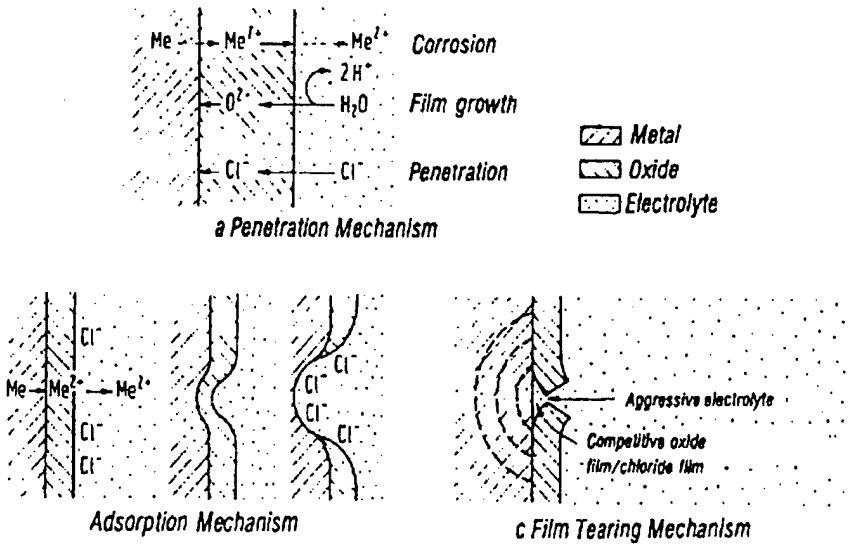

Figure 4.21 Schematic sketch of three possible initiation process for pitting: a. through incorporation of anions into the passive oxide, b. through island adsorption of anions on the passive oxide, c. through tearing of the passive oxide (Kaesche 1985).

4.5.2 Mechanisms of pitting corrosion.

For many decades, numerous investigations have been conducted on the pitting corrosion of aluminum alloys. Pitting corrosion has been recognized as a multiple step process, which brings coherency between the different types of investigations performed on the pitting corrosion of aluminum alloys, over the years. It may be easier to recognize pitting corrosion as being part of these steps, in order to have a better understanding of the pitting mechanism. The following four steps are implied in the formation and growth of pits:

1. The adsorption of reactive anions in the aluminum oxide layer.
2. The chemical reaction between the absorbed anions and the aluminum oxide.
3. The thinning of the oxide film by dissolution.
4. The direct attack of the metal surface by the metal ions.

Most of the research has been done in salt (NaCl) solutions in a range of pH values.

Adsorption Step

The initial group of researchers has suggested that chlorine-ions are adsorbed in the aluminum oxide layer, causing these sites to be the primary sites for pit formation. In addition, other inorganic ions, besides chlorine ions, can be adsorbed in the oxide layer, when the latter is exposed to an electrolyte. Furthermore, no applied potential is necessary during the adsorption process. This than calls for the question of the nature of the compound formed upon adsorption. Moreover, the research implies that the ion adsorption takes place at flaws in the oxide layer (Foley 1986).

Considerable attention has been given to determining the pitting potential of aluminum, which is related to the pit initiation and propagation. Once the pit is initiated, the growth takes place at lower potential. The pitting potential has been found to decrease with an increase in the CI ion concentration, but this decrease does not occur linearly (Foley 1986). The rate of initiation on the other hand, increases with the increase in Cl ion concentration. However, the pitting potential can not be used as a measure for pitting susceptibility, since the adsorption of ions is not directly dependent on the alloy composition.

Chemical Reaction Step

Over the decades, it has been proven that intermediate soluble complex compounds are formed by chemical reactions, once the ions are absorbed in the oxide layer. The nature of these compounds is pH related. It has been concluded that the Cl^- ion reacts directly with the surface to promote pitting, and that chloride is aggressive as a result of the solubility of the aluminum-chloride compound . The researchers have also suggested that $AlCl_3$ solutions could activate passive aluminum, and therefore initiate pitting. The formation of complex compounds can be understood with the following reactions:

$$Al^- + 2Cl^- = AlCl_2^+ \text{ (absorbed)} + 2e$$
$$AlCl_2 \text{ (absorbed)} = AlCl_2^+ + e$$

Thinning of the Oxide

Aluminum owes its corrosion resistance to the oxide layer that forms on the surface. As was

mentioned in the previous sections, the penetration of chlorine ions into the oxide layer is a cause for pitting corrosion. It has been proven that the oxide layer gets thinner when exposed to aqueous solutions. Furthermore, this oxide layer is not homogenous, which makes the dissolution process a flaw-assisted or a flaw-centered process. These flaws can be either mechanical or residual. Mechanical flaws involve scratches, defects, or presence of crystallographic asymmetry, while residual flaws involve the presence of second phase particles on the metal surface. These flaws are preferential sites for ion absorption, which will create active sites. These active sites will cause the accelerated thinning of the film.

Another group of researchers directed some studies towards the physical nature of the oxide film. The film was considered to be a face-centered γ-Al_2O_3 structure, and that some Al^{+++} ions were occupying oxygen position (Foley 1986). Under these circumstances, they have suggested that the corrosion reaction embraces the diffusion of aluminum ions and electrons through the oxide film via cation and anion vacancies (Buchheit 1997). Consequently, a high electrical field that draws the aluminum ions through the film is created with the adsorption of the anions in the oxide layer.

Direct Attack of Exposed Metal

During the first three steps defining pitting corrosion, Cl ions are adsorbed in the oxide layer, complex compounds are formed, and thinning of the film takes place. Thinning of these films take place at local areas, the attack to the metal will also be localized. This section is concerned with the growth of the pits. During the growth process there will be an interaction between the metal surface and the environment in which it evolves. This environment is constantly changing as the reaction proceeds. Furthermore, the composition of the solution inside the pits is different from the outside composition (Foley 1986).

Investigations have been directed towards the determination of the morphology of the pits. It has been suggested that the morphology of the pit changes with the types of aggressive anions, and with the applied potentials. Pits that grow near the pitting potential have a crystallographic nature, while pits growing away from the pitting potential have a smooth polished appearance.

Second phase particles are considered to be preferential sites for pitting corrosion. These segregated particles make the oxide film heterogeneous. The alloy's heterogeneity is the cause for an accelerated attack of the metal, since the second-phase particles create galvanic sites due to their potential differences.

Constituent Particles

In more recent years, investigations have been directed towards the presence of constituent particles or second-phase particles exposed on the metal surface, identifying their chemical composition, and the role they may have in the pitting mechanism (Wei et al 1996). Chen et al. (1996) suggest that these particles are preferential sites for pitting corrosion. Galvanic sites are created between these particles due to the difference in electrochemical activity.

The particles have different roles in the corrosion process. In accordance to Chen, et al. (1996) particles containing Al-Cu-Mg show to have a very anodic behavior. On the other hand, Al-Cu-Mn-Fe containing particles may have a more cathodic behavior. Consequently, galvanic couples

are created, which will promote localized attack (Schweitzer 1996).

According to Buchheit, et al. (1997), the Al_2CuMg particle, identified as the S-phase, show a dealloying behavior, whereby the particle will dissolve away leaving copper rich particles behind. These particles will then induce pitting to the surroundings. Furthermore, some of the copper particles may form a cluster and detach from the aluminum surface. These particles may then be transported away from the pit, either through the solution or by mechanical action of growing hydrous corrosion product.

4.5.3 Summary of Obispo's Contributions

Obispo found clusters of copper and copper-rich particles at inclusions or other surface sites after short-time corrosion testing in almost neutral (pH = 6), acid (pH = 3), and basic (pH = 11) sodium chloride solutions (0.6 M NaCl). The copper clusters had a microdendritic appearance. Similar copper clusters were observed on 2024 aluminum alloy surfaces after samples were immersed in the same solutions for 5 days.

A replica lift-off technique was used to remove copper particles along with other corrosion products from the samples after 5 days exposure to salt solutions. The copper clusters observed in the TEM have fine microdendritic appearance when exposed to a neutral and basic salt solution. However, when in acidic environments, the clusters had a more dense and nodular appearance, which indicates that the copper deposition process is pH dependent. These copper clusters appear to be growing randomly on the aluminum surface, and not only at specific sites where precipitate particles emerge.

The observations made in this work were very consistent with electrochemical displacement reactions where copper in Cl^- solutions is deposited on a more electropositive aluminum substrate. In the presence of sufficient Cl^- ions, the protective aluminum oxide layer is degraded, copper will then be released in solution, which will nucleate and grow on the aluminum surface, thereby causing further degradation or pitting of the surface, by releasing Al^{3+} and some Cu^{2+}.

Eight different types of second-phase particles were identified by TEM analysis done on the aluminum 2024 alloy samples. The five more prominent particles were Al-Cu-Fe-Mn, Al-Cu-Si, Al-Cu-Mg, Al-Cu-Fe-Mn-Si, and Al-Cu-Fe. The Al-Cu-Mg inclusions are not as prominent as documented by other researchers for 2024 aluminum. The copper clusters observed in the SEM were usually associated with Fe-containing particles, possibly indicating that the copper is depositing on the more electropositive Fe-containing inclusions.

The actual deposition of copper from dilute, aqueous solutions onto 2024 aluminum alloy surfaces as observed in this research represents a new concept, and indeed a new mechanism contributing to pitting corrosion in 2024 aluminum alloy, and possibly older copper-bearing aluminum alloys. Additional work on related aluminum alloy systems may shed more light on this concept, or validate the results observed here for 2024 aluminum.

Obispo, et al. (2000) have recently shown that the deposition of copper onto the surface of aluminum 2024 is a consequence of cementation. The copper ions (Cu^{+2}) in solution either from the particulates or from the matrix deposit as elemental copper on the aluminum surface. This leads to additional pitting. Figure 4.22 depicts the action of the mechanism .

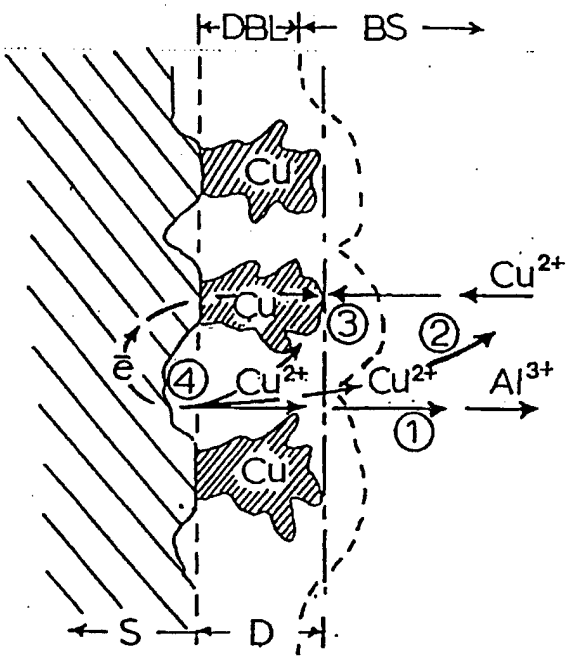

Figure 4.22 Schematic diagram depicting the copper deposition mechanism on aluminum matrix. At anodic areas Al^{3+} and Cu^{2+} ions are released from the alloy into the solution as the alloy corrodes (1 and 2). When the local copper concentration becomes sufficient, copper begins to surface. Electrons (e^-) are conducted from dissolution sites to the deposition sites (4), allowing the Cu deposit to grow. Figure Key: S -substrate, D — cu deposit, DBL — diffusion boundary layer, BS — bulk solution (NaCl), (Obispo, 1999).

4.6 A Corrosion Study of Aluminum 2524

The work of Cervantes (2001) was performed on samples of aluminum 2524 procured from Alcoa. The point of concentration for this study was guided by six objectives. These were, to::

1. Provide an elemental chemical analysis for the aluminum 2524 sample.
2. Expose aluminum 2524 samples to free corrosion testing in salt solutions with different pH values.
3. Expose samples to short-term corrosion testing at a controlled potential.
4. Observe, identify and categorize the microconstituents in aluminum 2524.
5. Observe and provide information on surface copper deposition.

6. Give a comparative overview between aluminum 2024 and aluminum 2524.

Samples of the aluminum 2524 alloy were observed under the scanning electron microscope. The energy dispersive X-ray spectrometer provided information the elemental composition of the constituent particles. A replica lift-off technique was used to remove the copper particles from the alloy's surface after the samples were subjected to corrosion testing. These replicas were observed under the transmission and scanning electron microscope.

The results of this study point to the involvement of electrochemical reactions in the deposition of copper on the surface of the aluminum 2524 alloy.

4.6.1 Aluminum 2524 Background

Recently, the aluminum alloy 2524 has been introduced and used on aircraft fuselage skin. (Staley, Liu and Hunt, 1997). This alloy exhibit improved fracture toughness and fatigue crack growth resistance when compared to the 2024 alloy. Studies performed by the team of Bray, Bucci, Colvin and Kulak, (1997) suggest that the fatigue strength of 2524 is 10% greater than the 2024 alloy and the lifetime to failure is 30 to 45% longer. The 2524 alloy shows a less damaging configuration of corrosion pits and exhibits a better fatigue crack growth resistance.

In aluminum alloys, high strength is achieved by the addition of copper as an alloying element. However, copper can lead to deleterious effects due to its corrosion activity resulting from the galvanic couples that exist between the copper rich inclusions and the copper depleted matrix. (Dimitrov, Mann and Sieradski, 1999).

Certain heavy metal ions such as Cu, Pb, Hg, Ni, and Sn and their corresponding potentials are an important factor when considering the corrosion resistance of aluminum alloys. Copper is the most common metal associated with aluminum alloys. Some metal ions are more cathodic than the solution and can be reduced to metallic form by aluminum. Usually, aluminum serves as the anode in galvanic cells. For each chemical equivalent of metal ion reduced, an equivalent of aluminum is oxidized. The reduction of these ions causes severe localized corrosion. The reduced metal ions plate onto the aluminum and galvanic cells are produced. These metallic ions are important in acidic solution. In alkaline solution, they usually show a lower solubility and less severe effects. The following factors are important to consider in the initiation of pitting on aluminum. They include (1) copper-ion concentration, (2) pH of the water, (3) chloride ion concentration and (4) if the pits are open or occluded. The low corrosion resistance of aluminum alloys results from the reduction of copper ions that are present in the corrosion product of the alloy. The corrosion rate of the aluminum coupled with copper in the presence of chloride ions is reduced in an environment that lacks oxygen (Jones, 1992).

Copper is a major alloying element in the 2xxx wrought and casting aluminum alloy series. These are in general, less resistant to corrosion when compared to other aluminum alloys of other series, which contain lower amounts of copper. The electrochemical corrosion is more of a problem in these alloys because after certain thermal treatments microscopic galvanic cells can develop

because of the particle deformation of copper. Resistance to corrosion decreases as the copper concentration increases. However, galvanic cells between the solid solution and second phase particles are not the most damaging aspect of this corrosion susceptibility. Rather, the galvanic cells created by the presence of copper particles and copper films which can be deposited on the alloy as a result of corrosion, can aggravate further corrosion damage. As the corrosion process proceeds, the copper ions first go into solution and then plate onto the alloy surface to form metallic copper cathodes. The reduction of the copper ions along with an increase in oxygen and hydrogen ion concentration enhances the corrosion rate (Jones, 1992).

The 2xxx aluminum alloys are solution heat-treated and can be used as either the naturally aged or the precipitation heat-treated temper. If a good heat-treated practice is in force, this can minimize the micro-galvanic cell effects on corrosion resistance.

In the work of Cervantes (2001) samples of aluminum 2524 were subjected to corrosion immersion experiments in salt solutions having different hydrogen-ion concentrations similar to those performed by Obispo. The results of Cervantes' study were consistent with those of Obispo, et al (2000). At an acid pH, the nodular copper deposits were evident near iron containing constituents. Copper clusters were seen over the surface of the alloy as well as the surface inclusions. Also, at pH 3, there is the presence of pit coalescing. At a basic pH, the copper deposit was dendritic. The constituents present at this pH were Al-Cu-Si-Mn. These may act as cathodic sites as elemental copper deposits on the surface of alloy. The results indicate that electrochemical reactions are at play.

The team of Obispo, Murr, Arrowood and Trillo, (2000), concluded that in the corrosion process of aluminum 2024, some particles act as cathodic centers while others are anodic. Copper ions are produced and dissolve in solution and then elemental copper deposits. The copper deposits may be nodular or dendritic. At acidic and neutral pH levels, copper deposits near iron rich particles and takes on a nodular appearance. Electrochemical activity is the process by which elemental copper deposits on the surface of the alloy.

4.6.2 Summary and Conclusions of Cervantes' Work

Samples of aluminum 2524 alloy were subjected to short-term and long-term corrosion test then observed using the scanning electron microscope. The energy dispersive X-ray spectrometer provided information on the elemental composition of the second-phase particles or inclusions. A replica lift-off technique was applied to remove the surface particles from the alloy's surface for TEM examination after the corrosion tests.

Samples of aluminum 2524 were subjected to corrosion tests at different hydrogen-ion concentrations in a 0.6 M sodium chloride solutions. Microstructure and elemental analyses reveal that copper is a major player in the corrosion process of the aluminum 2524 alloy. After the short-term potentiostatic tests in salt solutions at pH 3, pH 6 and pH 11, the SEM micrographs show the presence of free copper. The morphology of the copper deposits was nodular in all three environments. Copper clusters were evident over the entire surface of the alloy as well as in the surface inclusions. At pH 3, extensive pit coalescence was also visible (Figure 4.23).

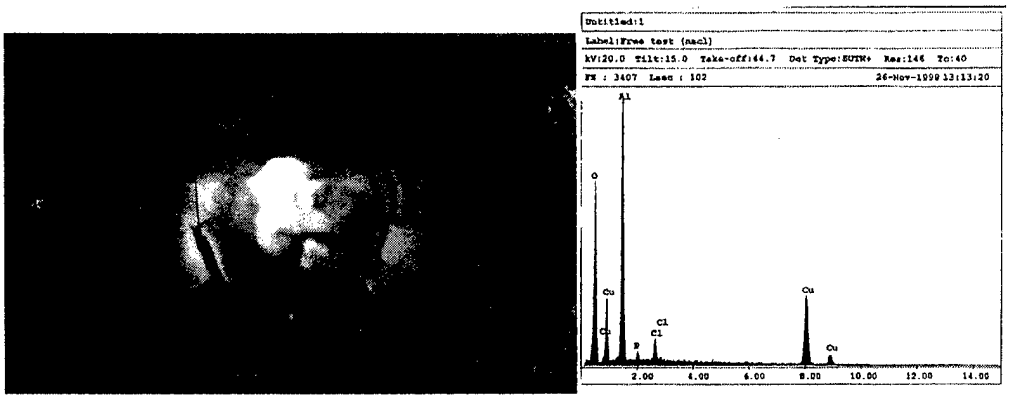

Figure 4.23 Shows a pit containing copper clusters on the surface of aluminum 2524 after corrosion tests in an acidic solution. The EDX shows presence of copper.

After a five-day exposure to a salt environment (0.6 M NaCl) at pH 3, pH 6 and pH 11, the aluminum 2524 samples were examined by the SEM. A replica lift-off technique was also used to remove the surface particles and/or inclusions from the alloy. The micrographs show a nodular morphology for the copper precipitate at pH 3 and pH 6. At pH 11, the morphology of the copper deposit was dendritic. These results are consistent with those cited by Obispo, et al., 2000. In the Obispo study, nodular copper deposits were found in aluminum 2024 after the free-corrosion tests were applied in salt solutions at pH 3 and pH 6. At the basic pH of 11, the dendritic copper deposit was identified. Consequently, the results of this study reproduce and confirm those of the Obispo research.

The results of Cervantes (2001) point to a link between the hydrogen-ion concentration and the morphology of the copper obtained through deposition. The nodular copper deposits in an acidic salt solution suggest that copper is depositing on the more electropositive matrix. Bray et al., (1997) maintains that the aluminum 2524 forms large pits through pit coalescence. The present study shows various SEM micrographs that point to pit coalescence. Aluminum 2524 seems to have fewer but large corrosion pits on its surface compared to Aluminum 2024. In a study of copper cementation on another alloy of aluminum, Murr and Annamalai (1978) suggest that a dendritic copper structure forms in a basic pH and low chloride ion concentration. The present study confirms the presence of a filamentous copper structure in a basic pH.

The observations from this study point to electrochemical reactions at play where copper in the presence of a chloride environment deposits onto an aluminum rich surface. The copper ions from the matrix concentrate in the solution layer at the metal's surface and deposit as elemental copper. The copper deposits promote further pitting in the alloy.

4.7 References

V. S. Agarwala, *Aircraft Corrosion in the Military - Maintenance and Repair Issues*, NACE International Corrosion/98 Conference, San Diego, CA, Paper No. 597, 1998.

Bray, C. H., R. J. Bucci, E. L. Colvin and Michael Kulak. "Effect of Prior Corrosion on the S/N Fatigue Performance of Aluminum Sheet Alloys 2024-T3 and 2524-T3," Effects of the Environment on the Initiation of Crack Growth, ASTM SW 1298. American Society for Testing and Materials, 1997.

R.G. Buchheit, E.P. Grant, P.F. Hlava, B. Mckenzie, and G.L Zender, *Journal of The Electrochemical Society,* 144 (8) (1997) 2621-2628.

Campuzano-Contreras, Ana Leticia, "Retrogression and Reaging Heat Treatment on Post-Service KC-135's Sections," Master of Science in Metallurgical and Materials Engineering, The University of Texas at EL Paso, May 2000

Robert Cervantes, "A Corrosion Study of Aluminum 2524 Microconstituents and the Consequent Mechanism for Copper Deposition on the Surface of the Alloy, "Master of Science in Metallurgical and Materials Engineering, The University of Texas at EL Paso, Dec. 2000.

G.S. Chen, M. Gao, and R.P. Wei, *Corrosion Science,* 52(1) (1996) 8-15.

B. M. Cina and B. Ranish, in *"Aluminum Industrial Products, Pittsburgh Chapter, Pittsburgh"* (ASM, Metals, Park, Ohio, 1974).

B. M. Cina and R. Gan, U.S. Cl. 148-159, Mar 13, 1973 Ser. No. 340,757. *Crystalline Solids,* Inst. Metals, London (1968) 36.

Dimitrov, N., J. A. Mann and K. Sieradzki. "Copper Redistribution During Corrosion of Aluminum Alloys," Journal of the Electrochemical Society. 146 (1) (1999) 98-102.

R.T. Foley, *Corrosion,* 42 (11) (1986) 277-288.

M. Habashi, E. Bante, J. Galland, and J.J. Bonda, *Corrosion Science*, **35**:14, (1983) 169 - 178.

J.E. Hatch, ed. Aluminum: Properties and Physical Metallurgy, American Society for Metals, Metals Park, Ohio, 1984, 242-319.

D.A. Jones, Principles and Prevention of Corrosion, Prentice Hall, Inc., New Jersey, 1992, 8, 9 and 200-214.

H. Kaesche, Metallic Corrosion: Principles of Physical Chemistry and Current problems, National Association of Corrosion Engineers, Houston, Texas, 1985, 321-359.

Murr, L. E. and V. Annamalai. "Characterization of Copper Nucleation and Growth from Aqueous Solution on Aluminum: At Transmission Electron Microscopy Study of Copper Cementation," Thin Solid Films. 54 (1978) 189-195.

J. K. Park and A. J. Ardell: *Metall. Trans. A,* **15A**, (1984) 1531-1 543.

Maria Posada, L. E. Murr, C.-S. Niou, D. Roberson, D. Little, Roy Arrowood, and Debra George, *Materials Characterization*, **38** (1997) 259-272.

Posada-Portillo, Maria, "Re-examination and Overview of Exfoliation Corrosion Occurring in

2024 A1 Alloy Aircraft Body Skins," Master of Science in Metallurgical and Materials Engineering, The University of Texas at El Paso, July 1998.

Obispo, Haydy, "Copper Deposition During the Corrosion of Aluminum Alloy 2024 in Sodium Chloride Solutions," Master of Science in Metallurgical and Materials Engineering, The University of Texas at El Paso, Dec. 1999

Obispo, H. M., L. E. Murr, R. M. Arrowood and E. A. Trillo. "Copper Desposition During the Corrosion of Aluminum Alloy 2024 in Sodium Chloride Solutions," Journal of Materials Science. 35(2000) 3479-3495.

K. Rajan, W. Wallace, J. C. Beddoes: *J. Mat. Sci.,* 17 (1982) 2817-2824.

M. J. Robinson, *Corrosion Science*, **23**:8 (1983) 887-894.

P.A. Schweitzer, ed., Corrosion Engineering Handbook, Marcel Dekker, Inc., New York, 1996,1-21 and 99-1 55.

Staley, J. T., J. Liu and W. H. Hunt. "Aluminum Alloys for Aerostructures," Advanced Materials and Processes. 10 (1997

Taylor, Edward, *Materials Performance* **36**:10 (1997) 66-69.

W. Wallace, J. J. Beddoes, and M. C. de Malherbe: *Canadian Aeronautics and Space Journal,* **27** (1981) 222-232.

R. P. Wei, M. Gao and C.-M. Laio, A*TEM Studies of Particle Induced Corrosion in 2024-T3 and 7075-T6 Aluminum Alloys@*, paper presented at 1997 TMS annual meeting, Orlando, FL, February 9 - 13, 1997.

R.P. Wei, C-M Liao, and M. Gao, *Metallurgical and Materials Transactions A,* 29A (1998) 1153-1160.

CHAPTER 5

LARGE AREA INSPECTION OF AIRCRAFT STRUCTURES USING VIBRATIONAL NONDESTRUCTIVE EVALUATION METHODS

5.1 Introduction

The main objective of this project was to develop vibrational nondestructive evaluation methods to inspect large areas of aircraft structures. The tools and methods developed relied on state-of-the-art laser instrumentation to perform modal analysis. A very comprehensive report describing the technical accomplishments under this project was submitted by Osegueda and Ferregut (2002). The contents of this chapter are a summary of the report.

5.2 Vibrational NDE

The theoretical developments of the vibrational NDE method and data fusion methodologies were developed and thoroughly documented in the report. Vibrational NDE for damage detection and assessment are based on experimental modal analysis testing to obtain the response characteristics. Since all forms of damage may cause changes in the structural stiffness, the damage is reflected in changes in the vibrational characteristics that can be measured. Since the dynamic characteristics of a structure are altered by the damage, then changes in frequencies, mode shapes and damping ratios or any value that derives from these changes can be used to detect damage. The vibrational NDE methods considered in this work are based on quantifying modal strain energy differences between the structure in a damaged state and a healthy state. From structural mechanics relationships, the differences in the strain energy can be evaluated using the measured modal shapes. From the static shapes of the modes, the strain energy distribution within the structure is computed by curvefitting or using finite element models. Since experimental modes are only obtained at the sampling points, curve-fitting and/or finite element techniques are required to complete the missing components of the modes. The energy differences of equally scaled modes before and after damage are normalized. This is necessary in order to combine information from multiple modes. Damage in an element causes changes in the modal shapes in the vicinity of or at the location of damage. The damage location is indicated as an apparent strain energy increase. The damage detection formulation relies on the features of the differences of modal strain energy when the modes are equally normalized giving collection sets of modal strain energy differences for the available modes. The distribution of the normalized strain energy differences also provide the mechanism to extract probabilities in support of damage and no damage at each location of the structure given the information in each mode. Information from modal pairs was then combined using data fusion techniques.

5.3 Vibrational NDE and Data Fusion in Beams

The Vibrational NDE and fusion methodologies were first developed and refined considering experiments on simple beams as illustrated in Figure 5.1. Modal vibration testing was conducted on beams to obtain their dynamic characteristics including, resonant frequencies,

damping ratios and mode shapes. The tests were conducted using accelerometers evenly spaced and one force transducer while the excitation force was provided by an electro-magnetic shaker. Two aluminum beams were subjected to 54 damage scenarios at different magnitudes and included damage at single and multiple locations. The different damage magnitudes helped test the ability and sensitivity of the methods to detect small defects (flaws or cuts) on the system. For each baseline and damage scenario, sets of FRFs and Coherence functions were obtained to extract the modal parameters of the first five bending modes. Graphical representations of the damage evaluation results were provided.

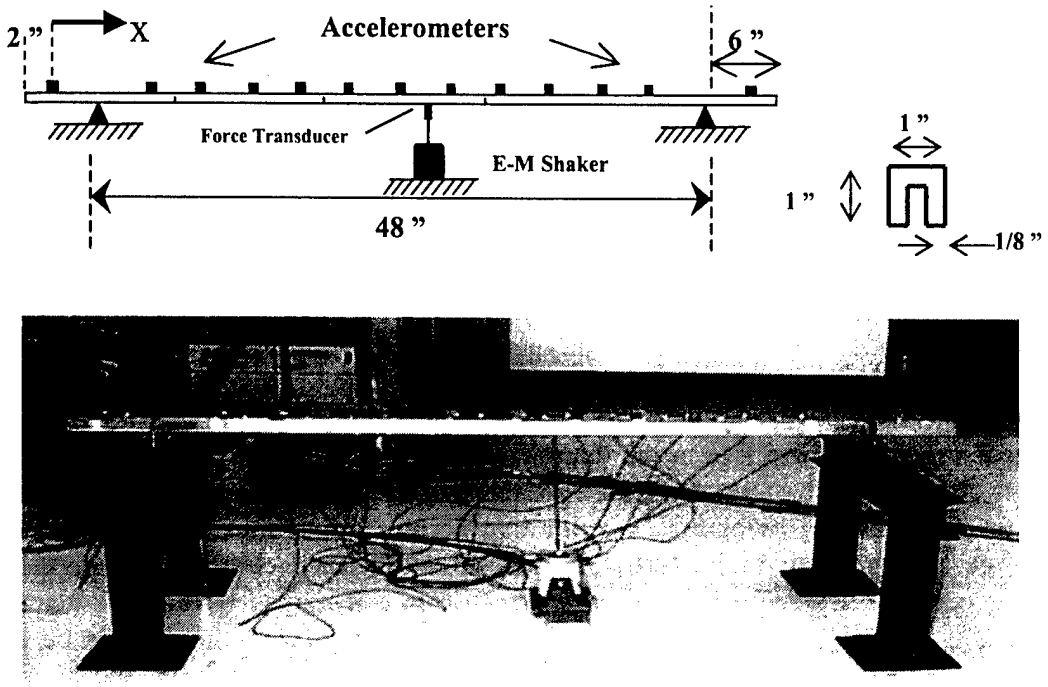

Figure 5.1. Structural System Set-Up.

5.4 Experiments on Large Plate Panel

The methods were applied to a large Aluminum stiffened plate laboratory structure which resembles aircraft construction as illustrated in Figure 5.2. The purpose of this work was to localize inflicted damage over a large area when the modal measurements are obtained with a scanning laser Doppler velocimetry (LDV). The data was processed using the methodologies and fusion techniques. The laboratory structure was a stiffened plate fabricated with aluminum sheet riveted to aluminum C-sections functioning as stringers and ribs. Two shakers were used at unsymmetrical points of the structure providing input force excitations. The LDV was used to sample the structure's response on the skin surface. The model was subjected to 22 different damage cases inflicted at eight different zones. The damage consisted of removal of bolts and cuts in the stiffening elements. Both forms of damage were caused at single and multiple locations. For each damage and baseline case, the FRF and Coherence functions with respect to

the two shakers were collected and processed to extract the vibrational characteristics. The modal assurance criterion (MAC) was used to correlate the mode shapes of the baseline to those of the damaged structure. The mode shapes were subjected to a curve-fit procedure to estimate modal bending and twisting curvatures of the front plate. These curvatures permitted the determination of the modal strain energies. The modal strain energy differences were determined for each mode and normalized using the standard norm. The damage indicators obtained from all available pairs of matching modes were combined by averaging the indicators. The results were presented in the form of damage maps. The experimental data was also used to obtain damage detection using likelihood ratio and evidential reasoning. The cases considered for the likelihood ratio and evidential reasoning methods were the cut damages in the stiffening elements. The statistical distribution of the normalized modal strain energy differences was approximated using the Kernel density estimator to obtain probabilities supporting damage and no-damage. From these probabilities, damage likelihood ratios were obtained for all locations given the modal inspection events. The second process consisted of using techniques of evidential reasoning to determine belief and plausibility in support of damage given the evidence in the modal strain energy differences.

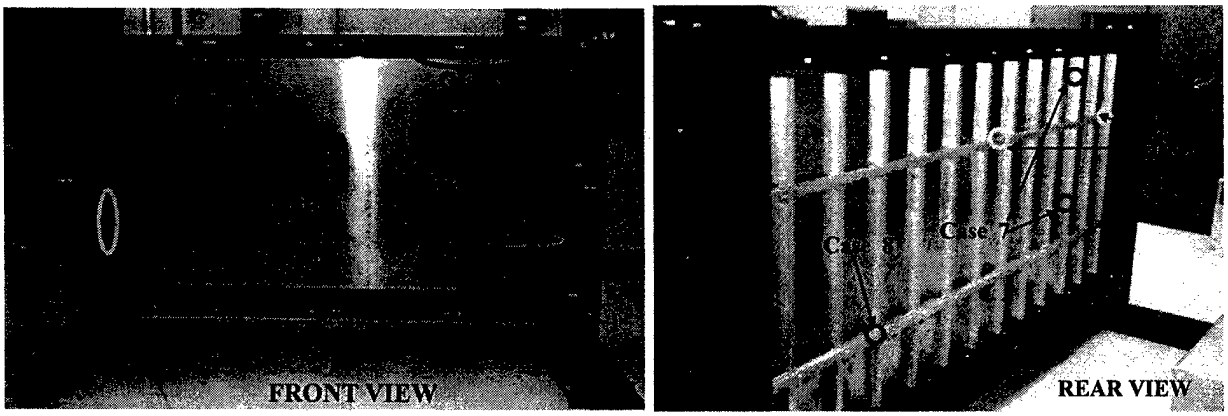

Figure 5.2. Stiffened Plate Panel Test Object

5.5 Experiments on Vertical Stabilizer Assembly

Extensive research was performed on a prototype of the vertical stabilizer assembly (VSA) of NASA's shuttle orbiter as depicted in Figure 5.3. This is an example how the large area inspection techniques could be implemented for aircraft structures. The purpose of the tests was to obtain a database that helped developed damage identification techniques. The data obtained during testing consisted of frequency response functions (FRF) and coherence functions for all scenarios (damage and repaired configurations). The data was used to extract the resonant frequencies and mode shapes. The measurements were taken with accelerometers and with the LDV. There were a total of eight damage cases. The first three cases were performed using accelerometer measurements only. The last five damage cases involved accelerometers and the LDV combined. The damages inflicted consisted of reversible and non-reversible scenarios with several levels of damage in each case. Damages inflicted on the VSA test article were at several locations. The mode-pairing between the baseline state and the damaged scenario was carried

out through the modal assurance criterion (MAC). In addition, the mode pairs which exhibit significant changes due to the inflicted damage were identified using a statistical analysis of the FRF data. The effects of mode-pairing was also studied by repeating the damage detection process using mode-pairs (a) identified by the MAC analysis with values greater than 0.9, (b) identified by the MAC analysis with values greater than 0.5; and by further refining the mode-pairing in both (a) and (b) using the Z-function analysis. The estimation of the strain energy content of the structure, due to the deflected modal shapes, was performed using a finite element approach. Four damage detection algorithms were considered: (1) averaging, (2) probability mass function method (PMF), (3) a weighted averaging method and (4) a weighted PMF method. Damage maps were obtained for all damage cases and damage levels using the four algorithms. The detectability was evaluated in terms of whether the correct location was detected. The number of false positives was obtained by counting the number of regions with high levels of potential damage depicted by the orange-red colors of the contours of the damage maps. A performance index was also evaluated in order to compare the efficacy of the detection methods as well as the mode-pairing approaches.

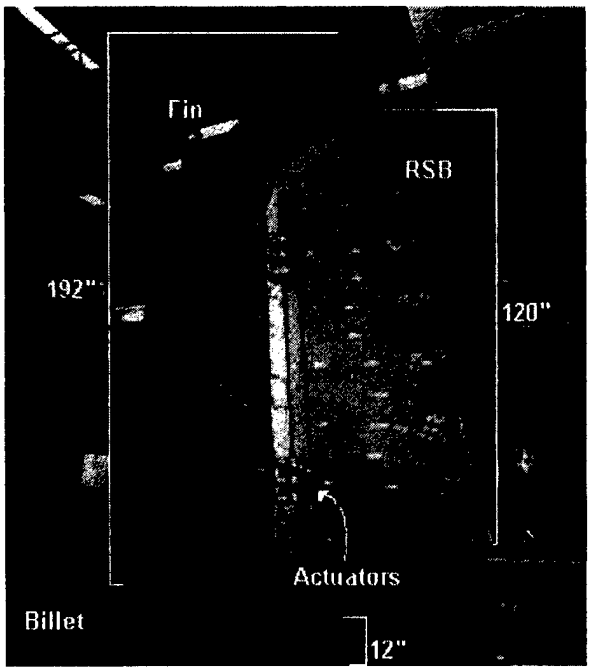

Figure 5.3. VSA Test Object

An extension of the VSA work was also performed where additional fusion approaches were applied to the VSA test structure while considering an improved finite element model. The finite element model to extract the complete modal information was modified to include additional bar elements of the model. The bar elements contributed significantly to the stiffness of the structure and affected the distribution of the strain energy. Prior work assumed the model to be at an undamaged state and no updating was performed when the inflected damage was irreversible. The work utilized model-updating due to the damage already present in some of the baselines. The damage detection results were then obtained using the Averaging, Bayes fusion,

and PMF methods. The methods were only applied considering mode-pairs identified with a MAC with and without the Z-function results. The results were presented in the form of damage maps and summarized in tables listing detectability, number of false positives (NFP) and detection performance in terms of a performance index (PI). The methods and the use of the Z-function were evaluated and compared as functions of detectability, the NFP and the PI.

5.6 Experiments on Curved Shell Test Article

Experimental work was also performed in a laboratory shell structure that resembles a fuselage structure as seen in Figure 5.4. Vibration tests were performed in a stiffened plate at damaged and undamaged states. The vibrational signatures of the structure were analyzed by applying the averaging method combined with the Z-function. Nine cases were studied involving a total of 28 reversible damage scenarios. Damage cases were selected so that regions of both, low and high strain energy content were affected.

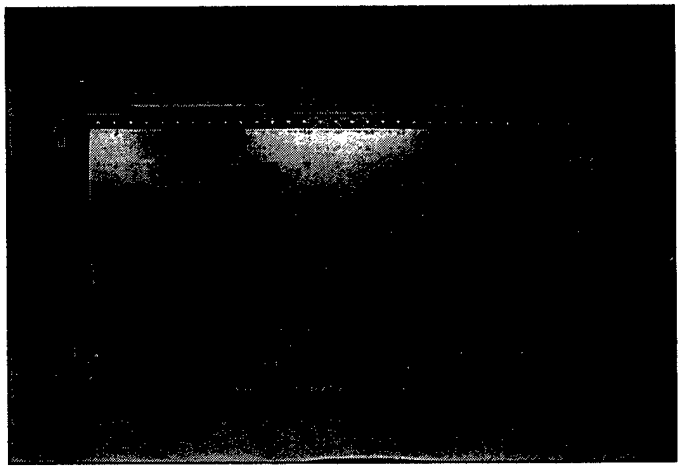

Figure 5.4. Shell Test Object

5.7 Summary of Conclusions

From the beam experiments the following conclusions were obtained. The single fusion technique that provided the best detectability was averaging, followed by the Bayes fusion methods. Averaging provided the least damage localization error. The likelihood ratio method exhibited the poorest detectability (74.1%); this was because of its tendency to intensify large-magnitude damages. The Bayes fusion method proved extremely valuable in enhancing the detection for the small-magnitude damage, at the expense of producing more false positives than other methods. The damage detectability for Beam 2 was 100 percent and that for Beam 1 was 83%; the detectability of the two beams combined was 88 percent. The damages that were not detected typically consisted of small magnitude accompanied with a large damage at another location. The number of false positives for the two beams combined was 20 locations out of a total of 54 damage locations.

The averaging technique when applied to the plate experiments was proven effective in detecting the damage inflicted to the stiffened-plate. Damage consisting in the removal of adjacent bolts was conclusively detected and located when five bolts were removed using the combined twisting and bending curvatures. Damage in the stiff parts of the structure (at supports) was not detected. This was primarily because of the low levels of vibrations compared to other parts of the plate; during the experiments the sensitivity of the laser was adjusted to the maximum level of vibrations. Damage consisting of the removal of bolts of the inner members of the stiffened plate was detected and located using the bending curvature in the direction of the damaged member. Damages in regions of low modal strain energy were not detected. Damage consisting of a cut of the inner stiffening members was detected. Damage was not detected when inflicted at the rigid support.

When the plate test data corresponding to the damage scenarios of the stiffening elements was processed using the likelihood ratio method and the evidential reasoning approaches, nine of ten cut damage locations were correctly detected. The one that was not detected was a damage of small magnitude accompanied with large magnitude damage at a different location. The number of false calls was larger for cases with small magnitude defects.

The major conclusions that can be stated for the tests conducted in the VSA prototype are as follows. The averaging method yielded the highest performance in locating damage when the Z-function analysis was not used. The weighted probability mass function method yielded the highest performance when the Z-function analysis was performed. Higher detection performance was generally obtained by considering mode-pairs matched with MAC values of 0.5 between the undamaged and damaged states of the structure. This was the case with or without the use of the Z-function analysis. The detections, considering the set of mode-pairs with MAC values greater than 0.9, provided a lower detection performance. The combination of using the Z-function analysis and MAC values greater than 0.5 yielded the highest damage detection performance of all the methods and mode-selection criteria.

The additional analyses on the VSA tests considering the averaging, Bayes fusion, and probability mass function (PMF) methods and the improved finite element model yielded the following conclusions. The inflicted damage was successfully detected in 9 of the 10 cases. The damages were correctly detected in 9 of the 10 cases by all three methods, individually. The averaging method yielded the best performance when the Z-Function analysis was used. Higher performance was obtained for the three methods when using the Z-Function analysis. Bayes Fusion, in general, yielded the worst performance of the three methods. This is due to a large number of false positives when compared to the other two methods.

From the work performed on the shell test articles, the following conclusions are stated. At least one damage map from each case detected the correct location with the exception of one case. This case had no significant global change according to the Z-functions analysis to indicate that the monitored modes were not sensitive to or affected by the inflicted damage. The damage maps obtained using the bending curvatures x and y were found to be the most likely to correctly display the damage. This was because of large strain energy content in the stiffening elements. In general, the higher the strain energy content in the damaged location, the higher the

probability of detection. All cases that correctly detected damage had at least a false positive damage. In general, the number of modes had no effect on the damage detection results.

The work on vibrational NDE methods reported in this document provides encouraging evidence that global NDE methods may be feasible for large area inspection of aircraft structures, in particular for detecting flaws in members located deep inside the aircraft which contribute significantly to the structure's stiffness. It is also clear that the methods described here can not be used to find small sized defects such as cracks in rivet holes. The methods also required careful processing of the modal test data using carefully tailored models. Further tools are needed to automate the process in order for implementation to be possible. Also, the refinement of the finite element models may limit the application of the methods.

5.8 References

Osegueda, Roberto and Ferregut, Carlos, "Large Area Inspection of Aircraft Structures Using Vibrational Nondestructive Evaluation Methods', FAST Center Report, The University of Texas at EL Paso, July 2002.

CHAPTER 6

INTELLIGENT NDE APPLICATIONS, MODEL VALIDATION AND PROBABILISTIC MODELING

6.1 Introduction

Perhaps one of the critical challenges of the research community is to investigate some of the fundamental issues associated with the development of hybrid NDE systems. For some time now, it has been recognized that all single NDE techniques have limitations on sensitivities to the size, type and location of the defects they can detect. No single method currently used is capable to detect all forms of defects. For that reason the development of hybrid systems that combine two or more NDE methods are attractive. Fundamental research issues that are critical here include the processing of the data coming from the systems at real time. Artificial neural networks (ANN) have the potential to provide the needed processing speed and robustness that multiple sensor NDE require. In this chapter several applications of ANN to the processing of NDE information are summarized.

One of the major elements that is usually ignored in NDE is the post-inspection decision making process. Among the issues that can be identified are the characterization of defects and the determination of their significance on the reliability of the structure. In most cases NDE techniques do not provide quantitative assessments about the integrity and reliability of the damaged structure. Two projects that explored the feasibility of probabilistic methods and fractal theory to assess the effect of pitting corrosion damage are also summarized in this chapter.

This chapter also summarizes the work conducted to develop a statistical approach to model validation when the data on a system's response is limited. The proposed approach should be useful in the validation of vibrational models using modal information of the real system.

6.2 Artificial Neural Networks Applications

The objectives of the projects reported in this section were to develop and test alternative methods for NDE data processing that: (1) would be computational faster that methods traditionally used; (2) will be more reliable in the detection of damage by better processing data sets which are contaminated with noise or incomplete; (3) will be more sensitive to the detect smaller defects; (4) will be able to discriminate among types of damage once damage is detected; and (5) will be able to detect the existence of multiple damages. Two applications of artificial neural network models on damage detection are reported; one uses vibrational data and the other uses ultrasonic Lamb waves.

A the third application, not related to damage detection, uses neural networks to predict the performance of rechargeable batteries in a renewable power supply system.

6.2.1 Mode Sensitive Neural Networks for Damage Assessment

Vibrational damage detection methods are based on the fact that as damage accumulates in a structure, the stiffness, mass, and damping of the structure experience a change. These changes, in turn, produce changes in the dynamic characteristics of the structure (i.e. resonant frequencies, mode shapes and damping ratios). The dynamic characteristics of a structural system before and after damage can be used to detect the location and magnitude of the damage. The techniques developed at the FAST center to perform these tasks were summarized in Chapter 5. An alternative approach to the techniques reported was the use of artificial neural networks methodology to process the before and after damage information for damage detection. An artificial neural network ability to discern patterns, and then interpolate similar patterns from information it is unfamiliar with, creates an appropriate tool for developing a damage assessment system that performs with relatively low computational time (Gutierrez et al. 1996).

Two Artificial neural network paradigms were utilized to create neural network systems to identify, quantify, and locate damage to an ideal three-degree-of-freedom system. Damage was defined as a percentage reduction in the properties of the elements comprising the three-degree-of-freedom system. An artificial neural network damage assessment system based on the back-propagation paradigm was created and its results were compared against an artificial neural network damage assessment system based on the Radial Basis Function Paradigm. Both systems utilized the same data, consisting of resonant frequencies and modes of vibration, to evaluate the condition of all elements of the three-degree-of-freedom system.

A linear and undamped three-degree-of-freedom system was chosen for this application. The three masses of the system were considered to have the same value. All spring constants were also taken the same. Several simulations were conducted to generate a data base of resonant frequencies and modes of vibrations as functions of the damage magnitude and location. Damage in the system was defined as the fractional reduction of mass or a fractional reduction of stiffness to a spring. Thus, six possible damage cases were assumed to occur in the system. Data was generated for a wide range of damage magnitudes ranging from 1% to 20% for each of the six damage cases. The data was then dichotomized into a training set and a testing set. The training set was used during the learning phase of each network to illustrate to the networks the patterns associated between vibration characteristics and damage to the elements of the model. The testing set was used to verify the networks ability to "learn" the patterns necessary to assess damage in the three-degree-of-freedom system. A total of three training cases (including the undamaged case) comprised the training data set and seventy two cases made the verification (testing) set.

The original goal of the project was to build an ANN that, when presented with any of the modes of vibration of the system, could predict whether or not the system had experienced a change (damage) in one of its dynamic properties, and if so, it would predict its location, determine the type of damage, and quantify its magnitude. To realize this goal, a back propagation ANN was designed with four processing elements (PEs) in the input layer, six PEs in the output layer, and one hidden layer of PEs. The input vector consisted of a natural frequency of the system and the corresponding mode of vibration. The output vector was a representation of the condition of each of the six elements in the model indicating the changes that occurred in each of the masses or spring constants of the system. In this way, the first three

elements of the output vector corresponded to spring constants and the last three represented the three masses of the system. A zero in one of the output PEs indicated no change in the property represented by that element. Conversely, a real positive value indicated a percentage change in the value of the property. The location of the damage was determined by the output PE that was activated (in other words, provided an output value larger than zero.)

This network was trained using all three natural frequencies and modes for a given damage case, the idea was to develop a network that could assess damage once presented with any of the modes of vibration of the system. Unfortunately, the network did not show a commensurable ability to generalize the training data. This failure to generalize the training data lead to a redefinition of the ANN damage assessment system. Thus a system of two layers of ANNs was conceived to handle the analysis of any of the three modes of vibration.

The new architecture consisted of four neural networks. The first network was designed to identify the vibrational mode being inputted. The input data to this network consisted of a natural frequency and the corresponding mode of vibration. The output was a binary variable that identified the mode inputted. Independently, three ANN were built to assess damage given a particular frequency and mode of vibration. That is, one network was trained with only the first mode of all damage cases, another was trained with the second mode, and so on. The input to each of the networks was the frequency and mode for which it was trained. The output represented the possible damage types (three masses and three springs) and the magnitudes of the damage. The way the overall system worked was: Modal data was fed into the first ANN to identify the type of mode that is being inputted. Using the output of this network, the same data was then fed into the network that assessed damage for the particular mode identified.

To identify the effectiveness of the networks built, three criteria were used to compare the two types of paradigms. The first was the average absolute error. This was the magnitude of the difference between the desired and actual output of each network for the entire testing set. The second criterion was the average percent error, average absolute error divided by the desired output, for each network; again for the entire testing set. Finally training time was taken into consideration. Given that both paradigms utilized the same training sets, training time or more specifically, number of training iterations, was another indicator of which systems generalized the training set more efficiently. Analysis of results indicated that the Radial Basis Function Network (RBF) outperformed the Back-Propagation Network (BP) in all three criteria. The comparison of the average absolute error to the average percentage error indicated that the BP's main weakness was in detecting small damages. The RBF demonstrated a better ability to not just classify damage types, but also generalize unfamiliar data more fully than the BP. The two paradigms work in a relatively expedient manner once training had been accomplished, far faster than classical approaches of analysis would have taken.

6.2.2. Artificial Neural Network Models for Damage Detection Using Lamb Waves

NDE techniques may be classified as "local" or "global" depending on the total surface of the structure to which they are applied. Global methods have the advantage of inspecting large areas or parts of structures. Local methods have proven over the years to be capable of detecting and quantifying small defects on structural components. Such local techniques include

ultrasonic testing, laser shearography, eddy current testing, thermography, magnetometry, radiography, and others.

Ultrasonic testing has been a field within the nondestructive evaluation techniques that have developed as a way of assessing damage in structures. Ultrasonic testing in metallic plates involves the propagation of waves within the body of the material. One such wave is the Lamb wave. Lamb waves propagate in the body of a solid whose thickness is comparable to the wavelength of the ultrasonic waves. In a solid plate (or layer) with free boundaries, Lamb waves generate displacements both in the direction of wave propagation and perpendicular to the plane of the plate.

Inspection of large components can be achieved by placing at one end of a plate a piezoelectric transducer exciting a wave that propagates along the plate. If a receiving transducer is positioned at a remote point on the structure, the received signal contains information about the integrity of the scanned section between the transmitting and receiving transducers. However, while this technique enables the detection of areas of structural damage, it does not allow for the quantification of the extent of that damage. One promising approach to infer the location and magnitude of damage in structures with the use of Lamb waves is ANN technology (Alvarez 2000). The seemingly overwhelming task of reviewing vast amounts of data generated from an ultrasonic scan can be easily carried out using this technology. Artificial Neural Networks models generally deal with pattern recognition, which may identify pattern changes (not necessarily linear) in the wave characteristics, between a transmitting and receiving transducer, associated with a damage location and magnitude.

One of the main problems concerning ultrasonic testing is the classification of defect characteristics (i.e. its location and size). Both in manual scanning and in more sophisticated scanning systems, a qualified NDT inspector usually performs the characterization. However, even though an expert, the best operator suffers from fatigue and loss of concentration, so human error cannot be neglected. Automated characterization offers the possibility of an impartial, standardized performance 24 hours a day. The use of artificial neural networks to assist in the automation process by providing a rapid and accurate characterization on the interaction of Lamb waves with damages was explored as part of the research activities reported in Chapter 3.

Lamb waves are basically two-dimensional waves, which attenuate less rapidly over large distances facilitating the capability of scanning large areas. Therefore, large plate-like structures have been tested using Lamb waves. In this application an aluminum plate with a notch, representing a plate-like structure with a crack, was considered.

The methodology proposed is illustrated in Figure 3.30 in Chapter 3. At one end of the plate a piezoelectric transducer excites a Lamb wave, which propagates through the plate and is reflected from the notch as well as from the ends of the plate. At another point, a receiving transducer measures the resulting time history. The measurements collected contain information about the notch characteristics, i.e. its location and depth. The aim is to obtain quantitative information about the notch characteristics on the basis of these measurements. This requires an inverse problem to be solved using neural networks to process the measured waves with the goal of determining the size and location of the notch.

For the training of the ANN, synthetically produced wave patterns were used. In this way the ANN builds up the wanted mapping between the time histories and corresponding notch characteristics.

Artificial neural networks are built based on historical data where there is an unknown relationship between a set of input factors and an outcome. To develop a neural network it is necessary to have a representative set of historical examples of this unknown mapping. These examples are then used to train and test the neural network model. In this application each example consisted of an input vector whose number of elements are defined by the number of time steps from the time response of the plate, and an output vector, which is defined by the quantity that the model will predict. In this case, the quantities are the location and depth of the damage. The investigated damage corresponded to certain forms of intergranular corrosion and cracking that occur at the surface of the plates.

The use of the finite element method in modeling the propagation of ultrasonic waves has gained popularity. The advantage of finite element modeling is that material properties and defect shapes associated with practical test situations can be easily modeled. In this application, a synthetic and comprehensive database was generated using finite element models to simulate and cover a wide range of possible damage scenarios.

An aluminum plate was considered for the application. The properties of the plate used for the model are shown in Table 6.1. The overall process employed to generate a synthetic data base is graphically depicted in Figure 6.1.

First, the parameters for the model need to be set (i.e. location of the transmitting and receiving transducers, location, L, and depth, H, of the notch on the plate). In this application, the first approach taken to solve the problem was to have a fixed source as a transmitting transducer and 16 receivers 2-cm equally spaced from the source as shown in Figure 6.1. Having a model with 16 receivers allowed to have 16 time responses for every notch location. This permitted to investigate the effect the distance between the transmitting and receiving transducers has on the ANN performance. The location of the notch was set randomly through out the plate with some restrictions. A restriction was set up limiting the notch location within the boundaries at 10-cm from the edges of the plate in order to avoid the effect of the edges of the plate on the time history results. Three notch depths where considered in this study, 25%, 50%, and 75% of the thickness of the plate.

Second, the finite element models of the aluminum plate were created using the parameters described in the previous paragraph. Third, the model was analyzed using the DYNA2D finite element program.

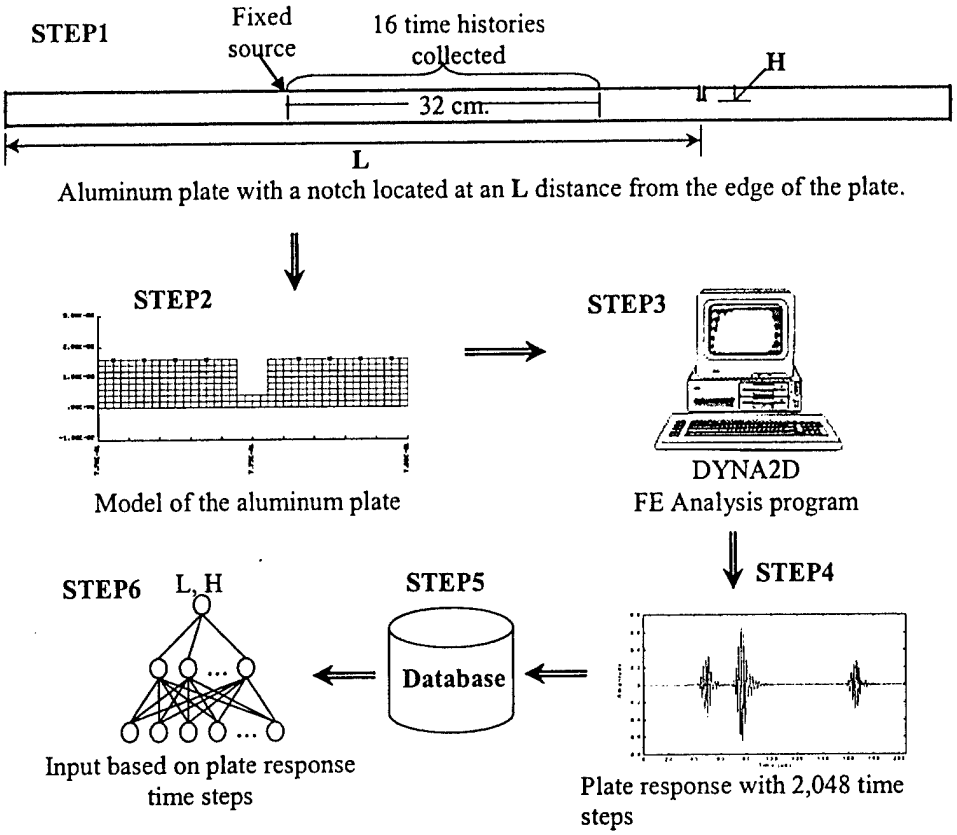

Figure 6.1 Synthetic Database Generation Process

Table 6.1 - Properties of aluminum plate (after Hibbeler, 1994).

Material	Aluminum 6061-T6
Thickness ($2d$)	1.6 mm
Density (ρ)	2,710 kg/cm^3
Modulus of Elasticity (E)	68.9 GPa
Poisson's Ratio (ν)	0.33

The results of the analysis were saved in an ASCII file. Such file contained the 16 time responses (one for each receiving transducer) of the plate. Each time response had 2,048 time steps. This process was repeated for every notch location on the plate until a comprehensive database was built. Finally, from this comprehensive database, training and testing time responses were selected to develop the ANN models. The number of PEs in the input layer of the ANN models was a function of the number of time steps in the time response.

All the neural networks models developed for this application were based on a multi-layer feed forward backpropagation algorithm. An adaptive gradient rate method was selected, as the learning rule, to estimate the weights for the links that join the processing elements

between two adjacent layers. The sigmoid function was used in the output layer to transfer the weighted sum to fit within certain specified bounds. The architectures for the final models consisted of three layers. The model with the best architecture was then tested and validated with a testing data file. A commercial software package, NeuralWorks Professional II by Neural Ware Inc., was used to build the ANN models.

The number of PEs in the input layer was defined by the number of time steps from the time response of the plate, which were initially 2,048. However, due to the limitations in the number of PEs of the software used to develop the ANN the number of PEs were reduced from 2048 to 256 PEs in the input layer. This was achieved by decimating the time history.

Decimation reduces the original sampling rate for a sequence to a lower rate. This process may be viewed as the opposite of interpolation. The decimation process filters the input data with a lowpass filter and then resamples the resulting smoothed signal at a lower rate. Figure 6.2 illustrates an example of the decimation of a time history. The Figure 6.2a shows the original time response measured by the receiving transducer in the case of an undamaged 1.6-mm thick aluminum plate. Figure 6.2b shows the corresponding decimated time response for the same plate. The decimated time history contains the same information about the integrity of the plate as the original signal. Thus, the number of time steps of the decimated time history defines the number of PEs in the input layer.

There were several ANN models developed in this work, each having one PE in the output layer. The number of PEs within the hidden layer was defined by trial and error depending on the model's performance.

There are three questions that arise when evaluating the integrity of a structure: 1) Is there a damage? If there is, 2) where is the damage? And, 3) how much damage there is? These questions influenced the development of the different types of ANN models in this work. One ANN model decided the presence of a defect; a second ANN model predicted the location. Once the decision that a defect is present and it is successfully located a third network was trained to predict the magnitude of the damage.

The first ANN was trained to return a yes/no value such that a value of 1 represented an affirmative presence of a defect and a 0 value registered a no defect. A performance of 90-100% correct classification was achieved by different architectures for the training set. When the ANN was tested with the cases from the testing set the performance varied from 92-95% correct classification. The ANN architecture with the best performance on the testing set was a the network with 256 PEs in the input layer, 12 PEs in the hidden layer and 1 PE in the output layer with a 95% correct classification.

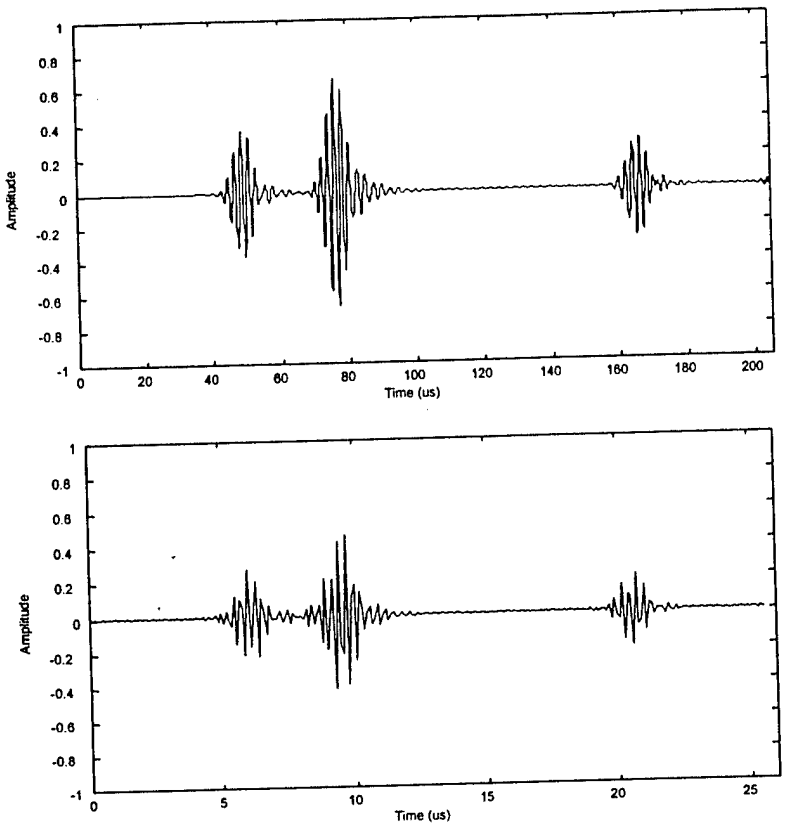

Figure 6.2 Time histories of the (a) original time response, and (b) decimated time response.

A second ANN model was trained to return the location of the notch. The undamaged case was not used for the development of this model. The ANN model with the best performance on the testing set was a network with the following architecture, 256 PEs in the input layer, 15 PEs in the hidden layer and 1 PE in the output layer. The ANN model performance was of a 95–100% correct prediction on the location of the notch for values of the training set. This ANN model had an efficiency of 86% correct prediction. This means that 62 out of the 72 cases of the testing set were predicted within an error of ±10% from the actual values.

The ANN model was also tested with cases with different notch depths. Two databases were created with notch depths of 25% and 75% of the thickness of the plate. From each database, testing sets were developed with the same notch locations as the first testing set. For the testing set of notch depth of 25% of the thickness of the plate, the ANN model had an efficiency of 60% correct prediction, which means that 43 out of the 72 cases were predicted within a ±10% error threshold. Similarly, the ANN model for the testing set of notch depth of 75% of the thickness of the plate had an efficiency of 75% correct prediction.

The third model develop predicted the depth of the notch. The training consisted of 108 time histories corresponding to 12 notch locations and 3 notch depths. The resulting ANN model

had an architecture of 256 PEs in the input layer, 15 PEs in the hidden layer and 1 PE in the output layer. The ANN model had a depth recognition of only 32% of the cases from testing set 1. For testing set 2, the network had a 67% depth recognition. For the testing set 3, the model had a 30% recognition of the depth.

The ANN developed were tested with experimental data to assess the reliability of the predictions. Tests were conducted in aluminum plates. The instrumentation used in the experimental investigation is shown schematically in Figure 6.3. A 500 kHz modulated tone burst was emitted by the signal generator (Stanford SRS 345 function generator) that delivered a 5-cycle tone burst to a 0.5" × 1", 0.5-MHz Technisonic transmitting transducer. The Lamb wave excited by the transmitting transducer propagated along the plate and was received by the receiving Digital Wave B1025 transducer. A Digital Wave 605,100 kHz – 25 MHz bandwidth acoustic emission preamplifier amplified the received signal and input to a Tektronix TDS420A oscilloscope for digital capture and display. In order to increase the signal noise ratio, 50 successive response signals captured by the digital oscilloscope were averaged. This was achieved by retriggering the system once the response of the plate to the previous input had decayed to zero.

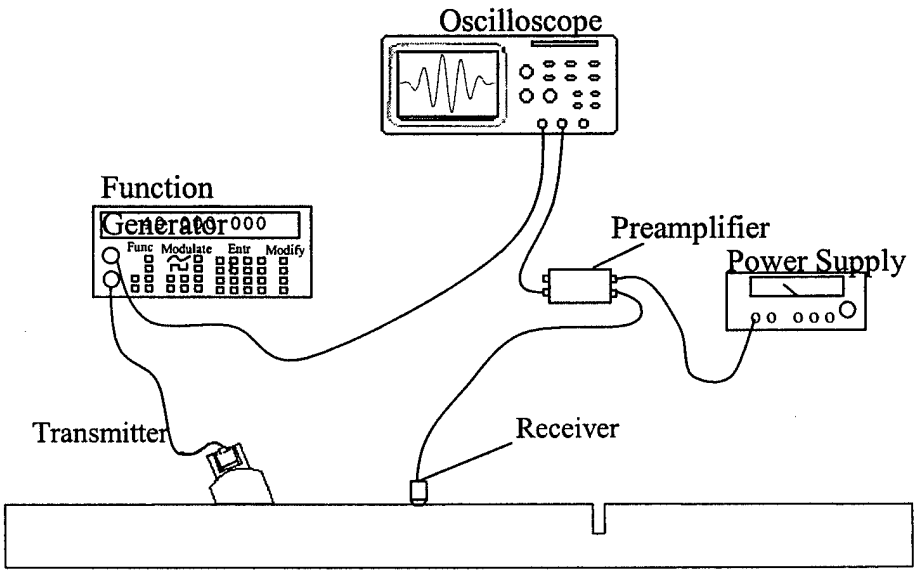

Figure 6.3 Schematic of Experimental Setup

The aluminum plates used in the experimental investigation were 1/16 in. thick, 2 ft. wide and 1 m long. Different plates were tested, one having no notch, and others having a notch as shown in Table 6.2. All notches were 0.8-mm-wide and 20 mm long. Figure 6.4 shows one of the actual notches tested in this study.

Table 6.2 – Characteristics of sample plates.

Plate	Notch	Width (mm)	Length (mm)	Depth (mm)	Location (mm)
1	No	-	-	-	-
2	Yes	0.8	20	1.2	750
3	Yes	0.8	20	0.4	530
4	Yes	0.8	20	0.8	640
5	Yes	0.8	20	0.8	820

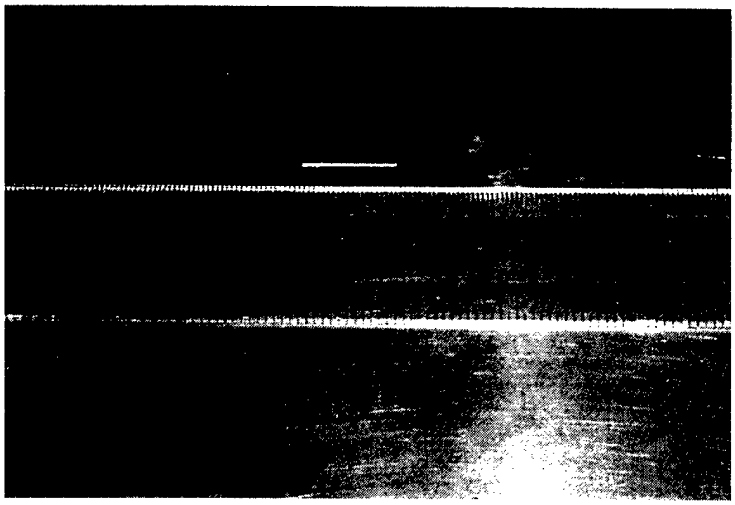

Figure 6.4 Example of notch milled on aluminum plate.

Three different scenarios were used to investigate the capability of the ANNs to detect and locate a damage independently of where the transmitter transducer was placed on the plate. The transmitter transducer was placed at 300 mm, 230 mm, and at 145 mm from the edge of the plate, this represented scenarios I, II and III respectively.

For the ANN model that detected the presence of a damage, the network returned a value of 1 for all damaged plates and a value of 0 for the undamaged plate successfully for the three scenarios investigated in this thesis.

For Scenario I, the ANN models that predicted the location and depth had a performance of 2.2 – 6.0% and a 0.0 – 50% error respectively. For Scenario II, the performance for the ANN models for damage localization was of a 0.4 – 24% error. The depth was predicted within a 6.2 – 25% error for all of the test plates. Scenario III had similar results as the other two, where the percent error fell between 1.6 – 13.9% and 0.0 – 25% for the localization and depth prediction respectively.

The ANN models for damage detection and localization showed good performance for the analytical and experimental data. However, the ANN model for depth prediction showed inconsistent results and larger errors. This is because there is a significant increase in the reflection modes amplitudes when comparing the time histories for notch depth of 25% and 50% of the thickness of the plate. In contrast, there is hardly any measurable increase in the reflection modes amplitudes when comparing the time histories from notch depths of 50% and 75%.

To make the use of ANN networks practical for this application it is necessary to carefully assess the experimental methodology in order to improve data collection of time histories.

6.2.3 Analysis or Rechargeable Batteries in a Renewable power Supply System

In this study, the behavior of rechargeable batteries, acting as a component of a renewable power supply system, was modeled and analyzed using the tools of probability and statistics. Stochastic and deterministic models were created to simulate the behavior of the various components of the energy system. These components included the solar energy (referred to as the solar resource), the photovoltaic power conversion, a rechargeable battery and a load profile. The proposed methodology included the modeling of two of the main components of the solar radiation as a Markov process, a Monte Carlo simulation of solar radiation data as well as characterization of the photovoltaic array and various load profiles. Of particular interest was the adaptation of an artificial neural network to model the damage, represented by a reduction in the maximum potential capacity, which occurs in lead-acid rechargeable batteries due to periods of discharge (Urbina 1999).

A rechargeable battery is an essential component for making the power from a photovoltaic system dispatchable. A photovoltaic-based power supply system sizes power generation to satisfactorily service the system load (if, indeed, load exists while the photovoltaic system generates power), and to charge an energy storage system (typically a lead-acid battery) that will service the system load when the photovoltaic system is not generating power. The system is optimally sized when, over the long term: (1) the photovoltaic component generates sufficient power to service the load while it is operating and, simultaneously, store enough energy to service the load when it is not operating, and (2) the rechargeable battery system services the load when the photovoltaic system is not generating power, and has sufficient capacity to avoid repeated "deep discharge" cycles. Discharge cycles accumulate damage in the batteries and the amount of damage is a function of the severity of the discharge event. This damage is manifested by a diminution of maximum potential capacity–i.e. the maximum capacity that a battery could reach at any given time. Cost constraints and the variability of the photovoltaic output depending on weather conditions makes it impractical to over-design the system sufficiently to entirely avoid periods of deficit charging. A predictive capability for the performance of the battery under the various design options was needed to optimize the system for the best trade off among cost, load requirements, and battery life.

The investigation created a framework for the analysis of rechargeable batteries acting as a component of a photovoltaic power supply system. The power supplied by the photovoltaic system was modeled as a stochastic process. Because solar radiation varies randomly as a function of time, and is equal to or less than some theoretical maximum value, the stochastic

process typically does not have a probability density function that is symmetric in its states, and therefore, cannot be accurately modeled as Gaussian. In this work, an approach that used a bivariate Markov process was used to simulate the two main components of the solar radiation. In addition the load profile was modeled as deterministic or stochastic, depending on its operating characteristics. The behavior of the rechargeable battery–in particular, the damage introduced by discharge cycles–was modeled by means of an artificial neural network (ANN). Data obtained experimentally serve as exemplars for training the ANN. (At the time this work was conducted, battery data that characterize damage associated with discharge periods were not available. Therefore, plausible, synthetic data were used for training.) These exemplars contain various charge/discharge profiles, including periods of deep discharge, for a particular type of battery. The ANN was used to map damage caused by discharge cycles to maximum potential capacity. Table 6.3 summarizes the models developed as well as their nature (stochastic, deterministic, ANN, etc.):

Table 6.3 Models Dveloped

Model	Model Type		
	Deterministic	Stochastic	Artificial Neural Network
Solar Resource		x	
Photovoltaic Array	x		
Rechargeable Batteries	(part) x		(part) x
Load Profile	x	x	

All these elements were combined into a single framework to yield a stochastic model for the power supply/storage/load system. The model was operated on the Monte Carlo principle to yield realizations of the stochastic processes characteristic of the operational phenomena, and these can be analyzed using the tools of statistics to infer the probabilistic behavior of the system. Ultimately, the model can be used to design and optimize the power supply/storage/load system. The proposed methodology is shown graphically in Figure 6.5. Each of the components in the figure was modeled by means of a series of computer programs written in MATLAB®, an object-oriented, modular-programming language.

The prediction model used measured data obtained from the National Solar Radiation Database which was compiled by the National Renewable Energy Laboratories (NREL) based in Golden, Colorado. Using the solar radiation data contained in the database, a stochastic framework (based on Markov chains) was created to simulate the joint realization of the direct normal and diffuse horizontal radiation components. Statistical analysis of this simulation showed a reasonable agreement between the measured and the simulated data.

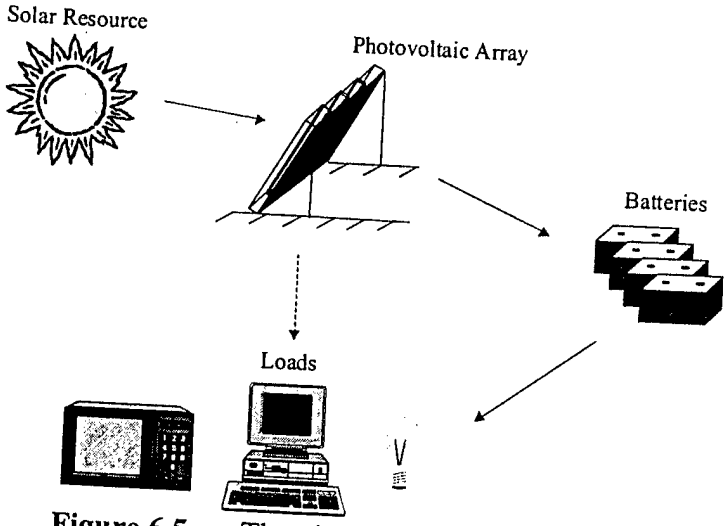

Figure 6.5 The photovoltaic power supply system

An artificial neural network (ANN) based model is a non-phenomenological modeling technique suited for complex system behavior maps. In this investigation the behavior of a rechargeable lead-acid battery was modeled using a combination of phenomenological and ANN models. In particular, the interrelation of the time and depth of discharge was mapped to the damage caused to the battery. This damage was represented by a diminution of the maximum potential capacity of the battery. Although experimental data had not been obtained, a tentative model was created and used to generate synthetic data to train the ANN. These data were deemed plausible and, at least qualitatively, correct. Validation of the proposed ANN model was recommended once the experimental data were obtained.

Using Monte Carlo simulations, a first passage probability analysis on the maximum potential capacity was performed to assess the reliability of the system. By noting the time at which a battery reaches a certain capacity threshold, it was shown that the system is sensitive to the particular load it services and, to a smaller degree, to the tilt angle of the photovoltaic array. Changing some of the operational parameters of the system can modify the reliability of the system. The software that was developed in this study should prove useful in predicting the life expectancy of a given system. By optimizing the operational parameters, the reliability of the system can be increased while maintaining a reasonable cost level.

6.3 Model Validation

Mathematical models are often used in engineering practice to connect system behavior to a specific phenomenology, to serve as an ordered framework for experimentally generated information, or to provide a structure for predicting future responses to inputs. Examples of mathematical models are: finite element models, finite difference models, modal models, and artificial neural network models. Sometimes test data for the model system are also available. In both phenomenological and non-phenomenological applications these data are often used to identify parameters of the mathematical model. Though ad hoc approaches are often developed

to characterize the accuracy of mathematical models, there are no generally applicable formal procedures for judging the quality of the mathematical models.

The bootstrap is a method for assessing the accuracy of arbitrary statistics of measured data. It was developed by Efron(1979) and is clearly explained in a text by Efron and Tibshirami (1993). It provides a means for the standard error, confidence intervals, and bias in statistical estimates. It was developed for situations in which the underlying data are non Gaussian, and the statistics are non-Gaussian and not Gaussian related. It can be used in the structural dynamics framework to assess the accuracy of structural response and characteristics of mechanical systems, for example, response spectral density, cross spectral density, frequency response function, modal parameters, etc.

A framework for the statistical validation of physical system models when experimental data are available was developed in this study. The procedure included the following steps. First, identify one or more measures of physical system character as the basis for validation of the mathematical model, for example, the first three modal frequencies of a linear system. Second, using the bootstrap and the experimental data from the physical system, estimate the confidence intervals on the modal frequencies, say at the 99%level (the 99% confidence intervals define the region within which we believe with 99% certainty the actual modal frequencies lie.) Third, evaluate the modal frequencies from the mathematical model and locate them relative to the confidence intervals from the bootstrap analysis. Now make a statistical hypothesis: the modal frequencies from the mathematical model are accurate representations of the corresponding modal frequencies from the actual system. Perform a statistical test of hypothesis. If the modal frequencies from the mathematical model fall within the confidence intervals on the modal frequencies from the bootstrap analysis then the hypothesis is accepted at the one percent level of significance. Otherwise is rejected.

6.3.1 The Bootstrap

The bootstrap is a data-based technique for estimating the accuracy of parameters derived from probability distributions. The bootstrap was developed by Efron(1979), and is readily applicable to estimating the accuracy of the mean estimate, the variance estimate, and the estimates of other probability distributions moments, as well as more complex statistics of random variable and random processes. The bootstrap is well suited to the estimation of bias, standard error, and confidence intervals of parameters derived from measured data. In the process of estimating confidence intervals the sampling distribution of the statistic of interest is approximated.

A bootstrap analysis is based on a sequence of data values, x_j, $j = 1,\ldots,n$. It is assumed that these values are produced by a source with an unknown probability distribution. The only knowledge of the source is the measured sequence of data values. Each observed data point is assigned a probability of occurrence of 1/n, where n is the number of measured data points. A bootstrap sample is created by selecting at random, with replacement, n elements from the measured data set. The creation of a bootstrap sample is illustrated in Figure 6.6. This procedure is readily implemented using a uniform random number generator which selects, with equal probability, integer values in the range 1 to n. Sampling is done with replacement, so each

bootstrap sample may have several occurrences of some data values and other data values may be absent.

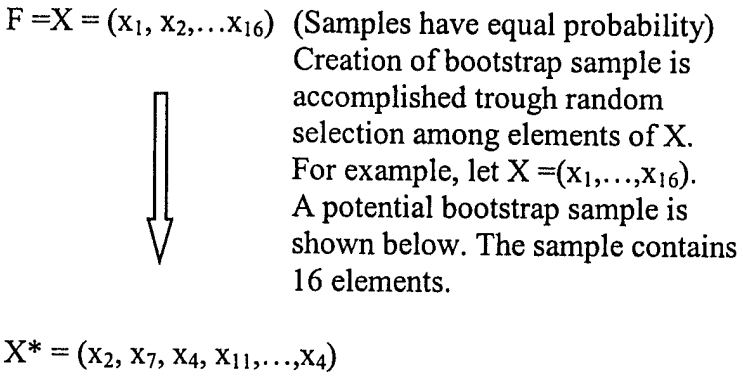

Figure 6.6 Obtaining a botstrap sample.

In a typical bootstrap analysis, numerous bootstrap samples X^{*b}, b = 1,..., B, are created. The statistic of interest is computed for each bootstrap sample; the resulting quantities are known as bootstrap replicates of the statistic of interest. The bootstrap replicates are denoted θ^* (b), b = 1,..., B, and are defined

$$\Theta^*(b) = s(X^{*b}) \qquad b = 1,...B \tag{1}$$

Where s(.) denotes the formula applied to the data to compute this statistic.

The hope in bootsrap analysis is that the bootstrap replicates are governed by a probability law that is approximately the same as the theoretical sampling distribution of the statistic of interest. The sampling distribution of the statistic of interest is the probability law that governs realizations of the statistic – the realizations that could be generated if unlimited data from the underlying source are available.

One class of applications of the bootstrap seeks to estimate standard error, confidence interval, and bias of the statistic of interest. The standard error is estimated using the bootstrap replicates in the usual formula for the standard deviation. Confidence intervals are estimated by sorting the bootstrap replicates and defining intervals associated with percentiles in the sorted list. However, this was not the class that was investigated here.

Bootstrap sampling provides an optimal estimate of the probability density function which characterizes the data source given that the knowledge of the source is limited to the measured data. Computation of a statistic from the bootstrap samples simulates computation of the same statistic on samples drawn from the real world distribution. Properties of the "real world" distribution are estimated in the "bootstrap world".

6.3.2. Confidence regions for measures of mechanical system behavior

The previous section briefly introduced the bootstrap as a technique for the analysis of the accuracy of random data. The boostrap was originally used to develop validation approaches for models of dynamic behavior using the first three modes information obtained from an aluminum beam in the laboratory (Paez et al. 1996). Later the approach was generalized to the validation of system models (Bartney et al 1997.) and to the validation of stochastic models of mechanical behavior (Hunter et al. 1997). The validation approach was also used in the validation of a finite element model of an aluminum plate (Perez et al. 1996).

The validation approach developed using bootstrap accounts for randomness in real system characteristics and the data measured from real systems. The approach is formal and systematic in that it is based on a well established statistical procedure, and it provides and objective measure of the interval that model parameters must occupy in order to be considered representative of the actual system at a particular level of significance. The approach is computer intensive; that is , it is time consuming to generate booststrap samples and replicates of the statistics of interest. However, its advantage is that it properly accounts for the non-Gaussian nature of the arbitrary statistics of interest.

It must be emphasized that the analyst who uses the proposed procedure for statistical model validation must be judicious in his or her choice of the specific measures and the number of measures of model performance use to validate the model. The number of measures should be neither too great nor too small, and should reflect the importance of the application. The specific measures of performance used should reflect the analyst's expectations of the model. Some measures of performance (like average measures of system behavior over a broad region) will be easier to validate than others.

6.4 Corrosion Damage Assessment

Corrosion is a degradation process essentially consisting of the reaction of a metal exposed to a reactive environment that can, in general, be divided into two main classes, general and local. Detection and characterization of corrosion at the initiation stage pose a great challenge to the inspection science and technology. Corrosion damage is a costly source of damage to aircraft and it carries the risk of loss of life as well as hardware in case of catastrophic failure.

Pitting corrosion is a form of localized corrosion that is exceedingly destructive since a perforation resulting from a single pit can cause complete failure. Furthermore, pits can produce premature service failure since they usually provide sites for crack initiation.

Aircraft materials, particularly those of high strength types, are susceptible to pitting corrosion in a favorable environment. Multiple-site pitting corrosion and corrosion fatigue represent two serious degradation mechanisms that affect the structural integrity and reliability of aging military and commercial aircraft. Corrosion pits influence the localized stress distribution and serve as crack initiation sites. The loss of material and consequently, the loss of strength of aircraft metals caused by corrosion can lead to a catastrophic failure of the aircraft when

combined with fatigue. Pit formation and their shapes are random phenomena; their formation depends upon material characteristics and electrochemical factors that are not well understood. At the present time, there is no nondestructive method that can provide precise or even reasonably accurate information on the spatial distribution of the pits and their geometrical characteristics. In addition, there appears to be no known quantitative measure of corrosion damage.

Two approaches for the quantification and assessment of corrosion seriousness were developed as part of this grant. One was based on probabilistic techniques and was aimed to quantify how pitting corrosion impacts the reliability of a structural element. The second approach was based on fractal theory and focused on quantifying corrosion damage.

6.4.1 Reliability-based corrosion assessment

Probabilistic models were used to assess the reliability of a structural element that has been affected by pitting corrosion. The uncertainties associated with the location and size of corroded areas, material properties, and loading, make it necessary to follow a probabilistic approach to the prediction of crack initiation. Finite element analysis (FEA) were used to compute the stress distribution on a corroded plate, the results of these analysis were combined with reliability methods to predict the probability of crack initiation. Results will be useful in the planning of aircraft inspections, and in making decisions about the integrity of corroded structures.

The corrosion assessment methodology was developed was developed with the aim to apply it to the reliability assessment of corroded plates and it is summarize in Figure 6.7. The steps include (Pardo 2000):

I. Obtain experimental or field data of corrosion pits

II. Develop statistical properties of the corrosion variables that define the pits. Fit probability density functions to pit density, pit depth, pit width, and pit location. Use the fitted probability distributions to generate a larger data sample using Monte Carlo simulation techniques.

III. Using the data simulated in step II, create finite element models of corroded plates. Use numerical methods (FEA) for stress field computations of the corroded plate. Determine the maximum node stress at every pit location.

IV. Fit a probability density function to the maximum node stresses.

V. Compute the the probability of crack initiation using the following failure criterion: $R - S \leq 0$. Where R is the fracture strength of the material and S is the maximum local stress.

VI. Compare computed reliability with target values to decide the criticality of the corrosion observed.

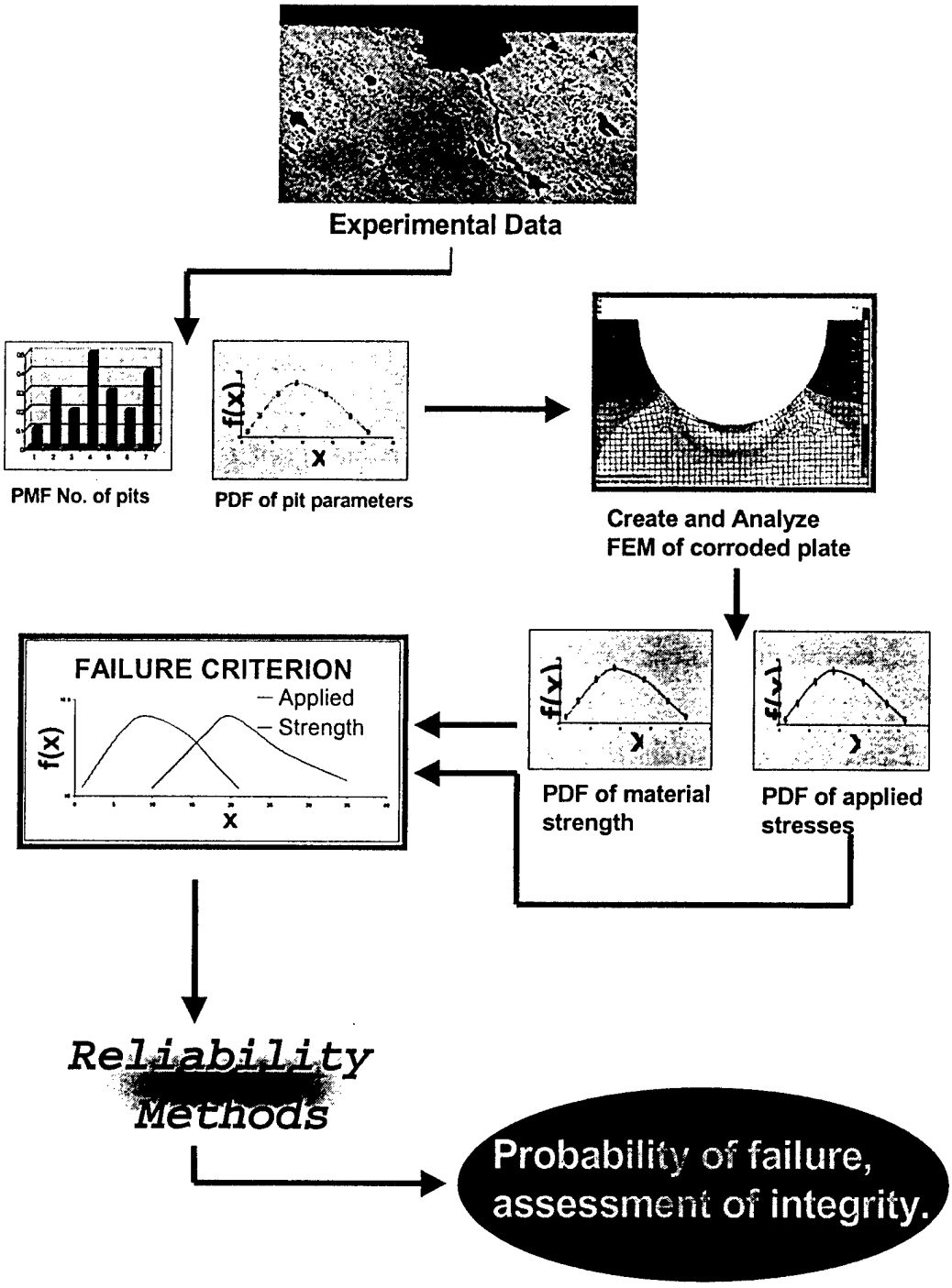

Figure 6.7 Reliability-based corrosion assessment approach.

For the purpose of developing the methodology shown in Figure 6.7, statistical data for corroded aluminum 2024 – T3 data were obtained from published sources.

A sample of a typical finite element model used in this study is shown in Figure 6.8. The number of corrosion pits, their location and the characteristics of each of them were defined by each of the Monte Carlo simulations generated.

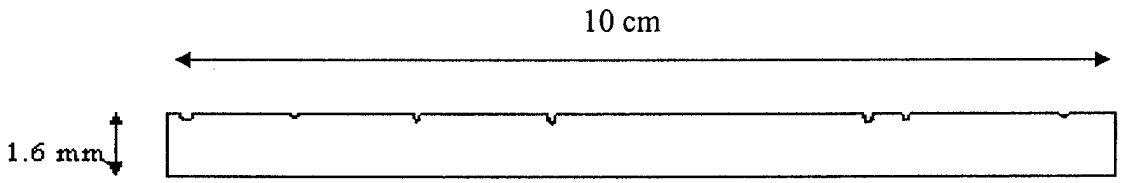

Figure 6.8 Finite Element Model of corroded plate

Each model was analyzed under an axial tensile load equal to the fracture strength of the material. Only the maximum stress was read at every pit location. For example, for a plate model containing 20 pits, only 20 node stresses were read for the entire plate. This was done to have the statistical distribution of the maximum stresses only. Figure 6.9 is a sample of a finite element model showing the stress distribution. The higher stress concentration at the bottom of the pits can be noticed. The probability density function that best fitted the maximum stress data was the Lognormal distribution. The fracture strenght was modeled using a Normal dentisty function.

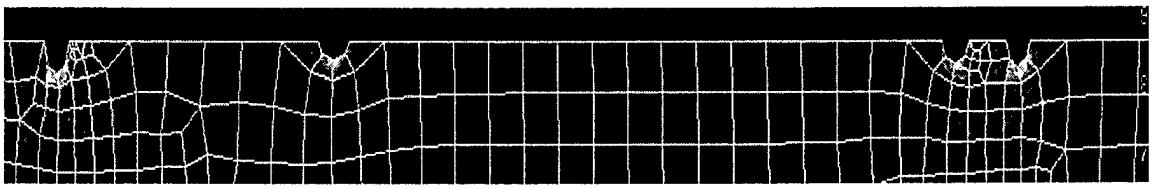

Figure 6.9 Typical local stress concentrations in corrosion pits.

First Order reliability methods were used in the computation of the probability of failure. A total of 10 simulated plates were analyzed. Results showed that the proposed probabilistic approach could be used in conjunction with NDE methods as a generic metric to assist in the process of decision making for inspections and maintenance scheduling.

6.4.2 Pitting Corrosion Quantification Using Fractal Theory

Complex forms and patterns, either existing in nature or artificially generated, are hardly characterized with simple mathematical concepts. However, there are theories that provide the understanding of random processes and natural phenomena. One of these theories is Fractal Theory. Fractal geometry deals with complex geometric objects that show a high-degree of irregularity that cannot be investigated by methods of classical geometry. Recently, a wide range of complex forms have been to the point of interest for scientists, engineers and physicians since these forms can be characterized using the idea of a *fractal dimension*.

A wide range of complex forms can be characterized using the idea of fractal dimension. The fractal dimension that lies between a line and a square is between 1 and 2. In the same manner, the fractal dimension that lies between a square and a cube has a value between 2 and 3. The simple way to fragment the length of a shape was by dividing it into segments of one arbitrary dimension, or creating similar copies of itself. Then, an algorithm can be developed to count the amount of segments needed to cover the entire shape and to define its fractal dimension. This process may be similarly applied to areas and volumes.

In this work the fractal dimension of corrosion pits was used as the measurable quantity to assess corrosion. The particular algorithm used to estimate the fractal dimension is known as the Box-counting method. This method is directly related to the mathematical definition of "covering dimension". If E is the fractal profile, $N(E, \varepsilon)$ is defined as the smallest number of boxes with linear size ε needed to cover E.

If the limit defined as:

$$\lim_{\varepsilon \to 0} \frac{\log N(E,\varepsilon)}{\log(\frac{1}{\varepsilon})} = D_b \qquad (2)$$

exists and is finite, then D_b is called the box-counting dimension of E (Carpinteri, 1989). From an operative perspective, the box-counting method is implemented by generating a square mesh of linear dimension ε_i and determining the number $N_i(E, \varepsilon)$ of boxes needed to totally cover the analyzed profile as shown in Figure 6.10. The procedure is repeated in a progressive manner with smaller boxes as shown in part b of Figure 6.10. Then, a linear regression with the logarithmic data on both axes ($\log N_i$ and $\log \varepsilon_i$) is performed. The fractal dimension is obtained from the slope of the best-fit line.

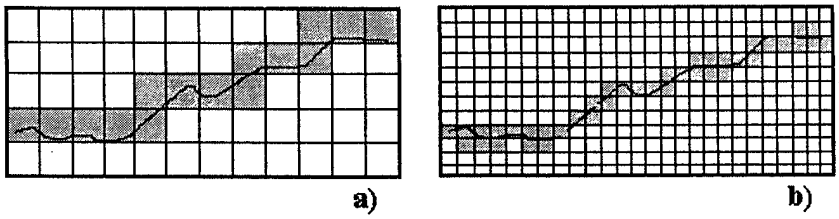

Figure 6.10 Box-counting method.

The Box-counting algorithm was implemented to characterize complex geometric patterns due to pitting corrosion. It has been found that surfaces of fracture, wear, erosion, corrosion, etc. are fractals (Russ, 1992). Thus, the purpose of the algorithm is to determine the fractal dimension considering that fractal dimension changes as texture of the metal surface results in a change.

In order to account for the relationship between corrosion and fractal dimension, images of corroded plates were obtained and then processed to create a black & white (binary) representation of the corroded regions, which represented the signature of the fractal. Then, the Box-counting algorithm was applied to the black and white images. The original images corresponded to corroded 2024-T3 aluminum plates. Regression formulas were used to obtain the fractal dimension (slope) once the algorithm was applied. As an example, an image is shown in Figure 6.11 which is a representation of a pitted region at the center of a corroded aluminum specimen. The pitted region belongs to a specimen exposed to (0.2 M) ferric chloride solution for 2 hours. From the image analysis, thresholding and filtering processes were done to produce a black and white binary image. After the algorithm and the regression formulas were implemented, the fractal dimension of the binary corroded patterns was obtained. According to the concept of fractal dimension, the negative of the slope of the line is the fractal dimension. In other words, the best fit-line, after the box-counting algorithm, is represented by a straight-line of slope -D = -1.16. Hence, the fractal dimension (D) is equal to 1.16 as shown in Figure 6.12.

In summary, the fractal dimension is important because it will characterize the different levels of corrosion at which the testing specimens will be subjected to. The steps of the process including the image analysis and implementation of the box-counting algorithm are the following:

a) The image is digitized, low-pass filtered, and thresholded.
b) The black and white binary image represents the actual pitted region.
c) The box-counting algorithm is applied to analyze the binary image.
d) The straight-line relationship is produced where the slope is negatively proportional to the slope of the line.

A schematic of the whole process is shown in Figure 6.13.

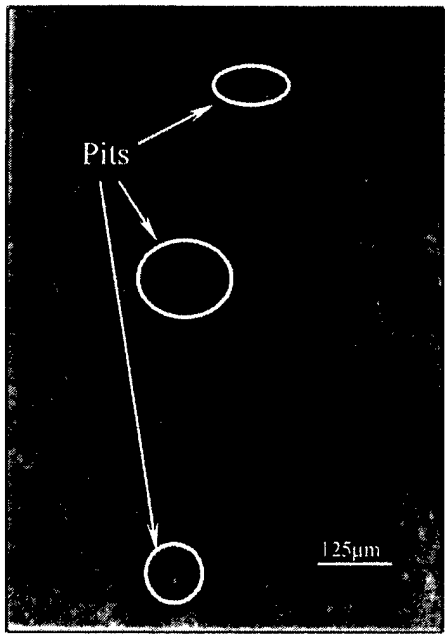

Figure 6.11 Pitted area of a corroded specimen at 2 hrs of exposure.

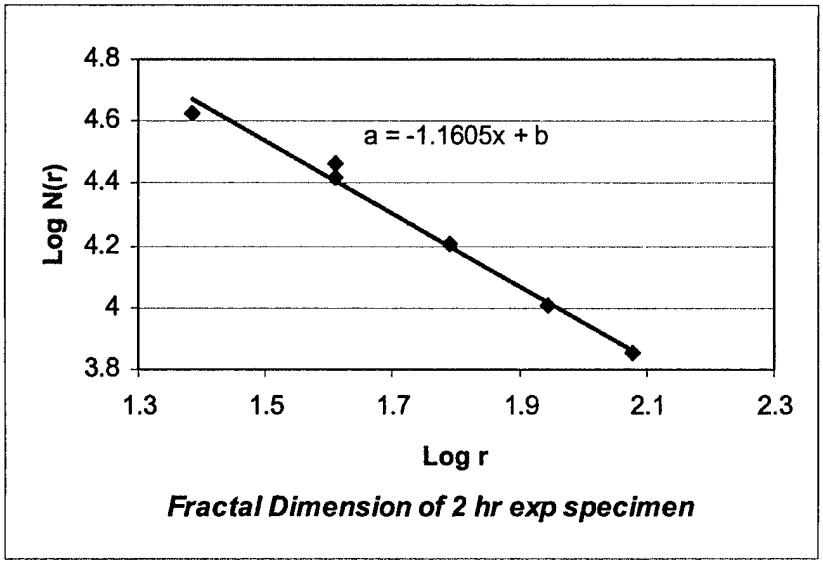

Figure 6.12 Fractal dimension for specimen exposed to 2hrs to a concentrated solution.

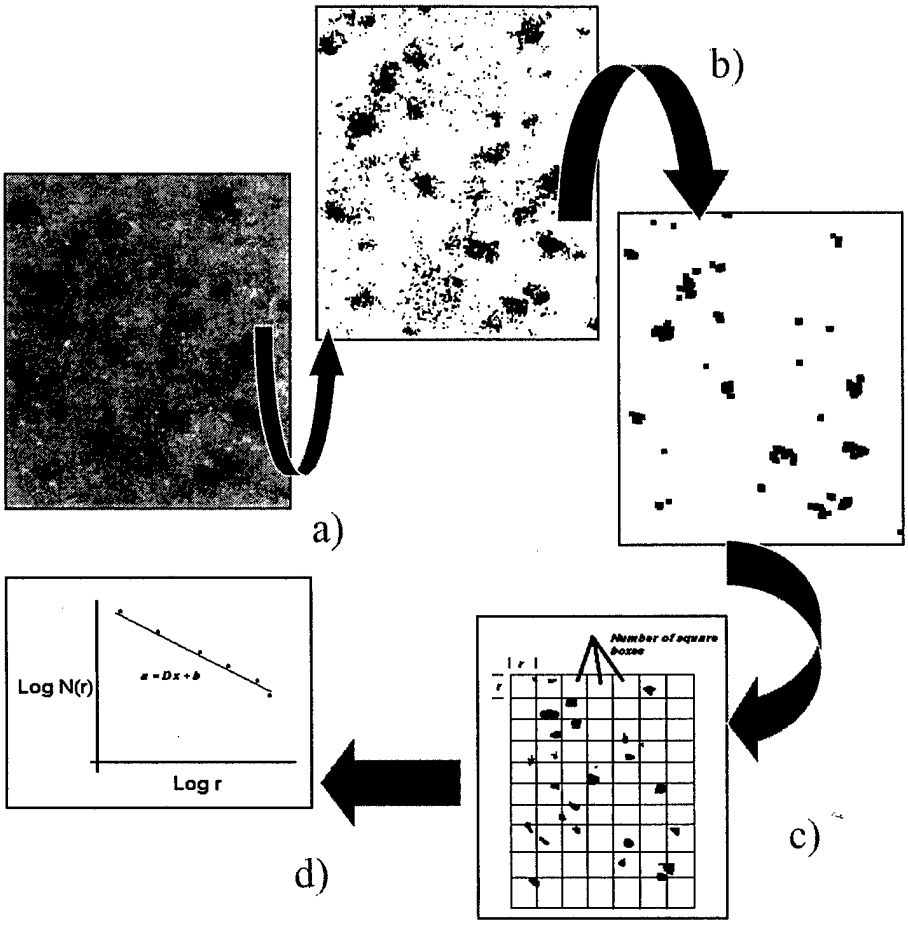

Figure 6.13 The schematic of Box-counting algorithm implementation.

This project also included the design of an experiment to obtain pitting corrosion information. The experiments were necessary to obtain corrosion patterns in the aluminum alloy using ferric chloride aqueous solutions. Test specimens were manufactured and machined to meet the standard requirement (E-8) of ASTM testing materials. The specimens were immersed in the aqueous solutions for several periods of time. The concentration in the solutions was also varied to create the different corrosive environments. Corrosion testing procedures were carefully reviewed to obtain the proper corrosive solution (DRAFT – API Revision 36). Finding the proper solution was of great importance because it was necessary to obtain specific corrosive patterns. Once the specimens were corroded at the desired levels, digitized images were extracted showing the pitting corrosion. The images were obtained with a visual high-resolution microscope. Next, the images were computer-analyzed to determine the pitting corrosion characteristics and thus define the morphology of corrosion patterns. Finally, the specimens were tested in pure tension to obtain the ultimate strength values of after corrosion. This data base was then used to develop a model that relates pitting corrosion characteristics, including fractal dimension, with the residual strength of the corroded material. The model was built using artificial neural networks techniques.

The project showed that the fractal dimension of a corrosion signature is a suitable metric to quantify corrosion damage and to determine the residual strength of a corroded specimen.

6.5 References

Alvarez, W., Artificial neural Network Models for Damage Detection Using Lamb Waves, Masters of Science Thesis, The University of Texas at El Paso, May, 2000.

Barney, P., Ferregut, C., Perez, L.E., Hunter, N.F., and Paez, T.L., "Statistical Validation of System Models," HICSS-30 Proceedings, Hawaii International Conference on Systems Science, University of Hawaii, Maui, Hawai, 1997

Efron, B., "Bootstrap Mehods: Another Look at the Jacknife," Annals of Statistics, vol 7, pp. 1-26, 1979.

Efron, B. and Tibshirani, R.J., An Introduction to the Bootstrap, Applied Monographs on Statistics and Applied Probability 57, Chapman and Hall 1993.

Gutierrez, J.M., Ferregut, C., and Osegueda, R.A., "A Comparative Study on Two Types of Mode Sensitive Neural Networks for Damage Assessment," Nondestructive Evaluation of Utilities and Pipelines, M. Prager and R.M. Tilley (Eds.), Proc. SPIE 2947, 1996, pp. 224-235.

Hunter, N.F., Barney, P., Ferregut, C., Perez, L.E., and Paez, T.L., "Statistical Validation of Stochastic Models," Proceedings of the 15th International Modal Analysis Conference, IMAC97, V.1, Society for Experimental Mechanics, Inc., Bethel, Connecticut, pp. 605-611, 1997.

Lopez, B., Pitting Corrosion Quantification Using Fractal Theory, Masters of Science Thesis, The University of Texas at El Paso, December, 2001.

Paez, T., Barney P., Hunter, N., Ferregut, C. and Perez, L.E., " Statistical Validation of Physical Systems Models, 67th Shock and Vibration Symposium, Monterrey, California, November 18-22, 1996 .

Pardo, H., Reliability-Based Corrosion Assessment Methodology, Masters of Science Thesis, The University of Texas at El Paso, December, 2000.

Perez, L.E., Ferregut, C., Carrasco, C., Paez, T.L., Barney, P. and Hunter, N.F., "Statistical Validation of a Plate Finite-Element Model for Damage Detection," in Smart Structures and Materials: Smart Systems for Bridges, Structures and Highways, 1997.

Urbina, A. Probabilistic Analysis of Rechargeable Batteries in a Renewable Power Supply System, Masters of Science Thesis, The University of Texas at El Paso, May 1999.

APPENDIX A

STUDENTS THAT HAVE PARTICIPATED IN UTEP'S FAST CENTER

A.1 Doctoral Graduates and Current Ph.D. Students

Dr. Gabriel Garcia

Doctor of Philosophy
Mechanical Engineering, Texas A&M University
Date: August 1996

Dissertation Title

Evaluation of relative performance of classification algorithms for nondestructive damage detection

Supervisor:

Dr. Norris Stubbs

Abstract

The objective of this dissertation is to evaluate the relative performance of five classification algorithms for nondestructive damage detection. The classification algorithms investigated here are as follows: (1) a quadratic classifier obtained from Bayes' rule (i.e., using unequal damage and undamaged covariance matrices), (2) a linear classifier obtained from Bayes' rule (i.e., using equal damage and undamaged covariance matrices), (3) a linear classifier obtained from Bayes' rule (i.e., assuming that the damaged and undamaged covariance matrices are equal to the identity matrix), (4) a classifier using Euclidean distance as a basis, and (5) a classifier using hypothesis testing. To meet this objective, an established theory of damage localization, which yields information on the location of the damage directly from changes in mode shapes, is selected. Next, the application of sophisticated techniques from pattern recognition, in the form of the five classification algorithms, is performed to the existing theory of damage localization. Expressions for pattern classification using discriminant functions obtained from Bayes' rule, distance as similarity, and hypothesis testing are generated. Criteria for the evaluation of the proposed pattern recognition models are generated. Using the enhanced model, the locating of damage is attempted in: (1) a numerical model of a space structure with simulated damage at various locations, and (2) a real structure damaged at known locations. Finally, the accuracy and reliability of the pattern recognition models are evaluated using the established criteria.

Publications

Garcia, G.V., and Stubbs, N., "Evaluation of Relative Performance of Classification Algorithms for Nondestructive Damage Detection", Report No. FAST-TAMU-96-01, Submitted to US Air Force Office of Scientific Research, Future Aerospace Science and Technology Program, Center for Structural Integrity of Aerospace Systems, University of Texas at El Paso, Contract Number 32525-47960-CE, July 1996.

Garcia, G.V. and Stubbs, N., "Modal Response of Finite Element Model of Space Truss Model of UTEP Space Structure", Report No. FAST-TAMU-96-02, "Submitted to US Air Force Office of Scientific Research, Future Aerospace Science, and Technology Program, Center for Structural Integrity of Aerospace Systems, University of Texas at El Paso, Contract Number 32525-47960-CE, July 1996.

Garcia, G.V. and Stubbs, N., "Application and Evaluation of Classification Algorithms to a Finite Element Model of a Three-Dimensional Truss structure for Nondestructive Damage Detection," in Smart Structures and Materials: Smart Systems for Bridges, Structures and Highways, SPIE Vol. 3043, pp. 205, March 1997.

Garcia, G. V., Stubbs, N., "Relative Performance Evaluation of Pattern Recognition Models for Nondestructive Damage Detection (NDD)," Proceedings of the 15th International Modal Analysis Conference, IMAC97, V.2, Society for Experimental Mechanics, Inc., Bethel, Connecticut, pp. 1822-1830, 1997.

Garcia, G.V., Butler, K., and Stubbs, N., "Relative Performance of Clustering-based Neural Network and Statistical Pattern Recognition Models for Nondestructive Damage Detection," Accepted for publication in Smart Materials and Structures Journal, May 1997.

Garcia, G.V., Osegueda, R. and Meza, D., "Comparison of the Damage Detection Results Utilizing and ARMA Model and a FRF Model to Extract the Modal Parameters", SPIE 98, Smart Structures and Materials Conference, San Diego, CA, March 1998.

Garcia, G., Stubbs, N. and Osegueda, R., "Pattern Recognition Approach to Damage Classification," Submitted for publication to Mechanical Systems and Signal Processing Journal.

Garcia, G.V. and Osegueda, R.A., "Damage Detection Using ARMA Model Coefficients," SPIE Conference, Smart Structures and Materials Conference, Newport Beach, CA., March 1999, Vol. 3671, pp. 289-296.

Garcia, G.V., Osegueda, R.A. and Meza, D., "Damage Detection Comparison Between Damage Index Method and ARMA Method," IMAC Proceedings of the 17th International Modal Analysis Conference, Kissimmee, FL, February 1999, Vol. 1, pp. 593-598.

Garcia, G.V. and Osegueda, R., "Combining Damage Index Method and ARMA Method to Improve Damage Detection", proceedings of IMAC 2000, San Antonio, TX, February 7-10, 2000, pp. 668-673.

Employment

Assistant Professor, Department of Mechanical Engineering, New Mexico State University
Las Cruces, New Mexico

Eulalio Rodriguez
Doctor of Philosophy
Electrical and Computer Engineering, UTEP
Date: December 1998

Dissertation Title

Non-Destructive Determination of Elasticity Constants of Composite Plates by the Acousto-Ultrasonic Method

Supervisors:

Drs. Joseph Pierluissi and Soheil Nazarian

Abstract

A nondestructive, reliable, and fast method for estimating the elasticity constants that characterize a fiber-reinforced polymer matrix composite plate is proposed. The proposed acousto-ultrasonic technique, which takes advantage of the spectral analysis of the ultrasonic plate waves, allows for the calculation and measurement of the dispersion curves of a plate wave propagating in the lowest symmetric mode. A dispersion curve is a plot of phase velocity versus frequency or wavelength. A narrow-spectrum ultrasonic pulse is applied to the surface of a plate by a broadband ultrasonic transducer. Time signals captured with two piezoelectric transducers in contact with the plate are first transformed to the frequency domain. The cross phase spectra is then calculated to obtain the phase shift, which in turn yields the phase velocity. The processing of the recorded signals involves a Fourier transform analysis to estimate the cross power spectrum of the received waves. The phase cross spectrum provides the phase shift over a frequency spectrum determined by the input pulse shape. The phase shift at each frequency is proportional to the distance between receivers and to the phase velocity of the ultrasonic wave. Since the receiver separation is known, the dispersion curve can be constructed in the frequency range where the input pulse contains significant energy. From the experimental dispersion curve, the stiffness constants of the plate are estimated. A theoretical dispersion curve is fitted to the measured dispersion curve using a plate model. The model relates the plate elasticity constants and thickness to the phase velocity of plate waves. An inversion algorithm was developed based on the general inverse theory, which rapidly converges to the desired elasticity constants. The experimental set up automatically and in real-time acquires the data through a digitizing oscilloscope. The accuracy of phase velocity measurements in aluminum plates was found to be, on the average, within ±1% when compared to the theoretical dispersion curves, and the inversion process yielded elasticity constants that were within 1% of the nominal values.

Publications

Keith Worden, Roberto Osegueda, Carlos Ferregut, Soheil Nazarian, Eulalio Rodriguez, Debra L. George, Mary J. George, Vladik Kreinovich, Olga Kosheleva, and Sergio Cabrera, "Interval Approach to Non-Destructive Testing of Aerospace Structures and to Mammography", In: Goetz Alefeld and Raul A. Trejo (eds.), Interval Computations and its Applications to Reasoning Under Uncertainty, Knowledge Representation, and Control Theory. Proceedings of MEXICON'98, Workshop on Interval Computations, 4th World Congress on Expert Systems, Mexico City, Mexico, 1998.

Rodriguez, E., Pardo, H., Nazarian, S. and Pierluissi, J.H., "Real Time Characterization of Isotropic Plates Using Lamb Waves," In Proc. of Workshop in Intelligent NDE Sciences for Aging and Futuristic Aircraft, Eds. Ferregut, Osegueda and Nunez, FAST Center for Structural Integrity of Aerospace Systems, The University of Texas at El Paso, ISBN: 97404-279-8, El Paso, Texas, January 1998, pp 257-266.

Employment

Army contractor, Fort Bliss, El Paso,Radar and Electronic Countermeasures analysis.

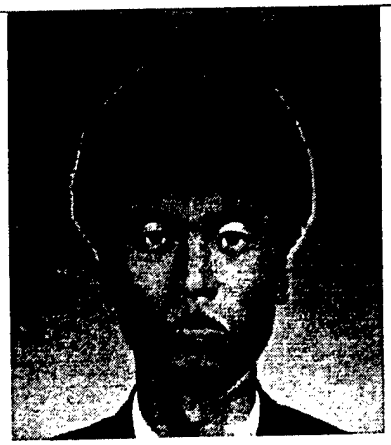

Dr. Sanghyun Choi
Doctor of Philosophy
Civil Engineering, Texas A&M University
Date: December 1999

Dissertation Title
Improved Performance of Damage Localization and Severity Estimation via Combining Multiple Damage Algorithms

Supervisor
Dr. Norris Stubbs

Abstract

To date, many non-destructive damage detection algorithms have been proposed and developed on various theoretical and experimental grounds. So far, however, it is observed that each and every algorithm has its limitations as well as advantages when applied to practical problems. To resolve these limitations, two ways to improve the performance of damage localization and severity estimation are explored in this study: (a) by enhancing the individual algorithms via utilizing more sensitive response measures to damage and (b) by combining multiple damage predictions from different algorithms. To these ends, specific algorithms using various types of response measures are developed from the generic expression of the two prominent damage detection algorithms: namely the algorithms that utilize the changes in the strain energy distribution and the flexibility distribution. The performance of damage detection using the specific algorithms is evaluated using data generated from numerical simulations. Then, various logical rules for combining the algorithms are proposed and the performances of damage detection using these rules are compared with the performance of individual algorithms. It is demonstrated that some response measures produce more accurate and consistent damage predictions than commonly used modal response measures and the damage prediction of the consensus of multiple damage algorithms may improve the performance of damage localization and severity estimation.

Publications

Choi, S. and Stubbs, N., "Nondestructive Damage Detection Algorithms for 2D Plates," in Smart Structures and Materials: Smart Systems for Bridges, Structures and Highways, SPIE Vol. 3043, pp. 193, March 1997.

Stubbs, N. and Choi, S., "Improved Non-destructive Damage Detection via Combining Individual Detection Theories," In Proc. of Workshop in Intelligent NDE Sciences for Aging and Futuristic Aircraft, Eds. Ferregut, Osegueda and Nunez, FAST Center for Structural Integrity of Aerospace Systems, The University of Texas at El Paso, ISBN: 97404-279-8, El Paso, Texas, January 1998, pp 23-35.

Employment

Research Associate, Civil Engineering Department, Texas A&M University.
To become Assistant Professor in College of Architecture at Texas A&M University effective September 2001

Dr. Cesar Carrasco

Doctor of Philosophy
Materials Science and Engineering, UTEP
Date: July 2000

Dissertation Title

Development of a Constitutive Microdamage Model for Simulation of Damage and Fracture of Metallic Plates Caused by Hypervelocity Impact

Supervisors

Drs. John Eftis and Roberto Osegueda

Abstract

A constitutive microdamage model is developed capable of simulating high shock compression, release, dilatation (tension), and microdamage evolution leading possibly to fracture and penetration of targets after hypervelocity impact. The microdamage constitutive model is applicable to polycrystalline metals and is appropriate in the lower range of hypervelocity impact velocity, i.e. approximately 2-7 km/s, over which the projectile and target materials remain in the solid state. The model implements the Mie-Gruneisen equation of state coupled with the Hugoniot relations along with expressions of non-linear elastic moduli (bulk and shear) as functions of volume strain, temperature and microdamage. The viscoplastic material response includes strain and strain rate hardening and temperature and microdamage softening. The microdamage evolution model is based on the micromechanics of an expanding void, and is capable of modeling void compaction and expansion that leads to spall-fracture as an evolutionary time dependent process. The constitutive microdamage model was implemented in the Autodyn™ software and a series of computer simulations of hypervelocity impact experiments on Al_{1100} plates with soda-lime glass spherical projectiles were conducted. The results of the simulations are compared with the laboratory experimental results in terms of crater, penetration hole and back-wall spallation geometry of the target plate.

Publications

Carrasco, C.J., Osegueda, R.A., Ferregut, C. and Grygier, M., "Damage Localization in a Space Truss Model Using Modal Strain Energy," Proceedings of the 15th International Modal Analysis Conference, IMAC97, V.2, Society for Experimental Mechanics, Inc., Bethel, Connecticut, pp. 1786-1792, 1997.

Perez, L.E., Ferregut, C., Carrasco, C., Paez, T.L., Barney, P. and Hunter, N.F., "Statistical Validation of a Plate Finite-Element Model for Damage detection," in Smart Structures and Materials: Smart Systems for Bridges, Structures and Highways, March 1997.

Carrasco, C.J., Osegueda, R.A., Ferregut, C.M., and Gryger, M. "Localization and Quantification of Damage in a Space Truss Model Using Modal Strain Energy," in Smart Structures and Materials: Smart Systems for Bridges, Structures and Highways, March 1997.

Osegueda, R.A., Carrasco, C.J. and Meza, R., "A Modal Strain Energy Distribution Method to Localize and Quantify Damage," Proceedings of the 15th International Modal Analysis Conference, IMAC97, V.2, Society for Experimental Mechanics, Inc., Bethel, Connecticut, pp. 1298-1304, 1997.

Meza, Jr. R., Carrasco, C.J., Osegueda, R.A., James, G., and Robinson, N., "Damage Detection in a DC-9 fuselage Using Laser Doppler Velocimetry," Proceedings of the 15th International Modal Analysis Conference, IMAC97, V.2, Society for Experimental Mechanics, Inc., Bethel, Connecticut, pp. 1779-1785, 1997.

Andre, G.C., Carrasco C.J., Osegueda, R.A., Ferregut, C.M., James III, G.H. and Grygier, M., "Comparison of Accelerometer and Laser Modal Tests of a Vertical Stabilizer Assembly," SPACE 98, ASCE, April 1998, pp.132-139.

Osegueda, R.A., Andre, G., Ferregut, C.M., Carrasco, C., Pereyra, L., James, G. III, Grygier, M. and Rocha, R., "A Strain Energy-Based Vibrational NDE Method Applied to an Aerospace Structure," 9th Annual Symposium on Non-Destructive Characterization of Materials, Sydney, Australia, July 1999.

Pereyra, L.R., Osegueda, R.A., Carrasco, C. and Ferregut, C.M., "Damage Detection in a Stiffened-Plate Using Modal Strain Energy Differences," SPIE Conference on Nondestructive Evaluation of Aging Aircraft, Airports, and Aerospace Hardware III, Newport Beach, CA, March 1999, Vol. 3586, pp. 211-222.

Pereyra, L.R., Osegueda, R.A., Carrasco, C. and Ferregut, C.M., "Structural Defects Detection Using Low Frequency Modal Testing With a Laser Vibrometer," ASNT Fall Conference and Quality Testing Show, Nashville, TN, October 1998, pp. 63-66.

R.A. Osegueda, M. Macias, G. Andre, C.M. Ferregut and C. Carrasco, "Fusion of Modal Strain Energy for Health Monitoring of Aircraft Structures", In Nondestructive Evaluation of Aging Aircraft, Airports, and Aerospace hardware IV, Ajit K. Mal, Editor, Proceedings of SPIE Vol. 3994, Newport Beach, CA, March 7-8 2000, pp. 117-127.

L.R. Pereyra, R.A. Osegueda, C. Carrasco and C. Ferregut, "Detection of Damage in a Stiffened Plate from Fusion of Modal Strain Energy Differences", proceedings of IMAC 2000, San Antonio, TX, February 7-10, 2000, pp. 1556-1562.

J. Eftis, C. Carrasco and R. Osegueda, "Modeling Dynamic Fracture Following High Shock Compression", In Damage and Fracture Mechanics VI Computer Aided Assessment and Control, Eds. A.P.S. Selvadurai and C.A. Brebbia, WIT Press, Southampton, Boston, 2000, ISBN: 1-85312-812-0, pp. 267-279

Internships

NASA Johnson Space Center, Houston, Texas, Summer 1995. Supervised by Dr. George James, III
NASA Johnson Space Center, Houston, Texas, Summer 1997. Supervised by Dr. George James, III

Employment

Assistant Professor at the Civil Engineering Department at the University of Texas at El Paso.

Arturo Revilla
Doctor of Philosophy
Electrical and Computer Engineering, UTEP
Date: December 2000

Dissertation Title
Predicting Probe Impedance Change in Eddy Current Nondestructive Testing Using Finite Elements

Supervisor
Dr. Joseph Pierluissi

Abstract

In recent times, the desire to extend the service life of aerospace structures to offset the cost of replacement has led to an increase in the need to accurately predict the state of a structure by means of nondestructive evaluations. One such type of inspection is that of eddy current nondestructive inspection. The inspection is however difficult, and the data interpretation requires a great deal of expertise and experience with these types of systems. In order to solve some of these problems the use of numerical models has been extensive and in particular, the modeling of eddy current nondestructive evaluation problems has been the subject of much research over the past few decades. The advent of faster computers has made the process of simulating the full three-dimensional space and the eddy current nondestructive inspection of parts feasible. However, in order to achieve full automation of the eddy current nondestructive inspection the availability of accurate models to predict the expected change of probe impedance due to a flaw within a structure are required. The purpose of such models is to generate quality synthetic data, which can, in some cases, be used to aid in the evaluation of data collected during the inspection process. The study presented in this dissertation probes the state of the art in eddy current modeling by making use of a commercially available finite element software package and examining the compromises, which must be made in order to generate quality synthetic data in a reasonable amount of time.

Publications

Osegueda, R.A., Revilla, A., Pereyra, L.R. and Moguel, O., "Fusion of Modal Strain Energy Differences for Localization of Damage," SPIE Conference on Nondestructive Evaluation of Aging Aircraft, Airports, and Aerospace Hardware III, Newport Beach, CA, March 1999, Vol. 3586, pp. 189-199.

"Predicting Probe Impedance change in Eddy Current Nondestructive Testing using Finite Elements", Arturo Revilla, UTEP, Dec. 2000.

Internships

Air Force Research Labs, Wright Patterson Air Force Base, Summer 1998.

Employment

Computer Engineer
U.S. Army Research Laboratory
Survivability/Lethality Analysis Directorate
White Sands Missile Range

Work with testing and evaluating Army Systems to ensure that they are "hacker" proof, i.e. Survivable under adverse conditions and able to perform there designated mission. The work involves security analysis; exploit research as well as the evaluation of the configuration of the systems.

Dr. Maria Estela Calixto

Chemistry
Universidad Nacional Autonoma de Mexico, UNAM
(National Autonomous University of Mexico)
June 2001

Dissertation Title

Characterization of Formation and Growth Mechanisms of Electro-Deposited $CuInSe_2$ Thin Films and their Applications to Solar Cells

Supervisor

Dr. Sebastian P. Joseph
Dr. John McClure supervised her work at UTEP

Abstract

In the present research project we studied the co-deposition of CIS thin films. A process for obtaining CIS thin film precursors with reproducible properties was developed. These precursors when subjected to a post-deposition thermal treatment in Se atmosphere showed characteristics similar to that obtained by thermal evaporation.

The films were grown by optimizing the deposition conditions. For this the deposition parameters such as, molar bath composition, pH of the solution, deposition potential and deposition time were varied (one at a time) to study their influence on film properties. From the results obtained from this analysis, we could establish the best deposition conditions for CIS thin films. Later on, a detailed study was carried out on the growth mechanism for CIS thin films. This study was performed using cyclic and linear sweep voltamperometry techniques on Cu-In-Se system in the interval, +0.3 to –0.7V/SCE and at a sweep velocity of 5 mV/s. To avoid the effect of oxidation during the potential sweep, the electrolyte was deoxygenated by flushing with nitrogen for 30 minutes. The nitrogen atmosphere was maintained on the electrolyte surface to avoid further oxygen entry into the electrolyte. The cyclic voltamperogram indicated that the CIS film formation is irreversible and only in the interval 0.3 to 0.7 V/SCE the reduction peaks were observed and there were no peaks corresponding to the oxidation during the reverse scan. The standard reduction potentials for Se, Cu and In are, 0.5, 0.1 and –0.5 V/SCE respectively. Taking these values as reference, reduction peaks observed at specific potentials in the voltamperogram were assigned for each element. In this way it is established that Se gets deposited first, followed by Cu and then In. For this reason CIS films were deposited at specific potentials close to those obtained from the voltamperogram peaks. The films were later on analyzed by x-ray diffraction. In this way it was established that it is possible to grow CIS thin films in the potential region –0.36 to –0.45 V/SCE. Once the deposition conditions were established for CIS, we decided to investigate in more detail the probable reaction mechanisms, which lead to the nucleation and growth of CIS films by electrodeposition.

This investigation was carried out by employing solid state as well as electrochemical characterization techniques. By the solid state techniques, the films grown on different substrates and by the electrochemical techniques, the growth processes for the CIS films were analyzed. This analysis established that the film formation is preceded by copper selenide (Cu_xSe) and indium selenide formation (In_2Se_3) and a chemical reaction between the two as indicated below:

$$2CuSe + In_2Se_3 \rightarrow 2CuInSe_2 + Se,$$

which explains the film formation and excess of Se in the film. This fact was verified by composition analysis done in the bulk and on the film surface. In addition, further complementary studies were carried out to analyze the structural, morphological and opto-electronic properties at different growth stages of the film

According to the results obtained from the physicochemical characterization of the films it was found that p-CIS films possess a band gap of E_g = 1.1 eV and a carrier density of the order of $N_A = 2.27 \times 10^{16}$ cm^{-3}. These films show stochiometry very close to that of CIS, the same may be obtained by a post-deposition treatment of the film at 500 °C in Se atmosphere. In this way one can get CIS thin films with suitable characteristics for their application in solar cells. This fact was further proved by fabricating CIS and $CuIn_xGa_{1-x}Se_2$ (CIS modified with Ga) based solar cells with electrodeposited precursors, which showed conversion efficiencies of 8% and 9.87% respectively. The solar cell structures were fabricated and tested under AM 1.5 conditions at the National Renewable Energy Laboratory, Golden, Colorado, USA

Publications

Calixto, M.E., McClure, J.C., Singh, V.P., Bronson, A., Sebastian, P.J. and Mathew, X., "Electrodeposition and Characterization of CdTe Thin Films on Mo Foils Using a Two Voltage Technique," presented at the International Materials Research Congress Cancun 99, Cancun, Mexico, August 1999.

Internships

Estela was sponsored by the FAST Center to spent one year at UTEP to perform her experimental work, to foster US-Mexico relationships

Employment

Will join husband who is pursuing Ph.D. at U.C. Berkeley.

Fariba Ansari
MS in Physics

Ph.D. Candidate
Materials Science and Engineering
Expected Graduation Date: December 2002

Tentative Dissertation Title

Determination of Composite Materials Properties using Lamb-Waves

Ms. Fariba Ansari is pursuing her Ph.D. in Materials Science and Engineering at the University of Texas at El Paso. Her research consists on developing inverse algorithms of the Lamb-Waves propagation characteristics to determine the materials elastic constants.

She is being supervised by Dr. Soheil Nazarian and expects to complete in December 2002.

A.2 Masters Graduates and Students

Raul Meza
B.S. in Civil Engineering
Master of Science in Civil Engineering
Date: July 1997

Thesis Title
Modal Tests of Composite Honeycomb Panels Using Laser Doppler Velocimetry for Damage Assessment

Supervisor
Roberto Osegueda

Abstract

Four composite panels consisting of 4-ply T300 graphite cloth laminate with a Nomex honeycomb core were modal tested using a Laser Doppler Velocimeter (LDV). One panel included no defects and the other three had engineered defects consisting of a disbond, a delamination and fluid ingress. The defects were within a 4-inch diameter circle at the center of the panels. The LDV scanned a grid of 23 points by 23 points of the surface of the panels when the panels were suspended and subjected to a random shaker excitation from 10 Hz to 1000 Hz. During the modal tests, random speckle dropout experimental noise, which was caused by a malfunction of the LDV optics, produced low coherences in the frequency response functions (FRF). This was partially solved by repeating each test four times and selecting the FRF with the highest coherence. The collected FRFs were curve-fitted using a poly-reference technique in the software SDRC I-DEAS to extract the modal parameters. A computer-assisted procedure was devised for visually identifying the outliers in the modal shape data for elimination in further analyses. The modal shapes were curve-fitted for the purpose of smoothing the modal shapes and extracting the modal slopes without loosing too much of the higher order content of the modes. The modal strain energy content of the elements was extracted using a finite element representation of the scanned area of the panels. Two energy-based damage detection methods were applied. The damage localization patterns obtained failed to indicate the known location of the damage.

Publications

Meza, Jr., R., Osegueda, R.A., Carrasco, C.J. and James III, G., "Modal Tests of Composite Honeycomb Panels Using Laser Doppler Velocimetry for Damage Assessment", Report FAST 96-02, FAST Center for Structural Integrity of Aerospace Systems, The University of Texas at El Paso, El Paso, Texas, 79968.

Meza, Jr., R., Carrasco, C.J., Osegueda, R.A., James III, G. and Robinson, N.A., "Damage Detection in a DC-9 Fuselage using Laser Doppler Velocimetry", Proceedings of the 15th International Modal Analysis Conference, Society of Experimental Mechanics, Orlando, Florida, Feb. 3-6, 1997.

Osegueda, R.A., Carrasco, C.J. and Meza, Jr., R., "A Modal Strain Energy Distribution Method to Localize and Quantify Damage", Proceedings of the 15th International Modal Analysis Conference, Society of Experimental Mechanics, Orlando, Florida, Feb. 3-6, 1997.

James III, G., Hansche, B., Meza, Jr., R. and Robinson, N., "Health Monitoring Studies on Composite Structures For Aerospace Applications", Proceedings of the 5th ASCE International Conference on Engineering, Construction, and Operations in Space - Space '96, Albuquerque, NM, June 1-6, 1996.

Robinson, N.A., Peterson, L.D., James III, G. and Meza, Jr., R., "Health Monitoring Studies for Aircraft Applications", Proceedings of the 1996 AIAA Adaptive Structures Forum in conjunction with the 1996 Structures, Structural Dynamics, and Materials Conference, Salt Lake City, Utah, April. 18-19, 1996.

Meza, Jr., R., Carrasco, C.J., Osegueda, R.A., James III, G. and Robinson, N.A., "Damage Evaluation in a DC-9 Fuselage using Laser Doppler Velocimetry Measurements", Proceedings of the 1997 SPIE Smart Structures and Materials Symposium, San Diego, CA, March 3-6, 1997.

Internship

FAA NDI Validation Center, Sandia National Labs, Albuquerque, New Mexico, supervised by Bruce Hansche and George James, Summer 1997.

Employment

Working for Robert Navarro & Associates, a structural engineering consulting firm, performing design/analysis of structures consisting mainly of buildings, water/wastewater treatment plants & lift stations, and other type reinforced concrete-steel structures.

Luis Perez
B.S. in Civil Engineering
Master of Science in Civil Engineering
Date: July 1997

Thesis Title
Statistical Validation of a Plate Finite Element Model for Damage Detection

Supervisor:
Dr. Carlos Ferregut

Abstract

Modal vibration testing was conducted on a suspended rectangular aluminum plate in order to obtain its corresponding frequency response functions of the plate were obtained by the use forty-nine accelerometers symmetrically mounted through out the plate. The input signal used to excite the plate consisted of a random shaker excitation from 10 to 2000 Hz. The collected frequency response functions were curve-fitted using a polyreference technique in the software SDRC I-DEAS to extract the plates dynamic characteristics, in particular the first two vibration modes. A finite element model of the plate was created in the computer code ALGOR to find the theoretical mode shapes of the plate. A model validation scheme based on the bootstrap statistical technique, was implemented as a means of providing a direct comparison between the experimental vs. theoretical dynamic mode shape behavior of the plate. The bootstrap used the experimental modal displacement data to estimate the confidence bounds of a statistic of interest of the vibration behavior of the plate. Hypothesis testing was then used to determine whether to accept or reject the finite element model created on the basis of the relative location of the predicted theoretical modes to the confidence region derived by bootstrapping the experimental data.

Publications

Paez, T., Barney, P., Hunter, N., Ferregut, C. and Perez, L.E., "Statistical Validation of Physical Systems Models," presented at 67th Shock and Vibration Symposium, Monterrey California, November 18-22, 1996.

Hunter, N.F., Barney, P., Ferregut, C., Perez, L.E., and Paez, T.L., "Statistical Validation of Stochastic Models," Proceedings of the 15th International Modal Analysis Conference, IMAC97, V.1, Society for Experimental Mechanics, Inc., Bethel, Connecticut, pp. 605-611, 1997.

Perez, L.E., Ferregut, C., Carrasco, C., Paez, T.L., Barney, P. and Hunter, N.F., "Statistical Validation of a Plate Finite-Element Model for Damage detection," in Smart Structures and Materials: Smart Systems for Bridges, Structures and Highways, March 1997.

Remarks

Started in FAST Center as an undergraduate Student

Employment

Worked at Boeing, Seattle, from August 1997 through July 1999. Then moved to Houston, Texas.

Working as a Design Engineer III at FMC SOFEC in Houston Texas, Responsible for the finite element analysis/verification of Single Point Moorings used by Floating Production Storage and Offloading (FPSO) Systems.

Murali Krishna
Master of Science in Computer Science
Date: July 1997

Thesis Title
Using Symmetries to Reduce the Size of a Fuzzy Knowledge Base, with an Application to Fault Detection

Supervisor
Dr. Vladik Kerinovich

Abstract
In many practical situations, we are interested in the value of a quantity y which is difficult to measure directly. For example, in non-destructive testing (NDT), we are interested in the location y of a (hidden) fault. To determine the value y, we measure related quantities $x_1,...,x_n$ and then reconstruct y from the results of these measurements. For example, in NDT, we can apply ultrasonic vibration to the tested object, and measure the vibration amplitude at different points. In some practical cases, we do not know the exact relation between y and $x_1,...,x_n$; instead, we have expert rules which describe this relation by using words of natural language such as "small", "large", etc. A special methodology called fuzzy logic has been developed to transform such "fuzzy" rules into a crisp computer algorithm which, given the measurement results $x_1,...,x_n$ estimates the value of the desired quantity y.

This methodology has been originally designed for handling simple rules, of the type "if x_1 is small, and x_2 is medium,...,then y is small". In some practical situations (in particular, in NDT) expert rules have a more complex form, such as "if two out of five measurements show increase, then...". In principle these complex rules can be represented as a sequence of several simple rules, but this representation leads to an exponential increase in the number of rules, which makes the resulting rule-based system non-feasible.

In this thesis, we show that using symmetries can drastically reduce the size of the resulting knowledge base and hence, make the fuzzy approach feasible. We illustrate our method on the example of NDT; for this example, fuzzy approach leads to very good fault detection.

Publications

Krishna, M., Kreinovich, V. and Osegueda, R.A., "Fuzzy Logic in Non-Destructive Testing of Aerospace Structures," 42nd Midwest Symposium on Circuits and Systems, Las Cruces, NM, August 1999.

Employment

Worked for one year as a web developer in Insight, Phoenix, Arizona. He currently works as a software consultant at Keane Inc., Syracuse, New York.

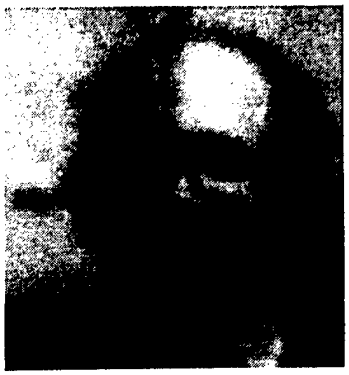

David C. Doran

BS in Mechanical Engineering
Master of Science in Civil Engineering
Date: July 1997

Thesis Title
Toward Strength Characterization of Connections Employed in Reticulated Structures

Supervisor
Dr. Carlos Ferregut

Abstract

The strength and failure mechanism characterization of elements and materials employed in the construction of structures is a critical prerequisite for the incorporation of such materials in common practice. The testing herein documented served to examine and document capacities and failure behaviors under a range of load conditions.

Tension, compression end buckling, and bending capacities have been tested with small sample populations, comparable to a number of other test series. Results have been compared with published results for similar elements when possible. For most test cases, probabilistic modeling has been conducted using available, applicable data to predict design loads for which a 95% confidence exists.

Two data screening tools are proposed for use in determining the applicability of the two-population modeling approaches employed in the probabilistic modeling effort. The two data screening tools are provisionally offered as aids, pending further development

Publications

Doran, D., Ferregut, C. Tirado, C. "Experimental Strength Characterization of Geometrica Connections Subjected to Tension, Compression and Bending," International Symposium on Shell and Spatial Structures, Singapore, November 10-14, 1997.

Remarks

Research performed at the FAST Center and sponsored by NASA

Employment

Upon Graduation, Mr. Doran went to work for the U.S. Civil Service, Kelly Air Force Base. Current whereabouts unknown.

Maria Posada-Portillo
BS in Metallurgical and Materials Engineering, Dec. 1995
Master of Science in Metallurgical and Materials Engineering
Date: July 1998

Thesis Title
Re-examination and Overview of Exfoliation Corrosion Occurring in 2024 A1 Alloy Aircraft Body Skins

Supervisors
Drs. Roy Arrowood and Lawrence Murr

Abstract
Exfoliation, a directional attack along elongated grain boundaries in rolled aluminum sheet and plate, has been examined in some detail for KC-135 aging aircraft body skin samples utilizing optical metallography, SEM and TEM. In addition, fine-probe backscatter EDX scans and micro-diffraction analyses have been made for both grain matrix and boundary-related precipitates, as well as matrix precipitates and their relationship to corrosion and corrosion nucleation. These observations suggest that anodic sites nucleating corrosion may not play a significant role in the nucleation and propagation of exfoliation corrosion. An interest stems form the directionality specific to exfoliation corrosion where there may exist a crystallographic origin or a unique crystallographic feature may characterize the elongated grain boundary and influence the corrosion path. TEM observations coupled with selected-area electron diffraction analyses were made to measure specific misorientations because misorientations are related to boundary energies. These observations were also compared with energy backscatter diffraction (EBSD) data performed on the aluminum skin for both in-plane and sheet thickness directions. There appears not to be a strong correlation between EBSD observations of misorientation with TEM measured misorientations for identically oriented grains used in comparing grain boundaries. The TEM data shows a bi-modal (high and low misorientation angle) distribution for the transverse (in-thickness) direction while the in-plane direction is more evenly distributed throughout which may suggest some crystallographic distinction. In addition, the role that hard corrosion products play appear to be significant in the propagation of the corrosion as they create wedging stresses between grain layers along the elongated grain boundaries.

Publications

L.E. Murr, Maria Posada, Roy M. Arrowood, Na D. Little, Some New Approaches to Understanding and Characterizing Exfoliation Corrosion in Aircraft Aluminum Alloy Sheet Metal, in: Proceedings of the workshop on Intelligent NDE sciences for Aging and Futuristic Aircraft, Sept. 30 -Oct. 2, 1997, C. Ferregut, R. Osegueda, A. Nunez. eds., Texas Western Press, UTEP.

Maria Posada, L.E. Murr, R.M. Arrowood, Observations of Exfoliation Corrosion in Aging Aircraft Body Skins: A search for Crystallographic Issues, in Microstructural Science, D.E. Alman, J.A. Hawk, J.W. Simmons, eds., 25(1997)131-138.

Maria Posada, L.E. Murr, C.-S. Niou, D. Roberson, D. Little, Roy Arrowood, and Debra George, Materials Characterization 38 (1997).

Remarks

Started in FAST Center as an undergraduate Student

Employment

Working as a Systems Planning, Research Development Engineering (SPRDE) Acquisition Intern assigned to Naval Sea Systems Command (NAVSEA). During my internship, I had rotational assignments to the Welding and NDE Branch at Naval Surface Warfare Center Carderock Division (NSWCCD) in W. Bethesda, MD and Naval Research Laboratory (NRL) in Washington, D.C. My current position is a Materials Engineer at NSWCCD for the Welding and NDE Branch. In my current position, I am working on various programs, which include friction stir welding, welding of HSLA-65, fabrication of Ti components for missiles, eddy-current sensor development, and thermal spray.

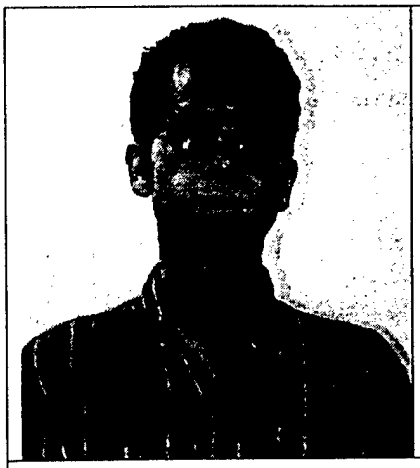

Miguel Castro
Master of Science in Physics
Date: July 1998

Thesis Title
Identification of Laser-Induced Lamb Waves in Aluminum Plates

Supervisors

Drs. Jorge Lopez and Roberto Osegueda

Abstract

The objective was to identify experimentally the propagating modes after short pulse 532 nm laser light from a Q-switched Nd:YAG was delivered on an aluminum plate. A laser line-shaped ultrasonic source induces Lamb modes. The analysis was carried out by detecting the ultrasonic modes through contact piezoelectric detectors along a wave propagation line. The two-dimensional fast Fourier transform aided processing the data. Good agreement is observed between theoretical and experimental dispersion curves for the first fundamental symmetrical and anti-symmetrical modes.

Publications

Castro-Colin, M., Lopez, J.A. and Osegueda, R., "Tuning Laser-induced Lamb Waves," Submitted for publication to the Journal for Non-Destructive Evaluation.

Employment

Ph.D. Candidate pursuing Ph.D. in Physics at the University of Houston, Houston, Texas. Expect to complete in May 2002.

Leopoldo Pereyra
B.S. in Civil Engineering
Master of Science in Civil Engineering
Date: December 1998

Thesis Title
Structural Damage Localization in a Stiffened-Plate Using Modal Analysis, Laser Velocimetry and a High-Order Curve Fit Method

Supervisor:
Dr. Roberto Osegueda

Abstract

An aluminum stiffened-plate resembling aircraft-fuselage construction was built and modal-tested in the laboratory with a Laser Doppler Velocimeter (LDV). The purpose of the test was to extract out-of-plane modal data before and after the infliction of damage, which was used to evaluate a global NDE damage localization technique. The NDE damage localization technique is based on modal strain energy differences between the undamaged and damaged states. To compute the modal strain energies and to enhance the resolution of damage detection, the modal bending and twisting curvatures were obtained using an iterative curve-fit procedure using estimated curvatures obtained from finite differences and curve fit of the experimental mode shapes. Strain energy differences between matching modes of the undamaged and damaged structure locate the inflicted damage by indicating apparent increases in the modal strain energy distributions. The damage indications provided by several modes were probabilistically combined to create damage maps that accurately predict the correct location of inflicted damage. The test article was excited at two points with shakers exerting uncorrelated continuous random forces from 0 to 300 Hz. Experimental frequency response functions and their corresponding coherence were extracted from 239 data points uniformly spaced. The model was subjected to 22 damage scenarios at eight different zones. This thesis presents the results, conclusions and recommendations of the global NDE technique used. Emphasizing the improved accuracy that resulted from combining probabilistic and modal information, and using high-order curve-fit algorithms to estimate curvatures.

Publications

Osegueda, R.A., Andre, G., Ferregut, C.M., Carrasco, C., Pereyra, L., James, G. III, Grygier, M. and Rocha, R., "A Strain Energy-Based Vibrational NDE Method Applied to an Aerospace Structure," 9th Annual Symposium on Non-Destructive Characterization of Materials, Sydney, Australia, July 1999

Pereyra, L.R., Osegueda, R.A., Carrasco, C. and Ferregut, C.M., "Damage Detection in a Stiffened-Plate Using Modal Strain Energy Differences," SPIE Conference on Nondestructive Evaluation of Aging Aircraft, Airports, and Aerospace Hardware III, Newport Beach, CA, March 1999, Vol. 3586, pp. 211-222.

Osegueda, R.A., Revilla, A., Pereyra, L.R. and Moguel, O., "Fusion of Modal Strain Energy Differences for Localization of Damage," SPIE Conference on Nondestructive Evaluation of Aging Aircraft, Airports, and Aerospace Hardware III, Newport Beach, CA, March 1999, Vol. 3586, pp. 189-199.

Pereyra, L.R., Osegueda, R.A., Carrasco, C. and Ferregut, C.M., "Structural Defects Detection Using Low Frequency Modal Testing With a Laser Vibrometer," ASNT Fall Conference and Quality Testing Show, Nashville, TN, October 1998, pp. 63-66.

L.R. Pereyra, R.A. Osegueda, C. Carrasco and C. Ferregut, "Detection of Damage in a Stiffened Plate from Fusion of Modal Strain Energy Differences", proceedings of IMAC 2000, San Antonio, TX, February 7-10, 2000, pp. 1556-1562.

R.A. Osegueda, H. Lopez, L. Pereyra, C.M. Ferregut, "Localization of Damage Using Fusion of Modal Strain Energy Differences", proceedings of IMAC 2000, San Antonio, TX, February 7-10, 2000, pp. 695-701.

Employment

Working as a Junior Project Manager at Lintel Corporation in Juarez, Mexico. Coordinating and supervising all the activities required to complete an industrial building. (Footings, Structure, Mechanical and Electrical Installations, finishes...In addition, the administration and scheduling of activities and resources in the construction site.
Also pursuing MBA at UTEP

Gabriela Andre
B.S. in Civil Engineering
Master of Science in Civil Engineering
Date: May 1999

Thesis Title
Comparison of Vibrational Damage Detection Methods in an Aerospace Vertical Stabilizer Structure

Supervisors
Drs. Roberto Osegueda and Carlos Ferregut

Abstract

The Vertical Stabilizer Assembly (VSA), a prototype of the upper section of an early version of a Shuttle Orbiter Vertical Stabilizer, was modal tested in the Vibration and Acoustic Test Facilities of the NASA Johnson Space Center. The purposes of the tests were (a) compare Laser Doppler Velocimeter (LDV) with accelerometer measurements and (b) to obtain a database to study vibrational nondestructive damage evaluation methods in complex aerospace structures. The VSA was subjected to several levels of damage.
This thesis considers four different vibrational damage detection methods based on modal strain energy differences between the undamaged and damaged states of a structure. Two of the methods are new and are based on probability ass functions defined with the positive regions of modal strain energy differences. A finite element model is used to extract complete mode shapes from modal measurements at few points and to compute modal strain energy distributions. The strain energy differences between modes of the undamaged and damaged states served as the basis for implementing the four detection methods. Damage maps were obtained using all methods and considering four different mode-selection criteria. One of the criteria is to use the results of a statistical analysis between the frequency response functions between the undamaged and damage states to identify modes of significant global change. The performance of the methods ad mode-selection criteria in detecting damage were evaluated in terms of detectability, false positives and compared. Valuable conclusions are presented.

Publications

Andre, G.C., Carrasco C.J., Osegueda, R.A., Ferregut, C.M., James III, G.H. and Grygier, M., "Comparison of Accelerometer and Laser Modal Tests of a Vertical Stabilizer Assembly," SPACE 98, ASCE, April 1998, pp.132-139.

Osegueda, R.A., Andre, G., Ferregut, C.M., Carrasco, C., Pereyra, L., James, G. III, Grygier, M. and Rocha, R., "A Strain Energy-Based Vibrational NDE Method Applied to an Aerospace Structure," 9th Annual Symposium on Non-Destructive Characterization of Materials, Sydney, Australia, July 1999.

R.A. Osegueda, M. Macias, G. Andre, C.M. Ferregut and C. Carrasco, "Fusion of Modal Strain Energy for Health Monitoring of Aircraft Structures", In Nondestructive Evaluation of Aging Aircraft, Airports, and Aerospace hardware IV, Ajit K. Mal, Editor, Proceedings of SPIE Vol. 3994, Newport Beach, CA, March 7-8 2000, pp. 117-127. **(BEST CONFERENCE PAPER AWARD)**

Internships

NASA Johnson Space Center, Summer 1997, supervised by George James.

Remarks
Thesis awarded the "Best University Thesis for 1999-2000 academic year.

Employment

Pipeline Project Engineering, Texas Utilities, Dallas, Texas

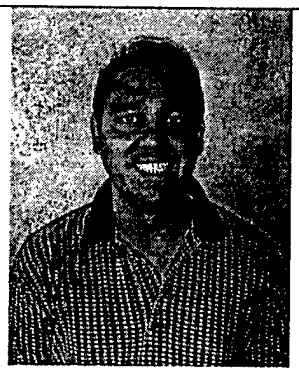

Angel Urbina
B.S. in Civil Engineering
Master of Science in Civil Engineering
Date: May 1999

Thesis Title
Probabilistic Analysis of Rechargeable Batteries in a Renewable Power Supply System

Supervisors
Drs. Carlos Ferregut and Thomas Paez

Abstract

A probabilistic model of the behavior of a rechargeable battery acting as the energy storage component in a renewable power supply system is developed. Stochastic and deterministic models are created to simulate the behavior of the system components. The components are the solar resource, the photovoltaic power supply system, the rechargeable battery, and a load profile. Artificial neural networks are incorporated into the model of the rechargeable battery to simulate damage that occurs during discharge cycles. The equations governing system behavior are combined into one set and solved simultaneously in the Monte Carlos framework to evaluate the probabilistic character of measures of battery behavior.

Publications

"Probabilistic Analysis of Rechargeable Batteries in a Renewable Power Supply System", Master's Thesis, The University of Texas at El Paso, El Paso, TX., 1999.

Urbina, A., Hunter, N., and Paez, T.L "Characterization of Nonlinear Dynamic Systems Using Artificial Neural Networks", Proceedings of the 69st Shock and Vibration Symposium, Minneapolis, MN, October 12-16, 1998.

Internships
Los Alamos National Laboratory, Fall 1997, supervised by Dr. Norm Hunter.
Sandia National Labs, Summer and Fall 1998, supervised by Dr. Thomas Paez

Employment

Working as a technical staff member at Sandia National Labs in the Experimental Structural Dynamics Department and currently in the Validation and Uncertainty Quantification Processes Department. Most of my work has been in the field of model validation especially structural dynamic models.

Cesar Tirado
B.S. in Civil Engineering
Master of Science in Civil Engineering
Date: May 1999

Thesis Title
Numerical Investigation on Propagation of Lamb Waves in Damage Plates

Supervisor
Dr. Soheil Nazarian

Abstract

The impact of damage on the propagation of Lamb waves was investigated using finite element analysis. The propagation of different modes of vibration of elastic waves in plates with and without defects, has been modeled and studied. Flaws representing cracks were introduced into the model. The effect of the size of the crack on the amplitudes of the waves and the presence of mode conversion was studied. An explicit finite element analysis software, DYNA2D, was used to model a simply supported plate with a plane strain geometry. Three materials were modeled for this purpose: Aluminum 6061-T6, Steel A36, and Graphite-Epoxy. The composite plate was analyzed in directions parallel and perpendicular to the fibers. Seven different crack depths, and three crack widths, were modeled to find the reflection and transmission ratios. The effect of the presence of damage on the propagation velocity was also studied. Low-frequency input signals were intentionally selected, so that basically the fundamental symmetric and antisymmetric modes could be excited. Furthermore, a two-dimensional Fourier transform (2D-FFT) method was introduced to identify and measure the amplitudes and velocities of individual Lamb wave modes propagating in a plate. Reflection and transmission ratios, obtained from both time domain records and from a 2D-FFT method, were found to be largely dependent on the crack depth and insensitive to notch crack

Publications

Tirado, C. and Nazarian, S., "Impact of Damage on Propagation of Lamb Waves in Plates," SPIE Conference on Nondestructive Evaluation of Aging Aircraft, Airports, and Aerospace Hardware III, Newport Beach, CA, March 1999, Vol. 3586, pp. 267-278.

Remarks

Started in FAST Center as an undergraduate Student

Employment

Started Ph.D. at Rice University in September 2000.

Haydy Obispo
BS in Metallurgical and Materials Engineering
Master of Science in Metallurgical and Materials Engineering
Date: December 1999

Thesis Title
Copper Deposition During the Corrosion of Aluminum Alloy 2024 in Sodium Chloride Solutions

Supervisor
Dr. Lawrence Murr

Abstract

Pitting corrosion on aluminum alloy airframe and airplane sheet materials is a common problem associated with aging aircraft. Pitting corrosion in particular, is a localized attack where the rate of attack is much faster at certain small specific areas on the surface. Copper plating and/or cementation from solution seems to have a direct influence on the pitting corrosion of aluminum alloy 2024, aircraft body skin sheets. After these sheets were exposed to acidic (pH = 3), almost neutral (pH = 6), and basic (pH = 11) 0.6 M NaCl solutions, copper and copper-rich particle clusters were observed to deposit on them.

Scanning electron microscopy (SEM) and EDX spectrometry were used to observe and analyze the copper particles, which often deposit close to iron-rich particles. A Hitachi-H 8000 scanning transmission electron microscope (STEM) was used to document the as-received microstructure, as well as to identify the constituent particles and particle regimes. Second-phase particles found in the alloy sheet include an Al-Cu-Mu, Al-Cu-Si, Al-Cu-Mg, Al-Cu-Fe-Mn-Si, among others.

In addition, a replica lift-off technique was used to remove corrosion products from the corroded samples. The STEM and an EDX spectrometer were then employed to reveal a wide range of copper deposits with microdendritic morphologies after being exposed to neutral and basic solution, and clusters with a more nodular appearance after being exposed to an acidic solution. These observations support a new concept for pitting corrosion in aluminum-copper alloys like 2024 aluminum.

Publications

Obispo, H. M., Murr, L. E., Arrowood, R. M., and Trillo, E. A., "Copper Deposition During the Corrosion of Aluminum Alloy 2024 in Sodium Chloride Solutions, Journal of Materials Science, 2000.

Remarks

Started in FAST Center as an undergraduate Student

Employment

Works at Dutch Petroleum Company, West Indies.

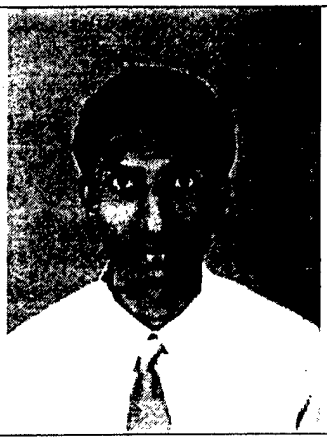

Sudhir Prabhu

Master of Science in Mechanical Engineering
Date: December 1999

Thesis Title

Damage Detection in a Stiffened Structure using Modal Strain Energy Differences and Finite Element Methods

Supervisor
Dr. Roberto Osegueda

Abstract

The modal testing of an aluminum stiffened plate panel, a prototype of an aircraft fuselage was performed in the laboratory using Laser Doppler Velocimeter to generate the modal data. The modal data obtained before and after the infliction of damage was used to identify and quantify the damage using the vibrational non-destructive damage evaluation method. The global NDE damage localization technique considered in this thesis is based on differences of modal strain energy densities between the undamaged and damaged states. A finite element model of the structure was modeled using MSC/NASTRAN and the experimental modal displacements were imposed on it, to compute the resonant frequencies and modal strain energy distributions. Strain energy differences between matching modes of he undamaged and damaged structure was used to locate the inflicted damage by indicating an apparent increase in the modal strain energy distributions. By combining the damage indications obtained from several modes, damage maps were created that accurately predict the correct location of the inflicted damage.

Also the study was extended to analyze the modal strain energy levels to detect damage in the structure. The strain energy distributions were categorized into high, medium and low zones to indicate the possibility of detecting the damage depending on its location.

Employment

Programmer Analyst, Supply Chain Consultants, Atlanta, GA.

Ana Leticia Campuzano-Contreras
B.S. in Metallurgical and Materials Engineering
Master of Science in Metallurgical and Materials Engineering
Date: May 2000

Thesis Title
Retrogression and Reaging Heat Treatment on Post-Service KC-135's Sections

Supervisor
Dr. Roy Arrowood

Abstract

KC-135s are unique and a valuable national resource. The importance of these aircraft has grown as in-flight refueling requirements have doubled in the past twenty years. The need to use these aging aircraft for forty more years has increased the interest in understanding corrosion damage in aircraft aluminum alloys.

Stringer ties from KC-135s, which have been in service, were analyzed after being exposed to different heat treatments. The stringer ties are made of aluminum alloy 7075-T6, which was high strength and low density but is prone to stress corrosion cracking (SCC). Corrosion resistance of this alloy can improve by over-aging the alloy to the T73 condition. This heat treatment (T7X) leads to a loss in the maximum strength of the alloy. A new heat treatment that can be used instead of T73 is retrogression and re-aging (RRA) heat treatment.

In 1973, Cina developed the RRA heat treatment to improve the resistance to stress corrosion cracking without sacrificing the strength of 7000 series aluminum alloys. The RRA treatment consists of a short time retrogression anneal in a temperature range within the two-phase ($\alpha+\eta$) region of the phase diagram, followed by water quenching and a final reaging treatment.

This study involves RRA heat-treating of post-service parts. Tensile tests were performed on sections that were subjected to a retrogression temperature of 220°C for 60 seconds, 5 minutes, and 30 minutes and were re-aged for 24 hours at 120°C. The samples have been examined by light microscopy and transmission electron microscopy (TEM). The effects of retrogression and reaging (RRA) heat treatment on post service parts revealed that the tensile strength increased and the corrosion susceptibility was reduced by a minimal amount. These findings are consistent with what other researchers have found.

Publication

Campuzano-Contreras, A.L., Arrowood, R.M., Murr, L.E., Little, D., Roberson, D., and Niou, C.S, "Characterization of Fuselage Skin Lap Joints", Microstructural Science Volume 25, 20-23, July 1997, Seattle, WA.

Internship

US Air Force, Oklahoma Air Logistic Center, Oklahoma City, OK, Summer 1997.

Employment

Boeing's Strategic Manufacturing Center at El Paso, TX
Materials and Processing Laboratory. Currently working at
ERC-CAS at Boeing-Irving Co. in Process Engineering.

Ravi Venugopalan

Master of Science in Electrical and Computer Engineering
Date: May 2000

Thesis Title
Structural Damage Localization in a Stiffened-Plate Using Laser Holography, Image Processing Techniques and a High-Order Curve Fitting Method

Supervisors:
Drs. Joseph Pierluissi and Roberto Osegueda

Abstract

An aluminum stiffened-plate panel resembling aircraft-fuselage was built and modal-tested in the laboratory using holographic methods. The purpose of the test was to extract out-of-plane modal data before and after infliction of damage, which were used later to evaluate a global Non-Destructive Evaluation (NDE) damage localization technique. The NDE damage localization technique is based on modal strain energy differences between the undamaged and damaged states. Digital image processing techniques were used to filter the data collected. To compute the modal strain energies and to enhance the resolution of damage detection, the modal bending and twisting curvatures were obtained through the adoption of an iterative curve-fit procedure using estimated curvatures obtained from finite differences and curve fit of the experimental mode shapes. Strain energy differences between matching modes of the undamaged and damaged structure help locate the inflicted damage by indicating apparent increases in modal strain energy distributions. The damage indications provided by several modes were probabilistically combined to create damage maps that attempt to predict the correct location of the inflicted damage. The test article was excited by a electromagnetic shaker exerting uncorrelated continuous random forces from 0 to 3500 Hz. Forty mode shapes were found within this range and mode shapes were extracted. This thesis presents the results, conclusions and recommendations of the global NDE technique used. Emphasizing the improved accuracy that resulted from combining probabilistic and fringe information, digital image processing techniques, and using high-order, curve-fit algorithms to estimate curvatures.

Presentation

R. Venugopalan, R. Osegueda and J. H.Pierluissi, " Structural Damage Localization in a Stiffened Plate using Laser Holography, image processing techniques and higher order curve fitting method," presented in the QNDE Conference, Iowa State University, July 20, 2000.

Employment

Design Verification Engineer, Microelectronics Division, IBM, Raleigh, North Carolina

Walter Alvarez
B.S. in Civil Engineering
Master of Science in Civil Engineering
Date: May 2000

Thesis Title

Artificial Neural Network Models for Damage Detection Using Lamb Waves

Supervisor
Drs. Carlos Ferregut and Soheil Nazarian

Abstract

This thesis describes work towards the development of a method for analysis of reflection and transmission characteristics of ultrasonic waves in aluminum plates to detect and localize possible damages. The proposed analysis approach is based on artificial neural networks. The proposed approach requires the excitation of an ultrasonic Lamb wave by a piezoelectric transmitting transducer, which propagates along the plate. If a receiving transducer is positioned at a remote point on the structure, the received signal contains information about the integrity of the scanned section between the transmitting and receiving transducers. A synthetic database was generated using a FE Model with several crack sized. This allowed building ANN models to predict the geometric characteristics of the defect based on the simulated data. Several network architectures were implemented and trained using the back propagation algorithm. At the end, three ANN models were created which determined the presence, location and magnitude of a defect. This thesis presents the results, conclusions and recommendation of the technique used.

Employment

Design Engineer, Paragon Project Consultants, Inc., Dallas, Texas
Provides project management services, highway, transportation and bridge design.

Mario Perez
B.S. in Civil Engineering
Master of Science in Civil Engineering
December 2000

Thesis Title

Performance of Vibrational Damage Detection Methods

Supervisor
Drs. Roberto Osegueda and Carlos Ferregut

Abstract

Vibration-based nondestructive damage detection methods are beginning to find application for the health monitoring of civil, aerospace and mechanical systems. The methods rely on the monitoring of vibrations signatures, such as resonant frequencies and mode shapes, in search of features that localize, quantify and assess potential damage. Although, the literature reports several successful applications, the methods seem to have limitations in the size of defects they can reliably detect. They are limited to mode sensitivity issues and noise in the measurements. The limitations depend on the location and magnitude of damage, the number of sensors and the number of modes available. This paper presents the results of an analytical study to find the effects of damage location, damage magnitude, number of global modes and number of sensors on the detectability of the damage.
The analytical model employed is a detailed three-dimensional finite element model of a simply supported beam. The vibration characteristics of the first nine bending modes of the undamaged model were obtained using linear modal analysis. Vertical cut damages ranging from a fraction of 0.02 to 0.10 the beam depth were simulated at 14 different locations along the beam length. For each case, the vibration characteristics were similarly obtained for the baseline case. For all cases, nondestructive damage detection methods were applied varying the input modal information by the number of sensors (from 113 to 15) and the number of modes (from one to nine). The results of this investigation consist of detectability of damage given the magnitude and location of damage, the number of sensors and the number of modes.

Presentation

Mario J. Perez, Roberto Osegueda and Sergio Castillo, "Damage Detectability Limits Using Vibration Measurements," SPIE Conference on Smart Structures and Materials, Newport Beach, CA, March 7, 2001

Remarks

Started in FAST Center as an undergraduate Student

Employment

Structural Engineer, The Crosby Group Company, San Francisco, California.
Design structures for seismic activity and perform lateral analyses on the structures.

Helder Lopez
B.S. in Civil Engineering
Master of Science in Civil Engineering
Date: December 2000

Thesis Title
Fusion of Strain Energy Differences for Damage Localization

Supervisor
Dr. Roberto Osegueda

Abstract

Aluminum beams resembling a part of an aircraft structure (rib or stringer) were built and modal-tested. Vibration testing conducted on the test articles provided us with modal response data of the structure before and after the infliction of damage, which was used to evaluate the global Non-destructive Evaluation damage localization technique. The NDE damage localization technique proposed is based on applying fusion techniques to modal strain energy differences.

A data fusion methodology with probabilistic and evidential reasoning features applied to the strain energy differences between the original and degraded states of the structure is proposed for damage detection. For proper evaluation of the strain energies and implementation of the methodology, modal curvatures are determined using an iterative curve-fit algorithm and enhance the resolution of damage detection. Five different techniques are presented and fused using the probabilistic features obtained from the strain energy differences, thus; providing features that indicate locations with potential damage. Scenarios with up to three damage locations are considered. The fusion results are plotted and analyzed applying the proposed damage assessing criteria.

This work includes results, conclusions and recommendations of the NDE damage detection technique used, as well as the features and limitations of the proposed damage assessing methodology and technique.

Publications

R.A. Osegueda, H. Lopez, L. Pereyra, C.M. Ferregut, "Localization of Damage Using Fusion of Modal Strain Energy Differences", proceedings of IMAC 2000, San Antonio, TX, February 7-10, 2000, pp. 695-701.

Employment

Project Engineer, MALOUF Engineering International, Inc., (MEI), Structural Engineering Consulting Firm specializing in the design and analysis of Telecommunication Structures.

Moises Macias
B.S. in Civil Engineering
Master of Science in Civil Engineering
Date: December 2000

Thesis Title

Health Monitoring of Aircraft Structures by Fusion of Modal Strain Energy Density

Supervisor:
Dr. Roberto Osegueda

Abstract

An early prototype of the Vertical Stabilizer Assembly (VSA) of the Shuttle Orbiter was modal tested at healthy and damaged states to study vibrational nondestructive damage evaluation in aerospace structures. Frequency Response and Coherence functions were collected with a Laser Vibrometer at 84 points when the healthy and damaged VSA was shaken with a continuous random force varying from 0 to 300 Hz. The measurements were used to extract the resonant frequencies and modal shapes for the healthy and damaged states. After pairing the mode shapes between the healthy and damaged states through the Modal Assurance Criterion (MAC) and an analysis of the differences in the Frequency Response Functions (FRFs), the strain energy densities of the elements due to modal deformations were determined through a finite element model. The energy densities were normalized so the total energy of the structure is the same for the mode pairs of the damaged and undamaged states. The differences in the modal strain energy densities between the healthy and damaged structures provide information that allow for the localization of damage. This is achieved by implementing fusion techniques that combine competing and complementing information obtained from the energy density differences of several mode pairs. This thesis considers three different fusion methods to localize damage in the VSA. These are averaging, Bayesian fusion, and Probability Mass Function (PMF) formulation.

Publications

R.A. Osegueda, M. Macias, G. Andre, C.M. Ferregut and C. Carrasco, "Fusion of Modal Strain Energy for Health Monitoring of Aircraft Structures", In Nondestructive Evaluation of Aging Aircraft, Airports, and Aerospace hardware IV, Ajit K. Mal, Editor, Proceedings of SPIE Vol. 3994, Newport Beach, CA, March 7-8 2000, pp. 117-127. **(BEST CONFERENCE PAPER AWARD)**

Employment

Structural Engineer, Henry K. Ng and Associates, Consulting Engineers Inc., El Paso, Texas

N/A	**Robert Cervantes** Master of Science in Metallurgical and Materials Engineering Date: December 2000 **Thesis Title** A Corrosion Study of Aluminum 2524 Microconstituents and the Consequent Mechanism for Copper Deposition on the Surface of the Alloy **Supervisor** Dr. Lawrence Murr

Abstract

Aluminum 2524 specimens were subjected to long-term corrosion treatment (5 days) in 0.6 M NaCl solutions ranging in pH values from 3 to 11. The resulting copper deposits on the alloy surface were observed to be in nodular and microdendritic form. These copper deposits were observed by SEM; EDX analysis confirmed the presence of copper. TEMand EDX spectrometry were used for additional analytic information. The experimental results confirm the involvement of an electrochemical cementation process during corrosion. In this process, copper ions from the alloy matrix which have gone into solution deposit as elemental copper on the aluminum alloy surface. This creates additional and accelerated corrosion phenomena.

Employment

Chemistry School Teacher
Ysleta Independent School District, El Paso, Texas

Miguel Orozco, Jr
B.S. in Civil Engineering
Master of Science in Civil Engineering
Date: May 2001

Thesis Title
Performance Verifications of the CONTOUR Dust Shield

Supervisor:
Drs. Roberto Osegueda and Cesar Carrasco

Abstract

Over a six-year period, CONTOUR "Comet Nucleus Tour", a NASA discovery mission will fly by two comets: *Encke* in 2003 and *Schwassmann-Wachmann-3* in 2006. CONTOUR will take images, make spectral maps, and analyze dust and gasses from the coma of the comets.

To successfully complete its mission, CONTOUR will be fitted with a dust shield that will protect the flight instruments as well as the data acquisition systems from the impact of millions of dust particles of varied sizes at velocities of 28.2 km/s from the first comet and 14.0 km/s from the second. The dust shield consists of four "bumpers" built with a high strength fabric and a backstop layer of epoxy fabric. These five layers of protection are placed 2.5 inches apart. The purpose of the bumpers is to "shock" and disintegrate and possibly melt and vaporize the impacting particles and the backstop functions as the last protective layer that should "catch" the remains of the dust particles that penetrate the last bumper.

The design of a typical spacecraft shield is based on a desired reliability (probability of no-penetration PNP) for the total duration of the mission. To design these shields accurate analysis of the probability of penetration must consider the fluence, velocity and angular distributions of comet dust particles, as well as shape and density distributions, the spacecraft geometry, and the penetration resistance of the structural components of the shield.

The purpose of this thesis is to describe the evaluation of the reliability of the CONTOUR dust shield based on predicted particle fluence data, and a series of "hypervelocity" impact tests were conducted at "*NASA's* White Sands Testing Facility" to predict the critical size of dust particles that would penetrate the CONTOUR's shield at the respective encounter velocities.

Publications

R.A, Osegueda, C.J. Carrasco, M. Orozco, J. Eftis, E. Reynolds and T.G. Sholar, "CONTOUR Dust Shield Performance", submitted for publication to Journal of Aerospace Engineering, 2001.

Internship

NASA Johnson Space Center, Hypervelocity Impact Testing Facilities, Houston, Texas, Summer 2000.

Remarks

Sponsored by project sponsored by APL.

Employment

Working as an engineering consultant at International Structural Products Corporation, EL Paso.

Sergio Castillo
B.S. in Civil Engineering
Master of Science in Civil Engineering
Date: July 2001

Thesis Title
Vibration-Based Damage Detection on a Curved, Aluminum-Stiffened Plate Resembling an Aircraft Fuselage.

Supervisor
Dr. Cesar Carrasco and Roberto Osegueda

Abstract

Vibration-based damage detection on a curved, aluminum-stiffened plate construction resembling an aircraft fuselage was conducted. The stiffened plate was modal tested with the aid of a Laser Doppler Velocimeter (LDV) that was used to obtain velocity readings at 112 uniformly distributed target points on the front of the structure. The objective of the experimental testing was to identify modes of significant global change in the FRFs between the undamaged and damaged states in order to increase the performance of a NDD method.

The method used is based on modal strain energies between damaged and undamaged states. This required the evaluation of mode shapes and their corresponding bending and twisting curvatures. In order to enhance their resolution and reduce experimental error, a smoothing algorithm was applied. The NDD method considered in this thesis is based on the fact that if damage is present in the structure, a loss of stiffness will occur in the location of damage. This is also reflected by a decrease in modal strain energy in that location. By comparing the strain energy distribution of the modes in the damaged and undamaged state, a prediction of the location of damage can be made. This is illustrated in the form of damage maps.

Nine damage cases that consisted of 28 reversible damages were inflicted to the test article. Findings, conclusions and recommendations of the NDD method in conjunction with the mode selection criteria used is presented in this thesis.

Publications

D.W. Allen, S. Castillo, A.L. Cundy, R.E. McMurry, "Damage Detection in Building Joints Through Statistical Analysis of Auto Regressive Models," in Proc.of IMAC XIX, Kissimmee, FL, February 2001.

Presentation

Mario J. Perez, Roberto Osegueda and Sergio Castillo, "Damage Detectability Limits Using Vibration Measurements," SPIE Conference on Smart Structures and Materials, Newport Beach, CA, March 7, 2001

Internship

Los Alamos National Laboratory, Structural Dynamics Group, Summer 2000

Remarks

Started in FAST Center as an undergraduate Student

Employment

Structural Engineer, MALOUF Engineering International, Inc., (MEI)

Francisco De Villa
B.S. in Civil Engineering
Master of Science in Civil Engineering
Date: July 2001

Thesis Title
Defect Detection in Thin Plates Using So Lamb Wave Scanning

Supervisor
Dr. Roberto Osegueda

Abstract

This thesis describes work towards the development of a Lamb wave scanning method for the detection of defects in thin plates. The approach requires the generation of an ultrasonic S_o-Mode Lamb wave using an incident transmitter excited with a tone burst centered at a near non-dispersive frequency. A pair of receiving transducers, with a fixed relative separation, remotely scans line sections of the thin plate. The global position of the receiver pair is moved to cover a large plate area. The arrival time information coming from incident and reflected waves contain information associated with the location of reflection surfaces or potential flaws. The cross-correlation between the excitation signal and the receivers' waveforms is obtained and subsequently demodulated using a quadrature amplitude method in order to facilitate the determination of arrival times. Distances from the source, to the reflection surface and to the receivers are found from the arrival times of the reflected waves and the Lamb wave phase velocity. The distances and the source and receiver locations are incorporated in an elliptical solution to find coordinates of the reflection points. In a line scanning the set of predicted reflection points define the extent of the defect. The Lamb wave scanning approach is tested using 1.6 mm-thick Aluminum plates with notches of various lengths and orientations from 0, 22.5, 45, 67.5 and 90 degrees with respect to the far edge of the plates. The results are summarized with defect maps that compare favorably to the actual notch locations.

Publications

Francisco DeVilla, E. Roldan, C. Tirado, R. Mares, S. Nazarian and R. Osegueda, "Defect Detection in thin plates using So Lamb wave scanning," in Proc. of NDE for Health Monitoring and Diagnostics, SPIE Vol. 4335, Paper 21, March 2001.

Remarks

Started in FAST Center as an undergraduate Student

Employment

Employed at Arredondo, Zepeda & Burnz, Dallas, Texas since August 2001.

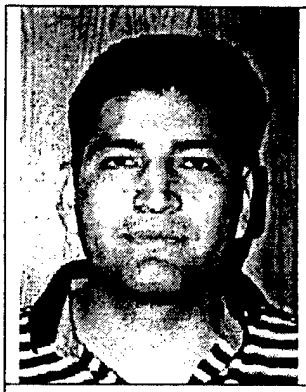

Hugo Pardo
BS in Civil Engineering, Dec. 1996
Master of Science in Civil Engineering
Date: December 2001

Thesis Title
A Reliability Based Corrosion Assessment Methodology

Supervisor
Dr. Carlos Ferregut

Abstract

Multiple-site pitting corrosion represents a serious degradation mechanism that affects the structural integrity and reliability of aging military and commercial aircraft. The uncertainties associated with the variables that control the initiation and growth of cracks from corrosion pits, make it necessary to employ a probabilistic rather than deterministic analysis to determine the probability of failure of an aircraft due to pitting corrosion. This thesis presents a methodology to assess the reliability of a theoretically corroded aluminum 2024 – T3 plate.
The proposed methodology requires the probability density functions (PDFs) of the pit characteristics, i.e. pit size, depth, location in the plate, and density. These PDFs are then used together with a Monte Carlo technique to randomly generate ellipsoids representing corrosion pits. These simulated ellipsoids are used to create 2D finite element (FE) models of corroded plates using FE software subjected to a uniaxial static tensile load. Each model represents a different potential corrosion situation that a plate might encounter during its life span. A PDF is fitted to the maximum stresses in the plates and to the material strength

Internship

University of California at LA, Mechanical Engineering Department, Summer of 1998. Worked under the Supervision of Dr. Ajit Mal.

Remarks

Started in FAST Center as an undergraduate Student

Employment

Structural Engineer, Jaster-Quintanilla, Inc., Dallas, Texas

Benjamin Lopez
BS Civil Engineering, May 2000
Started MS of Civil Engineering studies in June 2000

Thesis Title
Pitting Corrosion Quantification Using Fractal theory
December 2001

Supervisor
Dr. Carlos Ferregut

Thesis Abstract

This thesis describes the characterization and quantification of pitting corrosion of 2024-T3 aluminum alloy. A model for corrosion quantification was developed from an experimental analysis of aluminum alloy specimens by using the development of an algorithm based on fractal geometry techniques to characterize pitting corrosion and its effect on tension testing. The experimental analysis proposed was based in specimens submerged in a ferric chloride (FeCl3) aqueous solution at different times of exposure. The mathematical algorithm, based on the box-counting method, is used to search for a fractal size distribution to identify the parameter called fractal dimension. The characterization analysis consists in obtaining black and white images of pitted regions in the specimens. This is done in order to obtain data on pit density, pit size, and pit depth. Tension-Loading tests were performed to determine the remaining fracture strength. Thus, acquired data is implemented into a database which is used to develop a mechanistic model for the ultimate strength of the material as a function of pitting corrosion characteristics. The model was developed with the aid of correlation analysis and artificial neural networks (ANN).

Remarks

Started in FAST Center as an undergraduate Student

Victor Noriega
BS in Electrical Engineering, May 2000
Started MS in Electrical Engineering in June 2000

Thesis Title
" On-Line Data Fusion of Pulse-Echo Ultrasound for Testing Composite Materials
December 2001

Supervisors
Drs. Joseph Pierluissi and Roberto Osegueda

Abstract

An on-line fusion system for testing composite materials using ultrasound has been developed. A composite plate with known defect location is used to test the system. The system offers a solution to the problem of obtaining false defects caused by uneven surfaces of composite materials. The A-scan signal is a bandpass signal. Finding the complex envelope of the bandpass signal helps track the thickness of the composite material as the transducer moves over it. Real-time digital signal processing is used to create a C-scan image using the information of the complex envelope of the A-scan signal. Real-time digital signal processing also allows the C-scan image to be displayed as the system scans the composite plate. Four different fusion methods are used to create the C-scan image. The four methods include the average, maximum, front-and-back ratio, and Dempster-Shafer evidential reasoning method. All four methods detect the defects. It was found from the four methods used for generating a C-scan image that the Dempster-Shafer evidential reasoning method identified the defects more clearly than the other three methods.

Publications

V. M. Noriega, Jr., R. A. Osegueda, and J. H. Pierluissi , " On-Line Data Fusion of Pulse-Echo Ultrasound for Testing Composite Materials," to be published in Proc. of 28th Annual Review of Progress in Quantitative Nondestructive Evaluation on August 2, 2001.

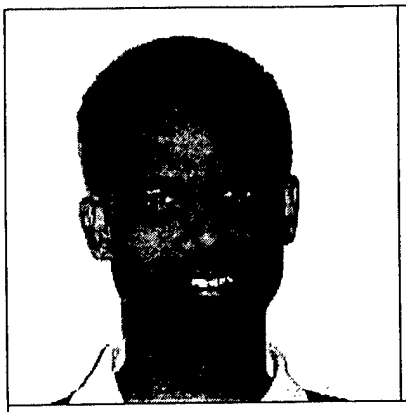

Rama Garigipati
Started MS degree in Civil Engineering in September 2000
Expected to complete in December 2002

Thesis Title
Flaw detection by Artificial Neural networks using Lamb Waves

Supervisor
Dr. Roberto Osegueda

Abstract

In order to ensure safety of the aerospace structures, periodic testing is necessary to make sure that thes structure does not have any defects. The Non-Destructive Testing(NDT) is used to test the structure as it is without having to dismantle it. The project 'flaw detection by artificial neural networks using lamb waves' makes use of the software WAVE 2000 to generate a database of time-histories for aluminium plates with notches of various lengths and at different angles to the horizontal. Ultrasonic waves are sent at a particular angle to the normal so that lamb waves are generated in the plates. Lamb waves are the waves whose wavelengths are comparable to the thickness of the plate and where the transverse wave and longitudinal wave travel at the same speed. When a comprehensive database is generated, an artificial neural network(ANN) is created and trained using back-propagation technique to predict the length and angle of the notch. For this purpose, the software NEURALSIM is made use of. The results obtained from the artificial neural network prediction are compared with the actual results to see if the model developed using ANN is effective in predicting the flaw in plates with notches at unknown location and dimesion.

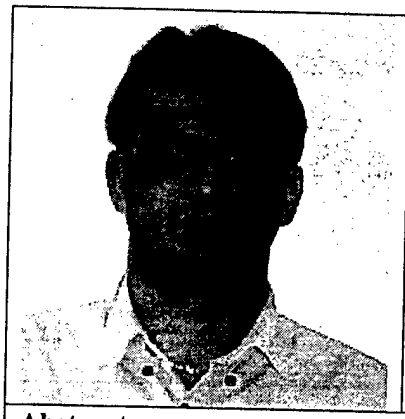

Ulas Toros
Started MS degree in September 2000.
May 2002 2001

Thesis Title
Damage Detectability from Modal Strain Energy Changes Under Uncertainties

Supervisor
Dr. Roberto Osegueda

Abstract

Analytical mode shapes of undamaged and damaged simply supported beams obtained from finite elements are considered. The mode shapes correspond to a beam with damage at various magnitudes and at various locations. Randomly distributed errors (noise) are introduced in the mode shapes of the undamaged and damaged beams at different levels to generate data for a Monte Carlo simulation. The modal strain energy difference method is applied to detect, locate, and quantify the damage using various detection strategies varying the numbers of sensors and modes. The predicted damage is compared to the actual damage and the efficacy of the detection is characterized using a given criteria. The Monte Carlo simulation provides data from which a quantification of the damage detectability can be extracted as a function of damage magnitude, noise level, number of modes, and number of sensors. The damage detectability was quantified using a curve-fit procedure of the simulation results using a detection tolerance of 1 in. The work illustrates a procedure to determine the probability of damage detection (detectability) considering a wide range of detection schemes, and provides tools to design instrumentation set-ups for optimal detectability

Remarks

Sponsored by NASA project

Manuel Celaya
Started MS in Civil Engineering in September 2000.

Thesis Title
Nondestructive Examination of Composite Cylinders by Using Lamb-Wave Scanning
July 2002

Supervisor
Dr. Roberto Osegueda

Abstract
The feasibility of using an ultrasonic Lamb wave approach to inspect thin and nested thick-walled rings and/or cylinders of composite materials is explored for application to kinetic energy flywheels. A computer-controlled ultrasonic scanning apparatus is designed and built suitable to inspect non-submersively composite rings and cylinders of various thickness and lengths. The scanner system is suitable for acquiring acousto-ultrasonic data for Lamb wave analysis and time history measurements for ultrasonic pulse-echo. Three different specimens are tested for Lamb-wave analysis and one cylinder specimen for pulse echo. The experimental data for the Lamb-wave analysis is processed by applying a double FFT and a transformation of axes to obtain experimental phase dispersion curves. The experimental curves are then correlated to analytical solutions obtained by a finite element method developed here. By matching the experimental and analytical dispersion curves, the elastic constants of the material are identified non-destructively.

The capabilities of the prototype scanner to inspect large cylindrical specimens using the pulse echo technique is also verified. A large cylinder specimen with internal delamination is scanned using the pulse-echo technique. The pulse-echo time history data was analyzed to determine the times of flight and amplitudes of echoes from potential internal reflection. Delamination maps in the composite specimen are obtained by mapping the ratio of the amplitudes of the outer- to inner-wall reflections.

Remarks

Sponsored partly by NIST

Gabriel Carrera
BS in Civil Engineering, December 200
Started MS in Civil Engineering in January 2001

Thesis Topic
Damage detectability limits in structures from vibration measurements using Monte Carlo Simulations

Supervisor
Dr. Cesar Carrasco

Project Description

The research consists of finding the detectability of damage in a beam using different modes shapes generated by Algor software. A program was developed in Matlab to perform the Monte Carlo Simulations introducing noise at different level in the mode shape data. The modal strain energy technique is used to solve for the damage magnitude and locations from the noisy data. The intent is to evaluate the effects of noise in detecting damage in real structures.

Remarks

Sponsored by NASA grant

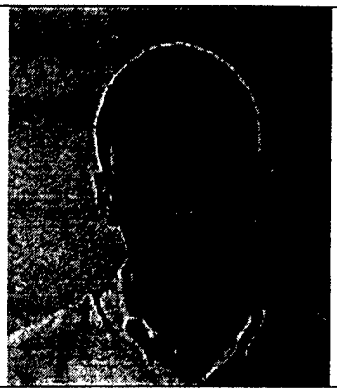

Mohammad Khatib
Started MS in Civil Engineering in January 2001
Started working at FAST Center in June 2001

Thesis Topic
No topic clearly defined yet

Supervisor
Dr. Cesar Carrasco

Description of Work at FAST

His work at FAST for the time being has been to get him acquainted with Smoothed Particle Hydrodynamics (SPH) for the modeling of dynamic problems such as elastic wave propagation, hypervelocity impact, etc. SPH is a technique for problem solving in Computational Continuum Dynamics (CCD), the method was used in astrophysical and cosmological problems and it is extended to treat the dynamic response of solids. SPH is a Lagrangian particle code, which uses no background spatial mesh, the method can handle large deformations in a pure Lagrangian frame. He is currently learning to use Autodyn Software.

Ana Cristina Holguin
BS in Mechanical Engineering, May 2001
Started MS in Mechanical Engineering in June 2001 at UTEP. Then transferred to University of Wisconsin at Madison.

Thesis Topic
Detection of Faults using Data Fusion and Lamb Waves

Supervisor
Dr. Roberto Osegueda

Abstract of Undergraduate Work

The high cost of replacing aged aircraft had led greater efforts on preventive maintenance and nondestructive evaluation (NDE) inspection to extend their serviceability. The use of multiple NDE techniques is mandatory because no single method is able to inspect all possible forms of defects. Thus, the fusion or combination of NDE inspection results is attractive.

This study utilizes two data fusion methods to combine NDE images obtained from a prototype patch for B-52 aircraft containing multiple forms of defects. The methods considered are (a) Dempster-Shafer evidential reasoning and (b) Statistical approach. The fusion results show that both methods reflect all the defect under the patch with a single image.

Presentations

Ana C. Holguin, "Fusion of NDE Data for Inspecting Composite Patches on Aging Aircraft," presented to NDE Branch, Air Force Materiel Command, AF Research Lab, Wright Patterson Air Force Base, March 2001.

Remarks

Started in FAST Center as an undergraduate Student.

Internship

University of Wisconsin, Madison, WI, Summer 2000, NSF – REU Internship.

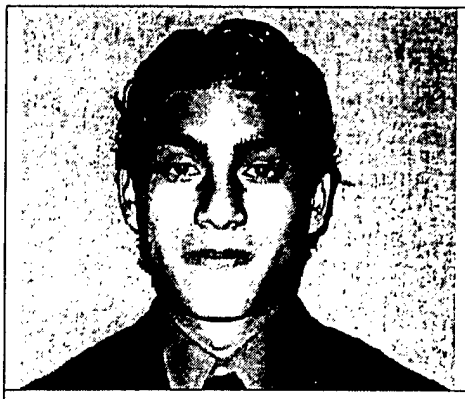

Enrique Roldan
BS in Civil Engineering, May 2001

Expected thesis title
Damage detection using S_0 Lamb wave scanning in thin plates with a rivet hole

Supervisor
Dr. Roberto Osegueda and Soheil Nazarian

Project Description

Lamb wave propagation in rectangular thin plates with a rivet hole resembling an aircraft structure is investigated for damage detection around the region of the hole. This investigation is tested on square Aluminum plates 30cm by 30cm and 1.6mm thick. For this experiment, Ultrasonic S_0 Lamb waves are generated using an incident transmitter and are propagated through the thin plate. The propagating waves are then recorded by a receiving transducer, which scans points in the plate surface and records time histories. Experimental results are then analyzed and in turn compared to simulations performed using a finite difference software.

Publication

C.W. Moloney, D.M. Peairs, E.R. Roldan,, "Characterization of Damping in Bolted Lap Joints," in Proc. of IMAC XIX, Kissimmee, FL, February 2001.

Remarks

Started in FAST Center as an undergraduate Student

Internship

Los Alamos National Laboratory, Structural Dynamics Group, Summer 2000

Jose Rodrigo Mares
BS in Civil Engineering, May 2001
Started MS studies in June 2001

Thesis Topic
Not defined yet but will be tailored towards Lamb Wave Scanning

Supervisor:
Drs. Roberto Osegueda and Soheil Nazarian

Description of Work

During his undergraduate work at the FAST Center, Rodrigo was trained in the area of NDE scanning using ultrasonic sensors. He assisted in performing scanning experiments for the work of Francisco De Villa. He has additionally been instrumental in the development of Lamb-Wave scanning for circular members such as rings and pipes.

Remarks

Started in FAST Center as an undergraduate Student

OTHER MS GRADUATE STUDENTS

Charles Miller obtained his MS in Mechanical Engineering in 1996 at Texas A&M University, under the supervision of Dr. Norris Stubbs. FAST Center partially sponsored his MS studies. He worked in Industry for two years and returned to Texas A&M University to pursue a Ph.D. degree in Mechanical Engineering.

Xiafang Mu started the MS studies in Electrical Engineering at UTEP in January 1997. He transferred to another university in May 1997.

Siria Espino started her MS studies in Civil Engineering in September 1998. She had received FAST Center support for one semester.

David Meza obtained is BS degree in Civil Engineering under FAST Center sponsorship. He continued his studies to pursue a MS degree in Civil Engineering. For financial reasons, he elected to take a full-time employment in a local engineering firm without completing his thesis work.

Anthony Prado obtained his BS degree in Metallurgical and Materials Engineering in May 2000. He started the MS program in Materials Science and Engineering in September 2000 under FAST sponsorship. Mr. Prado has not enrolled after December 2000.

A.3 BS Graduates and Students

Adrian Enriquez

BS in Civil Engineering
Date: May 1997

Supervisor
Dr. Carlos Ferregut

Adrian Enriquez worked for the FAST Center for two semesters. He contributed to development of modal analysis models based on finite elements in support of the work on global damage detection.

Upon graduation, he went to work for Anheiser-Busch, St. Louis, MO

James Brown

BS in Civil Engineering

Date: December 1996

Supervisor
Dr. Roberto Osegueda

He was active in using laser interfeometry to perform modal analysis testing. His research focused on the measurement on angular rotations using laser interferometry.

Worked at Boeing Co., Seattle for one year, then moved to Lockheed, Tempe, AZ

Internships

Sandia National Labs, Albuquerque, New Mexico, Summer of 1996. Supervised by Dr. Bruce Hansche

Brian Harms

BS in Civil Engineering

Date: December 1996

Supervisor
Dr. Carlos Ferregut

He was involved in performing finite element simulations of experimental set-ups for damage detection. He was involved in the modal testing of a space truss.

He works at a construction company in Dallas, Texas.

Internships

NASA Johnson Space Center Houston, Texas, Summer of 1995

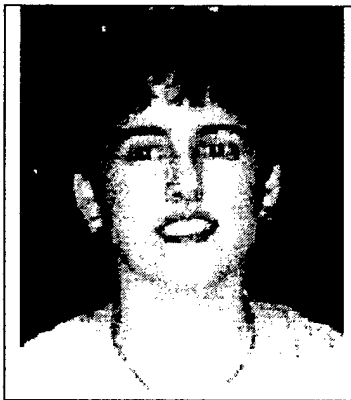

Daniella Martinez

BS in Metallurgical and Materials Engineering

Date: May 1997

Supervisor
Dr. Lawrence Murr

Daniella Martinez worked for the FAST Center during her senior year. Her work dealt with experiments on laboratory simulation of exfoliation corrosion in 2024 Aluminum, in support of other students.

She currently works at Exxon Co. USA, Houston, Texas

Jose Gutierrez

BS in Electrical and Computer Engineering

Date: December 1997

Supervisor
Dr. Carlos Ferregut

His work was very instrumental in the development of intelligent tools for NDE applications. In particular, Jose worked extensively in developing Neural Networks for damage detection. His focus was on the performance of the Neural Networks.

Upon graduation, he went to work for Raytheon Missile Systems, Dallas, Texas.

Publications

Gutierrez, J.M., Ferregut, C., and Osegueda, R.A., "A Comparative Study on Two Types of Mode Sensitive Neural Networks for Damage Assessment," Nondestructive Evaluation of Utilities and Pipelines, M. Prager and R.M. Tilley (Eds.), Proc. SPIE 2947, 1996, pp. 224-235

Osegueda, R.A., Ferregut, C. M., George, M.J., Gutierrez, J.M., and Kreinovich, V., "Computational Geometry and Artificial Neural Networks: A Hybrid Approach to Optimal Sensor Placement for Aerospace NDE", In Intelligent NDE Sciences for Aging and Futuristic Aircraft, Eds. Ferregut, Osegueda and Nunez, FAST Center for Structural Integrity of Aerospace Systems, The University of Texas at El Paso, ISBN: 97404-279-8, El Paso, Texas, January 1998, pp. 59-71.

Osegueda, R., Ferregut, C., George, M.J., Gutierrez, J.M. and Kreinovich, V., " Non-Equilibrium Thermodynamics Explains Semiotic Shapes: Applications to Astronomy and to Non-Destructive Testing of Aerospace Systems," Proceedings of the 1997 International Conference on Intelligent Systems and Semiotics, Gaithersburg, Maryland, September 22-25, (A.M. Meystel, Ed.), NIST Special Publication 918, 1997, pp. 378-382.

Internships

Sandia National Labs, Albuquerque, New Mexico, Summer of 1996 and 1997.

David Meza

BS in Civil Engineering

Date: May 1997

Supervisor
Dr. Roberto Osegueda

He mainly performed experimental work of test specimens to determine their vibrational characteristics. Involved in setting up the instrumentation and testing structural models in the laboratory.
He currently works in as a project engineer/manager for medium size projects in the El Paso area. My duties have included project scheduling/planning, project construction estimation, construction supervision, shop drawing's review, and miscellaneous construction tasks.

Publications

Garcia, G.V., Osegueda, R. and Meza, D., "Damage Detection using ARMA Model Coefficients," In Smart Systems for Bridges, Structures, and Highways, Ed. S.C. Liu, SPIE, Vol. 3671, Paper 3671-30, March 1999.

Garcia, G.V., Osegueda, R. and Meza, D., "Damage Detection Comparison between Damage Index Method and ARMA Method", in Proc. of 17th International Modal Analysis Conference, IMAC XVII, SEM, Orlando, FL. February 8-11, 1999.

Carrasco, C., Osegueda, R.A., Ferregut, C.M., Harms, B., Meza, D., and Grygier, M., "Comprehensive Modal Tests of a Space Truss Model for Damage Assessment," In Proc. Fifth International Conference on Space '96, June 1-6,1996, Albuquerque, NM, pp. 1141-1147.

Internships

NASA Johnson Space Center, Houston, Texas, Summer of 1995

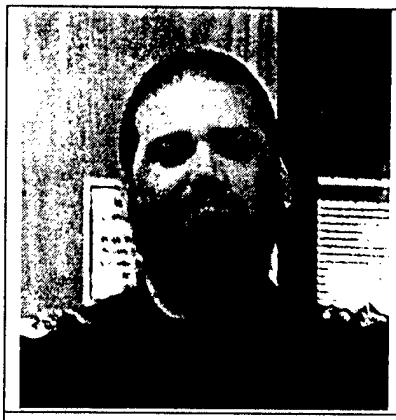

Daryl Little
BS in Metallurgical and Materials Engineering, May 1998

MS in Materials Sceince and Engineering, May 2001
University of Virginia

Continuing Ph.D. studies at Univ. of Virginia

Supervisor
Dr. Roy Arrowood

Daryl studied exfoliation corrosion of 2024 Al with Ms. Maria Posada, Corrosion of Lap skin joints, retrogression and Reaging of 7075 aircraft structure with Lety Campuzano, and my own research on the environmental embrittlement of AA7079 with Dr. Arrowood.

In May 2001, he obtained a MS degree in Materials Science and Engineering working at the Center for Electrochemical Science and Engineering (CESE) at the University of Virginia under the supervision of Dr. John R. Scully. (Thesis on "An Electrochemical Framework to Explain the Intergranular Stress Corrosion Path in Two Al-Cu-Mg-Ag Alloys, C415 and C416"). Started PhD program with same advisor May 2001 also studying corrosion for CESE.

Publications

A.L. Campuzano-Contreras, Roy Arrowood, D. Little, D. Roberson, L.E. Murr, and C-S. Niou, "Characterization of Fuselage Skin Lap Joints", Microstructural Science Volume 25, 20-23 July 1997, Seattle, Washington, Proceedings of the Thirtieth Annual Technical Meeting of the International Metallographic Society.

Maria Posada, L.E. Murr, C-S. Niou, D. Roberson. D. Little, Roy Arrowood, and Debra George, "Exfoliation and Related Microstructures in 2024 Aluminum Body Skins on Aging Aircraft", Materials Characterization, vol. 38, pp 259-272, 1997.

Internships

National Institute of Science & Technology, Maryland, Summer of 1997.

John Feighery

BS in Mechanical Engineering

Date: December 1998

Supervisor
Dr. Roberto Osegueda

His efforts concentrated on performing literature searches on laser-induced ultrasound for the generation of plate waves.

He currently works for an aerospace company at the Johnson Space Center, Houston, Texas.

Internships

NASA Johnson Space Center, Houston, Texas, Spring and Summer of 1997.

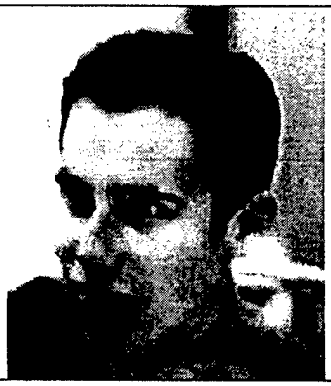

Patrick Dickerson

BS in Metallurgical and Materials Engineering

Date: December 1998

Supervisor
Dr. Roy Arrowood

Patrick studied corrosion of 2024 Al with Ms. Maria Posada, Corrosion of Lap skin joints, retrogression and Reaging of 7075 aircraft structure with Lety Campuzano.

He currently works at Raytheon Missile Systems, Tucson, AZ.

Alina Nunez

BS in Mechanical Engineering

Date: May 1999

Supervisor
Dr. Carlos Ferregut

Worked on the Data Fusion for NDE applications. She was influential in editing the proceeding of the Intelligent NDE Sciences Workshop held at the FAST Center in September 1997.

Currently works at Equilon Pipeline (a merger between Shell and Texaco), she supports the Control Center which monitors around 12,000 miles of pipeline in the US.

Publications

Ferregut, C.M., Osegueda, R.A., and Nuñez, A., (Editors), Intelligent NDE Sciences for Aging and Futuristic Aircraft, FAST Center for Structural Integrity of Aerospace Systems, The University of Texas at El Paso, ISBN: 97404-279-8, El Paso, Texas, January 1998.

Internships
Wright Patterson Air Force Base, Ohio, Summer of 1998

Oscar Moguel

BS in Mechanical Engineering
Date: May 1999

Supervisor:
Dr. Roberto Osegueda

Oscar was involved in experimental modal analysis testing to obtain mode shapes and natural frequencies in support of the Damage detection projects

He currently works at Exxon-Mobil as a machinery engineer.

Publications
Osegueda, R.A., Revilla, A., Pereyra, L.R. and Moguel, O., "Fusion of Modal Strain Energy Differences for Localization of Damage," SPIE Conference on Nondestructive Evaluation of Aging Aircraft, Airports, and Aerospace Hardware III, Newport Beach, CA, March 1999, Vol. 3586, pp. 189-199.

David Roberson

BS in Metallurgical and Materials Engineering, December 1999
MS in Materials Science and Engineering, May 2001

Supervisor
Dr. Lawrence Murr

His research at FAST Center was focused on the 7075 bulkhead forging for the KC-135. He continued as a graduate student in the Metallurgical and Materials Engineering Department, he graduated with his Master of Science in Metallurgical and Materials Engineering in May 2001.

He is currently employed with Intel of Albuquerque, NM.

Publications

Posada, M., Murr, L.E., Niou, C-S. Roberson, D., Little, D., Arrowood, R., and George, D., "Exfoliation and Related Microstructures in 2024 Aluminum Body Skins on Aging Aircraft," Material Characterization, Vol. 38, pp. 259-272, 1997.

Campuzano-Contreras, A.L., Arrowood, R.M., Murr, L.E., Little, D., Roberson, D., and Niou, C.S, "Characterization of Fuselage Skin Lap Joints", Microstructural Science Volume 25, 20-23, July 1997, Seattle, WA.

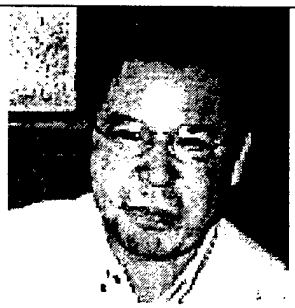

Miguel Kanakoqui

BS in Mechanical Engineering
Date: May 2000

Supervisor
Dr. Roberto Osegueda

Miguel Kanakoqi was trained to use finite elements to develop models of plate and shell systems. His participation in the FAST Center consisting of developing a FE model of the shell structure resembling a fuselage structure, tested by Sergio Castillo.

Current whereabouts unknown.

William Torres

BS in Civil Engineering

Date: May 2001

Supervisor
Dr. Roberto Osegueda

William Torres was trained in the experimentation of Lamb Waves. Unfortunately, he did not elect to pursue graduate studies for financial reasons. He received a Top-Ten Senior award for the University.

He currently works at Texas Department of Transportation, El Paso, Texas

Claudia De Leon

BS in Civil Engineering

Date: May 2001

Supervisor
Drs. Carlos Ferregut and Art Bronson

Claudia was sponsored by the FAST Center during her senior year. Her work consisted on performing corrosion tests in support of the work being performed bu Benjamin Lopez.

She currently works for CALTRANS, San Diego, California.

Debra George
BS candidate in Electrical Engineering

Supervisor

Drs. Roy Arrowood and Vladik Kreinovich

Debra George worked for the FAST Center for two years. She took an internship at Los Alamos National Laboratories and decided to switch major to Electrical Engineering and began working for a different research group on campus. She worked on Corrosion tests and NDE experiments.

Current whereabouts unknown.

Publications

Posada, M., Murr, L.E., Niou, C-S. Roberson, D., Little, D., Arrowood, R., and George, D., "Exfoliation and Related Microstructures in 2024 Aluminum Body Skins on Aging Aircraft," Material Characterization, Vol. 38, pp. 259-272, 1997.

Olga Kosheleva, Sergio Cabrera, Roberto Osegueda, Soheil Nazarian, Debra L. George, Mary J. George, Vladik Kreinovich, and Keith Worden, "Case study of non-linear inverse problems: mammography and non-destructive evaluation", In: Ali Mohamad-Djafari (ed.), Bayesian Inference for Inverse Problems, Proceedings of the SPIE/International Society for Optical Engineering, Vol. 3459, San Diego, CA, 1998

Keith Worden, Roberto Osegueda, Carlos Ferregut, Soheil Nazarian, Debra L. George, Mary J. George, Vladik Kreinovich, Olga Kosheleva, and Sergio Cabrera, "Interval Methods in Non-Destructive Testing of Aerospace Structures and in Mammography", International Conference on Interval Methods and their Application in Global Optimization (INTERVAL'98), April 20-23, Nanjing, China, Abstracts, 1998, pp. 152-154.

Worden, K., Osegueda, R., Ferregut, C., Nazarian, S., George, D.L., George, M.J., Kreinovich, V., Kosheleva, O. and Cabrera, S., "Interval Methods in Non-Destructive Testing of Material Structures", Reliable Computing, 2001

Internships

NASA Langley, Hampton Virginia, Summer of 1997 and Los Alamos Labs, Los Alamos, New Mexico, Summer of 1998

Hannah Jurado
Mechanical Engineering Major

Supervisor
Dr. Roberto Osegueda

Hannah attends UTEP to obtain a BS degree in Mechanical Engineering. Her research has focused on NDE of surface plates utilizing Lamb Waves. She has been influential in designing scanning systems.

Because of financial reasons, she has returned to full-time employment with the Boeing Co. at El Paso, but will continue her studies on a part-time basis.

Jessica Corral
Metallurgical Engineering Major

Supervisor
Dr. Lawrence Murr

Jessica's research has consisted of examining localized corrosion of friction stir welding of Al 2024 part. She is performing static immersion and potentio-dynamic tests in NaCl and NaOH solutions. Optical microscopy and scanning electron microscopy are being used in this investigation.

Jose Gabriela Mares
Civil Engineering Major

Supervisor
Dr. Cesar Carrasco

Gabriela started participating in the FAST Center in January 2001. She has been involved in documenting software and processes that have been used in some of the research projects. She is currently in a summer Co-op. Her stipend support has been provided by Alliance Minority Program (AMP) funded by NSF. Furthermore, she is also the recipient of a presidential scholarship.

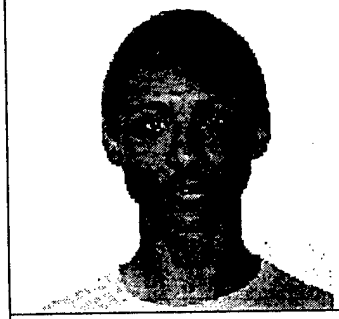

Vanol Francois
Mechanical Engineering Major

Supervisor:
Dr. Roberto Osegueda

Vanol started working in the FAST program in June 2001. He is being trained in several aspects of our research, which include: (a) modal testing using laser vibrometer (b) smooth particle hydrodynamics for elastic system analysis, (c) theory of elasticity.

OTHER UNDERGRADUATE STUDENTS

Adolfo Aguilera worked for the FAST Center during the Fall semester 1995. Graduate with a BS degree of Mechanical Engineering in December 1996.

Mary Jo George participated in the activities of the FAST Center from January 1996 through May 1997. She was an undergraduate student in Computer Science. She took a Coop position at Washington, DC. She has not returned since.

Jabel Morales worked for the FAST Center during the Fall semester of 1999. He was a CS major.

Greg Gelfond attended UTEP and transferred to Texas Tech University. During the Fall semester 1997, he was supported by the FAST Center. He was a CS major.

Jose Antonio Garcia was supported by the FAST program for the Fall semester 1997.He was a CS major.

Douglas C. Deming participated in the FAST Center activities in the Fall of 1995. He did not particpate in FAST in the Spring 1996 because of his commitment to UTEP Athletics. He graduated with honors in May 1996 and went to work for Sandia National Labs.

Scott Minke was sponsored by the FAST Center throughDr. Stubbs at Texas A&M University. Scott received his BS degree in Aerospace Engineering in December 1997 and went to work for Lockheed in Dallas-Fort Worth region.

APPENDIX B

PUBLICATION ABSTRACTS

Reference

Carrasco, C. J., Osegueda, R.A. and Ferregut C.M., "Modal Tests of a Space Truss Model and Damage Localization Using Modal Strain Energy," Report FAST 96-01, FAST Center for Structural Integrity of Aerospace Systems, The University of Texas at El Paso, El Paso, Texas, 79968, July 1996.

ABSTRACT

A three-dimensional scale model of a hexagonal boom truss of the then space station Freedom was built and tested in the laboratory. The purpose of the tests was to extract complete quality data of the vibrational characteristics of the structure, before and after damage, for use with damage detection/evaluation theories, that could eventually be implemented in a space environment. The vibration tests consisted of experimental modal analysis before and after the infliction of artificial damage. The structure was subjected to 18 different damage scenarios, the damage consisted of three different types of damage: a) cut damage, b) partial damage and c) complete damage, at single and multiple locations. The cut damage consisted of a cut through half the member at about three inches from one of the connections. The partial damage consisted of removing *50* percent of the area over the middle third of the element. The complete damage was simply caused by cutting through the complete cross section of the element. All damages were induced in such a way as not to change the mass properties of the structure through a specially design clamping device.

This report documents the details of the structure, the construction procedure, the testing procedure, the modal test results, the extracted modal shapes and an analysis implemented to localize the damage via modal strain energy distribution. The modal test results consist of the vibrational signatures due to different damages on the structure. The extracted modal results are implemented in a global damage detection/evaluation theory based on modal strain energy distribution. The strain energy distributions due to the static shapes of the modes are computed before and after the inflicted damage. The differences from the normalized strain energy distributions are multiplied times element weight factors proportional to the strain energy distribution of the undamaged structure. The weighted modal strain energy differences are lumped into the connecting nodes of the elements to provide indications of the location of the inflicted damage. The technique is able to locate the complete damage and the partial damage, but was not able to detect the cut damage.

Reference

Meza, Jr., R., Osegueda, R.A., Carrasco, C.J. and James, G., "Modal Tests of Composite Honeycomb Panels Using Laser Doppler Velocimetry for Damage Assessment," Report FAST 96-02, FAST Center for Structural Integrity of Aerospace Systems, The University of Texas at El Paso, El Paso, Texas, 79968.

ABSTRACT

Four composite panels consisting of 4-ply T300 graphite cloth laminate with a Nomex honeycomb core were modal tested using a laser Doppler velocimeter (LDV). One panel included no defects and the other three had engineered defects consisting of a disbond, a delamination and fluid ingress. The defects were within a 4-inch diameter circle at the center of the panels. The LDV scanned a grid of 23 points by 23 points of the surface of the panels when the panels were suspended and subjected to a random shaker excitation from 10 Hz to 1000 Hz. During the modal tests, random speckle dropout experimental noise, which was caused by a malfunction of the LDV optics, produced low coherences in the frequency response functions (FRF). This was partially solved by repeating each test four times and selecting the FRF with the highest coherence. The collected FRFs were curve-fitted using a poly-reference technique in the software SDRC I-DEAS to extract the modal parameters. A computer-assisted procedure was devised for visually identifying the outliers in the modal shape data for elimination in further analyses. The modal shapes were curve-fitted for the purpose of smoothing the modal shapes and extracting the modal slopes without loosing too much of the higher order content of the modes. The modal strain energy content of the elements was extracted using a finite element representation of the scanned area of the panels. Two energy-based damage detection methods were applied. The damage localization patterns obtained failed to indicate the known location of the damage.

Reference

Garcia, G.V., and Stubbs, N., "Evaluation of Relative Performance of Classification Algorithms for Nondestructive Damage Detection", Report No. FAST-TAMU-96-01, Submitted to US Air Force Office of Scientific Research, Future Aerospace Science and Technology Program, Center for Structural Integrity of Aerospace Systems, University of Texas at El Paso, Contract Number 32525-47960-CE, July 1996.

ABSTRACT

The objective of this report is to evaluate the relative performance of five classification algorithms for nondestructive damage detection. The classification algorithms investigated here are as follows: (1) a quadratic classifier obtained from Bayes' rule (i.e., using unequal damage and undamaged covariance matrices), (2) a linear classifier obtained from Bayes' rule (i.e., using equal damage and undamaged covariance matrices), (3) a linear classifier obtained from Bayes' rule (i.e., assuming that the damaged and undamaged covariance matrices are equal to the identity matrix), (4) a classifier using Euclidean distance as a basis, and *(5)* a classifier using hypothesis testing. To meet this objective, an established theory of damage localization, which yields information on the location of the damage directly from changes in mode shapes, is selected. Next, the application of sophisticated techniques from pattern recognition, in the form of the five classification algorithms, is performed to the existing theory of damage localization. Expressions for pattern classification using discriminant functions obtained from Bayes' rule, distance as similarity, and hypothesis testing are generated. Criteria for the evaluation of the proposed pattern recognition models are generated. Using the enhanced model, the locating of damage is attempted in: (1) a numerical model of a space structure with simulated damage at various locations, and (2) a real structure damaged at known locations. Finally, the accuracy and reliability of the pattern recognition models are evaluated using the established criteria.

Reference

Garcia, G.V. and Stubbs, N., "Modal Response of Finite Element Model of Space Truss Model of UTEP Space Structure", Report No. FAST-TAMU-96-02, "Submitted to US Air Force Office of Scientific Research, Future Aerospace Science, and Technology Program, Center for Structural Integrity of Aerospace Systems, University of Texas at El Paso, Contract Number 32525-47960-CE, July 1996.

ABSTRACT

The objective of this report is to provide the necessary modal information to repeat the numerical analysis of a three-dimensional 1:6 scale model of a typical hexagonal truss to be used in the construction of the Space Station Freedom. The modal displacements and frequencies for five modes of vibration for the undamaged structure and twenty damage scenarios are presented. Modal displacements and frequencies are obtained from an ABAQUS (1994) model of the test structure. The simulation of damage to the truss members of the finite element model is given in the report by Garcia and Stubbs (1996).

Reference

Paez, T., Barney, P., Hunter, N., Ferregut, C. and Perez, L.E., "Statistical Validation of Physical Systems Models," presented at 67th Shock and Vibration Symposium, Monterrey California, November 18-22, 1996.

ABSTRACT

It is common practice in applied mechanics to develop mathematical models for mechanical system behavior. Frequently, the actual physical system being modeled is also available for testing, and sometimes the test data are used to help identify the parameters of the mathematical model. However, no general-purpose technique exists for formally, statistically judging the quality of a model. This paper suggests a formal statistical procedure for the validation of mathematical models of physical systems when data taken during operation of the physical system are available. The statistical validation procedure is based on the bootstrap, and it seeks to build a framework where a statistical test of hypothesis can be run to determine whether or not a mathematical model is an acceptable model of a physical system with regard to user-specified measures of system behavior. The approach to model validation developed in this study uses experimental data to estimate the marginal and joint confidence intervals of statistics of interest of the physical system. These same measures of behavior are estimated for the mathematical model. The statistics of interest from the mathematical model are located relative to the confidence intervals for the statistics obtained from the experimental data. These relative locations are used to judge the accuracy of the mathematical model. A numerical example is presented to demonstrate the application of the technique.

Reference

Gutierrez, J.M., Ferregut, C., and Osegueda, R.A., "A Comparative Study on Two Types of Mode Sensitive Neural Networks for Damage Assessment," Nondestructive Evaluation of Utilities and Pipelines, M. Prager and R.M. Tilley (Eds.), Proc. SPIE 2947, 1996, pp. 224-235.

ABSTRACT

In order to create a method to monitor the structural integrity of aerospace systems that can utilize current technology, effectiveness of processing data produced by current instrumentation is desired. Utilizing modal vibration methods to measure the dynamic characteristics of a structure, an Artificial Neural Network's ability to discern patterns and then interpolate similar patterns from information it is unfamiliar with, creates an appropriate vehicle for developing a damage assessment system that performs, in a manner, with relatively low computational time. In this study, two Artificial Neural Network paradigms were utilized to create neural network systems to identify, quantify, and locate damage to an ideal three-degree-of-freedom system. Damage was defined as a percentage reduction in the properties of the elements comprising the three-degree-of-freedom system. An artificial neural network damage assessment system based on the Back-Propagation paradigm was created and then compared against an artificial neural network damage assessment system based on the Radial Basis Function paradigm. Both systems utilized the same data, consisting of resonant frequencies and modes of vibration, to evaluate the condition of all the elements of the three-degree-of-freedom system. Results show that the Radial Basis Function Network performed with a greater efficacy and robustness in assessing damage for this system.

Reference

Carrasco, C.J., Osegueda, R.A., Ferregut, C. and Grygier, M., "Damage Localization in a Space Truss Model Using Modal Strain Energy," Proceedings of the 15th International Modal Analysis Conference, IMAC97, V.2, Society for Experimental Mechanics, Inc., Bethel, Connecticut, pp. 1786-1792, 1997.

ABSTRACT

A three-dimensional scale model of a hexagonal boom truss of the then space station Freedom was built and tested in the laboratory. The purpose of the tests was to extract complete high-quality data of the vibrational characteristics of the structure, before and after damage, to validate damage detection/evaluation theories. The vibration tests consisted of experimental modal analysis before and after the infliction of artificial damage. The structure was subjected to 18 different damage scenarios, at single and multiple locations, of three types: a) cut damage consisting of a cut through half the depth of the element , b) partial damage removing 50% of the area over the middle third of the element, and c) complete damage caused by completely cutting through the member. All damages were induced without changing the mass properties of the structure through specially design clamping devices.

This paper summarizes the experimental program, the modal test results, the extracted modal shapes and an analysis implemented to localize the damage via modal strain energy distribution. The modal test results consist of the vibrational signatures due to different damages on the structure. The extracted modal results are implemented in a global damage detection/evaluation theory based on modal strain energy distribution. The strain energy distributions due to the static shapes of the modes are computed before and after the inflicted damage. The differences from the normalized strain energy distributions are multiplied times element weight factors proportional to the strain energy distribution of the undamaged structure. The weighted modal strain energy differences are lumped into the connecting nodes of the elements to provide indications of the location of the inflicted damage. The technique is able to locate the complete damage and the partial damage, but was not able to detect the cut damage.

Reference

Hunter, N.F., Barney, P., Ferregut, C., Perez, L.E., and Paez, T.L., "Statistical Validation of Stochastic Models," Proceedings of the 15th International Modal Analysis Conference, IMAC97, V.1, Society for Experimental Mechanics, Inc., Bethel, Connecticut, pp. 605-611, 1997.

ABSTRACT

It is common practice in structural dynamics to develop mathematical models for system behavior, and we are now capable of developing stochastic models, i.e., models whose parameters are random variables. Such models have random characteristics that are meant to simulate the randomness in characteristics of experimentally observed systems. This paper suggests a formal statistical procedure for the validation of mathematical models of stochastic systems when data taken during operation of the stochastic system are available. The statistical characteristics of the experimental system are obtained using the bootstrap, a technique for the statistical analysis of non-Gaussian data. We propose a procedure to determine whether or not a mathematical model is an acceptable model of a stochastic system with regard to user-specified measures of system behavior. A numerical example is presented to demonstrate the application of the technique.

Reference

Perez, L.E., Ferregut, C., Carrasco, C., Paez, T.L., Barney, P. and Hunter, N.F., "Statistical Validation of a Plate Finite-Element Model for Damage detection," in Smart Structures and Materials: Smart Systems for Bridges, Structures and Highways, March 1997.

ABSTRACT

It is common practice in applied mechanics to develop finite element models for mechanical system behavior. Most structural integrity monitoring techniques, proposed to date, rely on an accurate model of the structure at hand. In many situations the structure being monitored is already built; in those cases, it is good engineering practice to ensure that the finite element model matches the behavior of the physical structure. However, no general-purpose technique exists for formally, statistically judging the quality of the finite element model. This paper applies a formal statistical procedure for the validation of finite element models of structural systems, when data taken during operation of the system are available. The statistical validation procedure is based on the bootstrap, and it seeks to build a tool for assessing whether or not a finite element model is an acceptable representation of the structure. The approach uses experimental data to construct confidence bounds that permit the assessment of the model. The case of a finite element model of an aluminum plate is presented.

Reference

Carrasco, C.J., Osegueda, R.A., Ferregut, C.M., and Gryger, M. "Localization and Quantification of Damage in a Space Truss Model Using Modal Strain Energy," in Smart Structures and Materials: Smart Systems for Bridges, Structures and Highways, March 1997.

ABSTRACT

This paper addresses the issue of localizing and quantifying damage using changes in the vibrational characteristics of structures. The method considers the mode shapes of the structure pre- and post-damage measured via modal analysis. Values of the modal shapes are used to compute the strain energy distribution in the structural elements. Using the assumption that the element modal strain energy is the same pre- and post-damage, and characterizing the damage as a scalar quantity of the undamaged stiffness matrix, an expression is obtained for element damage factors that quantify the magnitude of the damage for each mode shape. Due to numerical instabilities in the computation of this expression, filters are applied that overcome some of the instabilities but reduce the true amplitude of damage. The modified-filtered expression was very effective in localizing the actual damage. After localization, the magnitudes of damage are computed using the original unfiltered expression.

The method is tested using experimental data from a three-dimensional scale model of a space structure, subjected to 18 different damage scenarios. The damage forms consist of a 180° cut (Type I), a 50% reduction of the area over one-third the element length (Type II), and a complete cut through the element section (Type III). These types of damages correspond to magnitudes of α equal to -0.17, -0.5 and -1.0, respectively. The method is able to detect Type I damage for only one of four cases, Type II for all the three cases and Type III damage for all single and double-location cases, excluding the cases that involves a damage insensitive element.

Reference

Choi, S. and Stubbs, N., "Nondestructive Damage Detection Algorithms for 2D Plates," in Smart Structures and Materials: Smart Systems for Bridges, Structures and Highways, SPIE Vol. 3043, pp. 193, March 1997.

ABSTRACT

The objective of this paper is to develop appropriate nondestructive damage detection algorithms for two-dimensional plates. Two methods, one using the local compliance and the other using local modal strain energy, are presented and compared in this paper. The compliance method is derived simply from the governing differential equations of motion presented in the classical plate theory. The second method is developed from expressions for the elastic strain energy of a plate. A damage index, used to indicate local damage, is defined and expressed in terms of modal displacements that are obtained numerically from mode shapes of the undamaged and the damaged structures. The possible damage locations in the structure are determined by the application of damage indicators according to previously developed decision rules. The damage indices, which are obtained for each mode, are transformed to probability space and superposed as weighted general means (WGM). In the WGM, the fraction of modal energy for the element is used as the weight of each mode. Each of the two methods is demonstrated by using a numerical example of a simply supported plate with simulated damage. Finally, the relative performances of the two methods are compared.

Reference

Garcia, G.V. and Stubbs, N., "Application and Evaluation of Classification Algorithms to a Finite Element Model of a Three-Dimensional Truss structure for Nondestructive Damage Detection," in Smart Structures and Materials: Smart Systems for Bridges, Structures and Highways, SPIE Vol. 3043, pp. 205, March 1997.

ABSTRACT

The objective of this paper is to apply and evaluate the relative performance of classification algorithms for nondestructive damage detection (NDD). The classification algorithms are obtained from various forms of Baye's Rule. An established theory of damage localization, which yields information on the location of the damage directly from changes in mode shapes, is selected. Next, the application of classification is performed to the existing theory of damage localization. Expressions for the classification algorithms using the damage indicator functions from the damage localization theory are generated. Criteria for the evaluation of the proposed classification algorithms are then generated. Using the classification algorithms, damage localization is attempted in a numerical model of a three-dimensional truss structure, which contains simulated damage at various locations. Finally, the accuracy and reliability of the classification algorithms is evaluated using the established criteria.

Reference

Osegueda, R.A., Carrasco, C.J. and Meza, R., "A Modal Strain Energy Distribution Method to Localize and Quantify Damage," Proceedings of the 15th International Modal Analysis Conference, IMAC97, V.2, Society for Experimental Mechanics, Inc., Bethel, Connecticut, pp. 1298-1304, 1997.

ABSTRACT

A method based on modal strain energy distributions is presented to localize and quantify damage in structural systems. The method is based on the fact that most forms of damage can be characterized as changes in the stiffness properties, reflecting localized increases in the structural compliance and changes in the modal shapes. The method considers a finite element representation of a system whose experimental modal parameters are known for the undamaged and damaged states. The strain energy stored in each of the elements due to the static shapes of the normalized modes are computed for the two states The differences in the modal strain energy reflect the location of the damage as apparent increases in the energy. Energy relationships between the two states provide the means for quantifying the magnitude of the damage. The method is validated with experiments conducted in cantilever beams. In the experiments, the modal parameters were measured through laser Doppler velocimetry. Four different double-cantilever aluminum beams were tested to generate ten different damage scenario. In all the scenarios, the damage was inflicted by milling out about one-tenth the thickness over one-tenth the length of the beam. For each case, 14 modes were extracted and used to localize and quantify the damage. A second set of experiments was also conducted on four different composite plates with a honeycomb core sandwiched between four ply T300 plane weave graphite cloth laminate. One of the plates was undamaged and the other three had engineered flaws which consisted of a) four-inch diameter disbond between the laminate and the core, b) four-inch diameter region of the honeycomb core filled with fluid and c) a four-inch diameter delamination between the plies of the graphite laminate. The modal strain energy distribution method was implemented for both systems. For the cantilever beam experiments, the location of the damage was accurately identified. The magnitude of the inflicted damage was predicted within a 10 percent margin of error. For the composite plate tests, difficulties were encountered in localizing the damage due to the fact that only two of the modes have significant energy content in the vicinity of the defect.

Reference

Meza, Jr. R., Carrasco, C.J., Osegueda, R.A., James, G., and Robinson, N., "Damage Detection in a DC-9 fuselage Using Laser Doppler Velocimetry," Proceedings of the 15th International Modal Analysis Conference, IMAC97, V.2, Society for Experimental Mechanics, Inc., Bethel, Connecticut, pp. 1779-1785, 1997.

ABSTRACT

A series of induced damage tests were conducted on the surface of the forward fuselage of a DC-9 aircraft and modal data acquired using a laser Doppler velocimetry. Damage was inflicted to a longitudinal stringer within the scanned area of the skin surface. The force was applied to the outer skin of the fuselage. The excitation force was a pure continuous 5-pound random signal with a lower frequency bound of 50Hz and upper bound of 1250 Hz. Data was acquired from a grid of 38 inches by 14 inches on a 1-inch spacing, producing 585 measuring points. The laser head was positioned at a working distance of 75 inches from the surface. The acquisition system calculated FRF's and coherence functions in real time and saved these functions for detailed post-test analysis. A Hanning window was used in the band of 0 to 1250 Hz with 10 averages and a block-size of 1024, with a 50 percent overlap. The object was tested at three states: undamaged, partial damage and complete damage. The stringer was initially cut through the flanges and web and then repaired with two splice plates bolted to its flanges, simulating the undamaged state. The partial damage scenario was simulated by cutting one of the splice plates; the complete damage was caused by cutting both splice plates. The acquired FRF's were used to extract the modal parameters and modal shapes within the frequency band tested. Because of inherent laser dropout errors, the modal shapes were contaminated with outliers. The modal shapes were corrected using a fourth-order sliding surface polynomial curve-fit, while extracting the modal slopes and curvatures. The corrected modal displacements and the extracted slopes were used as the input in a finite element representation of the scanned surface to compute the modal strain energy for the three states. Differences in the strain energy distributions between the undamaged and damage scenarios were used to localize the inflicted damage

Reference

Garcia, G. V., Stubbs, N., "Relative Performance Evaluation of Pattern Recognition Models for Nondestructive Damage Detection (NDD)," Proceedings of the 15th International Modal Analysis Conference, IMAC97, V.2, Society for Experimental Mechanics, Inc., Bethel, Connecticut, pp. 1822-1830, 1997.

ABSTRACT

In this work, pattern recognition techniques are utilized to improve the ability of nondestructive damage detection (NDD) methods to locate damage in structures. Pattern recognition models based on Bayes' Rule are formulated using an established theory of damage localization. This yields information on the location of the damage directly from changes in mode shapes. Damage localization is then attempted in a truss type structure that is damaged at known locations. To evaluate the relative performance of the pattern recognition models to locate damage in the structure, a set of criteria are established. Results from the relative performance evaluation suggest that the adaptation of pattern recognition techniques into the nondestructive damage detection models can lead to improvements in the ability of the models to localize damage in a structure.

Reference

Barney, P., Ferregut, C., Perez, L.E., Hunter, N.F., and Paez, T.L., "Statistical Validation of System Models," HICSS-30 Proceedings, Hawaii International Conference on Systems Science, University of Hawaii, Maui, Hawaii, 1997

ABSTRACT

We frequently develop mathematical models of system behavior and sometimes use test data to help identify the parameters of the mathematical model. However, no general-purpose technique exists for formally, statistically judging the quality of a model. This paper suggests a formal statistical procedure for the validation of mathematical models of systems when data taken during operation of the system are available. The statistical validation procedure is based on the bootstrap, and it seeks to build a framework where a statistical test of hypothesis can be run to determine whether or not a mathematical model is an acceptable model of a system with regard to user-specified measures of system behavior. A numerical example is presented to demonstrate the application of the technique.

Reference

Doran, D., Ferregut, C. Tirado, C. "Experimental Strength Characterization of Geometrica Connections Subjected to Tension, Compression and Bending," to be presented at International Symposium on Shell and Spatial Structures, Singapore, November 10-14, 1997.

ABSTRACT

Structural design standards already exist for common materials and forms including: common structural steel forms, reinforced concrete, and laminated wood products. No such standards are available for the design of structures that employ extruded or machined aluminum connectors with formed tubular steel or aluminum structural members. Characterization of the minimum capacities of such systems under a variety of load conditions is a necessary precursor to the establishment of such standards. A number of manufacturers offer a range of connectors and specify and fabricate members according to the particular requirements of a given project. This paper represents the results of recent strength characterization tests and some statistical analysis generated for one such connector series. Testing included tensile, compression and bending tests. Two specimen configurations tested in tension are covered herein. Five different configurations of specimens were subjected to compression tests. One configuration was tested in bending. An efficient statistical analysis approach is introduced to maximize the value, of the limited information provided by the results of the tests, in the determination of characteristic strengths.

Reference

Andre, G.C., Carrasco C.J., Osegueda, R.A., Ferregut, C.M., James III, G.H. and Grygier, M., "Comparison of Accelerometer and Laser Modal Tests of a Vertical Stabilizer Assembly," SPACE 98, ASCE, April 1998, pp.132-139.

ABSTRACT

A Vertical Stabilizer Assembly (VSA) prototype of the Space Shuttle Orbiter was modal tested with a Laser Doppler Velocimeter (LDV) and accelerometers in order to compile a database that can be used to benchmark several damage identification techniques. The VSA was instrumented with 56 accelerometers and one force link attached to a stinger connecting a 500-lb. shaker and the structure. The LDV was used to acquire data from 84 points on one side of the VSA, 35 of which matched with accelerometer locations.

Seven controlled damage scenarios were inflicted on the VSA. The test article was modal tested before and after the infliction of the damage. The damage consisted of removing bolts and rivets, disbonding of skin from the aluminum honeycomb, cutting through ribs, and skin removal. The data captured consisted of frequency response functions (FRFs) with accompanying coherence functions and time histories for two scenarios.

This paper presents the results and conclusions of the comparison of the laser and accelerometer data on the basis of noise levels and magnitudes of FRFs. In addition, the advantages and disadvantages of the two techniques are discussed with respect to the setup and data acquisition times, as well as the ability to measure data on different points of the structure.

Reference

Bar-Cohen, Y., Marzell, N., Osegueda, R and Ferregut, C. "Smart Sensor System for NDE Corrosion in Aging Aircraft," ASNT'98 Spring Conference, Joint with 9th Asia-Pacific Conference on NDT, and 7th Annual Research Symposium, Anaheim, CA, March 24-26,1998.

ABSTRACT

The extension of the operation life of military and civilian aircraft rather than replacing them with new ones is increasing the probability of aircraft component failure as a result of aging. Aircraft that already have endured a long service life of more than 40 years are now being considered for another 40 years of service. Such a life extension has added a great degree of urgency to the ongoing need for reliable and efficient NDE methods. In contrast to crack detection, for which many NDE methods are available, corrosion damage is difficult to detect particularly at the initiation stages. Corrosion damage is costly to the aircraft operators and, in case of catastrophic failure, carrying the risk of loss of life and hardware. A futuristic idea is presented herein to take advantage of the accumulating knowledge and understanding of material degradation caused by flaws. A knowledge-base system combined with a series of sensors that monitor the variations in the material state supported by effective computing power can be used to simulate the process of degradation and to establish a health monitoring system. While this paper concentrates on corrosion, the concept is generic and can be adapted to other type of flaws. Corrosion [1] is a complex electro-chemo-mechanical process of material degradation, which depends on a large number of variables, with some that are difficult to identify a *priori*. The idea is to model the corrosion growth as a mathematical transformation operator that transforms the material characteristic variables to a degraded state. Such a model can be used to simulate the corrosion process and incorporate the parameters that characterize the material state and the level of corrosion damage. The input to the corrosion simulation system emulates data that is obtained in real time from selected sensors. Data fusion of sensor signals and artificial neural network algorithms [2] can enhance the accuracy of the damage characterization and reduce the effect of uncertainties and nonlinearities. The monitoring system can be complemented by an expert system with knowledge base, which would contain the information and heuristic rules used by inspectors to make decisions regarding the integrity of a corroded structure. The developed hybrid system will improve the understanding of corrosion processes, the monitoring of the associated material degradation, and the integrity assessment of the instrumented structure.

Reference

Osegueda, R.A., Ferregut, C. M., George, M.J., Gutierrez, J.M., and Kreinovich, V., "Computational Geometry and Artificial Neural Networks: A Hybrid Approach to Optimal Sensor Placement for Aerospace NDE", In Intelligent NDE Sciences for Aging and Futuristic Aircraft, Eds. Ferregut, Osegueda and Nunez, FAST Center for Structural Integrity of Aerospace Systems, The University of Texas at El Paso, ISBN: 97404-279-8, El Paso, Texas, January 1998, pp. 59-71.

ABSTRACT

The ideal design of an airplane should include built-in sensors that are pre-blended in the perfect aerodynamic shape. Each built-in sensor is expensive to blend in and requires continuous maintenance and data processing, so we would like to use as few sensors as possible. The ideal formulation of the corresponding optimization problem is, e.g., to minimize the average detection error for fault locations. However, there are two obstacles to this ideal formulation:

- First, this ideal formulation requires that we know the probabilities of different fault locations etc., and there are usually not enough statistics to determine these probabilities.
- Second, even for a known distribution, finding the best locations is a very difficult computational problem.

To solve these problems, *geometric symmetries* are used; these symmetries enable to choose several possible sets of sensor locations; the best location is then found by using a *neural network* to test all these (few) selected locations.

Reference

Y. Bar-Cohen, "Autonomous Rapid Inspection of Aerospace Structures," In Proc. of Workshop in Intelligent NDE Sciences for Aging and Futuristic Aircraft, Eds. Ferregut, Osegueda and Nunez, FAST Center for Structural Integrity of Aerospace Systems, The University of Texas at El Paso, ISBN: 97404-279-8, El Paso, Texas, January 1998, pp 93-99.

ABSTRACT

Effective assurance of the integrity and performance of aging aircraft structures, particularly those that are made of composite materials, requires rapid inspection of large areas. Removal from the aircraft for N7DE at an inspection facility is not economical and preferably the inspection should be performed at the field setting. Detection and characterization of defects are labor intensive, time consuming and when the process is manual the results are subjected to human error. These limitations of the standard NDE methods created a need for portable, user-friendly inspection systems that can rapidly and automatically scan large areas of complex structures and locate all the detrimental material conditions. Addressing this need has been an evolutionary process that followed the technology trend, and unique devices were developed to perform field inspection. Such a development-required integration of expertise in multidisciplinary areas that include NDE, telerobotics, neural networks, materials science, imbedded computing and automated control. Various portable inspection systems have emerged and the trend is toward fully automatic systems that autonomously inspect aircraft

Reference

Rodriguez, E., Pardo, H., Nazarian, S. and Pierluissi, J.H., "Real Time Characterization of Isotropic Plates Using Lamb Waves," In Proc. of Workshop in Intelligent NDE Sciences for Aging and Futuristic Aircraft, Eds. Ferregut, Osegueda and Nunez, FAST Center for Structural Integrity of Aerospace Systems, The University of Texas at El Paso, ISBN: 97404-279-8, El Paso, Texas, January 1998, pp 257-266.

ABSTRACT

A fast and accurate technique to determine, in real-time, the elasticity constants of the material in isotropic thin plates using ultrasonic plate (Lamb) waves is described in this paper. It allows for the calculation and measurement of the dispersion curves of a plate wave propagating in the lowest symmetric mode. Time signals captured with two piezoelectric transducers in contact with the plate are first transformed to the frequency domain. Then the cross phase spectra is calculated to obtain the phase *shift,* which in turns yields the phase velocity. The experimental set up automatically and in real-time acquires and processes the data, finds the operating frequency range, and displays the results as dispersion curves. Ultimately, Young's and shear moduli are calculated from the measured dispersion curves by means of an inverting algorithm. The accuracy of phase velocity measurements in aluminum plates was found to be, on the average, within ± 1 % when compared to the theoretical dispersion curves, and the inversion process yielded elasticity constants that were very close to the nominal values.

Reference

Murr, L.E., Posada, M., Arrowood, R.M., and Little, D., "Some New Approaches for Understanding and Characterizing Exfoliation Corrosion in Aircraft Aluminum Alloy Sheet Metal," In Proc. of Workshop in Intelligent NDE Sciences for Aging and Futuristic Aircraft, Eds. Ferregut, Osegueda and Nunez, FAST Center for Structural Integrity of Aerospace Systems, The University of Texas at El Paso, ISBN: 97404-279-8, El Paso, Texas, January 1998, pp 123-139.

ABSTRACT

In the absence of evidence for elemental excess or depletion at elongated and exfoliating grain boundaries in 2024 aluminum alloy sheet samples from KC- *135* aircraft body skins, we are pursuing different analytical and experimental approaches involving the measurement and comparison of grain boundary geometry and crystallography as these relate to energetics. We have used electron backscatter diffraction in the scanning electron microscope to compare microtexture in the orthogonal sample planes along with mesotextures of special grain boundaries. These measurements are compared with transmission electron microscopy observations of grain boundary misorientations for [11 0] directions in identically oriented (110) and (112) neighbor grains. Fundamental issues involved in the development and propagation of exfoliation cracks within the elongated grain layers are discussed on the basis of these preliminary observations and comparisons, and a simple model is developed.

Reference

Stubbs, N. and Choi, S., "Improved Non-destructive Damage Detection via Combining Individual Detection Theories," In Proc. of Workshop in Intelligent NDE Sciences for Aging and Futuristic Aircraft, Eds. Ferregut, Osegueda and Nunez, FAST Center for Structural Integrity of Aerospace Systems, The University of Texas at El Paso, ISBN: 97404-279-8, El Paso, Texas, January 1998, pp 23-35.

ABSTRACT

The possibility of improving the performance of damage detection via combining the predictions of more than one damage theory is explored in this paper. The theories, which are utilized here to demonstrate the approach, incorporate changes in the strain energy distribution of an element and the flexibility distribution at a point in the structure. The basic elements of the approaches are summarized in the generic sense that various types of measurement sets (e.g., displacements, strains, curvatures, etc.) may be applied. The performance of each methodology is evaluated using the data generated in a space structure. Both static and dynamic measurements are utilized to increase the number of damage prediction sets. Three logical rules for combining the theories are proposed and the performances of these rules are compared with the performance of the individual theories.

Reference

Osegueda, R., Ferregut, C., George, M.J., Gutierrez, J.M. and Kreinovich, V., " Non-Equilibrium Thermodynamics Explains Semiotic Shapes: Applications to Astronomy and to Non-Destructive Testing of Aerospace Systems," Proceedings of the 1997 International Conference on Intelligent Systems and Semiotics, Gaithersburg, Maryland, September 22-25, (A.M. Meystel, Ed.), NIST Special Publication 918, 1997, pp. 378-382.

ABSTRACT

Celestial bodies such as galaxies, stellar clusters, planetary systems, etc., have different geometric shapes (e.g., galaxies can be spiral or circular, etc.). Usually, complicated physical theories are used to explain these shapes; for example, several dozen different theories explain why many galaxies are of spiral shape. Some rare shapes are still difficult to explain.

It turns out that to explain these "astroshapes", we do not need to know the details of *physical* equations: practically all the shapes of celestial bodies can be explained by simple *geometric* invariance properties. This fact explains, e.g., why so many different physical theories lead to the same spiral galaxy shapes.

This same physical idea is used to solve a different problem: the optimal sensor placement for non-destructive testing of aerospace systems.

Reference

Claus, R.O., Osegueda, R.A., Bar-Cohen, Y. and Castro, M., "Laser Induced Plate Waves Using Waveform Shaping Optics and Strain Sensing by Fiberoptics Cross-sensitivity Effect", Proceedings of the ASNT Fall Conference, ISBN: 1-57117-068-5, Pitt., PA, Oct. 20-23, (1997), pp. 241-243.

ABSTRACT

Aircraft are being used in service significantly longer than their original design life. This cost driven measure is subjecting aircraft structures to conditions that are increasing the probability of failure, particularly as a result of aging. Aircraft that already endured a long service life of more than *35* years are now being considered for additional *45* service years. This issue of long term usage and aging of aircraft is relevant to both military and commercial aircraft. The 1988 failure of the Boeing aircraft, which was operated by Aloha Airlines, heightened the level of attention of aircraft manufacturers, users and the Federal Aviation Administration (FAA) to the aging commercial aircraft. The increased usage of old aircraft has added a great degree of urgency to the ongoing need for reliable and efficient NDE methods of flaw detection and characterization in aircraft structures. Current technology is time consuming, demands great attention to details by the inspectors and, in many cases, requires a costly disassembly of the structure. The reliability of the test results depends heavily on the type of instrumentation that is used, the condition of the instruments, the methods and environment under which they are used and above all, the interpretation of the inspectors. While a large variety of NDE methods are available for inspection of aircraft structures, the speed of inspection, the need for coupling, and other constrains are imposing limitations on the field use of such methods.

Recent studies with plate waves [1] and particularly leaky Lamb waves have shown effective capabilities of quantitative evaluation of plate structures such as bonded joints and composite materials. Plate wave NDE methods can be used to determine the elastic properties of the adhesive and the composite laminates as well as to detect and characterize flaws. Models were developed assuming in the case of composite materials that they consist of transversely isotropic layers [e.g., 1-3]. Dispersion curves (phase velocity as a function of the thickness x frequency) are measured and are used to determine the properties by an inversion algorithm. Generally, a homogeneous composite laminate with the symmetric axis parallel to the surfaces supports the formation of two modes of propagation: symmetric and antisymmetric. The lowest symmetric (extensional) and antisymmetric (flexural) modes are the easiest to measure in an ultrasonic experiment and their velocity values are used to determine certain material constants. Unfortunately, the transmission of the ultrasonic signals for the leaky Lamb waves experiments require the use of water immersion or water injection through squirters. This water-coupling requirement restricts the field applicability of the method and is limiting the number of constants that can be measured. Particularly, the constant c_{11} is difficult to determine due to need for a pitch catch setting with small incidence angles. The application of a contact coupled guided wave methods offer the potential for the transition of plate wave techniques to field inspection. Efforts to develop contract type plate wave techniques were made by numerous investigators (see for example [4]). The flexural wave signals are mixed with reflected signals from the boundary if the lateral dimension of the specimen is small in relation to the wavelength or the structure geometry is complex. In this case, only the extensional mode can be identified clearly. The issue of the mode identification in contact coupled plate waves is currently under investigation, and the practical implementation is still unsatisfactory. Recently, the authored started addressing this issue by developing a shaped wave-front laser induced ultrasound and fiberoptics receiving technique with a broader goal of integration all the laser induced NDE methods into a single system.

Reference

Osegueda, R., Ferregut, C., George, M.J., Gutierrez, J.M. and Kreinovich, V., "Maximum Entropy Approach to Optimal Sensor Placement for Aerospace Non-Destructive Testing," Maximum Entropy and Bayesian Methods, G. Erikson (ed.) Kluwer, Dordrecht, 1997.

ABSTRACT

The ideal design of an airplane should include *built-in sensors* that are pre-blended in the perfect aerodynamic shape. Each built-in sensor is expensive to blend in and requires continuous maintenance and data processing, so we would like to use *as few sensors as possible.*

The *ideal* formulation of the corresponding optimization problem is, e.g., to minimize the average detection error for fault locations. However, there are *two obstacles* to this ideal formulation:

First, this ideal formulation requires that we *know the probabilities* of different fault locations and the probabilities of different aircraft exploitation regimes. In reality, especially for a new aircraft, *we do not have those statistics* (and for the aging aircraft, the statistics gathered from its earlier usage may not be applicable to its current state). Therefore, instead of a well-defined optimization problem, we face a problem of not so well defined problem of optimization under uncertainty.

Second, even if we know the probabilities, the corresponding optimization problem is very *computation-consuming* and difficult to solve.

In this paper, we overcome the first obstacle by using *maximum entropy* approach (MaxEnt) to select the corresponding probability distributions.

To overcome the second obstacle, we use the *symmetry* approach. Namely, the basic surface shapes are symmetric (with respect to some geometric transformations such as rotations or shifts). The MaxEnt approach results in distributions that are *invariant* with respect to these symmetries, and therefore, the resulting *optimality criterion* (be it the minimum of detection error, or the minimum of fault location error, etc.) is also *invariant* with respect to these same symmetries.

Reference

Posada, M., Murr, L.E., Niou, C-S. Roberson, D., Little, D., Arrowood, R., and George, D., "Exfoliation and Related Microstructures in 2024 Aluminum Body Skins on Aging Aircraft," Material Characterization, Vol. 38, pp. 259-272, 1997.

ABSTRACT

Exfoliation, a directional attack along elongated grain boundaries in rolled 2024 aluminum sheet and plate, has been examined in some detail for KG-135 aging aircraft body skin samples utilizing optical (light) metallography, SEM, and TEM. A detailed analysis and comparison of precipitates within the grains and in the grain boundaries was performed as well as an examination of elemental depletion profiles across grain boundaries. These observations suggest that corrosion-related anodic sites play a far less significant role in the propagation of exfoliation than the hard corrosion products creating wedging stresses within the elongated grain boundaries, which seem to demonstrate unique and unusual structural and/or energetic features.

Reference

Garcia, G.V., Butler, K., and Stubbs, N., "Relative Performance of Clustering-based Neural Network and Statistical Pattern Recognition Models for Nondestructive Damage Detection," in Smart Materials and Structures Journal, May 1997.

ABSTRACT

The objective of this paper is to compare and contrast the capabilities of neural networks and statistical pattern recognition to localize damage in three-dimensional structures. A theory of damage localization, which yields information on the location of the damage directly from changes in mode shapes, is formulated. Next, the application of statistical pattern recognition and neural networks for nondestructive damage detection (NDD) is established. Expressions for classification using linear discriminant functions and a two-stage supervised clustering-based neural network are generated. Damage localization is applied to a finite-element model (FEM) of a structure, which contains simulated damage at various locations. A set of criteria for comparing and contrasting statistical pattern recognition and neural network models is then established. Finally, the evaluation of the two models is carried out using the established criteria.

Reference

Olga Kosheleva, Sergio Cabrera, Roberto Osegueda, Soheil Nazarian, Debra L. George, Mary J. George, Vladik Kreinovich, and Keith Worden, "Case study of non-linear inverse problems: mammography and non-destructive evaluation", In: Ali Mohamad-Djafari (ed.), Bayesian Inference for Inverse Problems, Proceedings of the SPIE/International Society for Optical Engineering, Vol. 3459, San Diego, CA, 1998

ABSTRACT

The inverse problem is usually difficult because the signal (image) that we want to reconstruct is weak. Since it is weak, we can usually neglect quadratic and higher order terms, and consider the problem to be linear. Since the problem is linear, methods of solving this problem are also, mainly, linear (with the notable exception of the necessity to take into consideration, e.g., that the actual image is non-negative).

In most real-life problems, this linear description works pretty well. However, at some point, when we start looking for a better accuracy, we must take into consideration non-linear terms. This may be a minor improvement for normal image processing, but these non-linear terms may lead to a major improvement and a great enhancement if we are interested in outliers such as faults in non-destructive evaluation or bumps in mammography. Non-linear terms (quadratic or cubic) give a great relative push to large outliers, and thus, in these non-linear terms, the effect of irregularities dominate. The presence of the non-linear terms can serve, therefore, as a good indication of the presence of irregularities.

Reference

Keith Worden, Roberto Osegueda, Carlos Ferregut, Soheil Nazarian, Debra L. George, Mary J. George, Vladik Kreinovich, Olga Kosheleva, and Sergio Cabrera, "Interval Methods in Non-Destructive Testing of Aerospace Structures and in Mammography", International Conference on Interval Methods and their Application in Global Optimization (INTERVAL'98), April 20-23, Nanjing, China, Abstracts, 1998, pp. 152-154.

ABSTRACT

In many practical situations, e.g., in aerospace applications and in mammography, it is important to test the structural integrity of material structures. We show that interval methods can help.

Reference

Keith Worden, Roberto Osegueda, Carlos Ferregut, Soheil Nazarian, Eulalio Rodriguez, Debra L. George, Mary J. George, Vladik Kreinovich, Olga Kosheleva, and Sergio Cabrera, "Interval Approach to Non-Destructive Testing of Aerospace Structures and to Mammography", In: Goetz Alefeld and Raul A. Trejo (eds.), Interval Computations and its Applications to Reasoning Under Uncertainty, Knowledge Representation, and Control Theory. Proceedings of MEXICON'98, Workshop on Interval Computations, 4th World Congress on Expert Systems, Mexico City, Mexico, 1998

ABSTRACT

One of the most important characteristics of the plane is its weight: every pound shaved off the plane means a pound added to the carrying ability of this plane. As a result, planes are made as light as possible, with its "skin" as thin as possible. However the thinner the layer, the more vulnerable is the resulting structure to stresses and faults, and a flight is a very stressful experience. Therefore, even minor faults in the plane's structure, if undetected, can be disastrous. To avoid possible catastrophic consequences, before the flight, we must thoroughly check the structural integrity of the plane.

Reference

Y. Bar-Cohen, S.-S. Lih, A. K. Mal, and Z. Chang, "Rapid Characterization of the Degradation of Composites Using Plate Waves Dispersion Data", Review of Progress in Quantitative Nondestructive Evaluation, Vol. 17, D.O. Thompson and D. E. Chimenti, (Eds.), Plenum Press, New York, N.Y. (1998) pp. 1711-1176.

ABSTRACT

NDE methods are needed to determine the structure integrity, stiffness and durability (residual life) of structures and they can be extremely useful in assuring the performance of structures using smaller safety factors. While the integrity and stiffness can be extracted directly from NDE measurements, strength and durability cannot be associated with physical parameters and therefore, cannot be measured by NDE methods. Specifically, NDE methods are developed to detect and characterize flaws and to determine the material properties of test specimens. For many years, composites as multi-layered anisotropic media, have posed a challenge to the NDE research community. Pulse-echo and through-transmission are the leading methods that are used in practice to evaluate the quality of composites. However, these methods provide limited and mostly qualitative information about the material properties and many defects. Following the discovery of the LLW and the Polar Backscattering phenomena in composites [1, 2], numerous experimental and analytical studies have taken place using obliquely insonified ultrasonic waves [3-5]. These studies led to the development of effective quantitative NDE capabilities to determine the elastic properties, to accurately characterize defects and even to evaluate the quality of adhesively bonded joints [6, 7]. In spite of the progress that was made both theoretically and experimentally, oblique insonification techniques are still academic tools and have not yet become standard industrial test methods for NDE of composite materials. The authors investigated the issues that are hampering the transition of these methods to the practical world of NDE and are involved with extensive studies to address these issues. This paper covers the progress that was made by the investigators in tackling the theoretical and experimental issues to solidify the foundation of the techniques and their transition to practical NDE tools.

Reference

Y. Bar-Cohen, A. K. Mal and Z. Chang, "Defects Detection and Characterization Using Leaky Lamb Wave (LLW) Dispersion Data," ASNT '98 Spring Conference, Joint with 9th Asia-Pacific Conference on NDT, and 7th Annual Research Symposium, Anaheim, CA, March 24-26, 1998.

ABSTRACT

Composite materials are being used at a significant level of usage for flaw critical structures and they are taking a growing percentage of the makeup of aircraft and spacecraft. Composite structures are now reaching service duration, for which the issue of aging is requiring adequate attention. The key to efficient inspection of composites is the ability to determine their integrity and durability. Standard NDE methods, which were developed to inspect metallic structures, were adapted by the industry for inspection of composites partially accounting for the multi-layered anisotropic nature of these materials. These standard methods provide limited and mostly qualitative information about the material properties and defects. The discovery of the ultrasonic LLW and the Polar Backscattering phenomena in composites [1, 2] established the foundations for quantitative NDE of these materials as well as the extraction of detailed information about flaws and material properties. These phenomena are based on obliquely insonified ultrasonic waves and numerous analytical and experimental studies followed the discovery of these phenomena [e.g., 3-5]. These studies led to the development of quantitative NDE capabilities of determining the elastic properties, characterize flaws, and even the evaluation of adhesive bonded-joints' quality [6]. In spite of the progress that was made both theoretically and experimentally, oblique insonification techniques are still mostly academic tools and have not yet become standard industrial NDE methods for composite materials. In the last several years, the authors have investigated the issues that are hampering the transition of the LLW method to the practical NDE arena and are making efforts to overcome the method limitations. This paper covers the progress that was made by the investigators in developing the LLW method for characterization of flaw that are related aging aircraft.

Reference

Y. Bar-Cohen, A. Mal and Z. Chang, "Composite Material Defects Characterization Using LLW Dispersion Data" SPIE's NDE Techniques for Aging Infrastructure & Manufacturing, Conference NDE of Materials and Composites II, 31 March-2 April 1998, San Antonio, Texas. Paper No. 3396-25.

ABSTRACT

Leaky Lamb waves (LLW) propagation in composite materials has been studied extensively since it was first observed in 1982. The wave is induced using a pitch-catch arrangement and the plate wave modes are detected by identifying minima in the reflected spectra to obtain the dispersion data. The wave behavior in multi-orientation laminates was well documented and corroborated experimentally with a very high accuracy. The sensitivity of the wave to the elastic constants of the material and to its boundary condition led to several studies where the elastic properties were inverted and the characteristics of bonded joint were evaluated. Recently, the authors modified their experimental setup to allow measuring dispersion curves at a significantly higher speed than ever recorded. A set of 20 angles of incidence along a single polar angle of a composite laminate are acquired in about 45 seconds. The reflection spectra are acquired in real time while filtering the high frequency noise providing reliable data at amplitude levels that are significantly lower that were acquired in prior studies. This new method makes the LLW a practical quantitative tool for both inversion of the elastic properties and characterization of flaws. The emphasis of the current study is on the detection and characterization of flaws. The composite is modeled as transversely isotropic and dissipative medium and the effect of flaws is analyzed and compared to the experimental data using a C-scan mounted LLW scanner.

Reference

Y. Bar-Cohen, A. K. Mal and Z. Chang, "Characterization of Defects in Composite Material Using Rapidly Acquired Leaky Lamb Wave Dispersion Data", Proceedings of the 7th European Conference on Non-Destructive Testing, Session 4: Aerospace, Copenhagen, Denmark 26-29 May 1998.

ABSTRACT

The phenomenon of Leaky Lamb waves (LLW) in composite materials was first observed in 1982 using a Schlieren system. It has been studied extensively by numerous investigators and successfully shown to be an effective quantitative NDE tool. In spite of the success, the method has not become a standard inspection technique due to shortcoming that will be addressed in this manuscript. The LLW phenomenon is associated with an ultrasonic pitch-catch setup and involves the measurements of the guided wave dispersion curves by identifying the minima in the reflected spectra. The sensitivity of the wave to the elastic constants of the material and the boundary conditions led to the development of methods of inverting the elastic properties and the characterization of bonded joint. Recently, the authors modified their experimental setup to rapidly measure dispersion curves allowing data acquisition speed that is faster than ever before. The reflection spectra are acquired in real time while filtering the high frequency noise providing reliable data at amplitude levels that are significantly lower than were acquired in prior studies. This new method makes the LLW more practical as a quantitative tool for both inversion of the elastic properties and characterization of flaws. The emphasis of the current study is on the detection and characterization of flaws. The composite is modeled as transversely isotropic and dissipative medium. Further, the effect of flaws is analyzed and compared to the experimental data using a C-scan mounted LLW scanner.

Reference

Garcia, G.V., Osegueda, R. and Meza, D., "Comparison of the Damage Detection Results Utilizing and ARMA Model and a FRF Model to Extract the Modal Parameters", SPIE 98, Smart Structures and Materials Conference, San Diego, CA, March 1998

ABSTRACT

The objective of this paper is to make a comparison of the damage detection results obtained from an analysis of the modal parameters extracted from a time domain model and a frequency domain model. In this paper, an autoregressive moving average (ARMA) model and a FRF model will be utilized to extract the modal parameters of a beam. Expressions for the modal parameters using the ARMA model are developed. Next, an established theory of damage localization, which yields information on the location of the damage directly from changes in mode shapes, is selected. Expressions for classification algorithms using the damage indicator functions from the damage localization theory are then generated. Using the classification algorithms, damage localization is attempted for a pinned-pinned beam, which contains damage of various degrees. Finally, the modal parameters and damage detection results obtained from the two methods are compared.

Reference

Campuzano-Contreras, A.L., Arrowood, R.M., Murr, L.E., Little, D., Roberson, D., and Niou, C.S, "Characterization of Fuselage Skin Lap Joints", Microstructural Science Volume 25, 20-23, July 1997, Seattle, WA.

ABSTRACT

Fuselage skin lap joints, damaged by crevice corrosion, of a KC-135 fuel tanker were analyzed. The need to use these aging aircraft for 40 more years has increased the interest in understanding corrosion damage in aircraft aluminum alloys. Having a fundamental scientific understanding of crevice corrosion mechanisms that occur in sections of a KC-135 can help in planning for maintenance and nondestructive inspection to extend the life of the aircraft. Metallographic (light microscope) observations of the base metal illustrate the initial crystal structure or grain structure, and transmission electron microscopy shows precipitates and dislocation structures. Auger spectroscopy shows that different areas of the laps had different aluminum to oxygen composition ratios. X-ray diffraction and energy dispersive spectroscopy were other analytical techniques used.

The KC-135 fuel tankers, which are the Air Force's core tanker, have exceeded their design life; their average age in 1995 was 30.9 years (1). From a fatigue damage perspective the KC-135 aircraft are considered new since they only have approximately 15,000 hours of service. They were designed for 70,000 hours of service. The Air Force is considering the possibility of flying KC-135's until 2040 (2). This service life is calculated considering an uncorroded aircraft. The estimated direct maintenance cost due to corrosion is 1 billion dollars per year to the USAF (3). Therefore, it is important to implement an effective corrosion control and prevention program.

Much of the corrosion on the KC-135 is found between the skin and the spot welded doublers, 620/820/960 bulkheads, wing spar chords, upper wing skins, and section 41 fuselage skins. The doublers are cracking at the spot welds and in some cases dissimilar metal corrosion between aluminum and stainless steel is occurring. The main corrosion problems on the KC-135 are not in the lap joints (4). However, our lap joints from a decommissioned aircraft do show corrosion damage. It is probable that our samples are from a Boeing 707 commercial airliner, rather than a KC-135 military fuel tanker. (The 707 and the KC-135 are essentially the same aircraft.) Our purpose is to investigate rather generic corrosion phenomena in 2XXX aluminum aircraft skins, not to describe a problem unique to the KC-135.

Crevice corrosion is localized corrosion of a metal that occurs at areas that are shielded from full exposure to the environment. It can occur at lap joints where oxygen is restricted, often by the local breakdown of the protective passive layer.

Aluminum alloy skins from a decommissioned aircraft were characterized using a variety of analytical techniques to develop an overview of both macrostructural and microstructural aspects of crevice corrosion. Optical metallography, X-ray diffraction, scanning electron microscopy, energy dispersive spectrometry, auger electron spectroscopy, and transmission electron microscopy were the analytical techniques used in this investigation.

Reference

Posada, M., Murr, L.E., and Arrowood, R.M., "Observations of Exfoliation Corrosion in Aging Aircraft Body Skins: A Search for Crystallographic Issues", Microstructural Science Volume 25, 20-23, July 1997, Seattle, WA.

ABSTRACT

Exfoliation, a directional attack along elongated grain boundaries in rolled aluminum sheet and plate, has been examined in some detail for KC-135 aging aircraft body skin samples utilizing optical (light) metallography, SEM, and TEM. In addition, fine-probe backscatter EDX scans and microdiffraction analyses have been made for both grain boundary-related precipitates, and matrix precipitates and their relationship to corrosion and corrosion nucleation. These observations suggest that anodic sites nucleating corrosion may not play a significant role in the nucleation and propagation of exfoliation corrosion. Believing that the directionality specific to exfoliation corrosion observed may have a crystallographic origin or that crystallographically unique features may characterize the elongated grain boundaries, TEM observations coupled with selected-area electron diffraction analysis were made to measure specific misorientations. These observations were also compared with EBSD analysis in both the in-plane and sheet thickness directions. While the results are somewhat preliminary, there seems to be compelling crystallographic distinction for exfoliation. There appears not to be a strong correlation between EBSD observations of misorientation with TEM measured misorientations for identically oriented grains used in comparing grain boundaries.

Reference

Corral, J., Trillo, E.A., Li, Y. and Murr, L.E., "Corrosion of Friction-Stir Welded Aluminum Alloys 2024 and 2195," submitted to Corrosion 1999.

ABSTRACT

The susceptibility of the base metal and weld zone for the friction-stir welding (FSW) of Al 2024 and Al 2195 to corrosion in chloride and caustic solutions was studied. Pitting corrosion was examined and compared through potentiodynamic polarization experiments. The microstructures of the unwelded base metals were examined and compared by transmission electron microscopy with those of the FSW zone. In each case the FSW zone consisted of smaller, equiaxed, dynamically recrystallized grains measuring less than 10 μm. Residual micro hardness profiles through the weld zones were also measured and compared. In each case the FSW zone hardness was significantly lowered. The Al 2024 FSW zone exhibited exaggerated softening at the FSW zone boundaries where the hardness reduction in contrast to the unwelded base metal was nearly 70%. The Al 2195 samples exhibited generally superior corrosion resistance since there was little difference between the base metal and FSW zone corrosion after static immersion testing in chloride and caustic solutions. The FSW zone was noticeably corroded in caustic solution for the Al 2024 alloy. Anodic polarization curves showed that both the Al 2024 and Al 2195 alloys have nearly the same passive currents and corrosion potentials in chloride solution. However, consistent with immersion testing, the Al 2024 FSW zone did have a higher passive current density than the base metal in caustic solution.

Reference

Garcia, G., Stubbs, N. and Osegueda, R., "Pattern Recognition Approach to Damage Classification," Submitted for publication to Mechanical Systems and Signal Processing Journal.

ABSTRACT

The objective of this work is to investigate the utility of classification algorithms for damage localization in structures that utilize damage indicators (DI) to detect and localize damage. The classification algorithms presented here can be used by any damage detection method, which uses damage indicators to detect and localize damage. To accomplish this objective we will evaluate the relative performance of five classification algorithms for nondestructive damage detection. The classification algorithms investigated here are as follows: (1) a quadratic classifier obtained from Bayes' rule (i.e., using unequal damage and undamaged covariance matrices), (2) a linear classifier obtained from Bayes' rule (i.e., using equal damage and undamaged covariance matrices), (3) a linear classifier obtained from Bayes' rule (i.e., assuming that the damaged and undamaged covariance matrices are equal to the identity matrix), (4) a classifier using Euclidean distance as a basis, and *(5)* a classifier using hypothesis testing. First, expressions for pattern classification using discriminant functions obtained from Bayes' rule, distance as similarity, and hypothesis testing are generated. Next, an established theory of damage localization that yields information on the location of the damage directly from changes in a damage indicator function is selected. Criteria for the evaluation of the proposed pattern classification models are generated. Utilizing the enhanced models, the locating of damage is attempted in: (1) a numerical model of a space structure with simulated damage at various locations, and (2) a real structure damaged at known locations. Finally, the accuracy and reliability of the pattern classification models are evaluated using the established criteria.

Reference

Castro-Colin, M., Lopez, J.A. and Osegueda, R., "Tuning Laser-induced Lamb Waves," Submitted for publication to the Journal for Non-Destructive Evaluation.

ABSTRACT

We study experimentally the propagating modes of ultrasound waves produced by a pulse of 532 nm laser light delivered on an aluminum plate. The beam, shaped as a line, selectively induced Lamb modes according to the line length of the beam. The mode identification was performed by detecting the ultrasonic modes with piezoelectric detectors along a propagation direction, and using two-dimensional fast Fourier transform. Good agreement is observed between theoretical and experimental dispersion curves for the first fundamental symmetric and anti-symmetric modes. Comparative results are shown for 12 and 24 mm laser line-length at 13.6 and 16.8 ns pulse-width.

Reference

Nguyen, H.T., Kreinovich, V. and Wu, B., "Fuzzy/probability-fractal/smooth," International Journal of Uncertainty, Fuzziness, and Knowledge-Based Systems (IJUFKS), 1999.

ABSTRACT

Many applications of probability theory are based on the assumption that, as the number of cases increase, the relative frequency of cases with a certain property tends to a number - *probability* that this property is true. L. Zadeh has shown that in many real-life situations, the frequency oscillates and does not converge at all. It is very difficult to describe such situations by using methods from traditional probability theory. Fuzzy logic is not based on any convergence assumptions and therefore, provides a natural description of such situations. However, a natural next question arises: how can we describe this oscillating behavior? Since we cannot describe it by using a *single* parameter (such as probability), we need to use a *multi-D* formalism. In this paper, we describe an optimal formalism for describing such oscillations, and show that it complements traditional probability techniques in the same way as fractals complement smooth curves and surfaces.

Reference

Yager, R.R. and Kreinovich, V., "Decision Making Under Interval Probabilities," International Journal of Approximate Reasoning, 1999.

ABSTRACT

If we know the probabilities $p_1,\ldots,p_n$ of different situations $s_1,\ldots,s_n$, then we can choose a decision A_i for which the expected benefit $C_i = p_1 \cdot c_{i1} + \ldots + p_n \cdot c_{in}$, takes the largest possible value, where c_{ij} denotes the benefit of decision A_i in situation s_j. In many real life situations, however, we do not know the *exact* values of the probabilities p_j; we only know the *intervals* $\mathbf{p}_j = [p_j^-, p_j^+]$ of possible values of these probabilities. In order to make decisions under such interval probabilities, we would like to generalize the notion of expected benefits to interval probabilities. In this paper, we show that natural requirements lead to a unique (and easily computable) generalization. Thus, we have a natural way of decision making under interval probabilities.

Reference

Osegueda, R., Mendoza, Y., Kosheleva, O. and Kreinovich, V., "Multi-Resolution Methods in Non-Destructive Testing of Aerospace Structures and in Medicine," 14th IEEE International Symposium on Intelligent Control/Intelligent Systems and Semiotics ISIC/ISAS '99, Cambridge, MA, September 1999.

ABSTRACT

A fault in an aerospace structure can lead to catastrophic consequences; therefore, it is extremely important to test these structures regularly. Thorough testing of a huge aerospace structures results in a large amount of data, and processing this data takes a lot of time. To decrease the processing time, we use a "multi-resolution" technique, in which we first separate the data into data corresponding to different vibration modes, and then combine these data together. There are many possible ways to transform each mode's data into the probability of a fault, and many possible way of combining these mode-based probabilities; different approaches lead to different results. In this paper, we show how a general methodology for choosing the optimal uncertainty representation can he used to find the optimal uncertainty representations for this particular problem. Namely, we show that the problem of finding the best approximation to the probability of detection (POD) curve (describing the dependence of probability *p(a)* of detection on the size a of the fault, see [2, 6, 7]) can be solved similarly to the problem of finding the best activation function in neural networks. A similar approach can be used in detecting faults in medical images (e.g., in mammography).

Reference

Calixto, M.E., McClure, J.C., Singh, V.P., Bronson, A., Sebastian, P.J. and Mathew, X., "Electrodeposition and Characterization of CdTe Thin Films on Mo Foils Using a Two Voltage Technique," presented at the International Materials Research Congress Cancun 99, Cancun, Mexico, August 1999.

ABSTRACT

Polycrystalline thin film CdTe based solar cells are one of the most promising candidates for low-cost terrestrial conversion of solar energy because of the optimum energy band gap (Eg = 1.44 eV) and high absorption coefficient of CdTe.

In this work, a two-voltage electrodeposition technique has been used to prepare CdTe thin films from acidic solutions. At -300mV (SCE) a Te rich CdTe layer was deposited on the Mo foil substrate before depositing the final CdTe thin film at higher voltages. In this way, the polycrystalline CdTe showed good adherence to the substrate and very low contact resistance between the substrate and the film as well as nearly stoichiometric composition. From X-ray Diffraction results, the as deposited films show very small grain sizes but after annealing the grain size increases considerably showing very well defined peaks. The morphological, structural and composition results of CdTe thin films obtained by Scanning Electron Microscopy, X-ray Diffraction, and X-ray Fluorescence will be presented. Electrical properties such as conductivity type and contact resistance values for the Mo/CdTe structures will also be presented.

Reference

Mendoza, Y. and Osegueda, R., "Theoretical Explanation for the Empirical Probability of Detection (POD) Curve: A Neural Network-Motivated Approach," To appear in 42nd Midwest Symposium on Circuits and Systems, Las Cruces, NM, August 1999.

ABSTRACT

For non-destructive testing of aerospace structures, it is extremely important to know how the probability of detecting a fault depends on its size. Recently, an empirical formula has been found which described this dependence. In this paper, we provide the theoretical justification for this formula by using methods motivated by the neural network approach.

Reference

Kosheleva, O., Longpre, L. and Osegueda, R., "Detecting Known Non-Smooth Structures in Images: Fuzzy and Probabilistic Methods, with Applications to Medical Imaging, Non-Destructive Testing, and Detecting Text on Web Pages," The Eighth International Fuzzy Systems Association World Congress IFSA '99, Taipei, Taiwan, August 1999.

ABSTRACT

We show how probabilistic and fuzzy methods can be used in detecting non-smoothnesses in images; intended applications include medical imaging, nondestructive testing of aerospace structures, and search for text in web images.

Reference

Krishna, M., Kreinovich, V. and Osegueda, R.A., "Fuzzy Logic in Non-Destructive Testing of Aerospace Structures," To appear in 42nd Midwest Symposium on Circuits and Systems, Las Cruces, NM, August 1999.

ABSTRACT

In nondestructive testing, to locate the faults, we send an ultrasonic signal and measure the resulting vibration at different points. To describe and combine the uncertainty corresponding to different measurements and fuzzy estimates, we used fuzzy logic. As a result, we get reasonably simple computational models, which lead to as good fault detection as the known more complicated models.

Reference

Osegueda, R.A., Andre, G., Ferregut, C.M., Carrasco, C., Pereyra, L., James, G. III, Grygier, M. and Rocha, R., "A Strain Energy-Based Vibrational NDE Method Applied to an Aerospace Structure," 9th Annual Symposium on Non-Destructive Characterization of Materials, Sydney, Australia, July 1999.

ABSTRACT

An early prototype of the Vertical Stabilizer Assembly (VSA) of the Shuttle Orbiter was modal tested at healthy and damaged states to study vibrational nondestructive damage evaluation in aerospace structures. Frequency Response and Coherence functions were collected with a Laser Vibrometer at 84 points when the healthy and damaged VSA was shaken with a continuous random force from 0 to 300 Hz. The measurements were used to extract the resonant frequencies and modal shapes for the healthy and damaged states. After pairing of the mode shapes between the healthy and damaged states through the Modal Assurance Criterion, the strain energy of the modes were determined through a finite element model of the VSA and normalized. The localization of the damage is achieved through an analysis of the differences between the modal strain energy in the healthy and damaged states and a fusion on the information obtained from several modes. This paper evaluates the detectability and performance of four different methods.

Reference

Ross, T.J., Ferregut, C., Osegueda, R. and Kreinovich, V., "System Reliability: A Case When Fuzzy Logic Enhances Probability Theory's Ability to Deal With Real-World Problems," 18th International Conference of the North American Fuzzy Information Society NAFIPS '99, New York City, NY, June 1999, pp. 243-247.

ABSTRACT

In his recent paper "Probability theory needs an infusion of fuzzy logic to enhance its ability to deal with real-world problems", L. Zadeh explains that probability theory needs an infusion of fuzzy logic to enhance its ability to deal with real-world problems. In this talk, we give an example of a real-world problem for which such an infusion is indeed successful: the problem of system reliability.

Reference

Yam, Y., Osegueda, R. and Kreinovich, V., "Towards Faster, Smoother, and More Compact Fuzzy Approximation, with an Application to Non-Destructive Evaluation of Space Shuttle's Structural Integrity," 18th International Conference of the North American Fuzzy Information Society NAFIPS '99, New York City, NY, June 1999, pp. 243-247.

ABSTRACT

It is known that fuzzy systems are universal approximators, i.e., any input-output system can be approximated, within any given accuracy, by a system described by fuzzy rules. Fuzzy rules work well in many practical applications. However, in some applications, the existing fuzzy rule approximation techniques are not sufficient:

First, in many practical problems (e.g., in many control applications), derivatives of the approximated function are very important, and so, we want not only the approximating function to be close to the approximated one, but we also want their derivatives to be close; however, standard fuzzy approximation techniques do not guarantee the accuracy of approximating a derivative.

Second, to get the desired approximation accuracy, we sometimes need unrealistically many rules.

Reference

Pereyra, L.R., Osegueda, R.A., Carrasco, C. and Ferregut, C.M., "Damage Detection in a Stiffened-Plate Using Modal Strain Energy Differences," SPIE Conference on Nondestructive Evaluation of Aging Aircraft, Airports, and Aerospace Hardware III, Newport Beach, CA, March 1999, Vol. 3586, pp. 211-222.

ABSTRACT

An aluminum stiffened-plate panel resembling aircraft-fuselage construction was tested in the laboratory with a Laser Doppler Velocimeter (LDV). The purpose of the test was to extract out-of-plane mode shape data before and after the infliction of damage to evaluate a global NDE damage localization technique. The NDE damage localization technique is based on modal strain energy differences between the undamaged and damaged states. The modal strain energies were computed from bending and twisting curvatures obtained using an iterative bi-variate curve-fit procedure on estimated curvatures obtained from finite differences of the mode shapes. Strain energy differences between pairs of matching modes of the undamaged and damaged structure locate the inflicted damage by indicating increases in the modal strain energy. The damage indications provided by several modes are normalized using a standard norm and fused using an average approach to create damage maps.

The test article was excited at two points with shakers exerting uncorrelated continuous random forces from 0 to 300 Hz. Experimental frequency response functions and their corresponding coherence were extracted from 239 data points uniformly spaced. The model was subjected to several damage scenarios at different zones. The mode shapes of the undamaged and damaged structures were extracted using a poly-reference MDOF curve-fit technique.

This paper presents the results, conclusions and recommendations of the global NDE technique used. The emphasis is on the improved accuracy that resulted from combining the modal information and using high-order curve-fit algorithms to estimate curvatures.

Reference

Garcia, G.V. and Osegueda, R.A., "Damage Detection Using ARMA Model Coefficients," SPIE Conference, Smart Structures and Materials Conference, Newport Beach, CA., March 1999, Vol. 3671, pp. 289-296.

ABSTRACT

The objective of this paper is to perform damage detection utilizing the coefficients obtained from an ARMA model. The Damage Index Method has been proven to be one of the better modal based damage detection methods currently in use. One major draw back to this method is the need to determine mode shapes from the frequency response function (FRF) data. Extracting mode shapes from FRF data can be extremely time consuming and the results at times can be highly dependent on the users knowledge and the application of the software package being utilized to extract the modal parameters. In an attempt to minimize user interaction in the damage detection process and to eliminate the need to determine modal parameters, we will develop a method, which is capable of providing damage detection results from accelerometer time histories. This will be accomplished by utilizing the parameters of an ARMA model as damage indicators. Expressions for classification algorithms using the ARMA model parameters will be generated. Using the classification algorithms, damage localization is attempted for a simply supported beam, which contains damage of various degrees at several locations. The damage detection results will then be compared to the damage detection results obtained by the Damage Index Method.

Reference

Osegueda, R.A., Revilla, A., Pereyra, L.R. and Moguel, O., "Fusion of Modal Strain Energy Differences for Localization of Damage," SPIE Conference on Nondestructive Evaluation of Aging Aircraft, Airports, and Aerospace Hardware III, Newport Beach, CA, March 1999, Vol. 3586, pp. 189-199.

ABSTRACT

The fusion of multiple modal strain energy differences is proposed for the detection of damage at single and multiple locations. The approaches assume the existence of several modal shapes of the structure in the undamaged and damaged states. Modal curvatures obtained through iterative high-order spline fits of the shapes permit the determination of the modal strain energy content of the structure in both states. Locations with increases in the modal strain energy between the undamaged and damaged structure are indicative of possible damage. The damage indications resulting from multiple modes are fused according to three rules: (1) an Average Standard Norm, (2) a union of probability mass functions and (3) a weighted intersection of the probabilities that the strain energy are greater than zero. The third rule requires knowledge of the statistics of the modal shape measurements. While not strictly adhering to the classical data fusion methodologies such as, Dempster-Shafer or Bayesian, the combination of information at the probabilistic level yields results that are consistent with those expected in a formal data fusion formulation. The fusion algorithms for the localization of damage are tested using five modal shapes obtained from aluminum beams in undamaged and damaged states. One and two locations at different damage magnitudes are considered. The results indicate that the last two approaches are superior to the standard norm method.

Reference

Tirado, C. and Nazarian, S., "Impact of Damage on Propagation of Lamb Waves in Plates," SPIE Conference on Nondestructive Evaluation of Aging Aircraft, Airports, and Aerospace Hardware III, Newport Beach, CA, March 1999, Vol. 3586, pp. 267-278.

ABSTRACT

A consorted effort is ongoing to utilize spectral analysis of Lamb Waves to rapidly characterize and to detect damage in plates. To optimize test set-up, to understand the limitations of the methodology, and to verify the experimental results, an effort is under way to simulate conditions normally encountered in actual cases. The impact of propagation of Lamb waves in the presence or absence of damage has been simulated using a finite element algorithm. Two-dimensional (2D) Fourier transform can be used to identify individual modes, and to measure the amplitude and propagation velocity of each mode in a thin plate. Mode conversion due to the presence of a crack can be readily identified with this method. The damage was modeled as notches with different widths and depths. Three different materials were modeled for this purpose: Aluminum 6061-T6, Steel A36, and Graphite-Epoxy; the latter being analyzed in directions parallel and perpendicular to the fibers. The focus of the work was on low-frequency range where the fundamental symmetric and anti-symmetric modes are dominant. The ratio of notch depth to plate thickness and the absolute notch depth were considered as possible controlling parameters for the sensitivity in the damage detection. The effect of the width of the flaw on the transmissivity of the Lamb waves was also considered and found to be minimal.

Reference

Garcia, G.V., Osegueda, R.A. and Meza, D., "Damage Detection Comparison Between Damage Index Method and ARMA Method," IMAC Proceedings of the 17th International Modal Analysis Conference, Kissimmee, FL, February 1999, Vol. 1, pp. 593-598.

ABSTRACT

The objective of this paper is to make a comparison of the damage detection results obtained from the Damage Index Method and a method that utilizes the parameters obtained from an ARMA model. The Damage Index Method has been proven to be one of the better modal based damage detection methods currently in use. One major draw back to this method is the need to determine mode shapes from frequency response function (FRF) data. Extracting mode shapes from FRF data can be extremely time consuming and the results at times can be highly dependent on the users knowledge and the application of the software package being utilized to extract the modal parameters. In an attempt to minimize user interaction in the damage detection process and to eliminate the need to determine modal parameters, we will develop a method that is capable of providing damage detection results from accelerometer time histories. This will be accomplished by utilizing the coefficients of an ARMA model as damage indicators (DI's). Expressions for classification algorithms using the ARMA model coefficients are generated. Using the classification algorithms, damage localization is attempted for a simply supported beam that contains damage of various degrees at several locations. The damage detection results will then be compared to the damage detection results obtained by the Damage Index Method.

Reference

Pereyra, L.R., Osegueda, R.A., Carrasco, C. and Ferregut, C.M., "Structural Defects Detection Using Low Frequency Modal Testing With a Laser Vibrometer," ASNT Fall Conference and Quality Testing Show, Nashville, TN, October 1998, pp. 63-66.

ABSTRACT

The issue of aging of aircraft is of high priority in the safety of military and civilian flights. Its importance is because a considerable percentage of the fleet already endured the service life for which they were originally designed. The high cost of replacing aged aircraft structures had led to extend their serviceability long beyond the design service life while improving preventive maintenance and NDE inspections. Old aircraft must be subjected to frequent routine visual inspections and periodic maintenance where the aircraft are disassembled and inspected. However, visual inspections could result in reduced reliability of safety since human error is easily produced in a structure of this magnitude and complexity. Robust NDE methods having less susceptibility to human and environmental factors are essential to offset the increasing inspection burden. A less obvious but not less important benefit of improved inspection methods is that the development of reliable, cost effective NDE methods can reduce possible collateral damage associated with disassembly, re-assembly, and modification of airplane structures made during visual inspection. So far, various NDE techniques such as ultrasonics, Eddy current, thermography, and others are being effectively utilized for the detection of cracks, disbonds, and corrosion damage. These techniques are capable of detecting very small defects; however, their effectiveness depends on correctly placing their sensors on or in the vicinity of the defects. Because of this requirement, traditional NDE methods, such as those mentioned, are classified as "local". Vibrational NDE method, on the other hand, can be classified as global. They require measurements of the global dynamic response due to some "known" input force and the processing of these measurements for the numerical extraction of the global modal parameters. The measurements can be obtained from attached sensors or non-contactly via laser Doppler velocimetry (a laser vibrometer).

Global vibrational NDE methods utilize the changes in the modal characteristics of the structure (resonant frequencies, damping ratios and mode shapes) before and after a damage to localize, quantify and asses the inflicted damage. The methods have the potential of inspecting large areas of the structure. Many researchers have proven the efficacy of using mode shapes changes to detect damage in aerospace structures"[2]. This paper describes the process to localize inflicted damage in a laboratory structure resembling aircraft construction using modal information measured before and after damage with a laser vibrometer.

Reference

Obispo, H. M., Murr, L. E., Arrowood, R. M., and Trillo, E. A., "Copper Deposition During the Corrosion of Aluminum Alloy 2024 in Sodium Chloride Solutions, Journal of Materials Science, in press (2000).

ABSTRACT

Copper and copper-rich particle clusters were observed to deposit on aging aircraft skin material (Al 2024 sheet coupons) after corrosion immersion experiments for 5 days in acidic (pH 3) neutral (pH~6), and basic (pH 11) 0.6 M NaCl solutions. SEM analysis employing an EDX spectrometer showed a propensity of large Cu particle clusters on Fe-rich or Fe-containing areas while a TEM inventory of second-phase particles in the alloy sheet showed a propensity of Al-Fe-Cu-Mn and Al-Cu-Si particles along with Al-Cu-Mg and Al-Cu-Fe-Mn-Si particles and particle clusters. A modified replication technique was used to lift particles from the corroded coupon surfaces. TEM analysis employing an EDX spectrometer showed a wide range of copper deposits exhibiting microdendritic morphologies in basic and neutral environments, and botryoidal (or nodular) morphologies in acidic environments. The plating or cementation of copper from solution as an electrochemical displacement reaction appears to be a major contributor to the pitting corrosion of 2024 aluminum alloy.

Reference

J. Corral, E. A. Trillo, and L. E. Murr, "Localized Corrosion Analysis of Friction Stir Welded Aluminum Alloys", paper to be published in Mexican American Engineers and Scientists Society Proceedings, 2000.

ABSTRACT

The corrosion effects of three friction-stir welded (FSW) alloys were examined; Al 2024/2024, Al 2195/2195, and Al 2024/2195. Static immersion tests in 0.6M NaCl revealed that an even amount of corrosion by-product occurs on the samples that gradually increases with time. Potentiodynamic scans of the weld zone and the base materials show that there is no difference in the passive current densities of the different sections of the material in all three FSW samples. Immersion tests in 0.5M NaOH show preferential attack at the weld zone for the Al 2024/2024 FSW. This amount of attack is increased when a tunnel defect is present. Polarization curves also show that the weld zone has higher passive current densities than the base material. Immersion tests performed on the Al 2 195/2195 FSW do not reveal any preferential attack and the polarization curves are identical for the weld zone and base material. Tests performed on the Al 2024/2195 FSW show preferential attack on the Al 2024 side, not necessarily in the weld zone. In this system the weld zone has taken the corrosion characteristics of the Al 2195 material.

Reference

Ferregut, C., Osegueda, R.A., Mendoza, Y., Kreinovich, V., and Ross, T.J., "Aircraft Integrity and Reliability", In Booker, J., Parkinson, J., and Ross, T.R. (eds.), "Combined Fuzzy Logic and Probability Applications", SIAM Publ., Philadelphia.

ABSTRACT

In his recent paper "Probability theory needs an infusion of fuzzy logic to enhance its ability to deal with real-world problems", L. A. Zadeh explains that probability theory needs an infusion of fuzzy logic to enhance its ability to deal with real-world problems. In this chapter, we give an example of a real-world problem for which such an infusion is indeed successful: the problems of aircraft integrity and reliability.

Reference

Osegueda, R.A., Ferregut, C., Kreinovich, V., Seetharami, S., and Schulte, H., "Fuzzy (Granular) Levels of Quality, with Applications to Data Mining and to Structural Integrity of Aerospace Structures", proceedings of the 19th International Conference of the North American Fuzzy Information Society NAFIPS'2000", Atlanta, GA, July 13-15, 2000, pp. 348-352.

ABSTRACT

Experts usually describe quality by using words from natural language such as "perfect ' "good' etc. In this paper, we deduce natural numerical values corresponding to these words, and show that these values explain empirical dependencies uncovered in data mining and in the analysis of structural integrity of aerospace structures.

Reference

Starks, S.A., and Vladik Kreinovich, V., "Aerospace Applications of Soft Computing and Interval Computations (with an emphasis on multi-spectral satellite imaging)", Proceedings of the 2000 World Automation Congress, Maui, Hawaii, June 11-16, 2000.

ABSTRACT

This paper presents a brief overview of our research in applications of soft computing and interval computations to aerospace problems, with a special emphasis on multi-spectral satellite imaging.

Reference

Worden, K., Osegueda, R., Ferregut, C., Nazarian, S., George, D.L., George, M.J., Kreinovich, V., Kosheleva, O. and Cabrera, S., "Interval Methods in Non-Destructive Testing of Material Structures", Reliable Computing, 2001

ABSTRACT

One of the most important characteristics of the plane is its weight: every pound shaved off the plane means a pound added to the carrying ability of this plane. As a result, planes are made as light as possible, with its "skin" as thin as possible. However the thinner the layer, the more vulnerable is the resulting structure to stresses and faults, and a flight is a very stressful experience. Therefore, even minor faults in the plane's structure, if undetected, can be disastrous. To avoid possible catastrophic consequences, before the flight, we must thoroughly check the structural integrity of the plane.

Reference

R.A. Osegueda, M. Macias, G. Andre, C.M. Ferregut and C. Carrasco, "Fusion of Modal Strain Energy for Health Monitoring of Aircraft Structures", In Nondestructive Evaluation of Aging Aircraft, Airports, and Aerospace hardware IV, Ajit K. Mal, Editor, Proceedings of SPIE Vol. 3994, Newport Beach, CA, March 7-8 2000, pp. 117-127.

ABSTRACT

An early prototype of the Vertical Stabilizer Assembly (VSA) of the Shuttle Orbiter was modal tested at healthy and damaged states to study vibrational nondestructive damage evaluation in aerospace structures. Frequency Response and Coherence functions were collected with a Laser Vibrometer at 84 points when the healthy and damaged VSA was shaken with a continuous random force from 0 to 300 Hz. The measurements were used to extract the resonant frequencies and modal shapes for the healthy and damaged states. After pairing of the mode shapes between the healthy and damaged states through the Modal Assurance Criterion and an analysis of the differences in the frequency response functions (FRFs), the strain energy densities of the elements due to modal deformations were determined through a finite element model. The energy densities were normalized so that the total energy of the structure be the same for the mode pairs of the undamaged and damaged sates. The differences in the modal strain energy densities between the healthy and damaged structures provide features that allow for the localization of damage. This is achieved by implementing fusion techniques that combine competing and complementing information obtained from the energy density differences of several mode pairs. This paper evaluates the detectability and performance of two fusion methods to localize damage in the VSA. These are averaging and Bayesian fusion. The performance is based on detectability and the number of false calls.

Reference

Garcia, G.V. and Osegueda, R., "Combining Damage Index Method and ARMA Method to Improve Damage Detection", proceedings of IMAC 2000, San Antonio, TX, February 7-10, 2000, pp. 668-673

ABSTRACT

The objective of this work is to improve the probability of detecting damage and reduce the probability of false positives by combining the Damage Index Method and the ARMA method for damage detection. The Damage Index Method utilizes a comparison of the modal swain energies of the damaged and undamaged structure to determine if damage exists at a particular location. The ARMA method utilizes the coefficients of the AR1vIA model of the undamaged and damaged structure to perform damage detection. The ARMA coefficients are obtained from the time histories generated from a modal test. Generally, the modal parameters needed for the Damage Index Method are obtained from the frequency response function (FRF) data. The Damage Index method and the ARMA method utilize a damage indicator (Dl) to determine if damage is present in the structure. Since both methods utilize a damage indicator we combined the damage indicators into a single feature vector. Next we applied a classification algorithm to classify the feature vector as belonging to the undamaged or damaged class. To investigate the advantage of combining the two NDD methods we made a comparison of the probability of detecting damage and the probability of a false positive using the damage detection results using each method separately and then combined.

Reference

L.R. Pereyra, R.A. Osegueda, C. Carrasco and C. Ferregut, "Detection of Damage in a Stiffened Plate from Fusion of Modal Strain Energy Differences", proceedings of IMAC 2000, San Antonio, TX, February 7-10, 2000, pp. 1556-1562.

ABSTRACT

An aluminum stiffened-plate panel resembling aircraft fuselage construction was tested with a Laser Doppler Velocimeter (LDV). The purpose of the tests was to obtain mode shape data before and after the infliction of damage to evaluate global damage detection techniques. The technique considered here is based on the fusion of modal strain energy differences between the undamaged and damaged states by means of damage likelihood functions and evidential reasoning. The modal strain energies were estimated from bending and twisting curvatures obtained by performing an iterative bi-variate curve-fit on curvatures obtained from finite differences of the mode shapes. The test article was excited with two shakers exerting uncorrelated continuous random forces. The frequency response functions were measured with a laser vibrometer at 239 data points uniformly spaced. The article was subjected to several damage scenarios at different zones.

Reference

R.A. Osegueda, H. Lopez, L. Pereyra, C.M. Ferregut, "Localization of Damage Using Fusion of Modal Strain Energy Differences", proceedings of IMAC 2000, San Antonio, TX, February 7-10, 2000, pp. 695-701.

ABSTRACT

Techniques of data fusion of multiple modal strain energy differences between the undamaged and damaged states of the structure are proposed for the localization of damage at single and multiple locations. The approach relies on a set of modal shape pairs for the undamaged and damaged states. Differences in modal strain energy (or densities) obtained through spline fits or via finite element models provide features that reflect locations with damage with positive values. The features resulting from multiple modes are combined using data fusion techniques involving probabilistic and evidential reasoning methodologies. Fusion algorithms for the localization of damage are tested using modal shapes obtained from aluminum beams in undamaged and damaged states. Damage scenarios with up to three damage locations are considered. The results indicate that the fusion techniques not only improve detectability, but also provide confidence and evidential reasoning for decision-making, reducing the number of false calls.

Reference

J. Eftis, C. Carrasco and R. Osegueda, "Modeling Dynamic Fracture Following High Shock Compression", In Damage and Fracture Mechanics VI Computer Aided Assessment and Control, Eds. A.P.S. Selvadurai and C.A. Brebbia, WIT Press, Southampton, Boston, 2000, ISBN: 1-85312-812-0, pp. 267-279.

ABSTRACT

Constitutive-microdamage equations are developed that are capable of simulating thermo-mechanical material behavior following high shock compression, dilatation, microdamage evolution and fracture, caused by projectile-target impact at hypervelocity.

Reference

J. Eftis, C. Carrasco and R. Osegueda, "Elastic-viscoplastic-microdamage modeling to simulate hypervelocity projectile-target impact and damage", IMPLAST-2000, 7th Int. Symposium on Structural Failure and Plasticity, October 4-6, 2000, Melborne, Australia.

ABSTRACT

Constitutive-microdamage equations are developed that are capable of describing the full range of thermomechanical material behavior, microdamage evolution and fracture associated with hypervelocity projectile-target impact.

Reference

J. Eftis, C. Carrasco and R. Osegueda, "Constitutive Model Simulation of High Shock Compression, Micro-Damage Evolution and Fracture Associated with Hypervelocity Impact", In Mesomechanics-2000, Eds. G.C. Sih, Tsinghua Univ. Press, China, 2000, pp. 279-290.

ABSTRACT

Constitutive-microdamage equations are developed that are capable of simulating the thermo-mechanical material behavior, microdamage evolution and fracture caused by projectile-target impact at hypervelocity.

Reference

J. Eftis, C. Carrasco and R. Osegueda, "A Constitutive-Microdamage Model to Simulate Hypervelocity Projectile-Target Impact, Material Damage and Fracture", presented at the Hypervelocity Impact Symposium 2000, Nov. 6-9, 2000 Galveston, Texas.

ABSTRACT

A set of constitutive-microdamage equations are presented that can model shock compression and the microdamage and fracture that can evolve following hypervelocity impact. The equations are appropriate for polycrystalline metals. For impact at a projectile velocity of 6.0 km/s, numerical simulations are preformed that describe the impact of spherical soda-lime glass projectiles with aluminum 1100 rectangular target plates. Three ratios of the projectile diameter to the target thickness are chosen for the simulations, providing a wide range of damage features. The simulated impact damage is compared with experimental damage of corresponding test specimens, illustrating the capability of the model.